Epigenetic Dysregulation in Cadmium Urothelial Carcinogenesis

Lucinda Cowling

Doctor of Philosophy

University of York

Biology

September 2015

Abstract

The urothelium, the epithelial lining of the bladder, is exposed to urinary-excreted carcinogens from environmental, occupational and dietary sources. These carcinogens include heavy metals such as cadmium. As cadmium is a weak mutagen, this suggests that genetic mechanisms are not responsible for cadmium-induced carcinogenesis. Non-genotoxic carcinogenesis is relatively poorly understood, however recent advances show that epigenetic dysregulation of gene expression may play an important role. The aim of my research was to investigate epigenetic dysregulation as the candidate mechanism underlying cadmium carcinogenesis of human urothelial cells.

Normal human urothelial (NHU) cells were cultured as finite cell lines following isolation from surgical specimens. When established *in vitro*, NHU cells have a highly proliferative phenotype and can be induced to differentiate using two published methods: either through PPARγ-mediated differentiation or serum-mediated differentiation.

Exposure of NHU cells to cadmium inhibited expression of the tumour suppressor genes, p16, APC and RASSF1A. As dysplasia is axiomatic of carcinoma in situ, the precursor to muscle invasive urothelial carcinoma, the potential of NHU cells to differentiate in the presence of cadmium was investigated. Following exposure to cadmium, there was a failure to upregulate archetypical differentiation-associated genes, including uroplakin 1A and 2, and cytokeratins 13 and 20. Trichostatin A, a histone deacetylase inhibitor was able to reverse some of these changes.

Mass spectrometry and immunoblotting were utilised to investigate post-translational histone modification changes caused by cadmium exposure. Data showed that there was a change in histone modification marks present in NHU cell cultures exposed to cadmium that failed to upregulate differentiation markers. An increase in repressive histone marks such as methylation at H3K9 was found alongside a decrease in active marks such as acetylation at H3K18 and H3K23.

This study presents evidence that cadmium exposure changes the epigenome of NHU cells and leads to compromised urothelial differentiation and downregulation of tumour suppressor genes.

Table of Contents

Table of Figures

Table of Tables

Acknowledgements

I would like to thank Professor Jenny Southgate for her guidance, support and advice throughout my PhD project. I also thank my friends and colleagues, past and present, in the Jack Birch Unit for Molecular Carcinogenesis for all their help and support, with special thanks to Jenny Hinley, Ros Duke and Carl Fishwick for their technical assistance.

I would like to thank Dr Mark Dickman and Tom Minshull at the University of Sheffield for the work they carried out on the mass spectrometry quantification of histone modifications.

I would also like to thank my family and friends for their love and support throughout my PhD, especially my boyfriend James Branton.

Finally I wish to thank York Against Cancer for funding my PhD studentship.

Author's Declaration

The candidate confirms that the work submitted in this thesis is her own work and that appropriate credit has been given where reference is made to the work of others, or the efforts of collaborators. This work has not previously been presented for an award at this, or any other, University.

1 Introduction

1.1 Urothelium

The urothelium is a transitional epithelium that lines the mammalian urinary tract, including the renal pelvis, ureter, bladder and proximal urethra. It functions to provide a permeability barrier to urine thereby protecting the underlying stroma (Fellows & Marshall, 1972).

The urothelium is stratified into three cell layers; basal, intermediate and superficial (Figure 1.1) with each layer having a morphologically distinct cell type (Richter & Moize, 1963). The basal layer is composed of small closely packed cells of diameter 5-10 µm which form a single layer of cells that are in contact with the basement membrane. The basal cells support one to four layers of larger, polygonal intermediate cells that have a diameter of 20 µm. The most luminal layer consists of terminally differentiated superficial cells, otherwise known as umbrella cells because they cover several underlying intermediate cells. Superficial cells have a hexagonal shape, are often binucleated and have a diameter ranging from 50-120 µm (Lewis, 2000). The three cell zones can be distinguished through the differential expression of cytokeratin and claudin isotypes and the expression of uroplakins by the superficial cells.

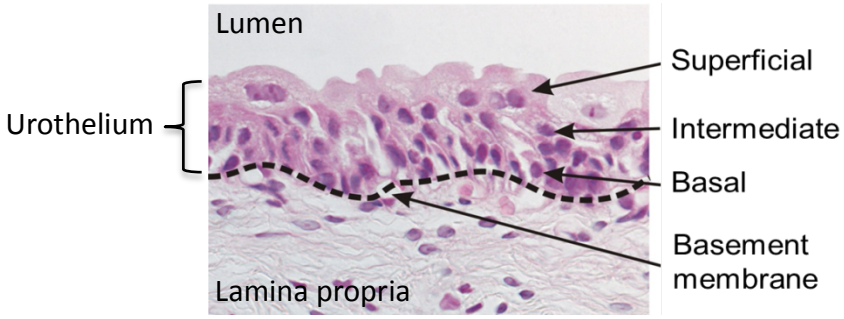

Figure 1.1. A haematoxylin and eosin stained section of human bladder tissue showing the multiple cell layers.

The urothelium is a mitotically-quiescent tissue in situ, but in response to injury or infection it possesses a high regenerative capacity (Hicks, 1975; Jost, 1989; Lavelle et al., 2002). This proliferation response to bladder injury is believed to be regulated by signal feedback between basal cells of the urothelium and the stromal cells that underlie them. Shin et al. (2011) showed that basal urothelial cells express the

secreted protein signal Sonic hedgehog (Shh), and in response to injury Shh expression in these basal cells increases and results in increased stromal expression of Wnt protein signals that lead to the proliferation of both urothelial and stomal cells. An additional study using a rodent damage model identified the involvement of the BMP4 signalling pathway during urothelial regeneration (Mysorekar et al., 2009).

1.1.1 Cytokeratins

Cytokeratins (CK) are keratin-containing intermediate filaments within the cytoplasm of epithelial cells. They exist as heterodimers which come together to form a tetramer by anti-parallel binding; these tetramers then form protofilaments which intertwine in pairs to form protofibrils. Four protofibrils represent one cytokeratin filament.

There are at least 20 different CK isotypes in humans and their expression profiles can be used to classify epithelia and to determine the differentiation stage (reviewed by Chu & Weiss, 2002; Southgate et al., 1999). CK20 is an indicator of terminal differentiation and is only found in the superficial cell zone of urothelium (Moll et al., 1992; Harnden et al., 1996). CK13 is an indicator of transitional differentiation and is expressed in the basal and intermediate cell zones (Achtstatter et al., 1985; Moll et al., 1988; Varley et al., 2004). CK7, CK8, CK18 and CK19 are expressed throughout the three cell layers (Schaafsma et al., 1989). CK14 is an indicator of squamous differentiation and is expressed in cases of squamous metaplasia (Harnden & Southgate, 1997).

1.1.2 Uroplakins

The apical surface of superficial cells is highly specialised, containing multiple thickened plaques of asymmetric unit membrane (AUM), which are comprised of the products of the urothelium-specific uroplakin genes (Wu et al., 1994; Sun et al., 1999). The AUM is thought to strengthen the urothelial apical surface, preventing the cells from rupturing during bladder distension and act to help prevent transcellular diffusion (Hu et al., 2002). Individual AUM plaques are surrounded by ‘hinge’ regions of normal symmetrical plasma membrane. There are five uroplakin proteins that have been identified in man: UPK1A, UPK1B, UPK2, UPK3A and UPK3B (Figure 1.2; Wu et al., 1990; Wu et al., 1994; Deng et al., 2002). UPK1A

and UPK1B are members of the tetraspanin family of proteins, which are a family of membrane proteins that have four transmembrane domains, whereas UPK2, UPK3A and UPK3B are single transmembrane domain proteins (Yu et al., 1994). UPK1A pairs with UPK2, and UPK1B pairs with either UPK3A or UPK3B to form the AUM plaques (Wu et al., 1994; Deng et al., 2002). Urothelial barrier function can be affected by impaired formation of the AUM plaques as demonstrated by UPK2 and UPK3A knockout mice, which showed increased water and urea permeability across the urothelium (Hu et al., 2000; Hu et al., 2002; Kong at al., 2004).

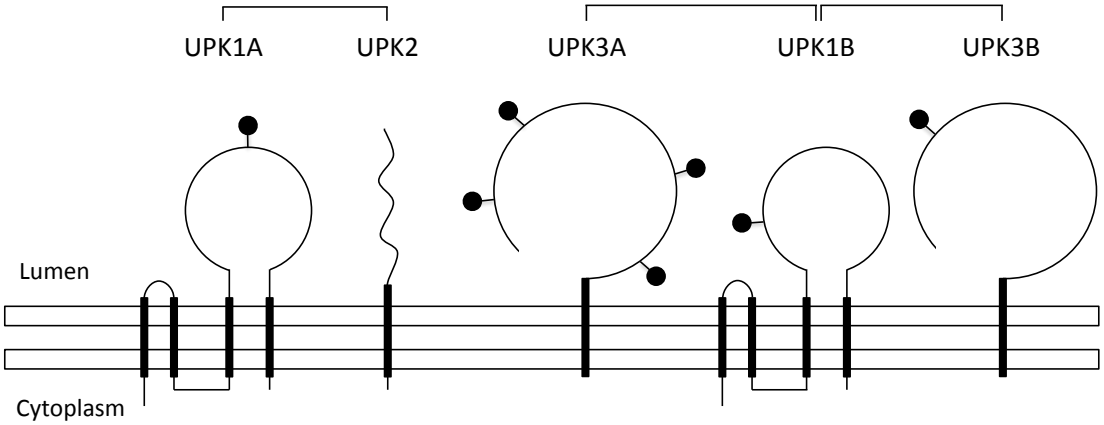

Figure 1.2. The uroplakins. UPK1A and UPK1B are members of the tetraspanning family of proteins. UPK2, UPK3A and UPK3B are single transmembrane proteins. The brackets denote known pairing interactions between UPK isoforms. Solid circles represent N-linked glycan sites. Figure adapted from Deng et al., 2002.

In normal human urothelium uroplakins are only expressed in terminally differentiated superficial 'umbrella' cells (Lobban et al., 1998; Varley & Southgate, 2008).

1.1.3 Tight junctions

Tight junction complexes prevent paracellular diffusion and help to establish polarity in mammalian epithelia. The tight junction barrier is formed by integral transmembrane proteins that seal the paracellular spaces. These proteins include occludin, junctional adhesion molecule and claudins (Figure 1.3). These transmembrane proteins attach to cytoplasmic proteins such as the zona occluden (ZO) proteins that act to cluster the barrier-forming proteins and link the tight junction to the actin cytoskeleton (Schneeberger & Lynch, 2004).

Claudins are small (20-27 kDa) transmembrane proteins. They are tetra-spanning proteins that have two extracellular loops and their N- and C-termini located in the cytoplasm (Schneeberger & Lynch, 2004; Krause et al., 2008). In humans there are 24 members of the claudin family. Claudins can interact homotypically and heterotypically to form fibrils; for example claudin 3 and 5 interact (Coyne et al., 2003; Angelow et al., 2008). Immunohistochemical localisation of claudins in human urothelium has shown that claudin 3 is expressed only at 'kissing points' between superficial cells. Claudin 4 and 5 were expressed at intercellular junctions in the superficial cell zone with claudin 4 also being expressed by the basal and intermediate cell zones and Claudin 7 was expressed by intermediate cells (Varley et al., 2006; Smith et al., 2015).

Zona occludens (ZO) proteins are part of a large family of membrane-associated guanylate kinase homologues. The C-terminus of all claudins except claudin 12, binds to proteins that contain a PDZ domain, which includes ZO-1, ZO-2 and ZO-3 (Itoh et al., 1999). ZO-1 and ZO-2 have been shown to be essential for spatial organisation of claudins in epithelial cells (Umeda et al., 2006).

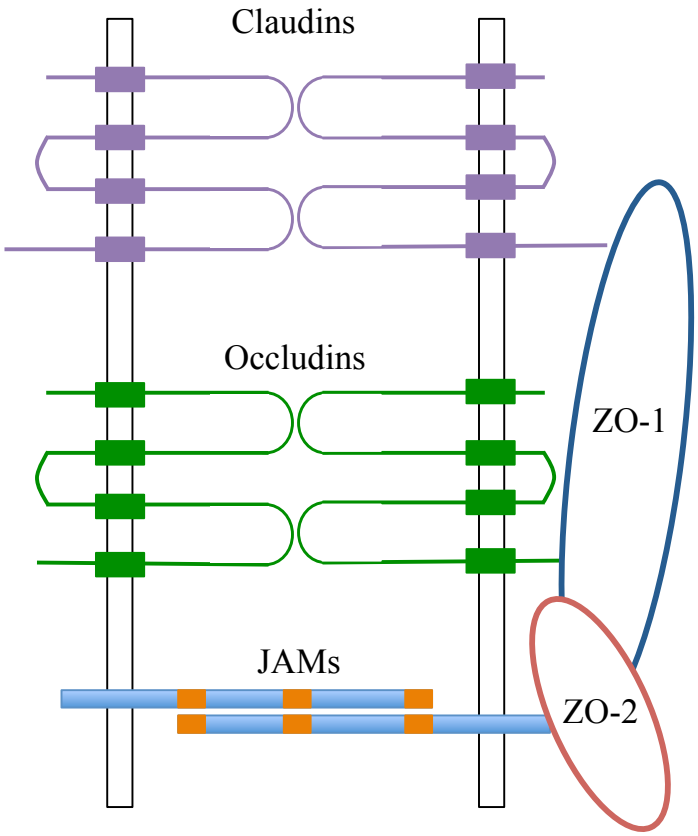

Figure 1.3. Structure of tight junctions.

1.2 Bladder stem cells and progenitor cells

Traditionally, epithelial stem cells reside in the basal cell layers as seen in skin, oral mucosa and the prostate (Bickenbach, 1987; Tsujimura et al., 2002). A DNA nucleotide labelling (BrdU) study in rats showed that potential bladder stem/progenitor cells were localised to the basal cell layer (Kurzrock et al., 2008). Additionally, Shh-expressing cells that have been shown to have long term regenerative capacity are proposed to be Keratin 5-expressing basal cells (Shin et al., 2011; Thangappan & Kurzrock, 2009).

However, from the use of fate mapping studies, Gandhi et al. (2013) observed that Keratin 5-expressing basal cells rarely produce intermediate or superficial cells. They found that P-cells, a transient urothelial cell type, are progenitors in the embryo and intermediate cells are progenitors in the adult urothelium and that both cell types require retinoids for their specification. Sun et al. (2014) found that label-retaining cells (BrdU or EdU) were distributed in all three cell layers of the urothelium and were most concentrated in the bladder trigone.

Wezel et al. (2014) used the expression of nerve growth factor receptor (NGFR), a cell surface-expressed marker that is restricted to basal cells, to isolate basal $NGFR^+$ and suprabasal $NGFR^-$ urothelial cells. Both basal and suprabasal cell populations showed long term proliferation and the capacity to form hierarchically organised differentiated urothelium similar to native urothelium. Colopy et al (2014) showed that UPEC-induced injury resulted in the loss of the superficial cell layer followed by the proliferation of label retaining cells in the basal and intermediate cell layers. This suggests that two distinct progenitor cell populations may exist in the basal and intermediate cell layers (Castillo-Martin et al., 2010; Colopy et al., 2014).

1.3 Urothelial cells *in vitro*

Numerous techniques for the growth of normal human urothelium *in vitro* have been reported (Reznikoff et al., 1983; Kirk et al., 1985; Dubeau & Jones, 1987; Rahman et al., 1987; Hutton et al., 1993; Southgate et al., 1994; Southgate et al., 2002). Human urothelium can be isolated from surgical specimens, disaggregated and then grown in monolayer culture as finite Normal Human Urothelial (NHU) cell lines (Southgate et al., 1994; 2002). When established in a low calcium keratinocyte serum-free medium (KSFM), NHU cells have a highly proliferative phenotype which is driven by the mitogen-activated protein kinase (MAPK) signalling cascade downstream of an epidermal growth factor receptor (EGFR)-activated autocrine signalling loop (Varley et al., 2005). Analysis of CK, claudin and uroplakin expression shows that in serum free conditions NHU cells are non-differentiated and adopt a squamous basal-like phenotype (Southgate et al., 1994; Lobban et al., 1998; Varley et al., 2006).

1.3.1 Differentiation of NHU cell cultures

Differentiation of NHU cell cultures can be induced by two methods: one involves subculture of NHU cell cultures in medium containing serum (Cross et al., 2005), while the other involves pharmacological activation of peroxisome proliferator-activated receptor gamma (PPARγ) and concurrent inhibition of the EGFR autocrine signalling loop (Varley et al., 2004).

1.3.1.1 Serum- mediated differentiation

NHU cells subcultured in medium supplemented with 5% bovine serum and near physiological calcium (2 mM) reproducibly differentiate to form a stratified urothelium, consisting of basal, intermediate and superficial cells, with an efficient barrier function demonstrating low diffusive permeability to urea and water (Cross et al., 2005). Barrier function can be assessed by transepithelial electrical resistance (TER) to determine the potential difference across an epithelial sheet. An epithelia is considered to have a 'tight' barrier function with a resistance >500 $\Omega.cm^2$, whereas a 'leaky' epithelia has a TER <500 $\Omega.cm^2$ (Fromter & Diamond, 1972; Lewis, 2000). The urothelium has one of the highest recorded TER for any tissue with a TER typically greater than 2500 $\Omega.cm^2$ (Lewis & Diamond, 1975; 1976; Hu et al., 2002). When NHU cells were seeded on permeable membranes and maintained in 5% bovine serum and physiological calcium, cultures developed a high TER greater than

3000 Ω.cm^2 (Cross et al., 2005). Cells differentiated using 5% bovine serum and 2mM calcium switch from a proliferative/squamous phenotype to a transitional cell phenotype confirmed by the expression of tight junction components ZO-1, occludin, claudin 4 and an increase in the number of cells expressing CK13 alongside a decrease in those expressing CK14 (Cross et al., 2005).

1.3.1.2 PPARγ-mediated differentiation

PPARγ is a member of the nuclear receptor family and is a ligand-activated transcription factor. It is the highest expressed PPAR isoform in human urothelium (Guan et al., 1997). The heterodimerisation of ligand-bound PPARγ with retinoid X receptor results in formation of an active transcription factor that binds specific regions of DNA in the promoters of target genes called peroxisome proliferator response elements (PPRE) (Blanquart et al., 2003). PPARγ activation has been shown to have roles in the differentiation of numerous cell types including adipocytes (Lowell, 1999).

Activation of PPARγ in NHU cell cultures with troglitazone (TZ) can induce upregulation of the urothelial differentiation marker UPK2 (Varley et al., 2004a) and induce transitional differentiation as demonstrated by the gain of CK13 and loss of CK14 protein expression (Varley et al., 2004b). Due to autocrine EGFR activity in NHU cells (Varley et al., 2005) which phosphorylates and inhibits PPARγ, PPARγ-mediated differentiation requires the concurrent inhibition of EGFR with PD153035 (PD) or the downstream MAPK/ERK protein inhibitor U0126. This allows for a more robust expression of uroplakins as well as cytokeratins and tight junction proteins (Varley et al., 2006).

1.3.1.3 Transcription factors involved in urothelial differentiation

Transcription factors upregulated by PPARγ activation have been shown to be involved in the expression of differentiation markers. The hypothesis that intermediary factors may be involved came about because the differentiation marker UPK2 does not contain a PPRE in its promoter region and because upregulation of UPK2 mRNA levels does not occur until 24-48 hours after PPARγ activation. This is later than other markers of differentiation such as FABP4 and AQP3 that contain a PPRE in their promoter region and are upregulated within six hours (Flemming, 2008). Varley et al. (2009) identified several transcription factors including

interferon regulatory factor (IRF1) and forkhead box A1 (FOXA1) that were upregulated within 12 hours of induction of differentiation and which had PPREs in their promoter regions. Both IRF1 and FOXA1 were shown to bind the promoter region of UPK2 and their knockdown inhibited differentiation. Other transcription factors that have been shown to be involved in urothelial differentiation include grainyhead-like protein 3 homolog (GRHL3), ETS-related transcription factor Elf-3 (ELF3), krueppel-like factor 5 (KLF5) and GATA-binding protein 3 (GATA3) (Yu et al., 2009; Bell et al., 2011; Bock et al., 2014).

1.4 Bladder Cancer

The majority of bladder cancers arise from the urothelium and in its most aggressive form, where urothelial carcinoma (UC) invades the detrusor smooth muscle of the bladder wall, it is associated with a high mortality (<50 % 5yr survival). The classical understanding of UC is based on clinical and genetic evidence which suggests that UC develops via two pathways: the Ta tumour pathway and the carcinoma in situ (CIS) pathway (Figure 1.4). The Ta/T1 pathway is characterised by low-grade frequently recurrent superficial tumours, which rarely progress to the muscle invasive stage (70–80% of human UC cases), whereas CIS lesions are high grade and often progress to muscle invasive carcinomas (20–30% of human UC cases). The two pathways are associated with different initiating mutations. Low grade superficial UCs frequently have activating mutations in the fibroblast growth factor receptor 3 (FGFR3) gene (75%) (Cappellen et al., 1999; Billerey et al., 2001), or in genes of the RAS pathway (10-15%) (Jebar et al., 2005) both of which activate the MAPK pathway. By contrast the high-grade muscle invasive tumours contain mutations in genes encoding the tumour suppressor p53 and/or retinoblastoma protein (RB) leading to a loss of function (Hartmann et al., 2002; Hopman et al., 2002; Hurst et al., 2008). Loss of PTEN function and activation of the Wnt signalling pathway have also been proposed to play a role in muscle-invasive bladder tumours (Puzio-Kuter et al., 2009).

Recent genome-wide expression and sequencing studies have identified distinct basal and luminal molecular subtypes of muscle-invasive bladder cancer (MIBC) that share molecular features with basal and luminal breast cancers (Sjodahl et al., 2012; 2013; Choi et al., 2014; Damrauer et al., 2014). Luminal MIBCs are enriched for uroplakins, KRT20, ERBB2 and differentiation markers such as FOXA1, GATA3, TRIM24 and PPARγ, while basal MIBCs are enriched for KRT5, KRT6, KRT14, CD44 and CDH3. Luminal MIBCs frequently have papillary morphology and FGFR3 upregulation or mutation.

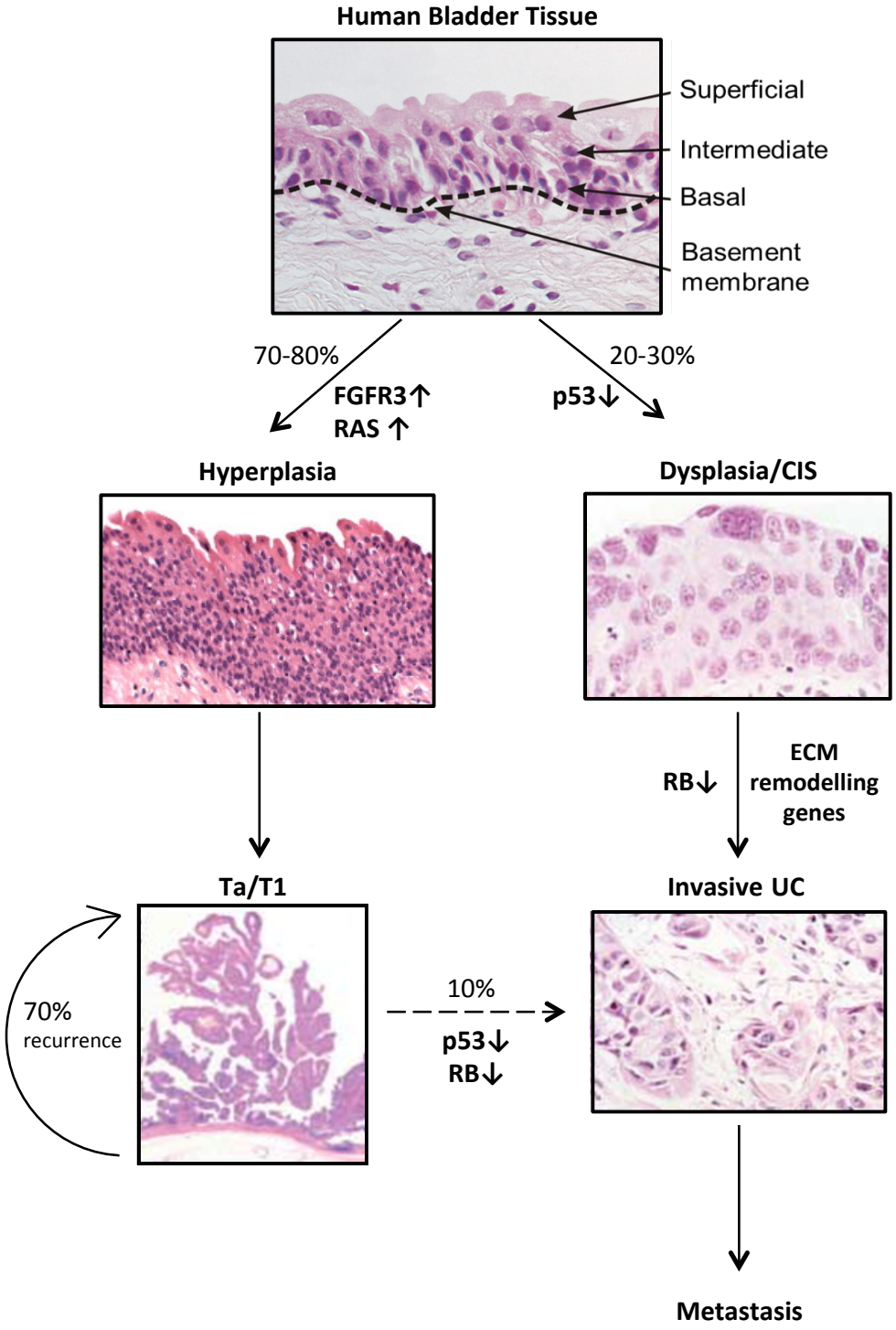

Figure 1.4. Diagram of urothelial carcinoma progression. Low grade, non-invasive papillary tumours are associated with activating mutations in FGFR3 and RAS. High grade muscle-invasive tumours are associated with loss of p53 or RB function. Later stage and carcinoma *in situ* tumours express extracellular matrix remodelling genes. (Cappellen et al., 1999; Billerey et al., 2001; Jebar et al., 2005; Hartmann et al., 2002; Hopman et al., 2002; Hurst et al., 2008).

1.5 Epigenetics

Epigenetics is defined as heritable changes in gene expression that are not accompanied by changes in DNA sequence (Jones & Baylin, 2007). Major epigenetic mechanisms include DNA methylation, post-translational modifications of histones and non-coding RNA-mediated gene silencing. Epigenetic mechanisms are essential for normal development as they regulate the expression of genes involved in key biological processes. However epigenetic changes have also been shown to play a role in cancer; this was first shown back in the 1980s when global DNA hypomethylation was reported in human tumours (Feinberg & Vogelstein, 1983). Since then many other epigenetic mechanisms have been implicated in cancer including histone modifications, microRNA expression and nucleosome positioning.

1.5.1 DNA methylation

DNA methylation is the most well studied epigenetic alteration. The DNA methyltransferase (DNMT) family mediates the methylation of cytosines through the transfer of a single methyl group from S-adenosyl methionine (SAM) to cytosine forming 5-methyl cytosine (5-MeC). DNA methylation silences genes by preventing access of transcription factors to their respective binding sites either directly by methylation of transcription factor binding sequences or indirectly through the recruitment of methyl-CpG-binding domain (MBD) proteins. MBD proteins can directly block transcription factor binding or they can recruit chromatin modifiers that alter the chromatin structure into a more repressive environment (Newell-Price et al., 2000).

1.5.2 Histone modifications

DNA is packaged into chromatin, which may be partitioned into condensed regions called heterochromatin or into more relaxed accessible regions called euchromatin (Felsenfeld & Groudine, 2003). The fundamental repeating unit of chromatin is the nucleosome, consisting of 147 bp of DNA wrapped approximately 1.7 superhelical turns around a core histone octamer, comprising two H2A/H2B dimers and a H3/H4 tetramer (Luger et al., 1997). Chromatin structure affects every DNA-based process including gene transcription, DNA replication and DNA repair (Kouzarides, 2003). One approach to establish, maintain and modulate chromatin structure involves post-

translational modification of histones, particularly of histone N-terminal tails (Bannister & Kouzarides, 2011).

The N-terminal tail domains of the core histones contain an extraordinary number of sites that can be subjected to post-translational modification (Grant, 2001; Goll & Bestor, 2002; Turner, 2002). Some modifications, such as acetylation and phosphorylation, can alter the charge of the tails and, therefore, have the potential to influence chromatin through electrostatic mechanisms. However, the primary mechanism by which histone modifications act appears to be through altering the ability of non-histone proteins to interact with chromatin (Martin & Zhang, 2005; Grewal & Moazed, 2003; Iizuka & Smith, 2003; Jenuwein & Allis, 2001).

The acetylation of histone tails by histone acetyltransferases (HATs) induces chromatin decondensation, whereas the removal of acetyl groups by histone deacetylases (HDACs) promotes a tighter binding of the histone to the DNA. Methylation of histones can be associated with either euchromatin or heterochromatin depending on the target histone residue. For example, the tri-methylation of histone H3 lysine 27 (H3K27me3) is implicated in gene repression by promoting a compact chromatin structure (Ringrose et al., 2004), whereas di/tri-methylated histone H3 lysine 4 (H3K4me2/me3) is associated with transcriptional activation, with the highest levels of this modification being observed near transcriptional start sites of highly expressed genes (Shi et al., 2004). The enzymes that add or remove methylation marks on lysine residues are known as lysine methyltransferases (KMTs) and lysine demethylases (KDMs) (Allis et al., 2007).

1.5.3 Epigenetic modifiers

Trichostatin A and 5-aza-deoxycytidine are two epigenetic modifiers that are widely used in studies to examine epigenetic mechanisms. Trichostatin A (TSA) is a *Streptomyces* metabolite, which specifically inhibits mammalian histone deacetylase at nanomolar concentrations and causes accumulation of highly acetylated histone molecules in mammalian cells (Yoshida et al., 1995). 5-aza-deoxycytidine (5aza) is an epigenetic modifier that inhibits DNA methyltransferase activity, which results in DNA demethylation (hypomethylation) and gene activation by remodelling chromatin (Creusot et al., 1982; Taylor & Jones, 1982; Christman et al., 1983). This

remodelling of chromatin structure allows transcription factors to bind to the promoter regions, assembly of the transcription complex, and alters gene expression.

1.6 Epigenetic Silencing in Bladder Cancer

In 2006, Stransky et al. developed a systematic approach, using a combination of transcriptome correlation map analysis and comparative genomic hybridization array data, to identify regional transcriptional deregulation that occurs independently of DNA-copy number changes. Using this approach they were the first to identity the long range silencing of numerous chromosomal regions by epigenetic silencing. In 2011, Vallot et al., extended this approach to identify seven chromosomal regions of genes that were silenced by epigenetic mechanisms in bladder tumours; they defined this simultaneous silencing of several chromosome regions as a new phenotype termed the multiple regional epigenetic silencing (MRES) phenotype and showed how the genes associated with this phenotype overlapped with the 100 genes of a gene expression signature for carcinoma in situ found by Dyrskjot et al. (2004). Vallot et al. showed that the mechanism of epigenetic silencing of these regions was associated with histone H3K9 and H3K27 methylation and H3K9 hypoacetylation and not DNA methylation. This study also highlighted that the silenced regions in the MRES phenotype contained known or potential tumour suppressor genes such as PLCD1, DLEC1 and HOXA5.

Nishiyama et al. (2010) carried out DNA methylation studies comparing urothelia from normal urothelium, non-cancerous urothelium from patients with UC and samples of urothelial carcinoma. They found that non-cancerous urothelia from patients with UC had methylated regions similar to UC samples, but distinct from normal urothelium samples. Methylation patterns were able to discriminate patients who suffered from recurrence after surgery from patients who did not. This study showed that DNA methylation profiling could provide indicators for carcinogenic risk estimation and prognosis.

Several groups have described differential methylation of promoters of genes known to have altered expression in UC such as RASSF1A, APC and p53 (Maruyama et al., 2001; Catto et al., 2005). This has been linked to the altered expression of DNMT1 during urothelial carcinogenesis as reported by Nakagawa (2005). Dhawan et al. (2006) found that aberrant promoter methylation occurs early in urothelial carcinogenesis. A follow up study by the same group was performed investigating the relationship between DNA methylation, histone methylation and gene expression

(Dudziec et al., 2012). They profiled two repressive histone modifications (H3K9me3 and H3K27me3) using ChIP-Seq, cytosine methylation using MeDIP and mRNA expression in normal and malignant urothelial cell lines. H3K27me3 was found to occur around genes with low expression in all cells, whereas H3K9me3 was only weakly associated with repression in a subset of genes with DNA methylation. DNA methylation itself was more closely related to gene expression in malignant rather than normal cell lines.

Chromatin-remodelling genes have been found to exhibit genetic mutations in bladder cancer. These include KDM6A, which encodes a histone demethylase; MLL/KMT2A, MLL2/KMT2D and MLL3/KMT2C, which encode histone methyltransferases; AT-rich interactive domain 1A (ARID1A) which encodes a component of the SWI/SNF chromatin-remodelling complex; E1A-binding protein p300 (EP300) and CREB-binding protein (CREBBP), which encode histone acetyltransferases; and nuclear receptor co-repressor 1 (NCOR1), which encodes a histone deacetylase (Gui et al., 2011; Guo et al., 2013).

1.7 Non-coding RNAs in Bladder Cancer

Many non-coding RNAs have been reported to show abnormal expression in bladder cancer tissue. Micro RNAs (miRNAs) are small (18-25 nucleotides) molecules that regulate gene expression post-transcriptionally. Altered miRNA expression in bladder cancer was first reported in 2007 with ten miRNAs (miR-221, -223, -23a, -185, -103-1, -205, -23b, -26b, -203 and -17-5p) found to be upregulated in bladder cancers compared to normal bladder mucosa (Gottardo et al. 2007). The majority of studies involving miRNA and bladder cancer have compared miRNA expression between normal bladder tissue, muscle-invasive bladder cancer (MIBC) and non muscle-invasive bladder cancer (NMIBC). The general trend is that miRNAs are upregulated in MIBC and downregulated in NIMBC (Catto et al., 2009; Veerla et al., 2009; Neely et al., 2010; Han et al., 2011; Guancial et al., 2014). Catto et al. (2009) found that MIBC was characterised by miRNA upregulation, including miR-21, which has previously been shown to downregulate the p53 pathway (Papagiannakopoulos et al., 2008), and miR-373, which promotes tumour invasion and metastasis (Huang et al., 2008). NMIBC tumours exhibited downregulation of many miRNAs including the loss of miR-99a and miR-100, which led to the upregulation of FGFR3 (Catto et al., 2009).

Recent studies have shown how miRNAs may promote bladder cancer progression. These include a study that has shown miR-96 may function as an onco-miRNA and that the upregulation of miR-96 may contribute to aggressive malignancy via suppressing CDKN1A protein expression in bladder cancer cells (Wu et al., 2015). Sun et al. (2015) found that the suppression of miR-138 in bladder cancer may promote ZEB2-mediated cancer invasion and metastasis.

Long non-coding RNAs (lncRNAs) are RNA molecules with a length of more than 200 nucleotides. Han et al. (2013) reported upregulated expression of the lncRNA MALAT1 in high-grade versus low grade carcinomas and also in invasive compared to non-invasive carcinomas. The long intergenic non-coding RNA UBC1 was upregulated in bladder cancer tissues compared with normal adjacent tissues, and linc-UBC1 overexpression was shown to correlate with lymph node metastasis and poor survival (He et al., 2013). Functional studies found linc-UBC1 associates with

polycomb repressive complex 2 (PRC2) and regulates the histone modification status of target genes.

H19 is a long non-coding RNA that harbours pro-tumorigenic properties (Barsyte-Lovejoy et al., 2006; Matouk et al., 2007; Yang et al., 2012). Luo et al. (2013) found that H19 expression is increased in bladder cancer tissues and was associated with disease progression, with functional studies suggesting H19 may regulate metastasis by associating with enhancer of zeste homolog 2 (EZH2) and inhibiting E-cadherin expression.

1.8 Metals in Cancer

Epidemiological, animal and cell culture experimental studies have shown that an increase in cancer incidence is associated with exposure to non-genotoxic metals such as nickel, arsenic and cadmium.

Nickel compounds are known human non-mutagenic carcinogens that target the respiratory system. This targeting is due to bioavailability rather than a tissue-restricted effect, as the route of exposure of the nickel compounds is through inhalation. Both water soluble and insoluble nickel compounds have been implicated in human lung and nasal cancers, with insoluble nickel compounds shown to be more potent carcinogens (NTP 1996a, 1996b). Epigenetic changes implicated in nickel-induced carcinogenesis include gene silencing by DNA hypermethylation (Lee et al., 1995), decreased histone acetylation of H2A, H2B, H3 and H4 (Broday et al., 2000; Golebiowski & Kasprzak, 2005; Ke et al., 2006), increases in histone H3 Lysine 9 dimethylation (Chen et al., 2006) and increases in histone ubiquitination H2A and H2B (Karaczyn et al., 2006).

Arsenic and inorganic arsenic compounds are known human carcinogens which target multiple sites including the lung, skin and urinary bladder. Inorganic arsenic is able to be methylated during its metabolism in the liver using S-adenosyl methionine (SAM) as the methyl donor to form monomethylarsonic acid and dimethylarsinic acid (DMA(V)). DMA(V) has been shown to induce urinary bladder carcinomas in rats that were orally exposed in either their water supply or by addition to their food (Wei et al., 1999). Epigenetic changes implicated in arsenic-induced carcinogenesis include increased DNA methylation of the p53 promoter (Mass & Wang, 1997), and alterations in global histone H3 methylation, with decreases in H3K27 trimethylation and increases in di- and trimethylated H3K4 (Zhou et al, 2008).

Arsenic treatment has also been shown to increase cell proliferation through the activation of signal transduction pathways. Mice that were treated with sodium arsenite in their drinking water developed hyperplasia of the bladder urothelium within 4 weeks of exposure. In the same study, it was found that arsenic can stimulate the growth of UROtsa cells, an immortalized human urothelial cell line (Simeonova et al, 2000). It had also been shown using the UROtsa cell line that arsenic exposure leads to c-Src-dependent activation of the EGFR and MAPK

pathway (Simeonova et al., 2002). This proliferation-enhancing effect of arsenic may also contribute to its ability to cause cancer.

1.8.1 Cadmium

Cadmium is a toxic transition metal that has been classified as a known human carcinogen by both the International Agency for Research on Cancer and the National Toxicology Program of the USA (IARC, 1993; NTP, 2000). The classification of cadmium as a human carcinogen is based on epidemiological studies in humans (Waalkes, 2000) and experimental studies in animals which show cadmium as a multiple tissue carcinogen (Takenaka et al., 1983; Waalkes et al., 1999). Cadmium has a long biological half-time in humans which is estimated to be between 15-20 years (Jin et al., 1998). The human body has a limited capacity to limit the harm of cadmium exposure as the metal cannot be metabolised to less toxic species and is poorly excreted, effectively making it a cumulative toxin (Goering et al., 1994).

1.8.2 Sources of Exposure

Occupational exposure to cadmium comes from activities such as lead and zinc smelting, melting or welding cadmium-coated steel, using cadmium-containing solders and the use, processing and production of cadmium powders for nickel-cadmium batteries (IARC, 1993). Recently diesel fumes, which contain cadmium, have been shown to be carcinogenic to humans (IARC, 2012). It is thought that people in high-risk industries exposed to diesel fumes, such as miners, railway workers and truck drivers have about a 40% increased risk of developing cancer. The general population can be exposed to cadmium via contaminated food or drinking water and by the inhalation of cigarette smoke (Jarup & Akesson, 2009; Adams et al., 2011). It is believed that the smoking of cigarettes can double the lifetime body burden of cadmium (Tokar et al., 2011).

1.9 Cadmium and Bladder Cancer

High-grade bladder cancer is particularly common in South Yorkshire, with some health regions having higher-than-average incidence rates (Figure 1.5). This reflects local clinical observations of increased high-grade bladder cancer risk amongst metal workers exposed to cadmium (J Catto, personal communication).

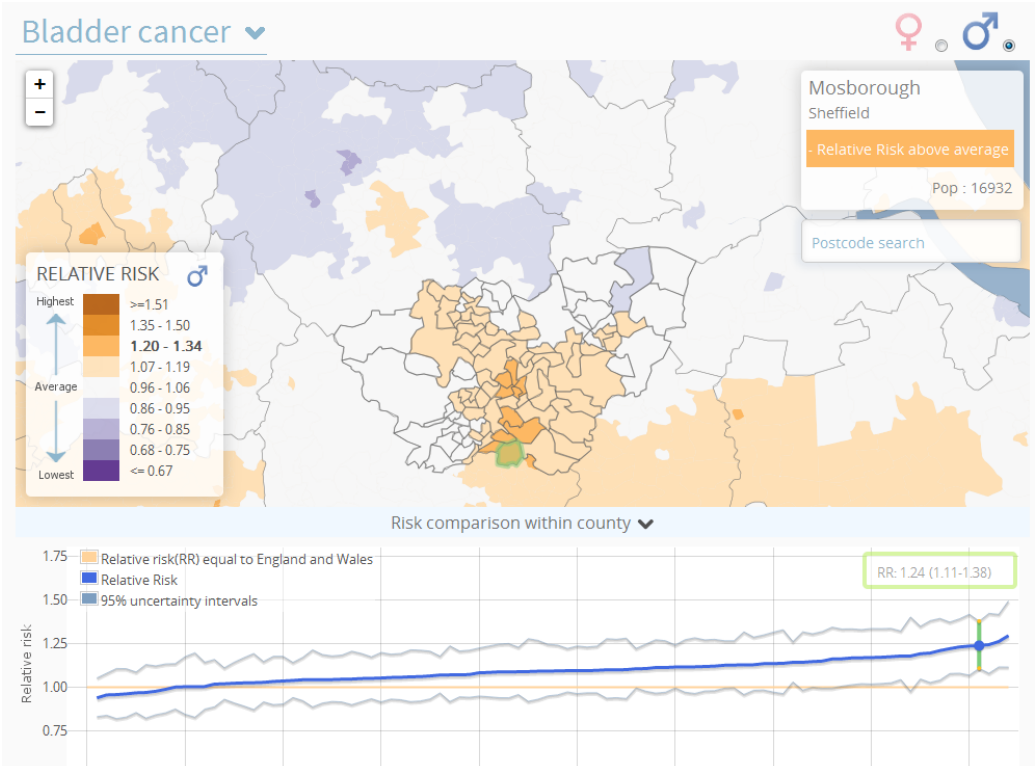

Figure 1.5. Bladder cancer risk for men in Yorkshire. From the Environment and Health Atlas for England and Wales (www.envhealthatlas.co.uk) produced by the UK Small Area Health Statistics Unit at Imperial College London.

A meta-analysis looking at the association between bladder cancer incidence and occupation found that metal workers were at an increased risk (Reulen et al., 2008).

1.9.1 Epidemiological and clinical studies

Evidence in support of cadmium being a bladder carcinogen includes a 1994 population-based case-control study of the associations between various cancers and occupational exposures which found evidence suggesting a link between cadmium exposure and cancer of the urinary bladder (Siemiatycki et al., 1994). This is supported by a Belgian case-controlled study which suggested that individuals with increased exposure to cadmium have an increased risk of bladder cancer, using blood cadmium levels as a marker for cadmium exposure (Kellen et al., 2007). Blood

cadmium is considered to reflect current exposure rather than whole body burden, while urinary cadmium reflects the total burden of cadmium (ATSDR, 1999). A further case-controlled study from Tunisia observed that an increased risk of bladder cancer was associated with an increase in cadmium blood concentrations (Feki-Tounsi et al., 2013). A follow up study by Feki-Tounsi et al. (2014) investigating levels of toxic metals in patients with bladder tumours was performed. It was found that cadmium concentrations were significantly elevated in normal tissues adjacent to tumours compared to controls.

A study in 1998 based on ten patients with bladder cancer used atomic spectrometry to measure urinary cadmium concentrations. It was found that in 60% of the patients urinary cadmium was increased, implying an involvement of cadmium in bladder cancer (Darewiczet al., 1998).

An investigation measuring metallothionein-bound cadmium concentration in urine using size exclusion chromatography coupled to inductively-coupled mass spectrometry found that in bladder cancer patients MT-bound cadmium was significantly elevated compared to the control group (Wolf et al., 2009).

Finally a case-control study that examined the association between the expression of metallothioneins and bladder tumours, and also compared cadmium levels in tissue and hair of 37 bovine bladder tumours against 17 controls, found that increased expression of metallothioneins was associated with bladder tumours and that cadmium concentrations in hair were significantly higher in the bladder tumour group compared to the control group (Amaral et al., 2009).

1.9.2 Experimental studies

Few animal studies have focused on cadmium-induced cancers. Injection, inhalation or ingestion of cadmium into animal models has been shown to cause cancer in several sites (Waalkes et al., 1999a; 1999b), however, only one study has showed that injection of cadmium led to the development of a bladder tumour (Waalkes et al., 2000).

In vitro studies indicating cadmium as a potential human bladder carcinogen include a study which demonstrated that cadmium is able to induce malignant transformation of immortalized human urothelial cells *in vitro* (Sens et al., 2004). It was demonstrated that long-term exposure to 1 μM Cd resulted in UROtsa cells that were

able to form colonies in soft agar and tumours when heterotransplanted into nude mice. Tumour heterotransplants produced by these cadmium-transformed cells were epithelial in character and had features consistent with urothelial carcinoma (Sens et al., 2004).

1.10 Cadmium Carcinogenesis

Cadmium compounds are not mutagenic in bacterial assays (Beyersmann & Hartwig, 1994) and cadmium salts did not cause DNA damage in cell extracts or with isolated DNA (Valverde et al., 2001). This implies cadmium-induced carcinogenesis may be mediated through non-genotoxic or indirect genotoxic mechanisms. Proposed mechanisms for cadmium carcinogenesis have been outlined below (Figure 1.6).

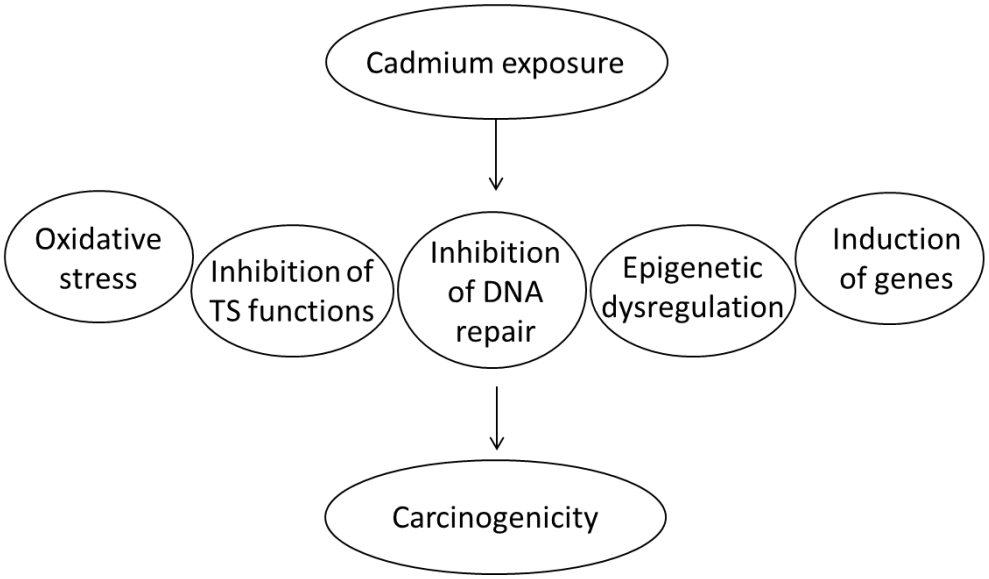

Figure 1.6. Proposed mechanisms involved in cadmium-induced carcinogenicity.

1.10.1 Oxidative stress

Cd^{2+} does not catalyse the Fenton-type production of free radicals because it does not accept or donate electrons under physiological conditions. However, increased levels of reactive oxygen species have been observed *in vitro* and *in vivo* (Liu et al., 2009). This is believed to be caused by the inhibitory effect of cadmium on antioxidant enzymes such as catalase, superoxide dismutase, glutathione reductase and glutathione peroxidase (Stohs et al., 2001; Valko et al., 2006). Cadmium compounds have been shown to induce DNA strand breaks and oxidative DNA base modifications in mammalian cells, but effects were small and restricted to high concentrations (Dally & Hartwig, 1997; Schwerdtle et al., 2010). The induction of DNA strand breaks and chromosomal aberrations by cadmium in mammalian cells could be suppressed by antioxidants and antioxidative enzymes (Ochi et al., 1987; Stohs et al., 2001; Valko et al., 2006). Oxidative DNA damage does not appear to be sufficient to explain the carcinogenicity of cadmium.

1.10.2 Induction of genes

Exposure to cadmium has been shown to induce the expression of many genes including immediate early response genes (IEGs) and stress response genes including metallothionein genes and heat-shock genes.

Immediate early response genes are genes that are activated rapidly and transiently after a variety of cellular stimuli. IEGs encode transcription factors and DNA-binding proteins that regulate cell growth and differentiation. The IEGs most studied with respect to cadmium toxicity and carcinogenesis are c-fos, c-jun and c-myc. These genes are overexpressed in response to cadmium exposure *in vitro* and *in vivo* (Achanzar et al., 2000; Jin & Ringertz, 1990; Matsuoka & Call, 1995).

Cadmium exposure to cells and whole animals has been shown to result in the induction of several stress response genes, including those involved in metallothionein synthesis (Hart et al., 1996), genes involved in the synthesis of glutathione (Hatcher et al., 1995), and genes encoding heat shock proteins (Lee et al., 2002). Cadmium has been shown to induce heat shock protein genes by generating denatured or abnormal proteins by reacting with thiol groups or by substituting for zinc in proteins (Parsell & Lindquist, 1994). Both metallothionein and glutathione play a role in cellular defence against cadmium toxicity and carcinogenesis by scavenging and sequestering the Cd^{2+} ion to prevent its interaction with critical cellular targets.

Metallothioneins (MTs) are a family of cysteine-rich low molecular weight proteins that bind heavy metals. There are eleven functional MT isoforms in humans that are divided into four classes, MT1 to MT4. MT1 and MT2 are expressed in many cell types and their function is to maintain cellular zinc homeostasis and protect against heavy metal and oxidant damage. MT1/2 transcription is regulated by the metal regulatory transcription factor 1 (MTF1), a zinc-sensing zinc-finger transcription factor that binds to short DNA sequence motifs termed metal response elements (MREs) present in the promoter region of metallothionein genes (Stuart et al., 1985). Upon cadmium exposure, MT-bound Zn^{2+} is replaced by Cd^{2+} which then activates MTF1 (Figure 1.7; Günther et al., 2012).

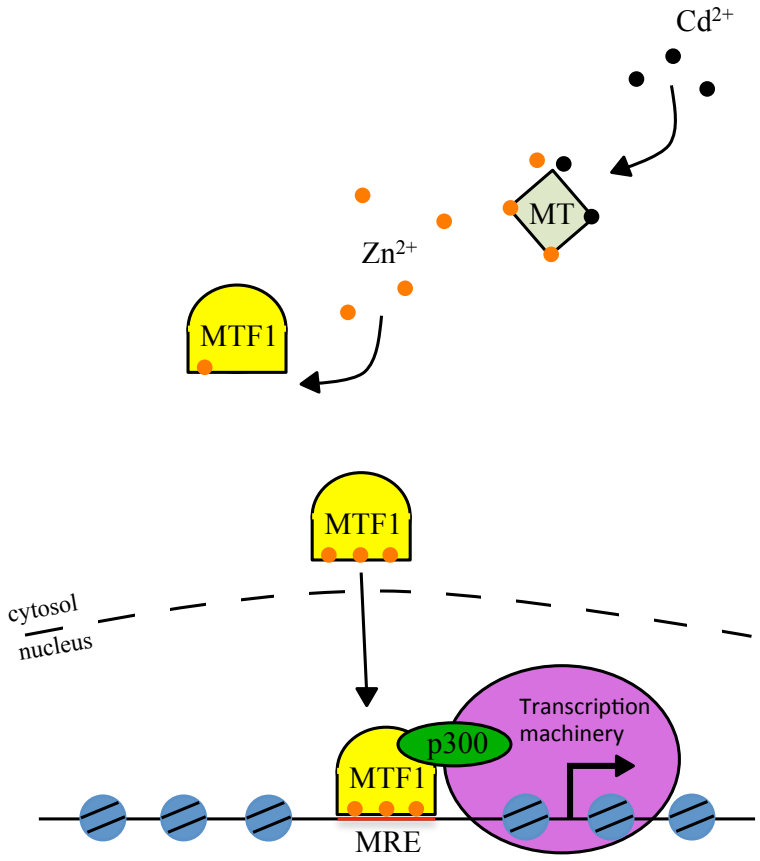

Figure 1.7. Proposed molecular mechanism of MT transcription in response to cadmium exposure. MTF1 can be activated directly by zinc or indirectly by release of zinc from metallothioneins upon cadmium exposure (Zhang et al., 2003). Upon zinc binding MTF1 translocates to the nucleus where it binds to metal response elements (MRE) located upstream of the MT gene coding sequences. MTF1 interacts with other transcription factors and recruits the histone acetyltransferases p300 resulting in increased MT transcription.

1.10.3 Inhibition of DNA repair

Inhibition of DNA repair has been identified as a mechanism contributing to the carcinogenic potential of cadmium. DNA damage can be caused by environmental agents or endogenous factors and is repaired by DNA damage repair pathways. These include base-excision repair, nucleotide-excision repair, recombinational repair and mismatch repair. Low concentrations of cadmium have been demonstrated to inhibit the repair of oxidative damage in mammalian cells (Dally & Hartwig, 1997). During nucleotide-excision repair cadmium was shown to inhibit the removal of thymine dimers generated by UV-irradiation by interfering with the first step of the repair pathway. Cadmium was shown to inhibit two proteins, Fpg and XPA (Asmuss et al., 2000); these proteins are zinc-finger proteins and the inhibitory

effect of cadmium was believed to be due substitution of zinc by cadmium (Hartwig, 2001).

1.10.4 Epigenetic mechanisms

Although cadmium can induce oxidative stress, it is poorly mutagenic and has a weak DNA binding affinity; therefore it is believed that another way cadmium may promote carcinogenesis is through epigenetic mechanisms.

1.10.4.1 DNA methylation

To date, the most reported epigenetic changes associated with cadmium exposure relate to changes in DNA methylation; however cadmium exposure has been shown to cause both hypermethylation and hypomethylation. Takiguchi and colleagues showed that cadmium is an effective inhibitor of DNA methyltransferases (DNMTs) and initially induced DNA hypomethylation in TRL1215 rat liver cells *in vitro*. However prolonged exposure led to the emergence of cadmium-transformed cells which exhibited increased DNA methylation and DNMT activity (Takiguchi et al., 2003). The study showed that acute cadmium exposure led to reduced DNA methyltransferase activity both *in vitro*, in TRL1215 liver cells, and in an *ex vivo* system using purified bacterial DNA methyltransferase. Kinetic analysis performed indicated that cadmium interacts with enzymes at sites other than the catalytic site. The authors put forward the DNA binding site of the DNMTs as a strong candidate as it contains numerous cysteines, which are known to bind cadmium. A later study using cadmium-transformed human prostate epithelial cells showed that increased DNMT enzymatic activity was associated with over-expression of DNMT3b without changes in DNMT1 (Benbrahim-Tallaa et al., 2007). The over-expression of DNMT3b correlated with reduced expression of the tumour suppressor genes, RASSF1A and p16. It was reported that the promoter regions of these genes were heavily methylated, indicating gene silencing due to DNA hypermethylation. Additionally the expression of these genes could be restored by treatment of the cells with 5-aza-2'-deoxycytidine, a DNA demethylating agent, giving evidence that chronic cadmium exposure induces gene-specific DNA hypermethylation and gene silencing. The overall effect of cadmium exposure on DNA methylation suggests that short exposures are associated with DNA hypomethylation whereas chronic

exposures are associated with DNA hypermethylation (Martinez-Zamudio & Ha, 2011).

1.10.4.2 Histone modifications

Few studies have been performed investigating histone modification changes due to cadmium exposure. One study looking at changes in histone modifications caused by direct cadmium exposure, used cadmium-transformed immortalized human urothelial cells to determine if epigenetic modifications control urothelial metallothionein 3 (MT-3) gene expression (Somji et al., 2011). The study found that in non-transformed UROtsa cells the MT-3 gene is silenced by a mechanism involving histone modification of the MT-3 promoter. Transformation of the UROtsa cells with Cd^{2+} modified the chromatin of the MT-3 promoter to a bivalent state with both active (H4 acetylation, H3K4 methylation) and repressive (H3K9 and H3K27 methylation) histone marks present.

However, other changes in histone modifications have been reported due to cadmium. In a study reporting the epigenetic and genotoxic effects of cadmium telluride quantum dots in human breast carcinoma cells, free cadmium ions released in the cells led to chromatin condensation and histone hypoacetylation (Choi et al., 2008). The hypoacetylation of histone H3 was detected by both immunofluorescence and western blotting, with the hypoacetylation being reversed by treatment with trichostatin A, a histone deacetylase inhibitor.

1.10.4.3 Non-coding RNA expression

Peripheral blood leukocytes from 63 workers at an electric-furnace steel plant were analysed after exposure to particular matter containing cadmium. miR-146a was found to be negatively correlated to occupational cadmium exposure while miR-222 and miR-21 were significantly increased after 3 days exposure to the metal-rich particulate matter (Bollati et al., 2010). Cadmium has been shown to affect miRNA levels *in vitro*. miRNA expression was analysed after cadmium exposure in a human hepatocellular carcinoma cell line using an Agilent microarray. Several differentially expressed miRNAs were found, some of which were members of the let-7 family, which exhibit oncosuppressor functions (Fabbri et al., 2012).

Two studies have reported changes in lncRNA expression upon cadmium exposure. Human-induced pluripotent stem cells treated with cadmium showed an increase in

the expression levels of two lncRNAs GABPB1-AS1 and LINC00152 (Tani et al., 2014). Zhou et al. (2015) reported aberrant expression profiles of lncRNAs in Cd^{2+}-transformed human bronchial epithelial cells (16HBE) compared to untreated 16HBE cells with lncRNA-ENST00000414355 showing the highest expression out of ten of the most significantly upregulated lncRNA when validated by real time PCR. The authors showed that expression of ENST0000041435 was detected in the blood and urine of workers exposed to cadmium, with a strong positive correlation between found blood ENST0000041435 and urine cadmium. Additionally, expression of ENST00000414355 increased in a dose-dependent manner in the lungs of Cd^{2+}-exposed rats.

1.11 Thesis aims

The urothelium is exposed to urinary-excreted carcinogens from environmental, occupational and dietary sources. These carcinogens include heavy metals such as cadmium; however, cadmium is a weak mutagen suggesting that genetic mechanisms are not responsible for cadmium carcinogenesis. Non-genotoxic carcinogenesis is relatively poorly understood, however recent advances show that epigenetic dysregulation of gene expression may play an important role.

The aim of this thesis was to investigate cadmium carcinogenesis of human urothelial cells and the role that epigenetic dysregulation of gene expression may play.

The working hypothesis is that exposure of the urothelium to cadmium leads to epigenetic dysregulation of gene expression, including down-regulation of tumour suppressor genes, causing field changes within the urothelium characteristic of dysplasia/carcinoma in situ (loss of differentiation), which is the best characterised precursor of invasive carcinomas.

The specific objectives of this thesis were to:

- Determine the effect of cadmium exposure on proliferative and differentiated NHU cells *in vitro*.
- Investigate whether the effects of cadmium can be reversed using two well-characterised epigenetic modifiers (TSA and 5-azacytidine).
- Assess the effect of cadmium on tumour suppressor gene expression.
- Analyse Agilent microarrays to identify gene expression changes that occur when urothelial cells are differentiated in the presence of cadmium and TSA.
- Examine proliferative and differentiated cadmium-treated NHU cell cultures for changes in global levels of post-translational histone modifications.

2 Materials and Methods

2.1 Practical work and collaborations

All practical work was carried out in the Jack Birch Unit for Molecular Carcinogenesis in the Department of Biology at the University of York with the following exceptions. Microarray experiments were carried out in the Genomics Department of the Technology Facility at the University of York. The quantification of post-translational histone modifications by LCMS/MS was carried out in collaboration with Dr Mark Dickman and Tom Minshull from the Department of Chemical and Biological Engineering at the University of Sheffield.

2.2 Suppliers

Commercial suppliers and manufacturers are indicated at the first mention of the reagent or equipment in the text. A complete list of suppliers' names and web addresses is provided in Appendix 1.

2.3 Stock Solutions

Recipes for all stock solutions are listed in Appendix 2. General laboratory solutions were prepared using deionised water (dH_2O). Tissue culture grade solutions were prepared with ultra-pure water from a Purelab Ultra Genetic (Elga) ultra violet water purification unit. Heat stable solutions were sterilised by autoclaving at 121°C (1 bar) for 50 minutes, and other solutions were sterilised by syringe filtration through filters with 0.2µm pore size (VWR).

2.4 Reagents

2.4.1 Antibodies

Primary antibodies used in this study are listed in (Table 2.1). Antibodies were titrated on known positive cell or tissue controls in order to establish the optimal concentration prior to use. Primary antibodies were aliquotted and stored as recommended by the manufacturer. Fluorophore-conjugated secondary antibodies were titrated prior to use and stored in the dark at 4°C (Table 2.2). Representative western blot images for each antibody are shown in Appendix 3.

Table 2.1. Primary Antibodies. Table listing primary antibodies used throughout this study along with their use (WB: western blotting, IF: immunofluorescence, IHC: immunohistochemistry, ChIP: Chromatin Immunoprecipitation). Antibodies used for western blotting also include molecular weight of protein.

Antigen	Host	Supplier	Catalogue Number	Use	Molecular Weight
β-actin	Mouse	Sigma	A5441	WB (1:250000)	42 kDa
CK13	Mouse	Abnova	MAB1864	WB (1:1000) IF (1:500) IHC (1:500)	50 kDa
CK14	Mouse	Serotech	MCA890	WB (1:1000)	50 kDa
CK14	Mouse	ICRF		IF (1:5)	
CK20	Mouse	Cymbus Bioscience Ltd		IF (1:100)	
Claudin 4	Mouse	Zymed	32-9400	WB (1:1000)	22 kDa
Claudin 5	Mouse	Invitrogen	35-2500	WB (1:250)	22-24 kDa
H2AK5ac	Rabbit	Cell Signalling	2576	WB (1:1000)	14 kDa
Histone H3	Rabbit	Abcam	ab1791	WB (1:1000) ChIP: 2.4 µg for each ChIP	17 kDa
H3K4me3	Rabbit	Cell Signalling	9751S	WB (1:1000)	17 kDa
H3K9ac	Rabbit	Cell Signalling	9671	WB (1:1000)	17 kDa
H3K9me2	Rabbit	Diagenode	060-050	WB (1:1000) IF (1:500)	17 kDa
H3K9me2	Mouse	Abcam	ab1220	WB (1:1000)	17 kDa
H3K9me3	Rabbit	Diagenode	056-050	WB (1:1000) IF (1:500) ChIP: 2.4 µg for each ChIP	17 kDa
H3K9/14ac	Rabbit	Diagenode	005-050	WB (1:1000)	17 kDa
H3K18ac	Rabbit	Millipore	07-354-S	WB (1:10000)	17 kDa
H3K23ac	Rabbit	Millipore	07-355-S	WB (1:10000)	17 kDa
H3K27me3	Rabbit	Cell Signalling	9733S	WB (1:1000)	17 kDa
H4K8ac	Rabbit	Cell Signalling	2594	WB (1:1000)	11 kDa
H4K20me3	Rabbit	Diagenode	057-100	WB (1:1000)	11 kDa
p16	Mouse	Santa Cruz	Sc-1661	WB (1:1000)	16 kDa
Rabbit IgG	Goat	Rockland	611131122	ChIP: 2.4 µg for each ChIP	
SOX9	Goat	Santa Cruz	Sc-17341	IF (1:50)	

Table 2.2. Secondary Antibodies.

Antigen	Conjugate	Host	Supplier & Cat. Number	Application
Mouse IgG	Alexa 680	Goat	Life Technologies, A21057	WB (1:10000)
Rabbit IgG	IR Dye 800	Goat	Rockland, 611-132-122	WB (1:10000)
Goat IgG	Alexa 594	Donkey	Life Technologies, A11058	IF (1:500)
Mouse IgG	Alexa 488	Goat	Life Technologies, A11001	IF (1:500)
Mouse IgG	Alexa 594	Goat	Life Technologies, A11005	IF (1:700)
Rabbit IgG	Alexa 488	Goat	Life Technologies, A11008	IF (1:400)
Rabbit IgG	Alexa 594	Goat	Life Technologies, A11012	IF (1:500)

2.4.2 Chemicals and Agonists/Antagonists

Chemicals and agonists/antagonists were reconstituted in sterile H_2O or tissue culture grade dimethyl sulfoxide (DMSO; Sigma) according to the manufacturer's instructions and stored in single use aliquots at -20°C. Prior to use, dilutions were made from the stock solutions into growth medium, for vehicle controls 0.1% DMSO (v/v) was added to medium (Table 2.3).

Table 2.3 Chemicals and Agonists/Antagonists

Compound	Target	Supplier & Catalogue Number	Stock concentration	Effective concentration in medium
PD153035 (PD)	EGFR inhibitor	Calbiochem, 234490	10 mM in DMSO	1 µM
Troglitozone (TZ)	PPARγ agonist	Tocris, 3114	100 mM in DMSO	1 µM
Cadmium chloride ($CdCl_2$)	-	Sigma, 202908	0.1 M in ddH_2O	10 nM - 20 µM
Trichostatin A (TSA)	Histone deacetylase inhibitor	Sigma, T8552	4 mM in DMSO	400 nM
5-Azacytidine (5aza)	DNA methyltransferase inhibitor	Sigma, A1287	500 µM in KSFMc	1 µM

2.5 Cell Culture

2.5.1 General

All tissue culture work was undertaken using aseptic techniques within a class II laminar flow safety cabinet with HEPA filtration (Envair or Medical Air technology). Surfaces were cleaned with 70% (v/v) ethanol before and after use.

Waste media and cells which did not contain cadmium chloride were aspirated by vacuum into a Buchner flask containing 10% (w/v) Virkon® sterilising agent (SLS) for decontamination. Waste medium containing cadmium chloride was aspirated using disposable sterile pipettes (Sarstedt) then put into bottles containing 10% (w/v) Virkon® for decontamination of medium and cells and disposed of via Biology Department internal chemical waste disposal. All used plastic-ware contaminated with cadmium chloride was placed in a double-bagged clinical waste bag for disposal by incineration.

Cultures were maintained in HeraCell 240 incubators (Thermo Scientific) at 37°C in a humidified atmosphere of 5% CO_2 in air. Culture medium was replaced on cell monolayers every 2 to 3 days.

All tissue culture centrifuge steps were carried out in a Sigma benchtop swing-angled centrifuge (Philip Harris) at 250 g for 5 min at ambient temperature.

An inverted Nikon phase-contrast microscope was used for observation of cell cultures. Monochrome images were captured using a Nikon Coolpix 4500 digital camera.

2.5.2 Primary Urothelial Cell Culture

2.5.2.1 Plastic-ware

Primary urothelial cell lines were maintained in Primaria® (Becton Dickinson) or Cell$^+$ (Sarstedt) flasks and dishes. These flasks and dishes have a mixture of negative, positive and nitrogen containing functional groups on the polystyrene surface that help to support the attachment of the primary urothelial cells to the surface.

2.5.2.2 Tissue Specimens

Human urological specimens of urinary bladder, ureter and renal pelvis were obtained from patients with no history of urothelial neoplasia. All specimens were collected following ethical approval from an NHS Research Ethics Committee and with the patient's written informed consent where required. On arrival each tissue sample was allocated an arbitrary laboratory record number (Y-number, e.g. Y1019). Details of tissue samples and subsequent cell lines used in this study are listed in Table 2.4. Specimens were collected in 25 mL plastic universal tubes containing sterile transport medium (Appendix 2) and were stored at 4°C until processed.

Table 2.4. Source and demographics of tissue samples and subsequent NHU cell lines.

Cell line	Surgical Procedure	Origin of Tissue	Donor Age (years)	Donor Sex (M/F)
Y1019	Unknown	Ureter	43	F
Y1054	Unknown	Ureter	57	M
Y1075	Pyeloplasty	Bladder	21	M
Y1141	Pyeloplasty	Renal pelvis	32	M
Y1160	Pyeloplasty	Ureter	25	M
Y1183	Nephrectomy	Ureter	75	M
Y1197	Pyeloplasty	Renal pelvis	73	M
Y1202	Nephrectomy	Ureter	56	F
Y1226	Nephrectomy	Ureter	78	M
Y1233	Nephrectomy	Ureter	81	F
Y1236	Nephrectomy	Ureter	57	M
Y1237	Nephrectomy	Ureter	73	M
Y1244	Pyeloplasty	Renal pelvis	43	M
Y1270	Nephrectomy	Ureter	76	F
Y1279	Pyeloplasty	Renal pelvis	52	F
Y1335	Nephrectomy	Ureter	70	M
Y1357	Nephrectomy	Ureter	38	F
Y1441	Renal transplant	Ureter	57	M
Y1445	Renal transplant	Ureter	79	F
Y1451	Nephrectomy	Ureter	61	F
Y1456	Renal transplant	Ureter	78	F
Y1529	Nephrectomy	Ureter	68	F

2.5.2.3 Isolation and culture of primary human urothelial cells

Primary Normal Human Urothelial (NHU) cell lines were established from urological specimens as previously described (Southgate et al., 1994; Southgate et al., 2002). Samples were removed from the plastic universal tubes by pouring into a clean sterile Petri dish (Nunc) along with the transport medium the sample came in. Unwanted connective and fatty tissue was removed using sterile scissors and forceps. A small representative sample of each specimen was fixed overnight in 10% (v/v) formalin in PBS for routine histology. The remaining tissue was cut into 1 cm^2 pieces and incubated in 10 mL stripper medium (Appendix 2) for 4 hours at 37 °C or 16 hours (overnight) at 4 °C. Sheets of urothelial cells were gently separated from the stroma using forceps, collected by centrifugation and then resuspended in 2 mL (100 U/mL) collagenase type IV (Appendix 2) and incubated for 20 minutes at 37 °C. Cells were collected by centrifugation, counted with a haemocytometer and seeded at a minimum density of 4 $x10^4$ cells/cm^2 in Keratinocyte Serum-Free Medium (KSFM; Invitrogen), supplemented with 5 ng/mL recombinant human epidermal growth factor (rhEGF; Invitrogen), 50 µg/mL bovine pituitary extract (BPE; Invitrogen) and 30 ng/mL cholera toxin (Sigma). This complete medium (KSFMc) was used for all experiments.

2.5.2.4 Subculture of NHU cell lines

NHU cell cultures were passaged when they reached near confluence by incubating cell monolayers in PBS with 0.1% (w/v) EDTA (Sigma) for 5 minutes at 37 °C, until the cells began to round up and dissociated from each other. Cultures were then incubated in a minimal volume (0.3 - 1 mL, dependent on size of dish or flask) 0.25% (w/v) trypsin (Sigma Aldrich) and 0.02% (w/v) EDTA in Hank's balanced salt solution (HBSS; Invitrogen) for 2 minutes at 37 °C. Cells were harvested into 5 mL KSFMc containing 1.5 mg/mL soybean trypsin inhibitor (Sigma). Cells were collected by centrifugation and resuspended into KSFMc before being seeded into fresh sterile dishes or flasks. NHU cells were passaged at split ratios between 1:3 and 1:6. All experiments were performed on NHU cells of passage 2-5.

2.5.2.5 Cryopreservation

NHU cells from one T75 cm^2 flask were harvested as for passaging, collected by centrifugation and resuspended in 6 mL ice-cold KSFMc containing 10% (v/v) FBS

(Seralab) and 10% (v/v) tissue culture grade DMSO, which inhibits the formation of ice crystals during cryopreservation. 1 mL of cell suspension was aliquoted into 1 mL polypropylene cyrovials (Greiner) and transferred to an isopropanol-filled freezing container (Sigma Aldrich) at -80°C. This allowed cells to cool at a rate of approximately 1°C per minute. Cells were kept at -80°C overnight and transferred to a liquid nitrogen-containing storage dewar at -196°C. Cells were recovered by rapid thawing in a 37°C water bath. Cells were then diluted with 5 mL pre-warmed KSFMc, centrifuged and resuspended in KSFMc and plated at the required density. Medium was changed after 24 hours to remove any unattached cells.

2.5.3 *In vitro* differentiation of NHU cell cultures

Differentiation of NHU cell cultures was induced by two established methods:

1) pharmacological activation of peroxisome proliferator-activated receptor gamma (PPARγ) by the PPARγ agonist, troglitazone, and concurrent inhibition of the EGFR autocrine signalling loop, through the use of an EGFR tyrosine kinase inhibitor, PD153035 (Varley et al., 2004)
2) a 'biomimetic model' that involves subculture of NHU cell cultures in medium containing adult bovine serum and a near physiological calcium concentration of 2 mM (ABS/Ca^{2+}) (Cross et al., 2005).

2.5.3.1 Pharmacological Differentiation

Troglitazone (TZ) (Sigma Aldrich) was solubilised in tissue grade DMSO (Sigma), to a final molarity of 100 mM. PD153035 (PD) (Calbiochem) was solubilised in DMSO, to a final molarity of 10 mM.

NHU cells were cultured to 80% confluence in KSFMc. For differentiation, medium was replaced with KSFMc containing 1 μM TZ and 1 μM PD diluted in DMSO totaling 0.1% of the medium volume. For control experiments performed without the presence of TZ and PD, KSFMc with 0.1% DMSO (v/v) was added as a vehicle control. After 24 h, medium was replenished with KSFMc containing 1 μM PD for differentiation-induced cells, or with 0.1% (v/v) DMSO for control cells. Cells were cultured up to 7 days with medium replaced every 2-3 days.

2.5.3.2 Biomimetic Differentiation

NHU cells were cultured to 80% confluence in KSFMc. Medium was then replaced with KSFMc supplemented with 5% (v/v) adult bovine serum (ABS, Seralab). Cells were cultured in 5% ABS for five days with media changed after 2/3 days. Cells were harvested and then either seeded into more flasks or onto Snapwell™ culture inserts (Fisher Scientific) or ThinCert 0.4 micron transparent inserts (Greiner Bio-One) for electrophysiological studies. Cells were seeded at $5x10^5$ cells per insert in 500 µL volume and 3 mL culture medium placed into the basal chamber. After 24 hours the exogenous calcium concentration was increased to 2 mM using a 1M $CaCl_2$ stock. Cell cultures were then maintained in medium containing 5% ABS and 2 mM Ca^{2+} with medium being replaced every 2-3 days.

2.5.4 Treatment of NHU cell cultures with Cadmium Chloride, TSA and 5-azacytidine

Cadmium chloride was solubilised in ddH_2O then sterilised by syringe filtration through filters with 0.2µm pore size (VWR), TSA was reconstituted in tissue grade dimethyl sulfoxide (DMSO, Sigma) and 5-azacytidine was solubilised in KSFMc.

5-azacytidine and TSA treatments were applied to NHU cell cultures at the same time point as TZ/PD treatments, with TSA being added to stock concentrations of TZ and PD in DMSO to give a final concentration of 0.1% DMSO in growth medium.

2.5.5 Proliferation Assay

An alamarBlue® assay quantitatively measures proliferation by using a fluorometric growth indicator based on mitochondrial enzyme activity. NHU cells were seeded at a concentration of $2x10^4$ cells mL^{-1} in to 96-well plates, treated with cadmium chloride concentrations and underwent alamarBlue® assays at 1, 3, 5, 7 and 9 days post cadmium treatment. alamarBlue® solution was diluted 1:10 with KSFMc and then incubated with the cells for four hours at 37°c. Absorbance was measured at 570 and 630nm. Results were normalised against no cell controls and the percentage reduction in alamarBlue® calculated.

2.5.6 Population Doublings

Cell counts were performed using an “Improved Neubauer” haemocytometer (VWR) by placing 10 µL of cell suspension under each side of the coverslip on to a

haemocytometer. Cells were counted in four grids and the average cell number was equivalent to the cell density in $1x10^{-4}$ mL of medium. Once cells were counted they were seeded onto Primaria® flasks. When cultures reached 80% confluence cells were passaged, counted and then seeded onto new Primaria® flasks. Number of populations doublings equals $\log_2$ (CMF), where CMF (cell multiplication factor) equals the final cell number divided by the initial cell number.

2.5.7 Fixation of cultured cells in formaldehyde for ChIP experiments

Cells were cultured in 10 cm Primaria® dishes and treated with 10 mL medium containing required compounds. Dishes were placed on an orbital shaker and 189 µL of 37% (w/v) formaldehyde added drop-wise directly to the medium to a final concentration of 1%. After 10 min, cross-linking was quenched by addition of 798 µL 125 mM glycine to a final concentration of 12.5 mM, followed by incubation at ambient temperature for 5 min. Cells were rinsed and scrape harvested in PBS and then transferred to 15 mL centrifuge tubes. Cells were pelleted by centrifugation at 800 g for 5 min, and the supernatants thoroughly aspirated and cell pellets stored at -80°C until use.

2.5.8 Measurements of transepithelial electrical resistance (TER)

TER can be used as an indicator of barrier function by cultured epithelial cells. Differentiation was induced using the "biomimetic" protocol as described above (section 2.5.3.2). The barrier function of cultured urothelium established on Snapwell™ or Griener membranes was monitored over 6-9 days using an EVOM™ Epithelial Voltohmmeter (World Precision Instruments) under sterile conditions.

2.5.9 Scratch-wounding

Differentiated NHU cell cultures grown on Snapwell™ or Griener membranes were scratched with a P10 pipette tip. Barrier recovery was monitored by measuring transepithelial electrical resistance.

2.5.10 Dispase (II) lifting of differentiated cell sheets

To conserve differentiated sheets for histological analysis, culture medium was removed from the Snapwell™ or Greiner inserts, before cell cultures were washed twice with 1x Dulbecco's phosphate-buffered saline (DPBS) (without Mg^{2+} and Ca^{2+} ions; Gibco) heated to 37 °C. Wells were flooded with 2% dispase II (Sigma) and

incubated at 37 °C for 30-60 minutes, until intact sheets were detached and able to be lifted from the membrane. Differentiated sheets were collected in a Cellsafe Capsule (Cell Path), before being fixed in 10% (v/v) formalin in PBS overnight. After overnight fixation, samples were placed in 70% (v/v) ethanol until embedding took place.

2.6 Western Blotting

2.6.1 Protein Extraction

Culture medium was aspirated and cells were washed twice with cold PBS before aspirating PBS. Cells were scrape-harvested in 100 µL 2% (w/v) SDS sample buffer containing protease inhibitors (Appendix 2) and transferred to a cold 1.5 mL micro-centrifuge tube. Lysates were sonicated on ice for two ten-second bursts with a ten second rest between bursts, using a Branson Sonifier set to 25 W, 40% amplitude. Whole cell lysates were left to chill on ice for 30 minutes before centrifuging at 18,000 g for 30 minutes in a centrifuged chilled to 4 °C. Supernatant was collected, aliquoted and stored at -80 °C until use.

2.6.2 Protein Quantification

Total protein concentration of each sample was determined using a Coomassie® protein assay reagent kit (Pierce), which is based on the Bradford colorimetric assay. Samples were diluted 1:12.5 in dH_2O. 10 µL of each sample was aliquoted in duplicate into a 96-well plate with 200 µL Coomassie reagent. The absorbance of samples was measured at test and reference wavelengths of 570 and 630nm, respectively using a MRX II 96-well plate spectrophotometer (Dynex). Samples were measured alongside bovine serum albumin (BSA) (Pierce) diluted to concentrations ranging from 0 to 1000 µg/mL in dH_2O. The Revelation software package (Dynex) was used to plot the BSA standard curve and calculate the R^2 value. The average of duplicate absorbance readings from each sample was used to estimate the protein concentration by comparison with the BSA standard curve.

2.6.3 SDS-Polyacrylamide Gel Electrophoresis

Protein samples were mixed with 4x LDS (Lithium Dodecyl Sulfate) (Life Technologies) and 10x reducing agent (Life Technologies). Reagents were diluted to a final concentration of 1x with dH_2O into volumes suitable to fit into wells (10-well

gels have a 40 µL maximum limit per well and 15-well gels have a 26 µL maximum per well), and then heated at 70 °C for ten minutes.

Proteins were resolved by electrophoresis through 1 mm thick 10 or 15 well 4-12% Bis-Tris NuPAGE pre-cast polyacrylamide gels using the Novex system (Invitrogen). The gel and wells were rinsed in dH_2O and assembled in to the Novex tank according to the manufacturer's instructions. 5 µL of All-Blue pre-stained marker (BioRad) was run as a protein size marker. Bis-Tris gels were run in either 1x MES buffer or 1x MOPS buffer (Life Technologies). 500 µL antioxidant (Life Technologies) was added to the inner chamber of the tank during electrophoresis, which was carried out at 200 V for 50 minutes, or until the running buffer reached the foot of the gel.

2.6.4 Western blotting using LI-COR Odyssey

Polyvinyldifluoride (PVDF) sheets (Millipore) were cut to size and dipped in methanol to wet, rinsed in H_2O and equilibrated in transfer buffer (Appendix 2) for 10 min. Protein was transferred to PVDF by semi-dry transfer between fibre blotting pads (Life Sciences, E-PAGE Blotting Pads) and filter paper (Whatman Grade 1, 150 mM) at 30 V for 2 h, keeping the tank on ice. PVDF membrane was rinsed in Tris buffered saline (TBS) (pH 7.4). Transferred protein was visualised by reversible staining with 42 mM Ponceau red in 3 % (v/v) trichloroacetic acid, and washed off in dH_2O.

To block free protein-binding sites and minimise non-specific binding, membranes were incubated in Odyssey blocking buffer (LI-COR) diluted 1:1 (v/v) with TBS for 1 hour at ambient temperature on an orbital shaker. Odyssey blocking buffer is also optimised to reduce autofluorescence of the membranes at detection wavelengths of the LI-COR scanner system. Membranes were probed with primary antibody diluted in blocking buffer and TBS-0.1% Tween 20 for 16 hours at 4 °C with shaking. 0.1% (w/v) NaN_3 was included in the primary antibody solutions as a preservative. Membranes were washed four times with TBS-0.1% Tween 20 (Appendix 2) and were then probed with secondary antibody, diluted in blocking buffer and TBS-0.1% Tween 20, for one hour at ambient temperature with shaking. Membranes were washed four times for five minutes in TBS-0.1% Tween before one wash in TBS.

Membranes were scanned on the LI-COR Odyssey scanner (Odyssey CLx Scanner, LICOR). The LICOR uses laser excitation at 685 and 785 nm to stimulate emission from the Alexa-conjugated secondary antibodies and a scan-head with 700 and 800 nm filters to detect their respective emissions. Scans were analysed using Odyssey v1.1 software (LI-COR). Band intensities were measured using the Odyssey software by drawing boxes around the protein band to calculate densitometry following background subtraction.

2.6.5 Recycling western blot membranes

Membranes were stripped to allow re-probing. Membranes were stripped by incubating in high pH Western Blot Recycling Kit reagent (Source Bioscience Autogen) for 30 minutes at ambient temperature on an orbital shaker. After stripping, secondary antibody was applied and membrane scanned as above to confirm removal of primary antibodies. Membranes were then washed in TBS, re-blocked and re-probed as in section 2.6.4 above.

2.7 Immunofluorescence labelling

2.7.1 Slide Preparation

12–well slides (CA Hendley) were wiped with 70% (v/v) ethanol, placed into a metal rack in a pipette box and autoclaved to sterilise. Slides were placed in to individual chambers of Heraeus boxes (Greiner) using sterile forceps. Cells were seeded in 50 µL droplets at $1x10^5$ cells mL^{-1} for proliferative studies or $3x10^5$ cells mL^{-1} for differentiation studies. Cells were left to attach for four hours at 37 °C, before the chambers of the Heraeus box were flooded with 5 mL of medium. Cells were treated the following day (as indicated for each experiment) with medium replaced every 2-3 days. At the desired time point cells were washed in PBS and fixed. Slides were fixed in methanol:acetone in a 1:1 mixture for 30 seconds before being air-dried and stored in cling film desiccated at -20 °C until use.

2.7.2 Immunolabelling

Primary antibodies were diluted in TBS containing 0.1% (w/v) BSA and 0.1% (w/v) NaN_3, pH 7.6. In order to contain the antibodies within individual wells, wells were surrounded by liquid repellent grease (Dako Pen, Dako). 20 µL of primary antibody solution or TBS (negative control) was added to each well. Cells were incubated with

antibodies overnight at 4 °C and then slides were washed three times with PBS on an orbital shaker. From this point slides were protected from UV light using aluminium foil in order to protect the fluorophores. 20 µL of appropriate secondary antibody diluted in TBS containing 0.1% (w/v) BSA and 0.1% (w/v) NaN_3, pH 7.6, was applied to each well for one hour at ambient temperature. Slides were then washed with PBS containing 0.25% (w/v) Tween 20 for 5 minutes on an orbital shaker. Nuclei were stained by incubation with Hoechst 33258, diluted to 0.1 µg/mL in PBS, for 5 minutes at ambient temperature. Slides were washed once in PBS and then rinsed in distilled water. Slides were mounted in antifade solution (appendix 2) and sealed under glass coverslips using nail varnish.

2.7.3 Fluorescence microscopy

Labelled immunofluorescence slides were viewed under epifluorescence illumination using an Olympus BX60 microscope with x20, x40 and x60 oil immersion objectives. The microscope was equipped with appropriate excitation and emission filters for bisbenzimide (blue), and dual and specific filters for FITC (green) and Texas Red (red). Images were captured using an Olympus DP50 digital camera and Image- Pro® Plus software.

2.7.4 Quantification using TissueQuest

TissueQuest (TissueGnostics) is analysis software for cells and stained areas in samples stained with immunofluorescent markers. TissueQuest software was used to quantify CK13, CK14 and CK20 protein expression from immunofluorescence microscopy images acquired as described in section 1.7.3. Samples were only comparable if labelled at the same time and if TissueQuest settings were unaltered after initial optimisation.

Hoechst 33258 labelling of nuclei was used as a master marker for cell identification. Furthermore, the average nuclear size, discrimination area, discrimination grey value and background threshold for the master marker was specified. Immunolabelling intensity was quantified using the appropriate cellular mask parameter. Masks projecting from identified cell nuclei were adjusted using the scale settings until cell boundaries were clearly identified. Labelling within the masks was quantified and data was displayed as dot plot scattergrams indicating arbitrary fluorescence intensity values. In order to differentiate between positive and negative cells, cut-offs based on

visual assessment were set in the dot plots. The percentage of positively labelled cells was then determined.

2.8 Histology

2.8.1 Tissue embedding and sections

Tissue samples were fixed overnight in 10% (v/v) formalin in PBS and transferred to 70% (v/v) ethanol until required. Samples were encased in embedding cassettes and submerged in fresh 70% ethanol for 10 minutes on an orbital shaker. This was followed by three changes in absolute ethanol, two changes in propan-2-ol and four changes in xylene for 10 minutes each. Samples were transferred to molten paraffin wax (Thermo) at 60 °C for 15 minutes, followed by three further 15 minute incubations in fresh wax. Tissue samples were orientated within a metal mould, embedded in wax and allowed to solidify on a cold table (RA Lamb). 5 μm sections were cut using a Leica RM2135 rotary microtome and collected onto electrostatically charged Super Frost Plus™ microscope slides (BDH). Sections were allowed to dry and then baked on a hot plate (RA Lamb) at 50 °C for one hour then stored at ambient temperature until use.

2.8.2 *In vitro* cell sheets

Formalin fixed differentiated cell sheets lifted by dispase (II) (section 2.5.10) were submerged in fresh 70% (v/v) ethanol for 5 minutes on an orbital shaker. Samples were then sequentially submerged in absolute ethanol (x3), propan-2-ol (x2) for 5 minutes each. The alcohol was removed from cell sheets with xylene (4 washes of 5 minutes each). Cell sheets were then transferred to molten paraffin wax (Thermo) at 60 °C for 10 minutes, followed by three further 10 minute incubations in fresh wax. Cell sheets were then orientated, embedded in wax and cut as previously described in section 2.8.1.

2.8.3 Haematoxylin and eosin staining

Sections were de-waxed with two 10 minute washes in xylene followed by two one minute washes in xylene then rehydrated by three one minute washes in absolute ethanol and one minute wash in 70% (v/v) ethanol. Sections were then washed for one minute under running tap water before staining in haematoxylin for two minutes. Slides were washed in running water for one minute before a one minute wash in

Scott's tap water followed by another wash in running water for one minute. Sections were stained in eosin for 30 seconds before being washed in running water for one minute. Sections were dehydrated with a one minute wash in 70% (v/v) ethanol followed by three one minute washes in absolute ethanol and two one minute washes in xylene. Slides were mounted with DPX (Cell Path) and sealed under glass coverslips.

2.9 Immunohistochemistry

Immunolabelling was performed using an indirect streptavidin 'ABC' immunoperoxidase method. A CK7 positive control and negative control, where TBS was substituted for primary antibody, were used in every experiment.

2.9.1 Dewaxing tissue sections

Paraffin wax-embedded sections were de-waxed with two 10 minute washes in xylene, followed by two one minute xylene washes. Sections were rehydrated by three one minute washes in absolute ethanol, a one minute wash in 70% (v/v) ethanol and a one minute wash under running tap water.

2.9.2 Antigen retrieval

Antigen retrieval was performed to restore the immunoreactivity of antigens masked by tissue processing. The method of antigen retrieval used in this study was trypsinisation followed by citric acid heat retrieval. Trypsinisation was performed by incubating sections in 100 mL of 0.1% (w/v) trypsin (Sigma) in 0.1% (w/v) $CaCl_2$. pH 7.8, for 1 minute at 37 °C. This was followed by citric acid heat retrieval where slides were microwaved in a Pyrex dish containing 10 mM citric acid buffer, pH 6.0 (appendix 2). The dish was covered with punctured Clingfilm, microwaved on full power for 13 minutes and then rapidly cooled on ice. Following antigen retrieval slides were washed under running tap water.

2.9.3 Blocking of endogenous sites

Slides were placed in Shandon Sequenza units (Thermo) and washed once with TBS (appendix 2). Endogenous avidin sites were blocked with 100 µL of avidin followed by 100 µL biotin from the blocking kit (Vector Labs). Sections were incubated for 10 minutes at ambient temperature for each blocking step with two TBS washes after each step. Non-specifc antibody binding was eliminated by blocking each section

with 100 µL of normal rabbit serum (10% (v/v) in TBS for 5 minutes at ambient temperature.

2.9.4 Steptavidin 'ABC' Immunoperxidase method

100 µL of CK13 primary antibody, or CK7 primary antibody (positive control) or TBS (negative control) was applied to the slides and incubated at 4 °C overnight. Primary antibody was washed off with three washes of TBS. 100 µL of biotinylated secondary antibody was applied to each slide for 30 minutes at ambient temperature, followed by two washes with TBS. 100 µL steptavidin-biotin HRP complex (Vector Labs), prepared according to the manufacturer's instructions, was applied to each slide and incubated for 30 minutes at ambient temperature. Slides were then washed twice with TBS and once with distilled water. Bound antibody was visualised using a Diaminobenzidine (DAB) substrate prepared using Sigma Fast DAB tablets dissolved in 5ml dH_2O. Slides were incubated with 200 µL DAB solution for a maximum of 15 minutes before being washed twice with distilled water.

2.9.5 Dehydration and mounting of sections

Slides were removed from the Shandon Sequenza units and placed into staining racks. Slides were counterstained for 5-10 seconds with haematoxylin and washed under running tap water. Sections were dehydrated through 70% and absolute ethanol and four changes of xylene. Slides were mounted in DPX (Cell Path) and sealed under glass coverslips.

2.9.6 Quantification using HistoQuest

Images of whole tissue sections were captured using an AxioScan.Z1 slide scanner (Zeiss) and Zen 2012 blue edition software (Zeiss). Images were stored as .czi files and opened using HistoQuest software (TissueGnostics) in order to quantify CK13 expression on differentiated cell sheets treated with or without cadmium. HistoQuest is brightfield image analysis software for the FACS-like analysis of samples stained with immunohistochemical or other stains.

Haematoxylin staining was used as a master marker for cell identification on the basis of nuclear detection. Furthermore, the average nuclear size, discrimination area, discrimination grey value and background threshold for the master marker was specified. DAB intensity was quantified using the inside and outside cellular mask

parameter to produce scattergrams displaying arbitrary intensity values. In order to differentiate between positive and negative cells, cut-offs based on visual assessment were set. The percentage of positively labelled cells was then determined.

2.10 Analysis of Gene Expression

2.10.1 General

For RNA work, all solutions were made with ultra pure dH_2O treated with 0.1% (v/v) diethyl pyrocarbonate (DEPC) at ambient temperature overnight. 13 mL polypropylene tubes and caps (Starstedt) were also incubated overnight with 0.1% (v/v) DEPC to inhibit RNase activity. DEPC was then destroyed by autoclaving. RNase/DNase free microfuge tubes and pipette tips (Axygen) were used for all RNA experiments. RNase Zap (Ambion) was used to clean the bench and pipettes before use.

2.10.2 RNA Extraction

Culture medium was aspirated from cell cultures. Trizol™ solution was added to 25 cm^2 flasks (2.5 mL) or Snapwell membranes (1 ml per Snapwell) and left to incubate on a rocking platform for 5 min before scrape-harvesting and transferring to a DEPC-treated 13 mL centrifuge tube. At this point samples can be stored at -80 °C until further processing. Lysates were thawed on ice then left at ambient temperature for five minutes to allow complete dissociation of nucleoprotein complexes. 0.2 mL chloroform was added per millilitre of Trizol reagent. Lysates were vortexed for 15 seconds and incubated at ambient temperature for two minutes, followed by centrifugation at 12,000 g for 15 minutes at 4 °C. Centrifugation was performed in a Sorvall RC-5 using rotor SM-24. The upper aqueous phase, containing the mRNA, was collected and transferred to a fresh DEPC-treated centrifuge tube. RNA was precipitated by the addition of 0.5 mL propan-2-ol per millilitre of Trizol and incubated at ambient temperature for 10 minutes. RNA was centrifuged at 12,000 g for 20 minutes at 4 °C. Following centrifugation the supernatant was discarded. The RNA pellet was washed with 75% (v/v) ethanol and centrifuged at 7500 g for 10 minutes at 4 °C. Ethanol was removed and pellets air-dried. Pellets were resuspended in 30 µL nuclease free DEPC treated ddH_2O then stored at -80 °C.

2.10.3 DNase Treatment

RNA samples were treated with the DNA-easy kit (Ambion) to remove any DNA contamination. 3 µL DNase 1 Buffer was added to RNA followed by 1 µL rDNase 1 (2 U/µL). After mixing by pipetting the sample was incubated for 30 minutes at 37 °C. DNase Inactivation Reagent was resuspended by vortexing to tube to form a slurry, 3.3 µL was then added to each sample to terminate the digestion. Samples were incubated at ambient temperature for two minutes then centrifuged for 90 seconds at 10,000g. RNA contained in the aqueous phase was collected and placed into a new microfuge tube then 1 µL (40 U/µL) of RNaseOUT (Life Technologies) was mixed into samples to prevent degradation of RNA by RNases.

2.10.4 Quantification of RNA

RNA was quantified by UV spectrophotometry. Samples were measured directly using a Nanodrop ND-1000 Spectrophotometer. Optical densities (ODs) were measured at 260 and 280nm and concentration calculated from the Nanodrop software. Sample purity was derived from the OD_{260}/OD_{280} ratio, which is 2.0 for pure preparations of RNA.

2.10.5 cDNA synthesis with Random Hexamers

DNA-free RNA was reverse transcribed using Invitrogen's SuperScript® II First-Strand Synthesis Kit and 50 ng random hexamers primers. 1 µg of DNase treated RNA was mixed with 1 µL (50 ng/µL) random hexamers and nuclease-free H_2O in a final volume of 12 µL. Samples were incubated at 65°C to anneal primers to RNA. To each sample the following volumes of reagents from the kit were added: 4 µL 5x First-Strand Buffer, 2 µL 0.1 M DTT and 1 µL dNTP mix (10 mM each). Samples were incubated at 25°C for two minutes. As a control for the presence of contaminating DNA, two of each sample was prepared and at this stage one sample was mixed with 1 µL (50 U/µL) of Superscript II reverse transcriptase, and the other with 1 µL nuclease-free H_2O. Samples were incubated at 25 °C for ten minutes followed by 42 °C for 50 minutes and then heated at 70 °C for 15 minutes in order to inactivate the enzyme. cDNA samples were then used neat for RT-PCR reactions or diluted 1in 5 for RTQPCR.

2.10.6 Primer Design

Primers were designed against target regions using the NCBI primer-BLAST tool (http://www.ncbi.nlm.nih.gov/tools/primer-blast/). Primers used for SYBR-green QPCR were designed using Primer express Software v.3 (Applied Biosystems) using recommended optimal parameters. The top ranked primers were checked for specificity using the NCBI primer-BLAST search facility. Primers were ordered from MWG Eurofins and stock made in nuclease free ddH_2O. Primer sequences used in this thesis are detailed in Table 2.5.

Table 2.5. Primers used for RTPCR and RTQPCR in this study. Primers for SYBR-green QPCR were designed to have an amplicon length between 50 and 125 bases.

Gene	Primer Sequence (5'-3')	Amplicon Length
APC	For – GGCTTCTTCTGGACAGATTGATTT Rev - ATCCTTCCCGGCTTCCATA	125
ELF3	For – GTTCATCCGGGACATCCTC Rev - GCTCAGCTTCTCGTAGGTC	160
FOXA1	For - CAAGAGTTGCTTGACCGAAAGTT Rev - TGTTCCCAGGGCCATCTGT	75
GAPDH	For – ACCCAGAAGACTGTGGATGG Rev - TTCTAGACGGCAGGTCAGGT	201
GAPDH (QPCR)	For - CAAGGTCATCCATGACAACTTTG Rev - GGGCCATCCACAGTCTTCTG	90
GATA3	For – TCCAGACACATGTCCTCCCT Rev - TGGTGTGGTCCAAAGGACAG	113
GRHL3	For – GTGACAAGGGAGCTGAGAGG Rev - CAGTCTCTGGCCGAAGGTAG	153
IRF1	For – TGCATTTATTTATACAGTGCCTTGCT Rev - CCCTCCCTGGGCCTGTT	79
KDM3A	For – CTGTCAAAGGTGTTCGAGAAATGT Rev - CACCCAGTGCAGGTTGAAGA	65
KDM3B	For – CCCAACTTTCTTGACCACATCA Rev - CCCGCTTTGAAGCATCTGA	70
KDM4A	For – CCCAGGAAGTGCTCAAAGCT Rev - GGGAAATCAGGGTCATCTTGTG	59

Gene	Primer Sequence (5'-3')	Amplicon Length
KDM4B	For – CCCTCCAAAAGCCGTCAGA Rev - GCCAGAGGTGAAGCACATCTC	60
KDM4C	For – GGCTATGAGAAGCCCGAGAA Rev - CAGGTGACTTTGGCCATGAA	58
KDM4E	For – GCCAACTGTTCAGCCTGCAT Rev - TTGAGCTCTACTCCTTGTACCCATT	61
KDM7A	For – GTGATGGATGTGGAACGTTATGTAG Rev - TGCCTCGCCACATCAATG	65
KDM7B/PHF2	For – CAAGCGGGTCCTCAACGT Rev - CCACGAAGCTGGACATTCG	62
KDM7C/PHF8	For – GGCTCCATTCCCCTAACCA Rev - GACAGCCTGGACATGGACACT	59
KLF5	For – GACACCTCAGCTTCCTCCAG Rev - ACTCTGGTGGCTGAAAATGG	232
KRT13	For – CTGATGTCCGTAGGCCTTAAATCT Rev - GGGAACTGCCGGCTCTCT	83
KRT14	For - CGGCCTGCTGAGATCAAAGA Rev - ATCTGCAGAAGGACATTGGCA	107
KRT20	For – CAAAAAGGAGCATCAGGAGGAA Rev - CAACCTCCACATTGACAGTGTTG	71
NR3C1	For – GAGGAGGAGCTACTGTGAAGGTTT Rev - TTCGCTGCTTGGAGTCTGATT	78
P16INK4A	For - GCGGAAGGTCCCTCAGACA Rev - TGATCTAAGTTTCCCGAGGTTTCTC	73
RASSF1A	For - ACAAGGGCACGTGAAGTCATT Rev - GCTCAGCGCGCTCAAAG	91
SOX9	For – AGCGACGTCATCTCCAACATC Rev - GTTGGGCGGCAGGTACTG	66
UPK1A	For – CATTCTTGCTGAACCGTTTGTG Rev - GTGACCGTGACAGAACTCTCATG	77
UPK2	For - CAGTGCCTCACCTTCCAACA Rev - TGGTAAAATGGGAGGAAAGTCAA	77

2.10.7 Polymerase Chain Reaction

PCR was performed using a T100 thermal cycler (BioRad) and the GoTaq® reagent kit (Promega). PCR reactions were made to total volumes of 20 µL, with 8.5 µL ddH_2O, 4 µL GoTaq® buffer, 0.4 µL dNTPs (10 mM), 2 µL $MgCl_2$ (25 mM), 2 µL forward primer (10 µM), 2 µL reverse primer (10 µM). 0.1 µL GoTaq® polymerase and 1 µL test cDNA or ddH2O (negative control) or genomic DNA (positive control). DNA underwent a two minute initial denaturation step at 95° C, followed by 25-35 cycles of denaturation for 30 seconds at 95 °C, annealing for 30 seconds at 50-65 °C (depending on optimal temperature for primers) and 1 min/Kb DNA at 72 °C for extension. A final extension stage of five minutes at 72 °C was followed by incubation at 4 °C.

2.10.8 Gel Electrophoresis

DNA was visualised under UV light after separation by gel electrophoresis. Electrophoresis grade agarose was boiled in 1x Tris-Borate-EDTA (TBE) buffer (Appendix 2) and cooled to 50 °C before adding 1/10,000 (v/v) GelRed (Cambridge Bioscience), which fluoresces under UV light when it intercalates with double stranded DNA. Gels were cast and then allowed to set before PCR products and Hyperladder I or IV (Bioline) were electrophoresed on the gel submerged in 1x TBE at 80V for 30 minutes. Gel images were captured digitally using a Gene Genius Gel Imaging System (Syngene) with GeneSnap software.

2.10.9 SYBR® Green Quantitative PCR

Quantitative polymerase chain reaction (QPCR) is a powerful method that enables the accumulation of PCR products to be measured over time. The binding of SYBR® Green I Dye to double-stranded DNA emits a fluorescent signal. The increase in fluorescence over time is proportional to the accumulation of PCR products. Fast SYBR® Green Master Mix (Applied Biosystems) containing the SYBR® Green I Dye, AmpliTaq® Fast DNA Polymerase, dNTPs, Uracil-DNA Glycosylase and a passive internal reference (ROX) was used. 5 µL of cDNA was mixed with 10 µL of the 2x Fast SYBR® Green Master Mix, 3.8 µL ddH_2O and 0.6 µL each of the forward and reverse primers (10 mM) in the wells of a optical 96-well plate (Applied Biosystems). Each cDNA sample was amplified by QPCR in triplicate wells and negative control samples (where the reverse transcriptase was omitted during cDNA

synthesis) were included. The plates were sealed with optical adhesive covers (Applied Biosystems) and briefly centrifuged. Plates were run on a StepOnePlus™ Real-Time PCR System (Applied Biosystems) and analysed with StepOne™ Software. The thermal profile used was: incubation at 95 °C for 20 seconds, followed by 40 cycles of denaturation at 95 °C for 3 seconds and elongation at 60 °C for 30 seconds.

During each cycle the fluorescence of the SYBR® Green I Dye was detected for every well. This fluorescence signal was normalised against the fluorophore ROX (yielding the normalised reporter value) to account for any changes in plate fluorescence that were unrelated to product amplification.

A final stage was included to establish the melting profiles of the products and give dissociation curves. This involved incubation for 15 seconds at 95 °C, 60 °C and finally 95 °C to ensure only one product was produced. Dissociation curves confirmed both the presence of a single amplification product and the absence of primer dimers for each primer set (example shown in Figure 2.1).

Amplification plots were generated by the StepOne™ Software. Threshold values were set in the region of exponential amplification across all of the plots. Threshold cycle (Ct) values were obtained as the cycle at which the fluorescence generated within a reaction crosses the threshold value. QPCR results were expressed as relative quantification (RQ) (relative expression/fold change). This is calculated using the following calculations:

Sample values were calculated relative to GAPDH to give ΔCt:

$$\Delta Ct = Ct\ target - Ct\ GAPDH$$

This was then calibrated to the control/calibrator sample to give ΔΔCt:

$$\Delta\Delta Ct = Ct\ test\ sample - Ct\ control/calibrator\ samples$$

Relative quantification was then calculated using:

$$RQ = 2^{\Delta\Delta Ct}$$

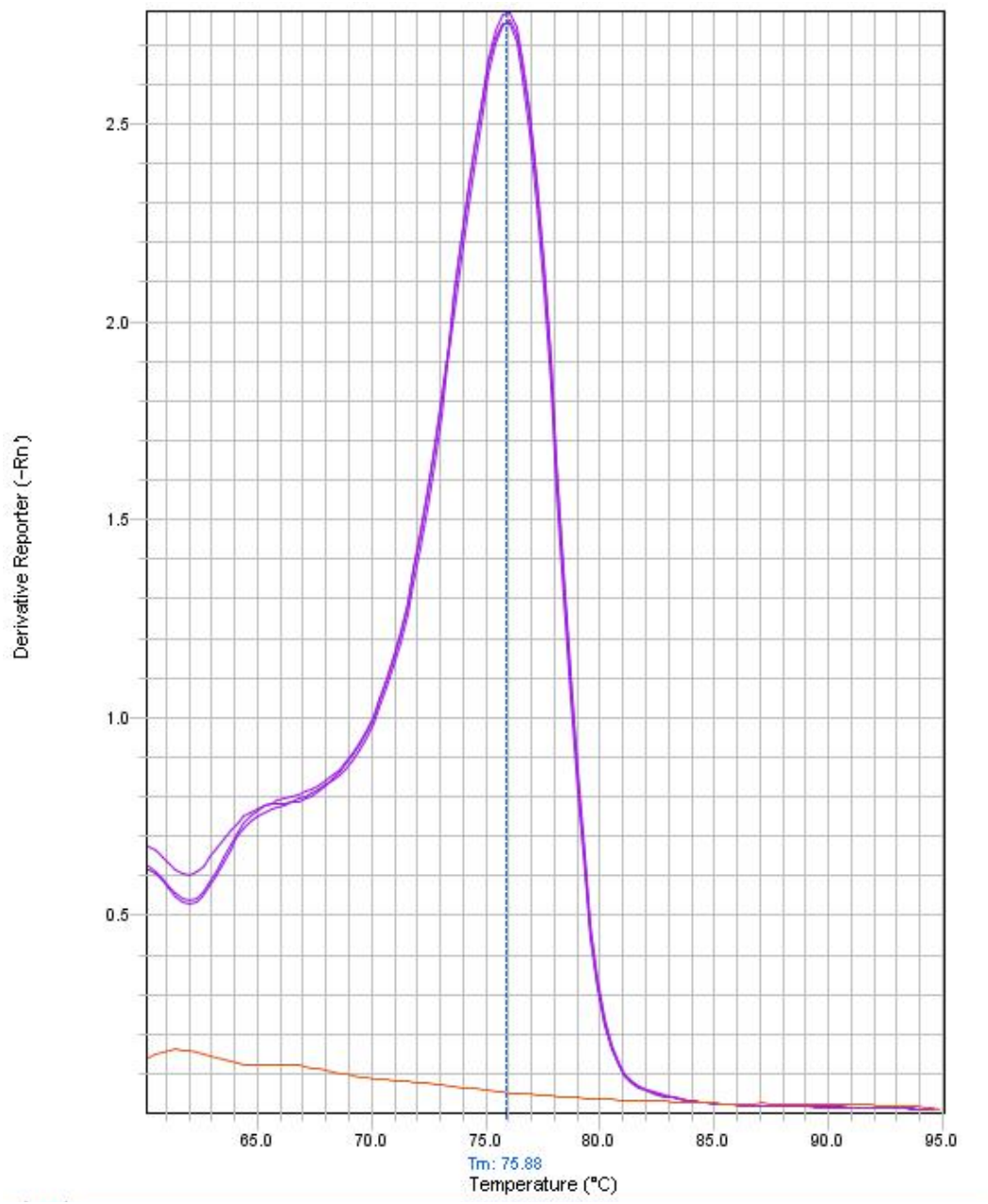

Figure 2.1. An example dissociation curve. Dissociation plot showing the change in fluorescence against temperature. Replicate cDNA samples are shown in purple and the corresponding negative control sample is shown in red. Note the presence of one peak, representing the dissociation curve of a product in each of the cDNA samples and the absence of product in the negative control. Also note the absence of primer dimers.

2.10.10 Microarrays

Two independent NHU cell lines (Y1441 and Y1451) were treated ± TZPD ± 10 μM CdCl2 ± 400 nM TSA for 3 days. RNA was extracted from the 8 treated NHU cell cultures as described in section 2.10.2, followed by DNase treatment (section 2.10.3). RNA was quantified using a ND-1000 Spectrophotometer (section 2.10.4) and 1 ug of RNA was synthesised into cDNA using random hexamers (section 2.10.5) in order to perform RTQPCR (section 2.10.9) to determine that the cadmium and TSA treatment had been successful prior to microarrays being perfomed.

Gene expression analysis was performed using Agilent SurePrint G3 Human Microarrays. Microarrays were carried out by the Genomics Department of the Bioscience Technology Facility at the University of York. Normalisation and fold change calculations were carried out by the Bioscience Technology Facility's Bioinformatics Laboratory using GeneSpring software (Agilent). Normalised intensity values and fold change data was supplied in the form of Excel spreadsheets.

2.10.11 Gene ontology and promoter analysis

Gene ontology enrichment analysis was performed using the PANTHER Classification System (http://pantherdb.org/) as described by Mi et al. (2013). Enrichment analysis finds which GO terms are over-represented (or under-represented) using annotations for that gene set.

Promoter analysis for the four differentiation genes (UPK1A, UPK2, KRT13 and KRT20) was carried out using the PSCAN promoter analysis tool, which was run against the JASPAR database of transcription factor binding profiles (http://159.149.160.51/pscan/) as described by Zambelli et al. (2009).

2.11 Chromatin Immunoprecipitation-(Q)PCR

Chromatin Immunoprecipitation (ChIP-QPCR) involves immunoprecipitation of formaldehyde fixed chromatin-DNA complexes followed by quantitative PCR (Figure 2.2). Cross-linked cell samples were subjected to hypotonic lysis and sonication to fragment chromatin. DNA-histone complexes were incubated with antibody:bead complexes, using antibodies raised against specific histone modifications. Protein:DNA complexes were then eluted from beads, cross-links

were reversed and ChIP-DNA was purified by phenol:chloroform extraction. ChIP-DNA was then analysed by PCR.

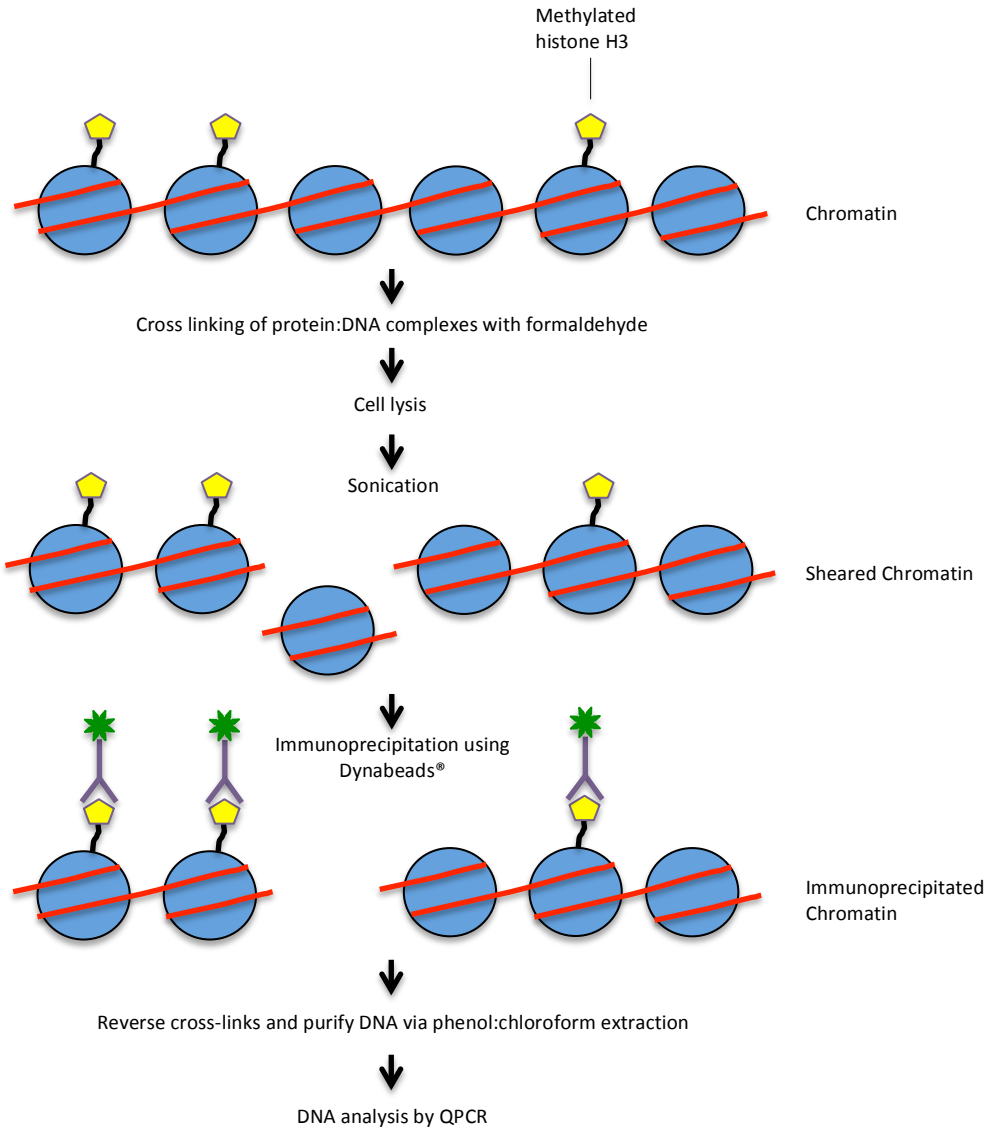

Figure 2.2. Cross-linking chromatin immunoprecipitation overview.

2.11.1 Blocking of Dynabeads®

Magnetic protein-G conjugated Dynabeads® (Novex) were used for immunoprecipitations (IP). Before beads were used for IP, beads were pre-blocked to reduce non-specific binding. Every 100 µL of bead suspension was mixed with 1 mL of RIPA buffer (Appendix 2), beads were then recovered on a magnet and mixed with another 1 mL RIPA buffer for a total of three washes. Beads were then mixed with 1 mL blocking buffer (0.2 mg/mL glycogen, 0.2 mg/ml BSA and 0.2 mg/mL yeast tRNA in RIPA buffer). Beads were incubated with blocking buffer overnight at

4 °C. Beads were recovered on a magnet and washed twice with RIPA buffer before diluted to starting volume in RIPA buffer.

2.11.2 Preparation of chromatin from formaldehyde fixed cell pellets

Cell pellets which had been fixed in formaldehyde (section 2.5.7) were thawed and resuspended in 1 mL of cold Swelling Buffer (Appendix 2) with freshly added 0.5% NP-40 and 1:500 protease inhibitors. Samples were transferred to a 1.5 mL micro-centrifuge tube and incubated for 20 minutes on ice on an orbital shaker. Samples were then centrifuged at 800 g for 5 minutes at 4 °C. Pellet was resuspended in 1 mL RIPA buffer containing protease inhibitors. Chromatin was sonicated on ice with a probe sonicator (50% power output, MSE Soniprep 150).

For initial optimisation, samples were sonicated for 10 cycles of 15 seconds with 30 second breaks between bursts. After each cycle a 50 µL aliquot was taken from the sample; the sample was then topped up with equal volume RIPA buffer. Aliquots were topped up to 250 µL with RIPA buffer, and then incubated at 65°C overnight to reverse cross-links. Samples were cooled to ambient temperature and 250 µL TE buffer (Appendix 2) and 10 µL of 10 mg/mL proteinase K was added to each aliquot before incubation at 37 °C for two hours. Fragmented DNA was purified by phenol:chloroform phase separation. To each aliquot, 500 µL of a 1:1 mixture of phenol:chloroform was added before vortexing for 30 seconds followed by centrifugation for 15 minutes at 14,000 g at ambient temperature. The upper phase was collected into a new 1.5 mL centrifuge tube. 50 µL of 3M sodium acetate was added along with 1 mL 100% ethanol before incubating the samples at -80 °C for one hour. Samples were centrifuged at 18,000g for 15 minutes at 4 °C, supernatant was removed then the pellet was washed in 1 mL 70% (v/v) ethanol before centrifugation for 15 minutes at 18,0000g at 4 °C. Ethanol was removed and the pellets were air-dried. Pellets were resuspended in 25 µL TE buffer. DNA was then electrophoretically separated on a 0.75% agarose gel. The number of cycles where the DNA was fragmented to 100-600 bp was chosen as the optimum number of cycles for sonication (8 cycles).

For all sonication performed, 50 µL aliquots were always taken after the final sonication cycle and subjected to purification, and fragmentation of DNA assessed by electrophoresis through agarose gels as above.

2.11.3 Quantification of DNA

DNA was quantified by UV spectrophotometry. Samples were measured directly using a Nanodrop ND-1000 Spectrophotometer (Thermo Scientific). Optical densities (ODs) were measured at 260 and 280nm and concentration calculated from the Nanodrop™ software.

2.11.4 Preparation of Antibody-Bead complexes

10 µL blocked Dynabeads® were used for each IP. Beads were washed twice with RIPA buffer. Beads were recovered using a magnetic rack. 2.4 µg antibody (H3 or H3K9me3) was added to each 10 µL beads, diluted to 100 µl using RIPA buffer then incubated for two hours on a rotator at 4 °C. For negative control samples Rabbit IgG was used.

2.11.5 Immunoprecipitation and Washes

2 µg chromatin was diluted with RIPA-ChIP Buffer (Appendix 2) to 100 µL. To pre-clear chromatin which binds non-specifically to Dynabeads®, blocked Dynabeads® that had been washed twice in RIPA-ChIP buffer were added to chromatin samples (10 µL beads per 100 µL chromatin) and then incubated with rotation at 4 °C for 90 minutes. Samples were placed on a magnetic rack and cleaned chromatin recovered.

100 µL pre-cleared chromatin was added into each 0.2 mL PCR tube containing antibody-beads complexes held to the wall in a magnetic rack on ice, and from which the RIPA buffer had been pipetted out. At this point 100 µL pre-cleared chromatin from each treatment sample was added to 1.5 mL centrifuge tubes to be used as the input chromatin. Samples were removed from the magnetic rack to release the antibody-bead complexes into the chromatin suspension and samples were then incubated on a rotator for two hours at 4 °C. Tubes were centrifuged for one second to bring down any solution trapped in the lid during incubation then immune complexes were captured by placing tubes in a chilled magnetic rack.

Supernatant was discarded, 100 µL ice cold RIPA buffer was added and the tubes were then removed from the magnetic rack to release the immune complexes into the buffer. The complexes were resuspended by gentle manual agitation and tubes were then placed on a rotator for four minutes at 4 °C. This step was repeated for a total of three washes in RIPA buffer. Tubes were briefly centrifuged, supernatant removed,

100 µL TE buffer added then incubated for four minutes on a rotator at 4 °C. Tubes were briefly centrifuged, placed on ice and then contents were transferred to separate clean 0.2 mL tubes on ice. The complexes were captured in the magnetic rack and TE buffer removed.

2.11.6 DNA Recovery by Phenol-Chloroform Extraction

150 µL complete elution buffer (Appendix 2) was added to each tube then incubated for two hours on a Thermomixer at 68 °C, 1300 rpm. Tubes were removed from the Thermomixer and briefly centrifuged before beads where captured on the magnetic rack. Supernatant was collected and placed in a clean 1.5 mL centrifuge tube. 150 µL complete elution buffer was added to the remaining ChIP material and incubated on the Thermomixer for five minutes at 68 °C, 1300 rpm. Tubes were removed from the Thermomixer, beads captured using the magnetic rack, supernatant collected and then combined with the first supernatant, 200 µL elution buffer was then to the combined supernatants.

Input chromatin samples were prepared by the addition of 200 µL elution buffer (Appendix 2) and 7.5 µL proteinase K (2 mg/mL). Samples were vortexed and then incubated for two hours on a heating block at 68 °C. Samples were removed from the heating block and 200 µL elution buffer was added.

DNA was extracted once with 500 µL phenol:chloroform. Samples were centrifuged at 14,000g for five minutes to separate the phases then 460 µL of the aqueous phase was transferred to a clean 1.5 mL centrifuge tube. DNA was then extracted with 460 µL chloroform. Samples were centrifuged at 14,000g for five minutes and 400 µL of the aqueous phase was then transferred to a clean 1.5 mL centrifuge tube. 44 µL 3M sodium acetate (pH 7.0) and 1 mL 100% ethanol was added to the aqueous phase, mixed thoroughly and then incubated for at least one hour at -80 °C. Samples were thawed and centrifuged at 18,000g for 15 minutes at 4 °C. Supernatant was removed, 1 mL 70% ethanol was added and then vortexed briefly to wash the DNA pellet then centrifuged at 18,000g for ten minutes at 4 °C. This step was repeated to give two ethanol washes. Ethanol was removed and DNA dissolved in 60 µL TE buffer. Samples were stored at -80 °C until use.

2.11.7 Analysis using PCR and QPCR

Chromatin Immunoprecipitation success was ascertained by ChIP-PCR. The Ensemble genome browser (www.ensemble.org) was used to identify the sequences for KRT13, KRT20, UPK1A and UPK2. These sequences were inputted into primer design software (http://www.ncbi.nlm.nih.gov/tools/primer-blast/). The software was instructed to design a PCR product of 50-150 bp (Table 2.6). The search target was the human reference genome (hg19) and all other settings were left as default. The highest ranked primer pair with no other hits in the genome was chosen.

Table 2.6. Primers for ChIP(Q)PCR.

Gene	Primer Sequence	Amplicon Length
KRT13	For - GAGCTCCTCTGCCAGCTATG Rev - CACCAAAACCACAGCTCACG	146
KRT20	For – TCAGTACAGTGGGCATGCAG Rev – TCACCGTGTGTCTGGAGTTG	99
UPK1A	For – TGCGGCAGCAGCGGA Rev – AATGATATTGCCCACAACTAGCAG	70
UPK2	For – CACCCCTGCTGCCCATC Rev – GCAGCCCCTGGGGACA	70

1 µL of purified ChIP-DNA and chromatin IP input were prepared for PCR using the GoTaq (Promega) PCR kit as described in section 2.10.7. PCR was performed using the conditions outlined in Table 2.7. 10 µL of PCR reactions were separated by electrophoresis on a 4 % agarose gel and gels photographed under UV light using a Gene Genius Gel Imaging System (Syngene) with GeneSnap software to visualise DNA bands.

Table 2.7. ChIP-PCR amplification settings.

Step	Temperature	Time
1	95 °C	2 min
2	95 °C	30 s
3	60 °C	30 s
4	72 °C	15 s
5	Go to 2	35 cycles
6	72 °C	5 min

SYBR® Green QPCR (as described in section 2.10.9) was then utilised to quantify the changes observed for four known differentiation genes KRT13, KRT14, UPK1A and UPK2. ChIP-DNA was diluted 1:2.5 with 5 µL DNA added to each reaction. Data was represented as % of input where % of input = $(2^{-Ct\ IP}/2^{-Ct\ input}) \times 100$.

2.12 Quantification of post-translational histone modifications using mass spectrometry

Quantification of global post-translational histone changes using mass spectrometry was performed in collaboration with Dr Mark Dickman and Tom Minshull from the Department of Chemical and Biological Engineering at the University of Sheffield. Quantification of post-translational histone changes was performed following the procedures in Figure 2.3. Cell culture treatments and preparation of histones was performed in York; RP-HPLC, LCMS/MS and MS analyses were performed by Tom Minshull in Sheffield.

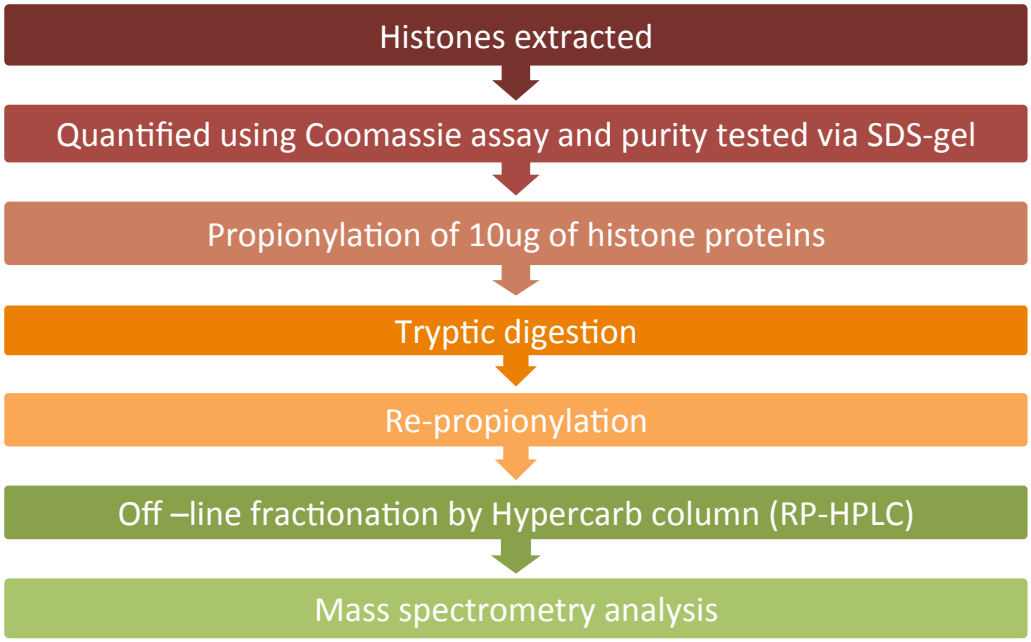

Figure 2.3. Work flow for the quantification of post-translational histone modifications by mass spectrometry.

2.12.1 Acid extraction of histones

Culture medium was aspirated from cell cultures in 75 cm^2 flasks. Cell monolayers were incubated in 0.1% (w/v) EDTA in PBS for 5 minutes at 37 °C, until the cells began to round up and dissociated from each other. Cells were then incubated in 1 mL of 0.25 % (w/v) trypsin (Sigma Aldrich) and 0.02% (w/v) EDTA in Hank's

balanced salt solution (Invitrogen) for 2 minutes at 37 °C. Cells were harvested into 5 mL KSFMc containing 1.5 mg/mL soybean trypsin inhibitor (Sigma). Cells were collected by centrifugation (10 min, 300g), supernatant was discarded and cell pellets were washed in PBS and centrifuged again at 300g for ten minutes. Supernatant was discarded; cell pellets were resuspended in 1 mL hypotonic lysis buffer (Appendix 2) and transferred to a 1.5 mL centrifuge tube. Samples were incubated for 30 minutes on a rotator at 4 °C to promote hypotonic swelling of cells and lysis by mechanical shearing during rotation. Intact nuclei were pelleted by centrifugation at 10,000g for ten minutes at 4 °C. Supernatant was discarded and nuclei were resuspended in 400 µL 0.4 N H_2SO_4 then incubated on a rotator for four hours at 4 °C. Samples were centrifuged at 16,000g for ten minutes at 4 °C to remove nuclear debris. Supernatant containing histones was transferred in to a clean 1.5 mL centrifuge tube. 132 µL trichloroacetic acid (Sigma) was added drop-wise to the histone solution (to give a final concentration of 33% TCA) after which the tube was inverted several times to mix the solutions. The samples were incubated overnight at 4 °C. Histones were pelleted by centrifugation at 16,000g for ten minutes at 4 °C. Supernatant was removed and the histones where then washed with ice-cold acetone to remove the acid from the solution without dissolving the protein pellet. Samples were centrifuged for ten minutes at 16,000g at 4 °C. The acetone washing step was performed twice before histones were left to air-dry at ambient temperature for 20 minutes before being dissolved in 100 µL ddH_20.

2.12.2 Quantification and purity testing of histones

The histone protein concentration of each sample was determined using a Coomassie® protein assay reagent kit (Pierce), which is based on the Bradford colorimetric assay. Samples were diluted 1:5 in dH_2O. 10 µL of each sample was aliquoted in duplicate into a 96-well plate with 200 µL Coomassie reagent. The absorbance of samples was measured at test and reference wavelengths of 570 and 630nm, respectively using a MRX II 96-well plate spectrophotometer (Dynex). Samples were measured alongside bovine serum albumin (BSA) (Pierce) diluted to concentrations ranging from 0 to 1000 µg/mL in dH_2O. The Revelation software package (Dynex) was used to plot the BSA standard curve and calculate the R^2 value. The average of duplicate absorbance readings from each sample was used to estimate the protein concentration by comparison with the BSA standard curve.

Histone purity was tested by SDS-Polyacrylamide gel electrophoresis. 2.5 µg histones samples were mixed with 4x LDS (Life Technologies) and 10x reducing agent (Life Technologies). Reagents were diluted to a final concentration of 1x with dH_2O into a total volume of 10 µL and then heated at 70 °C for ten minutes. Histones were resolved by electrophoresis through 1 mm thick 10 well 4-12% Bis-Tris NuPAGE pre-cast polyacrylamide gels using the Novex system (Invitrogen). The gel and wells were rinsed in dH_2O and assembled in to the Novex tank according to the manufacturer's instructions. 5 µL of All-Blue pre-stained marker (BioRad) was run as a protein size marker. Bis-Tris gels were run in 1x MES buffer (Life Technologies). 500 µL antioxidant (Life Technologies) was added to the inner chamber of the tank during electrophoresis, which was carried out at 200 V for 50 minutes. Gels were washed in dH_2O, stained with Coomassie Brilliant Blue solution (Appendix 2) for one hour and then rinsed in dH_2O for at least 30 minutes.

2.12.3 Chemical derivatization and tryptic digestion

In these procedures extracted histones were first derivatized using propionic anhydride to neutralise charge and block lysine residues before digestion using trypsin, which cleaved only the arginine residues as all lysine residues were blocked by endogenous modifications or chemically by conversion to propionyl amides, to give reproducible histone peptides.

10 µg histones were diluted with 5 µL 100 mM ammonium bicarbonate (pH 8) before 2 µL concentrated ammonium hydroxide was added to the sample. Fresh propionylation reagent was prepared by adding 75 µL propionic anhydride to 25 µL isopropanol. 10 µL propionylation reagent was added to histone samples followed by vortexing and then a short spin down in a mini-centrifuge. pH was then checked using pH indicator strips; if pH was less than 8, ammonium hydroxide was added dropwise until pH was approximately 8. Samples were incubated for 20 minutes at 51 °C. Samples were dried down to approximately 5 µL in a SpeedVac concentrator (Thermo Scientific) at ambient temperature for 20 minutes. Samples were diluted with 5 µL 100 mM ammonium bicarbonate (pH 8) before the propionylation reaction was performed a second time to ensure maximum conversion. 2 µL concentrated ammonium hydroxide was added followed by 10 µL propionylation reagent, pH was tested and then samples were incubated for 20 minutes at 51 °C.

50 µL 100 mM ammonium bicarbonate (pH 8) was added to the propionylated histones. Trypsin was added to the samples to make a 20:1 (w/w) protein:trypsin ratio and samples were then incubated overnight at 37 °C. The trypsin digestion was quenched by adding glacial acetic acid and pH was measured to make sure pH had dropped to about 3. Samples were then incubated at -80 °C for 10 minutes in order to inactivate the trypsin. Samples were dried down to approximately 5 µL in a SpeedVac concentrator before chemical derivatization with propionic anhydride was performed in order to convert the newly trypsin-generated N-termini on peptides to propionyl amides. 2 µL concentrated ammonium hydroxide was added followed by 10 µL propionylation reagent, pH was tested and then samples were incubated for 20 minutes at 51 °C. Samples were diluted with 5 µL 100 mM ammonium bicarbonate (pH 8) before the propionylation reaction was performed a second time to ensure maximum conversion. Samples were then dried down in a SpeedVac concentrator.

2.12.4 HPLC fractionation

Digested, propionylated histone samples were resuspended in 10 µL 0.1% trifluoroacetic acid (TFA) and were fractionated on the U3000 HPLC (Thermo Scientific) with a Hypercarb™ Column (50 x 2.1 mm, 5 µm particle size) (Thermo Scientific) running Chromleon software. Buffers used for HPLC: Buffer A contained 3% Acetonitrile (ACN) and 0.1% TFA and Buffer B contained 97 % ACN and 0.1% TFA. Parameters used: column temperature was 30 °C, UV was 214 mm (50 Hz) and flow rate was 0.2 mL/min. Gradient used is outlined in Table 2.8. Fractions were collected every 60 seconds (18 in total) in a 384 lo-bind deep well plate, starting at eight minutes. Following collection samples were transferred to lo-bind micro centrifuge tubes (Eppendorf), vacuum centrifuged to dryness and then stored at -80 °C.

Table 2.8. HPLC gradient for fractionation of histone samples.

% Buffer B	Time (min)	Flow rate (µL/min)
0	0	0.3
0	1	0.3
70	25	0.3
90	26	0.3
90	30	0.3
5	31	0.3
0	35	0.3

2.12.5 Mass spectrometry

All samples were re-suspended in 10 µL 0.1% TFA (LC-MS grade), and a proportion of this was used for LC/MS analysis. Peptides were separated on an Ultimate 3000 RSLC nano liquid chromatography system (Dionex), using a 150 mm x 75 µm i.d. PepMap reversed phase column (Dionex) online with the mass spectrometer. Elution of peptides occurred over 61 minutes with the following gradient (see Table 2.9). Buffers used: Buffer A contained 0.1% Formic acid (FA) and 3% ACN (LC-MS grade) and Buffer B contained 0.1% FA and 97% ACN (LC-MS grade).

Table 2.9. RP-HPLC gradient.

% Buffer B	Time (min)	Flow rate (µL/min)
3	0	0.3
3	2	0.3
25	30	0.3
50	40.1	0.3
90	41	0.3
90	47	0.3
3	48	0.3
3	55	0.3

MS/MS data was acquired using the MaXis Ultra high resolution quadrupole time-of-flight (Q-ToF) system (Bruker Daltonics) using a data dependent acquisition approach. A captive spray ESI was used to introduce the sample into the mass

spectrometer. MS and MS/MS scans (m/z 100-1800) were acquired in positive ion mode. Automatic internal calibration was performed using HP 1221.990364.

2.12.6 Analysis

Mass spectrometry analsysis (Figure 2.4) was performed as described by Dickman er al. (2013). Line spectra data was analysed in Data Analysis 4.1 software (Bruker Daltonics) and used to create .mgf files. The sum peak finder algorithm was used for peak detection using a signal to noise (S/N) ratio of 100 and an absolute intensity threshold of 3000. The .mgf files were then searched in MASCOT v2.5.1 using Mascot Daemon (Matrix science). MS and MS/MS tolerance were set at 0.15 Da, and searched against the SwissProt database with the Homo sapiens Taxonomy selected. Fixed modifications were set as propionylation (K & N-term) Variable modification selected were Methylpropionylation (K), Dimethylation (K), Trimethylation (K), Phosphorylation (S,T) and Acetylation (K) Enzyme selected was Arg-C (due to the propionylation reaction altering the specificity), with 2 missed cleavages allowed. Charge states searched were 2+, 3+ and 4+. All post-translational modifications were manually verified via manual assignments of MS/MS peaks. The relative abundance of histone peptides was determined by the integration of smoothed (gauss algorithm, 1 cycle) extracted ion chromatograms. This process was automated using Hist-o-matic VBscript. Finally, correction factor as detailed by Lin et al. (2014) were applied, to compensate for differences in ionisation efficiency between differently modified peptides.

Line spectra data was processed into peak list by DataAnalysis software (Bruker)

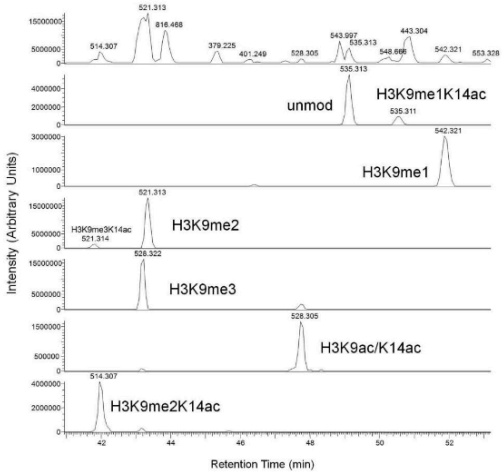

Example above shows total ion chromatogram and extracted ion chromatograms for various modified peptides ($[M+2H]^{2+}$ ions) spanning the 9–17 residues KSTGGKAPR. Labels indicate the particular modified form eluting in that peak.

All MS-MS spectra from modified peptides were manually inspected for accurate mass and correct fragmentation assignment (example below shows K23ac)

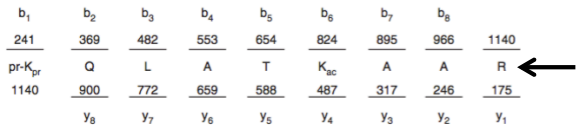

Predicted mass for b and y ions for acetylated 18-26 (KQLATKAAR) peptide at K23

Mass spectrum of the precursor parent ion differentiates this peptide as being acetylated as the experimental mass is consistent with an acetylation mark

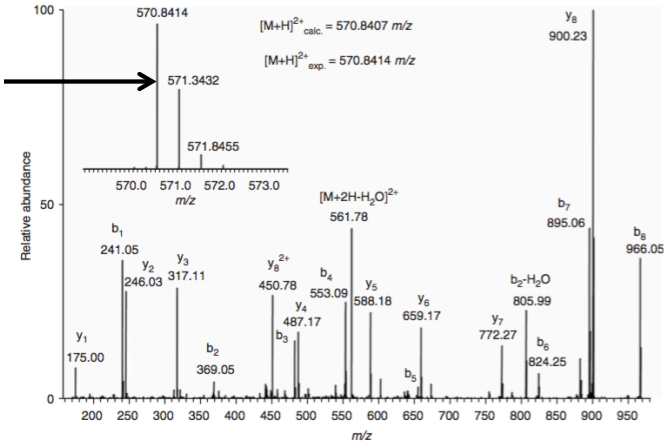

MS/MS spectrum of the $[M+2H]^{2+}$ precursor ion from the digest of propionylated histone H3. This peptide span residues 18–26 and was found to contain an acetylation (ac) modification on K23. b and y type ions are labeled.

Relative abundance of each modified peptide determined by integration of smoothed extracted ion chromatograms

Correction factor applied to compensate for differences in ionisation efficiency

Figure 2.4. Mass spectrometry analysis for quantification of post-translational histone modifications.

2.13 Statistical Analysis

Data is represented graphically using Microsoft Excel and GraphPad. Data is represented as the mean of all replicates with error bars representing ± one standard deviation. Statistical tests were performed using GraphPad Prism 6 software. One-way analysis of variance (ANOVA) tests were used to compare three or more sample means along with the appropriate post-test. Dunnett's post-test was performed to compare whether each treatment was significantly different to the control treatment. Tukey's post-test was performed to test which treatments were significantly different from each other. Details of statistical tests used are cited in the figure legends.

3 Effect of Cadmium on Proliferation and Differentiation of NHU Cell Cultures

3.1 Aim & Objectives

The aim of this chapter was to determine the effect that cadmium treatment had on proliferative and differentiated NHU cells in culture.

The working hypothesis is that exposure of the urothelium to cadmium leads to epigenetic dysregulation of gene expression, causing field changes within the urothelium characteristic of dysplasia/carcinoma in situ, which is the most common precursor of invasive carcinomas.

The specific objectives of this chapter were to assess the effect of cadmium on:

a) proliferative NHU cell cultures.
b) the differentiation potential of NHU cell cultures
   - ABS/Ca^{2+} and TZ/PD differentiating NHU cell cultures.
   - ABS/Ca^{2+} differentiated NHU cell cultures.
   - the expression of transcription factors involved in urothelial differentiation.
c) tumour suppressor gene expression in NHU cell cultures.

3.2 Experimental Approach

3.2.1 Proliferative NHU cell cultures

To investigate the effect that cadmium exposure had on proliferative NHU cell cultures, urothelial cell cultures were established in KSFMc, (Keratinocyte serum-free medium supplemented with 50 μg/mL bovine pituitary extract, 5 ng/mL epidermal growth factor and 30 ng/mL cholera toxin) then left to adhere overnight before addition of cadmium chloride.

alamarBlue® assays and population doubling calculations were used to assess the effect of cadmium on the proliferation of NHU cells. An alamarBlue® assay uses a mitochondrial enzyme assay in order to measure proliferation by using the assumption that mitochondrial activity is proportional to cell number. Number of population doublings equals $\log_2$ (CMF), where CMF (cell multiplication factor) equals the final cell number divided by the initial cell number.

3.2.2 Differentiated NHU cell cultures

In order to look at the effect cadmium had on differentiation, NHU cell cultures were established in KSFMc medium until cultures reached at least 80% confluence, at this point two methods to induce NHU cell differentiation were used as described in sections 2.5.3.1 and 2.5.3.2, with medium replaced every 2/3 days:

(1) 5% serum and 2 mM Ca^{2+} (Biomimetic)

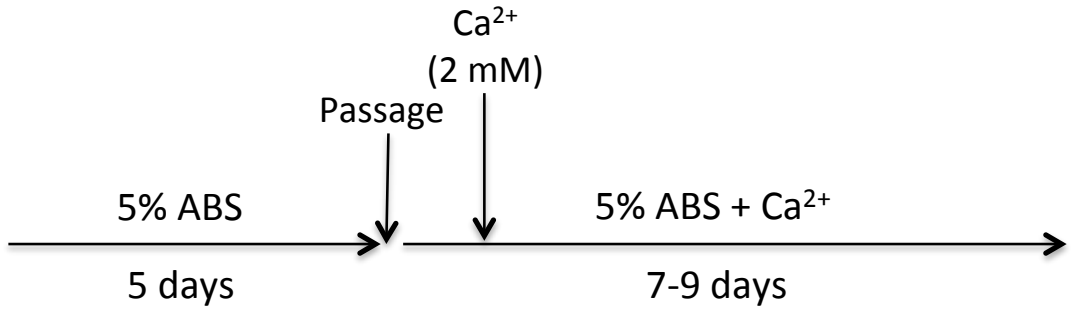

(2) Troglitazone and PD153035 (Pharmacological)

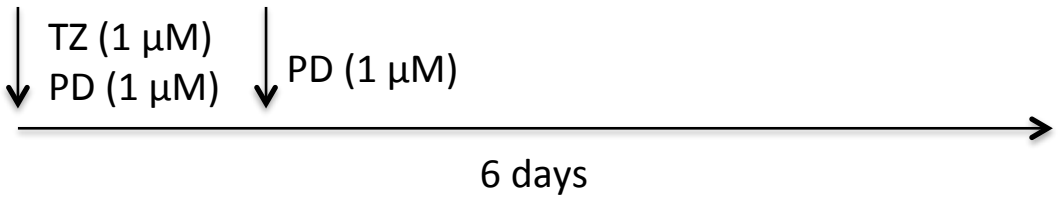

Using the ABS/Ca^{2+} method NHU cell cultures were exposed to cadmium before, during and after differentiation (Figure 3.1).

Cadmium treatments were applied to proliferative NHU cell cultures before the induction of differentiation in order to investigate whether cadmium exposure affected the potential of NHU cell cultures to differentiate. Immunoblotting was used to examine protein expression of differentiation markers, ie. claudins and cytokeratins.

ABS/Ca^{2+} differentiating cell cultures were treated with cadmium to test whether cadmium would affect the ability of cultures to form a functional barrier. Transepithelial electrical resistance (TER) measurements were used to monitor barrier formation.

ABS/Ca^{2+} differentiated cell sheets were exposed to cadmium once a stable barrier was formed to investigate whether NHU cell cultures were able to maintain a tight

barrier upon cadmium insult. Additionally, differentiated cell sheets were wounded in order to see if the presence of cadmium would affect their ability to recover. TER measurements were used to monitor barrier function.

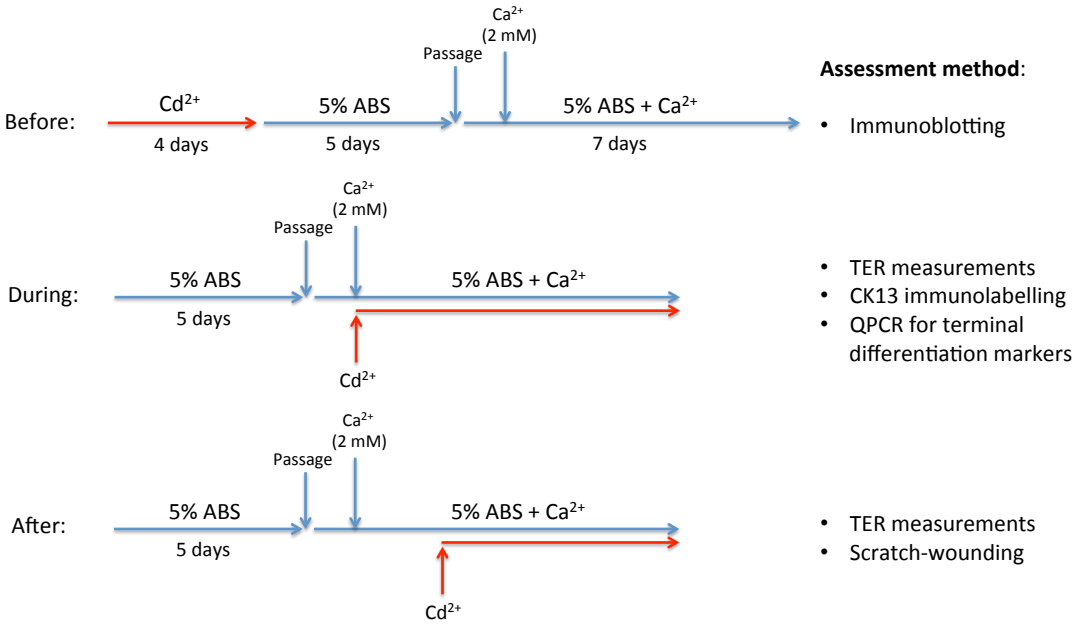

Figure 3.1. Experimental approach for cadmium chloride treatments using the ABS/Ca^{2+} method of differentiation induction.

Using the TZPD method, NHU cell cultures were exposed to cadmium before and during the induction of differentiation in order to investigate whether cadmium affected their ability to differentiate (Figure 3.2). Immunoblotting along with immunofluorescence microscopy was used to examine protein expression of differentiation markers.

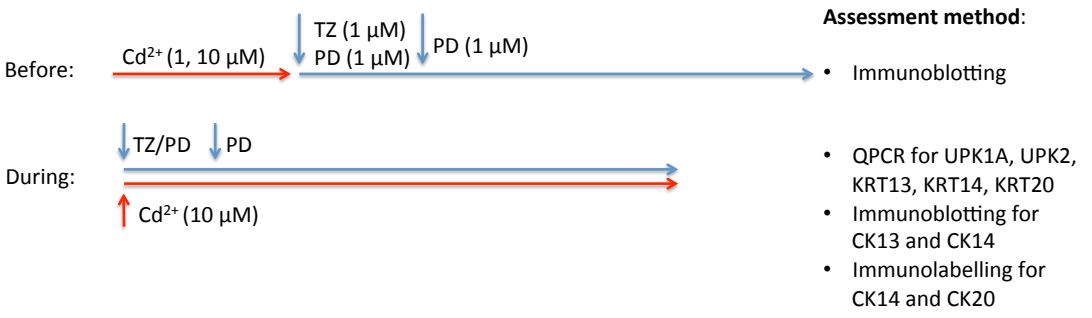

Figure 3.2. Experimental approach for cadmium chloride treatments using the TZPD method of differentiation induction.

RT(Q)PCR was used to assess transcript levels of differentiation-associated genes and transcription factors known to be involved in urothelial differentiation.

3.2.3 Tumour suppressor genes

RTQPCR was used to assess transcript levels of the tumour suppressor gene p16 in proliferative and TZPD-induced differentiated NHU cell cultures.

Immunoblotting was used to examine protein expression of p16 in proliferative NHU cell cultures exposed to cadmium for up to 22 days.

RTPCR was used to assess transcript levels of three tumour suppressor genes, (p16, RASSF1A and APC) in ABS/Ca^{2+} differentiated NHU cell cultures.

3.3 Results

3.3.1 Proliferation

NHU cells cultured in concentrations up to 10 µM $CdCl_2$ showed no differences in their proliferative ability to reach confluence over a 96 hour treatment period, however 100 µM $CdCl_2$ proved toxic to the cells within 48 hours (Figure 3.3). From further study it was found that constant exposure to 10 µM $CdCl_2$ was tolerated by the cultures, but more than 5 days treatment with 25 µM $CdCl_2$ was toxic, as at day 5 the cells had started to round up, indicative of cell death (Figure 3.4).

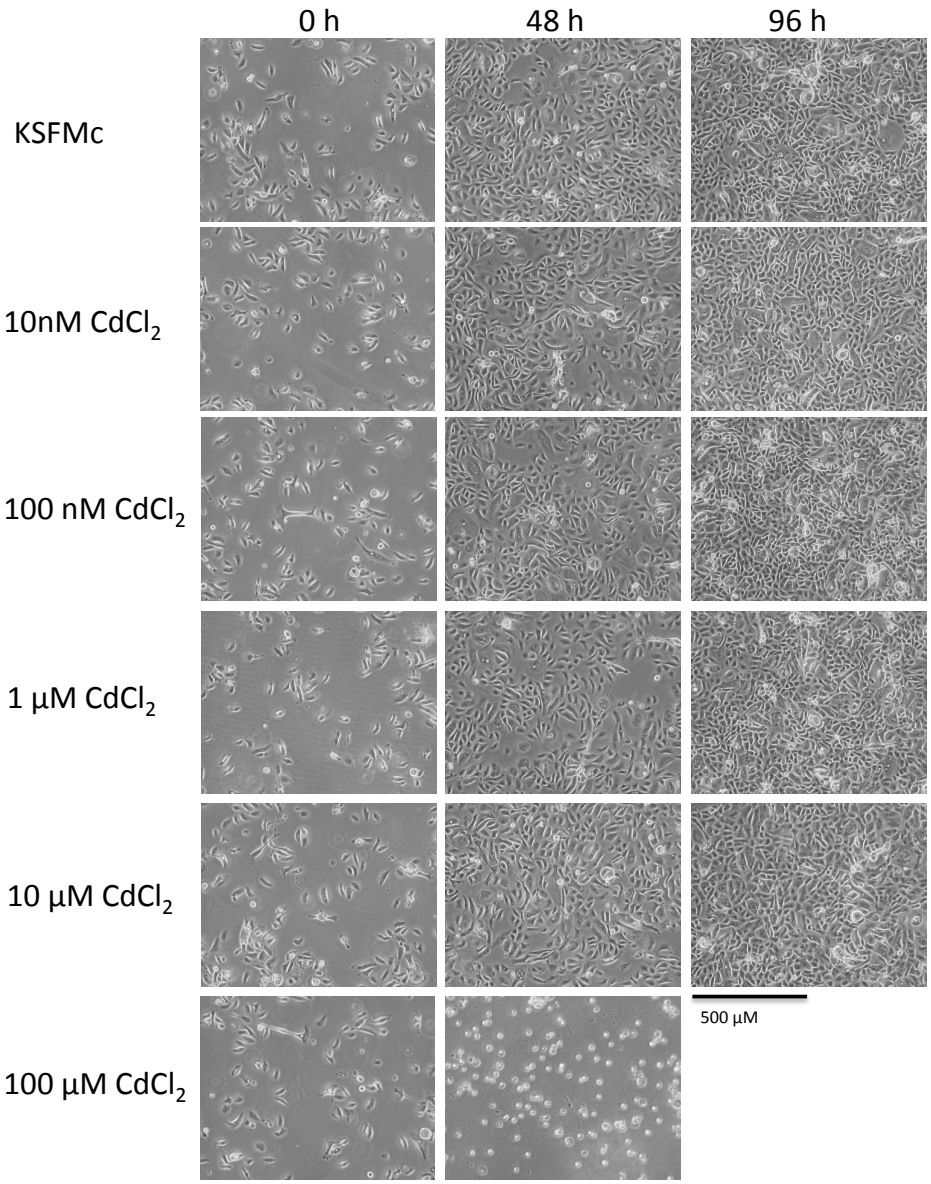

Figure 3.3. Phase contrast microscopy of proliferating NHU cell cultures. NHU cell cultures (Y1054) were treated with a range of cadmium chloride concentrations for 96 hours with images taken at time points 0, 48 and 96 hours.

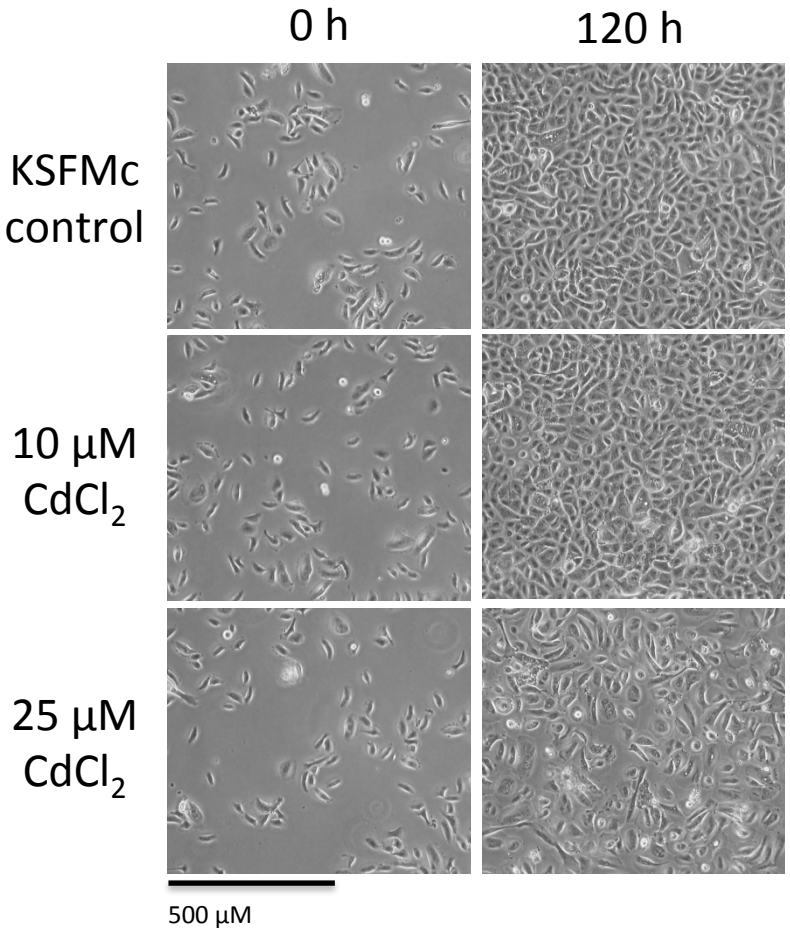

Figure 3.4. Phase contrast microscopy of proliferating NHU cell cultures. NHU cell cultures (Y1160) were maintained in KSFMc medium or treated with 10 µM or 25 µM cadmium chloride for 120 hours. Images taken at 0 hours and 120 hours.

An alamarBlue® assay showed that NHU cells treated with 1 and 5 µM $CdCl_2$ proliferated at the same rate as the KSFMc control whereas cultures treated with 10 µM $CdCl_2$ showed a reduced rate of proliferation but were still able to reach full confluence. Concentrations above 10 µM $CdCl_2$ proved toxic, with cultures failing to thrive (Figure 3.5 A).

Statistically significant differences in culture biomass were observed between KSFMc control and cultures in 10, 15, 20, and 25 µM $CdCl_2$ at day 3 (Figure 3.5 B). At days 5 and 7 there was still a statistically significant difference in biomass between cultures maintained in control medium and those treated with 10 µM $CdCl_2$; however, by day 9 there were no significant differences between cell cultures maintained in KSFMc or those treated with 1, 5 and 10 µM $CdCl_2$ (Figure 3.5 C).

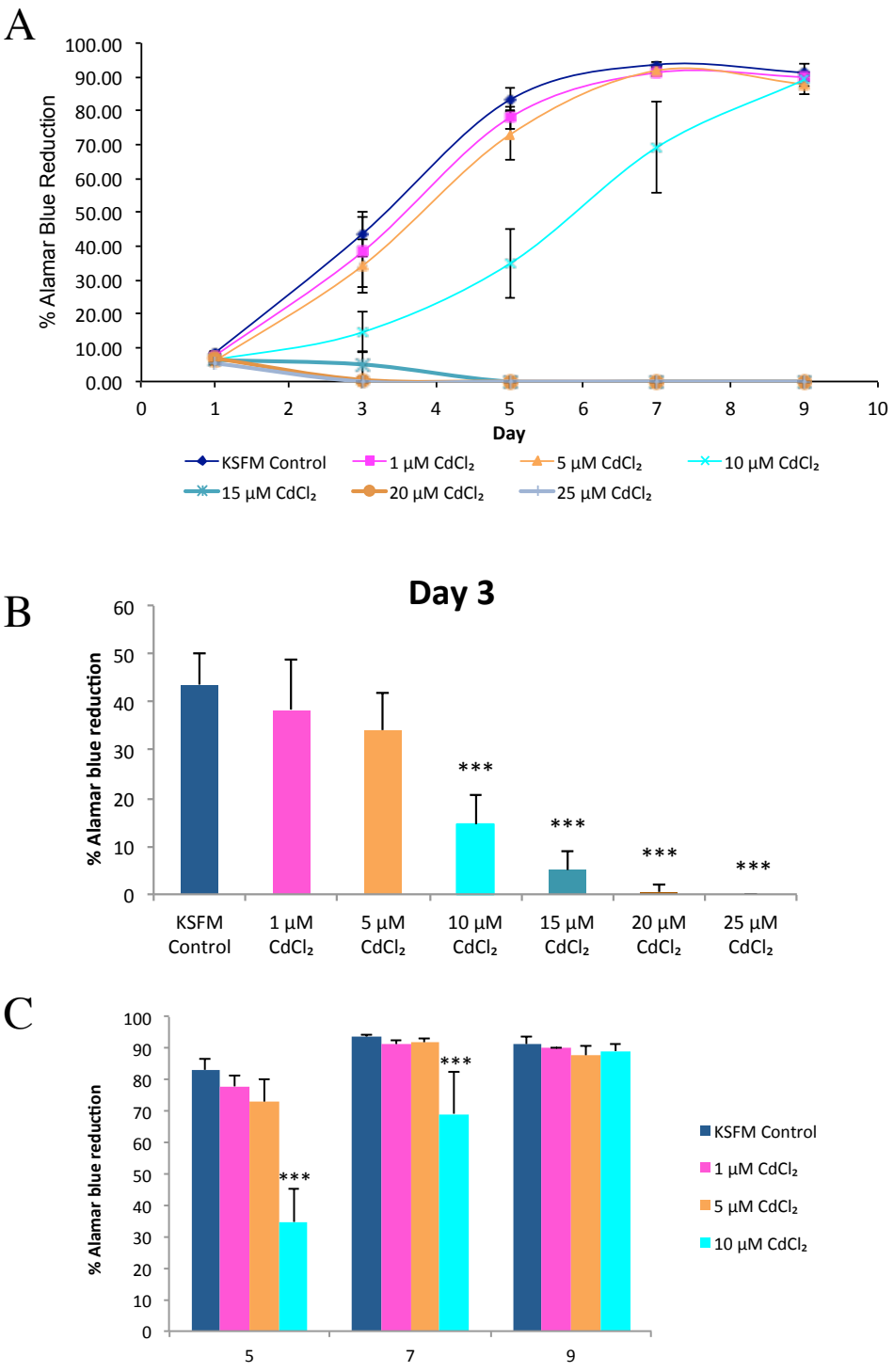

Figure 3.5. Effect of cadmium chloride on NHU cell growth. A) Y1237 NHU cells were seeded at a concentration of $2x10^4$ cells mL^{-1} in 96-well plates, treated with cadmium chloride concentrations and underwent alamarBlue® assays at 1, 3, 5, 7 and 9 days post cadmium treatment. Results were normalised against no cell controls and the percentage reduction in alamarBlue calculated. Each data point is the average of 6 replicates with standard deviations shown by error bars. B) alamarBlue® assays performed after 3 days of culture in KSFMc ± $CdCl_2$. (*p<0.001, ANOVA then Dunnett's post test). C) alamarBlue® assays performed after 5, 7, 9 days of culture in KSFMc ± $CdCl_2$. (***p<0.001, ANOVA then Dunnett's post test).**

Population doubling calculations were used to assess the cumulative effect that cadmium exposure had upon proliferating NHU cells over several generations. Proliferating NHU cell cultures were exposed to 1, 10 and 25 µM $CdCl_2$. Cumulative population doublings of continuous exposure in two cell lines (Figure 3.6) showed that NHU cell cultures exposed to 10 µM $CdCl_2$ showed growth attenuation; 25 µM $CdCl_2$ caused cell death; and no difference was seen in 1 µM $CdCl_2$ when compared to the medium only control.

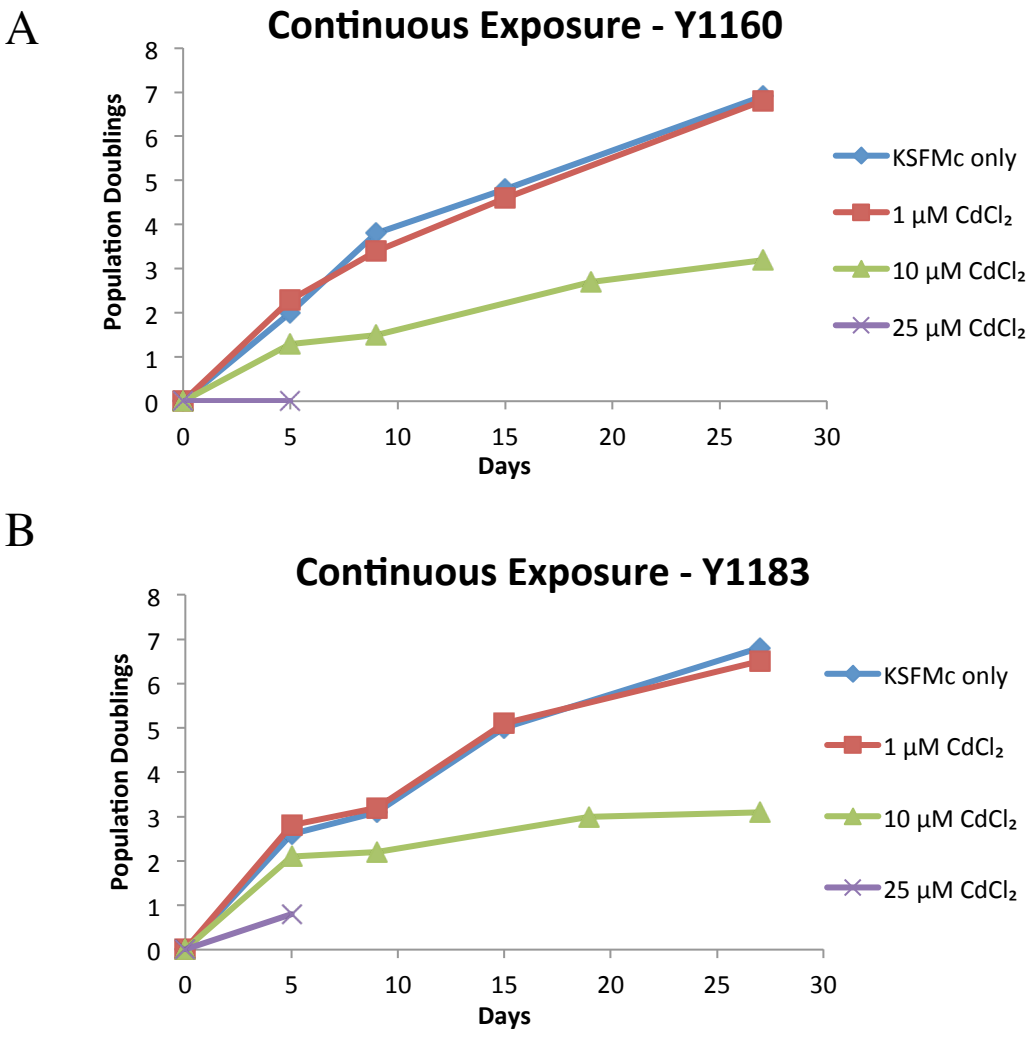

Figure 3.6. Growth curves showing cumulative population doublings of NHU cells as a function of time during continuous cadmium chloride exposure. Cells were counted with a haemocytometer then seeded into Primaria® flasks. Media were replaced after 48-72 hours. Once cultures reached 80% confluence cells were harvested, counted and then seeded into new Primaria® flasks. Number of population doublings equals log2 (CMF), where CMF (cell multiplication factor) equals the final cell number divided by the initial cell number. Points on the graph mark where cultures were subcultured.

As occupational or environmental exposure to cadmium is not constant, the ability for NHU cells to recover once exposed to cadmium was examined. NHU cells from two cell lines were transiently exposed to 1, 10 and 25 µM $CdCl_2$ for 5 days after which the cadmium was removed. At all concentrations used, including 25 µM $CdCl_2$, the cells recovered (Figure 3.7), although a lag phase occurred in cultures treated with 10 and 25 µM $CdCl_2$.

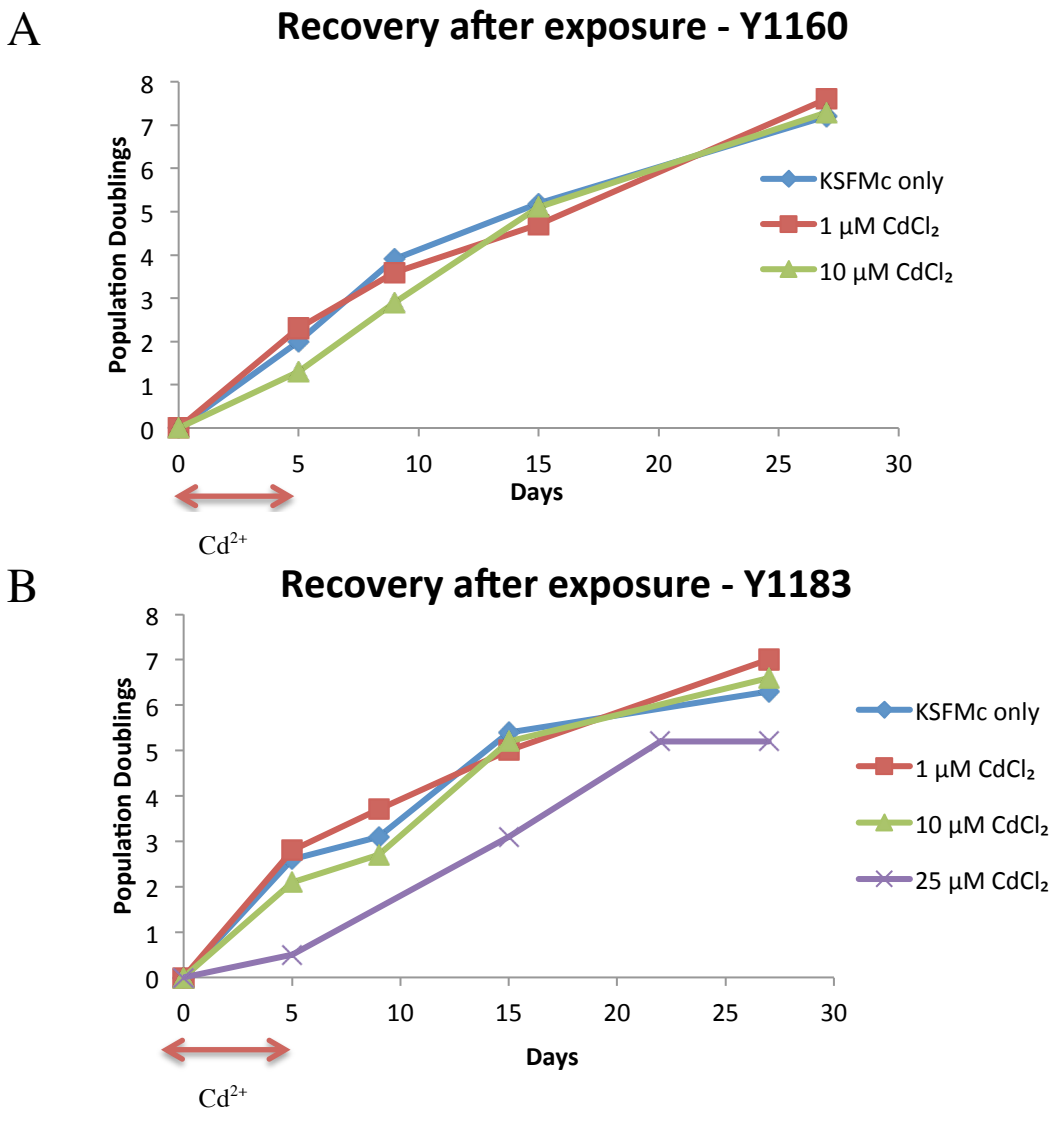

Figure 3.7. Growth curves showing cumulative population doublings of NHU cells as a function of time following transient exposure. Cells were counted with a haemocytometer then seeded into Primaria® flasks. Cultures were treated with cadmium for 5 days. Once cultures reached 80% confluence cells were harvested, counted and then seeded into new Primaria® flasks. Number of population doublings equals log2 (CMF), where CMF (cell multiplication factor) equals the final cell number divided by the initial cell number. Points on the graph mark where cultures were subcultured.

3.3.2 The effect of cadmium on differentiating NHU cells

The most common precursor to invasive urothelial cancer, carcinoma in situ (CIS), is associated with dysregulation of differentiation; therefore the potential of NHU cells to differentiate in the presence of cadmium was assessed.

Before cadmium treatments were performed, successful induction of differentiation using the ABS/Ca^{2+} and TZPD methods was confirmed.

Two markers of NHU cell differentiation, CK13 and claudin 5, were unregulated in whole cell lysates of ABS/Ca^{2+} treated NHU cell cultures (Figure 3.8A). The ability of ABS/Ca^{2+} treated cell cultures to form a functional barrier was demonstrated by cell sheets being able to form barriers greater than 2000 ohms.cm^2, an epithelium is considered tight and impermeable if it has a TER > 500 ohms.cm^2. Cell sheets were lifted off the permeable membranes they were cultured on, then fixed and processed into paraffin. The embedded cell sheets were sectioned and then stained with hematoxylin and eosin to show a stratified urothelia consisting of basal, intermediate and superficial cell layers (Figure 3.8B).

Upregulation of the terminal differentiation-associated gene UPK2 and the transitional differentiation marker, CK13, along side downregulation of CK14, a marker of proliferative NHU cells in culture, was demonstrated in TZPD induced differentiated NHU cell cultures (Figure 3.9).

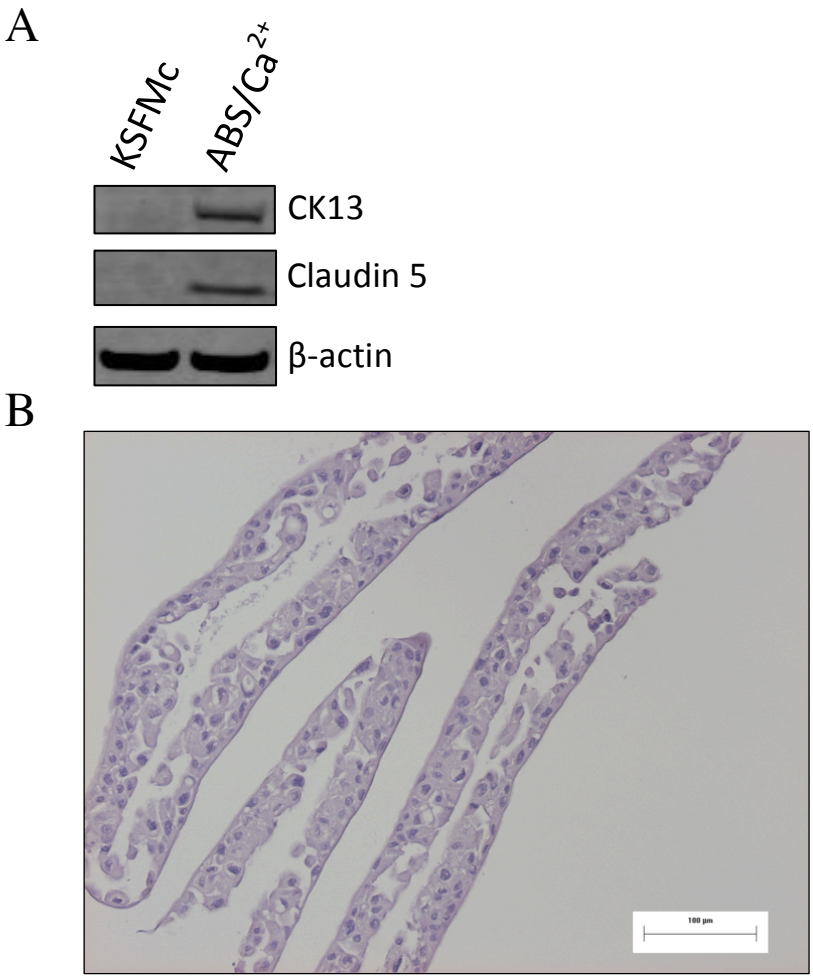

Figure 3.8. Confirmation of ABS/Ca^{2+} induced differentiation. A) Western blot showing upregulation of CK13 and claudin 5 in response to ABS/Ca^{2+} induced differentiation. Cells were lysed using SDS lysis buffer and then sonicated. Protein concentration was measured using a Bradford assay. 4-12% bis-Tris gels were loaded with 20 µg of protein and run at 200 V in MES running buffer. Protein was blotted on to PVDF membranes using the Novex apparatus for 2 hours at 30 V. Membranes were blocked in Odyssey blocking buffer, incubated with primary antibodies overnight at 4°c, and secondary immunoconjugates for one hour at ambient temperature then scanned on the Li-Cor imaging system. B) Hematoxylin and eosin stained cell sheet, showing stratified urothelia.

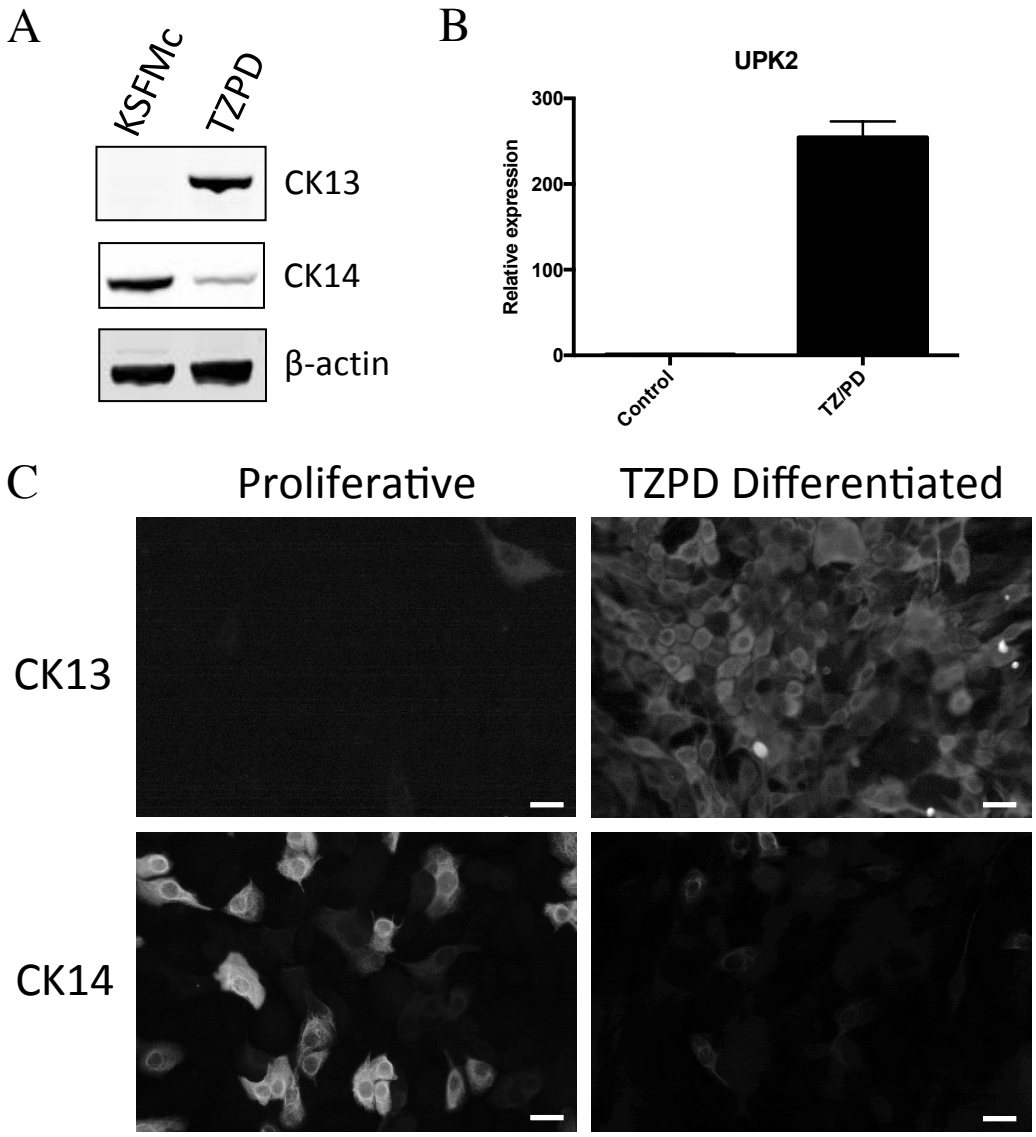

Figure 3.9. UPK2 and CK13 upregulation and CK14 downregulation in response in TZPD induced differentiation. A) Cells were lysed using SDS lysis buffer and then sonicated. Protein concentration was measured using a Bradford assay. 4-12% Bis-Tris gels were loaded with 20 µg of protein and run at 200 V in MES running buffer. Protein was blotted on to PVDF membranes using the Novex apparatus for 2 hours at 30 V. Membranes were blocked in Odyssey blocking buffer, incubated with primary antibodies overnight at 4°c, and secondary antibodies for one hour at ambient temperature then scanned on the Li-Cor imaging system. B) UPK2 RTQPCR results. mRNA was harvested from the cultures at day 3, with RTQPCR performed to quantify the relative expression of UPK2. Each value is the average of 3 replicates with standard deviations shown by error bars. C) Immunofluorescence microscopy images of CK13 and CK14. NHU cells were seeded at a concentration of $1x10^5$ cells mL^{-1} on to 12-well slides. Cells were cultured for 6 days ± TZ/PD before being fixed in methanol:acetone. Scale bar, 10 µM.

3.3.2.1 Differentiated NHU cells – ABS/Ca^{2+} method

Cadmium pre-treatment of NHU cell cultures before ABS/Ca^{2+} differentiation

To investigate whether pre-treatment of proliferative NHU cell cultures with cadmium affected their ability to differentiate, two NHU cell lines were treated with 1 and 10 μM $CdCl_2$ for 4 days. The cadmium was removed prior to pre-treatment of the cells with 5% ABS for 5 days then cultured in the presence of 5% ABS and 2mM calcium. Cells were lysed and western blots performed to look at markers of differentiation (Figure 3.10). Claudin 4, a tight junction protein upregulated in NHU cell differentiation, was shown to decrease slightly when cells were pre-treated with cadmium whereas claudin 5, another tight junction protein, was shown to increase slightly in both cell lines. In both cell lines CK13, a transitional differentiation marker was shown to decrease in cadmium pre-treated cells. By contrast CK14, a marker of squamous metaplasia, which is down regulated in differentiation, showed increases in one cell line but decreases in the other upon cadmium pre-treatment. Taken together these results indicate that cadmium pre-treatment of NHU cell cultures before ABS/Ca differentiation has a negligible effect upon differentiation.

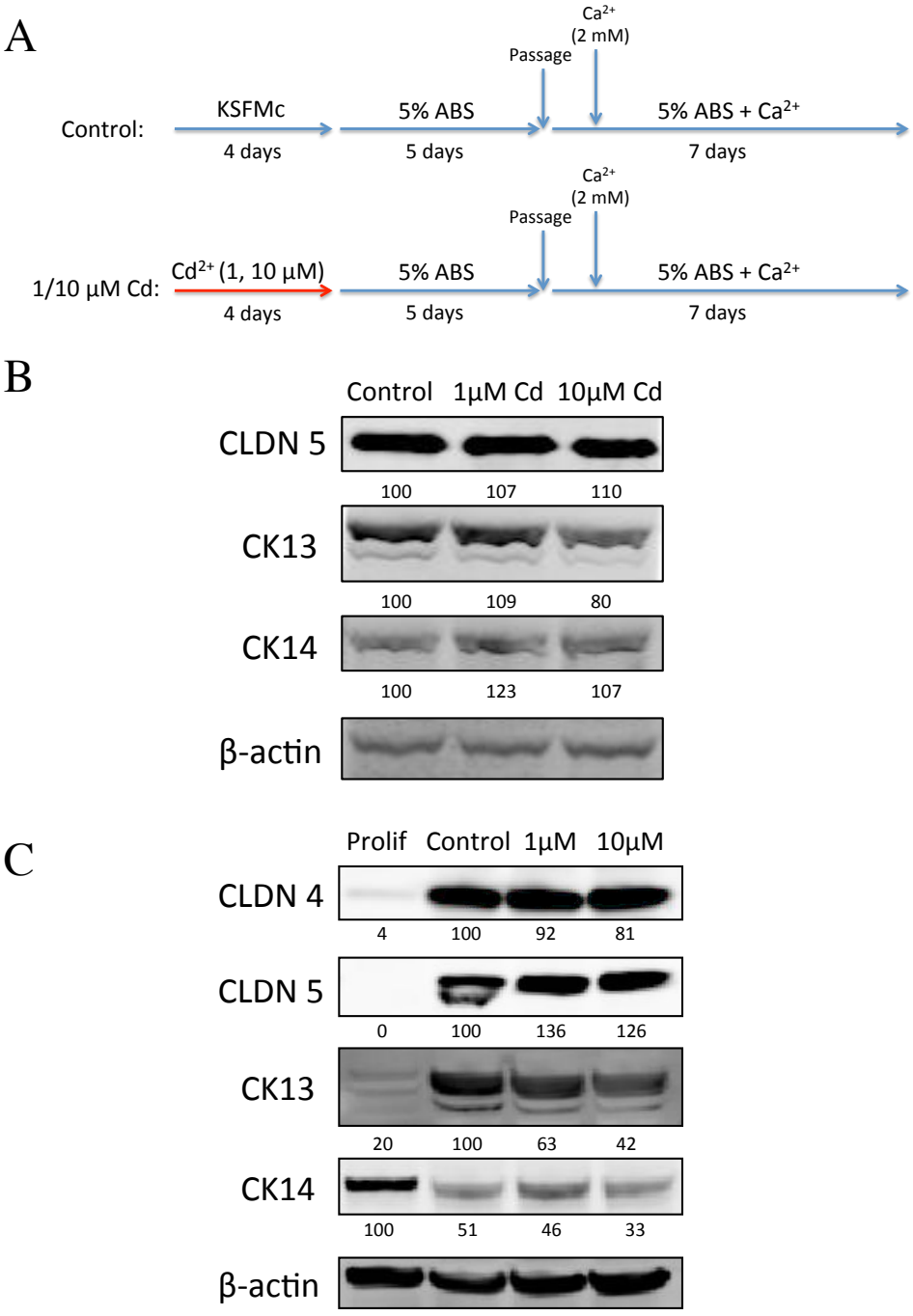

Figure 3.10. Western blot analysis of NHU cells maintained with KSFMc only (Control), 1 µM $CdCl_2$ and 10 µM $CdCl_2$ before undergoing ABS/Ca^{2+} differentiation. Cells were lysed using SDS lysis buffer and then sonicated. Protein concentration was measured using a Bradford assay. 4-12% Bis-Tris gels were loaded with 20 µg of protein and run at 200 V using MES running buffer. Protein was blotted on to PVDF membranes using the Novex apparatus for 2 hours at 30 V. Membranes were blocked in Odyssey blocking buffer, incubated with primary antibodies overnight at 4°C, and secondary antibodies for one hour at ambient temperature then scanned on the Li-Cor imaging system. The fluorescence of each band was quantified and normalised to the loading control β-actin using the Odyssey software. A) Treatment timelines. B) NHU cell line Y1019. C) NHU cell line Y1183.

Cadmium treatment during ABS/Ca^{2+} differentiation

To see if the presence of cadmium affected the ability of NHU cells to form a functional barrier urothelium, Y1183 NHU cells were exposed continually to either 1 or 10 μM $CdCl_2$ during ABS/Ca^{2+} differentiation. Transepithelial electrical resistance (TER) was used to monitor differentiation, with readings taken every day. Neither 1 nor 10 μM $CdCl_2$ produced any significant differences compared to the control (Figure 3.11B). Further cadmium treatments with an additional NHU cell line (Y1279) supported the initial observations with 1 and 10 μM $CdCl_2$, however a concentration of 20 μM $CdCl_2$ was shown to lead to a tightening of the barrier compared to the control, which was statistically significant at day 5 (Figure 3.11C).

At the end of the cadmium treatment time course mRNA was extracted from the differentiated cell sheets (Figure 3.11B) and RTQPCR was performed to quantify uroplakin 2 (UPK2) transcript expression as a measure of differentiation. It was found that UPK2 gene expression decreased with increasing concentration of cadmium chloride (Figure 3.12).

To follow up these observations, NHU cell cultures were maintained in either control 5% ABS KSFMc medium or treated with 5% ABS medium containing 10 μM $CdCl_2$ for 3, 6 and 9 days. At each time point the cells were harvested for mRNA with RTQPCR performed to measure the expression of differentiation markers. When NHU cell cultures were differentiated with ABS/Ca in the presence of cadmium, the expression of terminal differentiation-associated genes was suppressed by cadmium exposure (Figure 3.13).

Immunohistochemistry for CK13 was performed on paraffin embedded ABS/Ca^{2+} differentiated cell sheets that had been treated with 10 or 20 μM $CdCl_2$. Labelled cell sheets were imaged using a Zeiss AxioScan.Z1 slide scanner with representative images for each treatment shown in Figure 3.14A. When CK13 expression was quantified using HistoQuest software (TissueGnostics), cadmium exposure was shown to reduce expression of CK13 (Figure 3.14B).

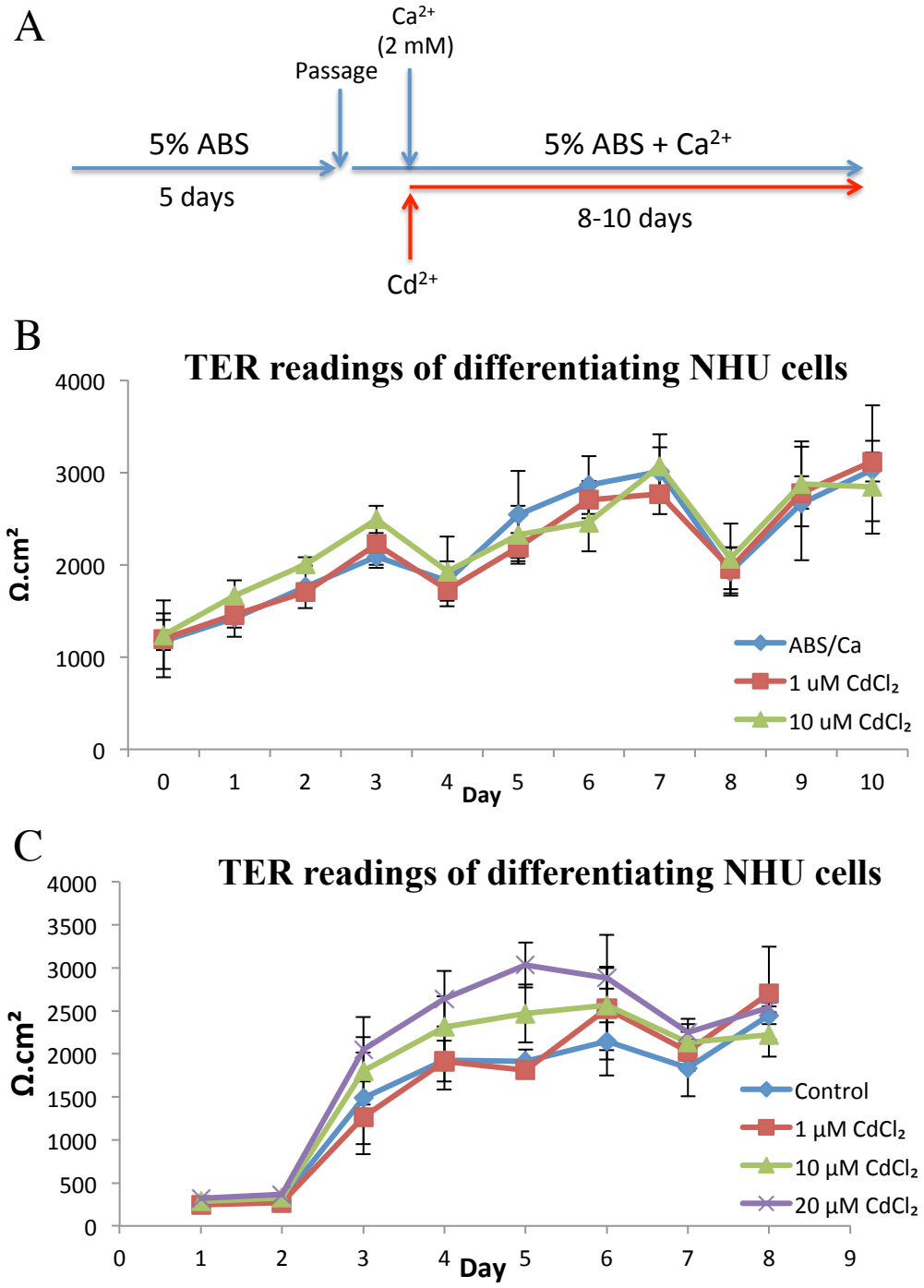

Figure 3.11. TER readings of NHU cells differentiating in the presence of cadmium. A) Treatment timeline: NHU cell cultures were pre-treated with 5% ABS for 5 days before 500,000 cells were seeded on to Snapwell or Griener membranes. Calcium concentration was increased to 2 mM 24 hours later at which point cadmium treatments started. B) NHU cell line Y1183. TER readings at day 4 and day 8 dip due to media changes having taken place. C) NHU cell line Y1279. Each data point is the average of at least 3 replicates with standard deviations shown by error bars.

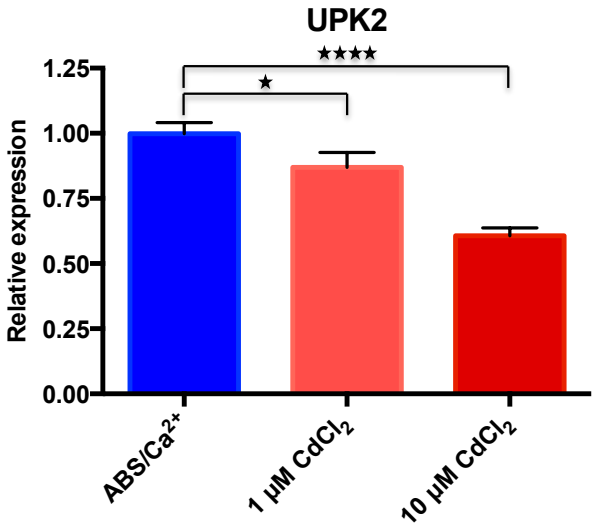

Figure 3.12. UPK2 expression in ABS/Ca^{2+} differentiated NHU cell cultures ± cadmium. Y1183 NHU cells were seeded on Snapwell™ membranes and then differentiated in the absence or presence of cadmium for 10 days at which point mRNA was harvested and UPK2 transcript expression quantified using RT-QPCR. Each value is the average of 3 replicates with standard deviations shown. One-way ANOVA with Tukey post testing was performed; where there are statistical differences between the treatments these are indicated on the graph. * p<0.05, **** p<0.0001

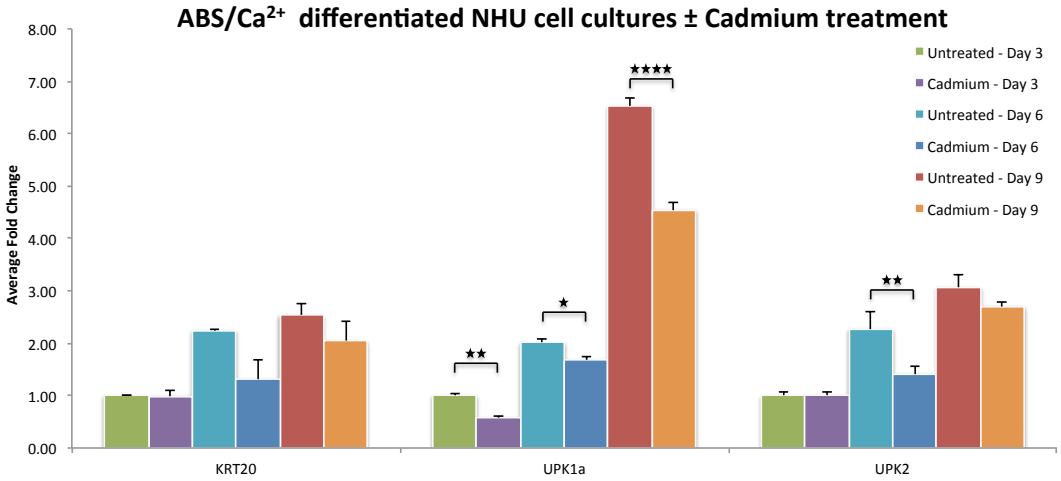

Figure 3.13. RT-QPCR results of mRNA expression for three archetypal differentiation-associated genes in ABS/Ca^{2+} differentiated cell cultures at day 3, 6 and 9. Each value is the average of 3 technical replicates with standard deviation shown. One-way ANOVAs with Turkey post testing was performed; where there are statistical differences between the treatments these are indicated on the graphs. * p<0.05 ** p<0.01, *** p<0.001, **** p<0.0001

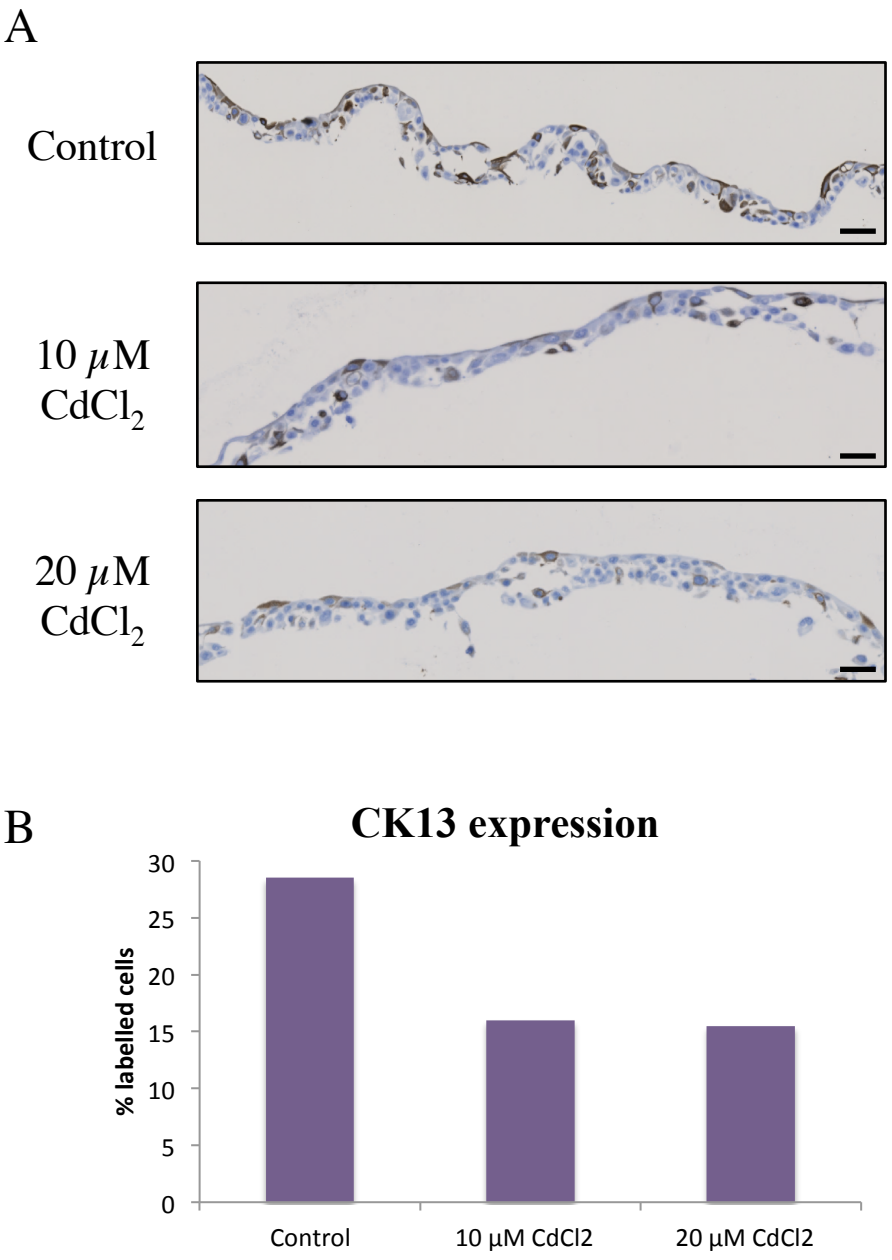

Figure 3.14. CK13 expression in cadmium exposed ABS/Ca^{2+} differentiated NHU cell cultures. A) NHU cells pre-treated with 5% ABS were seeded on to Snapwell™ inserts. Cells were cultured for 9 days ± 10 or 20 µM $CdCl_2$ before cell sheets were fixed in 10% (v/v) formalin. Cell sheets were embedded in paraffin wax before immunolabelling was performed using an indirect streptavidin 'ABC' immunoperoxidase method and then counterstained in haematoxylin. Cell sheets were imaged using a Zeiss AxioScan.Z1 slide scanner. Scale bar, 25 µM. B) Image analysis (HistoQuest by TissueGnostics) was used to quantify the percentage of CK13 labelled cells.

Cadmium treatment after ABS/Ca^{2+} differentiation

To study the effect cadmium had on already differentiated cells, ABS/Ca^{2+} differentiation was performed on NHU cell cultures to form cell sheets on Snapwell membranes. Once a stable barrier was formed (>2500 Ω.cm²), the differentiated cell sheets were exposed to 1, 10 or 20 µM $CdCl_2$ for 7 days in triplicate. The TER readings taken from cultures exposed to cadmium did not differ significantly from controls (Figure 3.15). At all cadmium concentrations the barrier was able to be maintained including at 20 µM $CdCl_2$ which was toxic to the proliferative NHU cells.

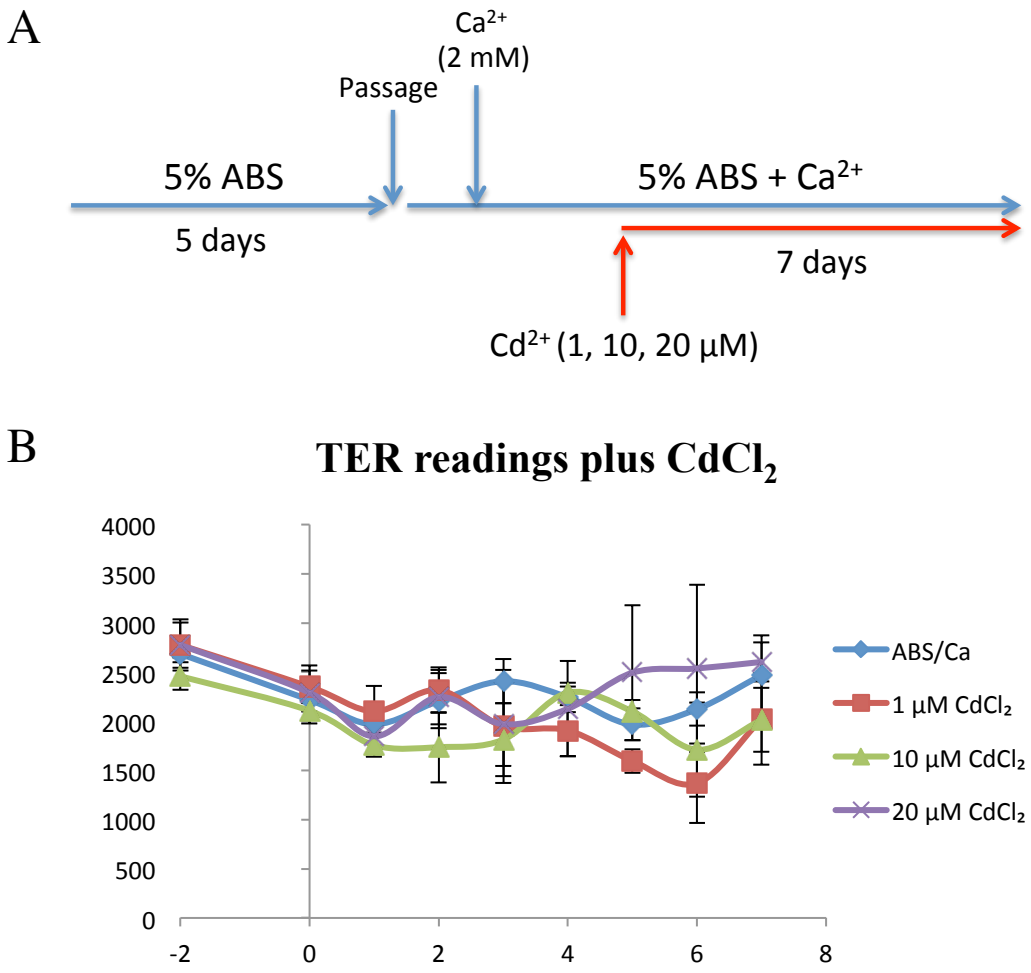

Figure 3.15. TER readings of differentiated cell sheets in the presence of cadmium. A) Treatment timeline: NHU cell cultures were pre-treated with 5% ABS for 5 days before 500,000 cells were seeded on to each Griener membrane, 24 hours later calcium was added. When all barriers exceeded 2500 Ω.cm² the cadmium was added. B) NHU cell line Y1237. Three replicates were performed for each concentration. Standard deviations are shown by error bars.

Wounding and recovery of differentiated cell sheets in the presence of cadmium

Differentiated cell sheets can be wounded and their ability to recover monitored by measuring TER. To see if the presence of cadmium affected this ability to recover, differentiated cell sheets were scratch wounded and then allowed to recover in presence of 1, 10 and 20 μM $CdCl_2$. TER readings were taken every 3 hours to monitor the recovery of the barrier (Figure 3.16 A). Although the barrier fully recovered at each cadmium concentration there was a delayed recovery after wounding in the presence of cadmium compared to the control. This was statistically significant at 6 and 9 hours for 10 μM $CdCl_2$ (Figure 3.16 B) and 6, 9 and 12 hours for 20 μM $CdCl_2$ (Figure 3.16 C). Repetitive wounding (3x) performed on cell sheets still led to barrier reformation with TER readings recovering to at least 4500 $\Omega.cm^2$ after each wounding (Table 3.1).

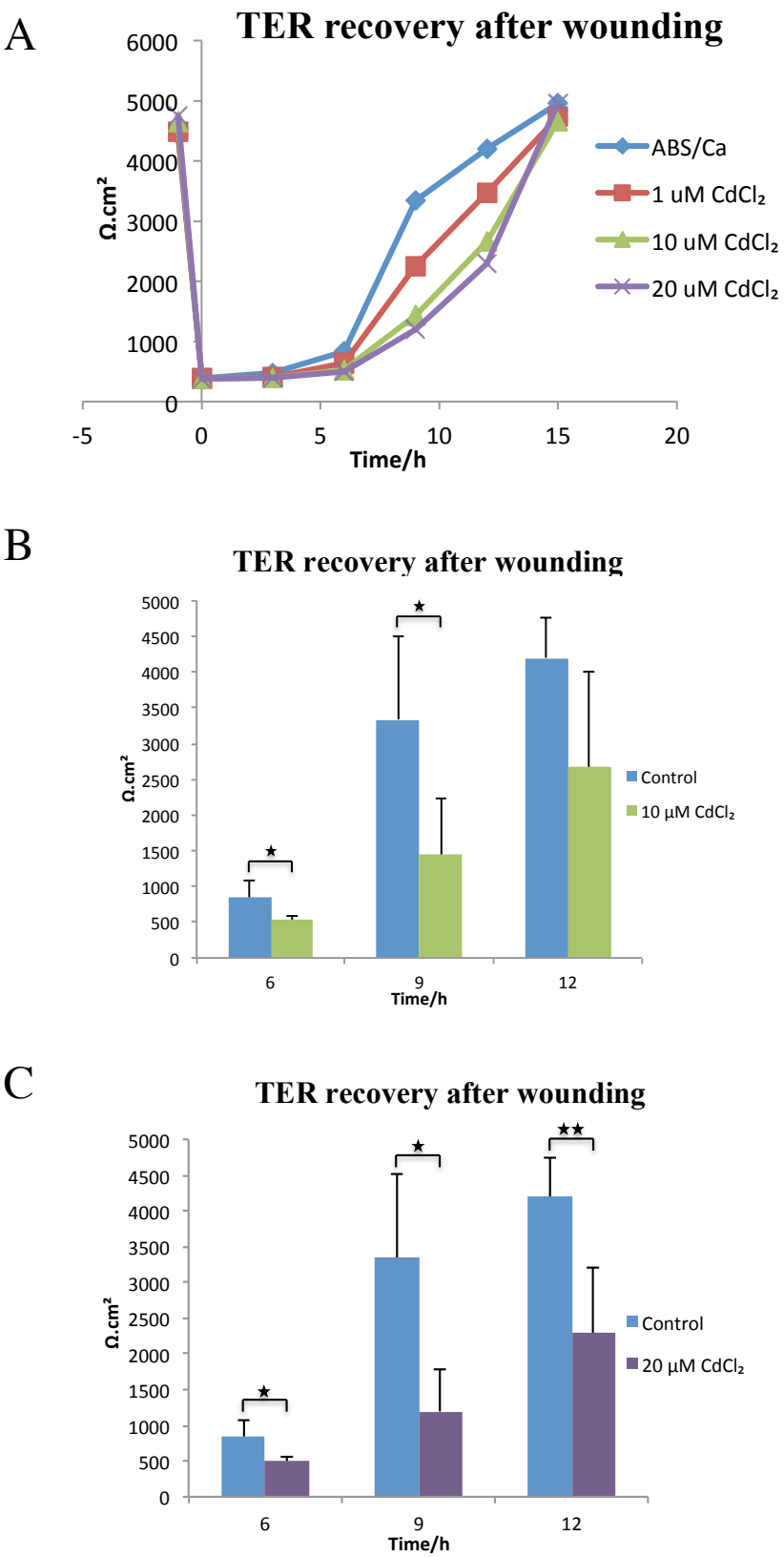

Figure 3.16. A) TER readings of barrier recovery in the presence of cadmium (Y1244). Graphs show TER readings of barrier recovery after wounding, in the presence of 10 (B) or 20 (C) µM cadmium chloride. Error bars represent the standard deviation of 4 experimental replicates. *p<0.05, **p<0.01 Unpaired t test with Welch's correction applied.

Table 3.1. TER readings of barrier reformation after repetitive wounding (Y1244). All values in Ω.cm² ± standard deviations.

	After 1st Wounding	After 2nd Wounding	After 3rd Wounding
ABS/Ca Control	5390 ± 496	4643 ± 448	4956 ± 806
1 μM $CdCl_2$	5643 ± 752	5252 ± 234	4735 ± 752
10 μM $CdCl_2$	5628 ± 416	4678 ± 1354	4660 ± 416
20 μM $CdCl_2$	5694 ± 292	4635 ± 926	4958 ± 292

3.3.2.2 Differentiated NHU cells – TZPD method

Cadmium pre-treatment of NHU cell cultures before TZPD differentiation

Proliferative NHU cell cultures were maintained in control KSFMc medium or treated with 1 or 10 μM $CdCl_2$ before undergoing TZPD differentiation. The cultures that were treated with 1 and 10 μM $CdCl_2$ were split in to two groups; one group had the cadmium removed before TZPD differentiation while the other group remained in cadmium while undergoing TZPD differentiation.

Cultures pre-treated with cadmium showed non-significant differences in the expression of differentiation-associated proteins (Figure 3.17). By contrast, cultures maintained in cadmium showed a decrease in the three differentiation markers Claudin 4 and 5 and CK13. CK14 a marker of proliferative NHU cells in culture remained high when cadmium was present.

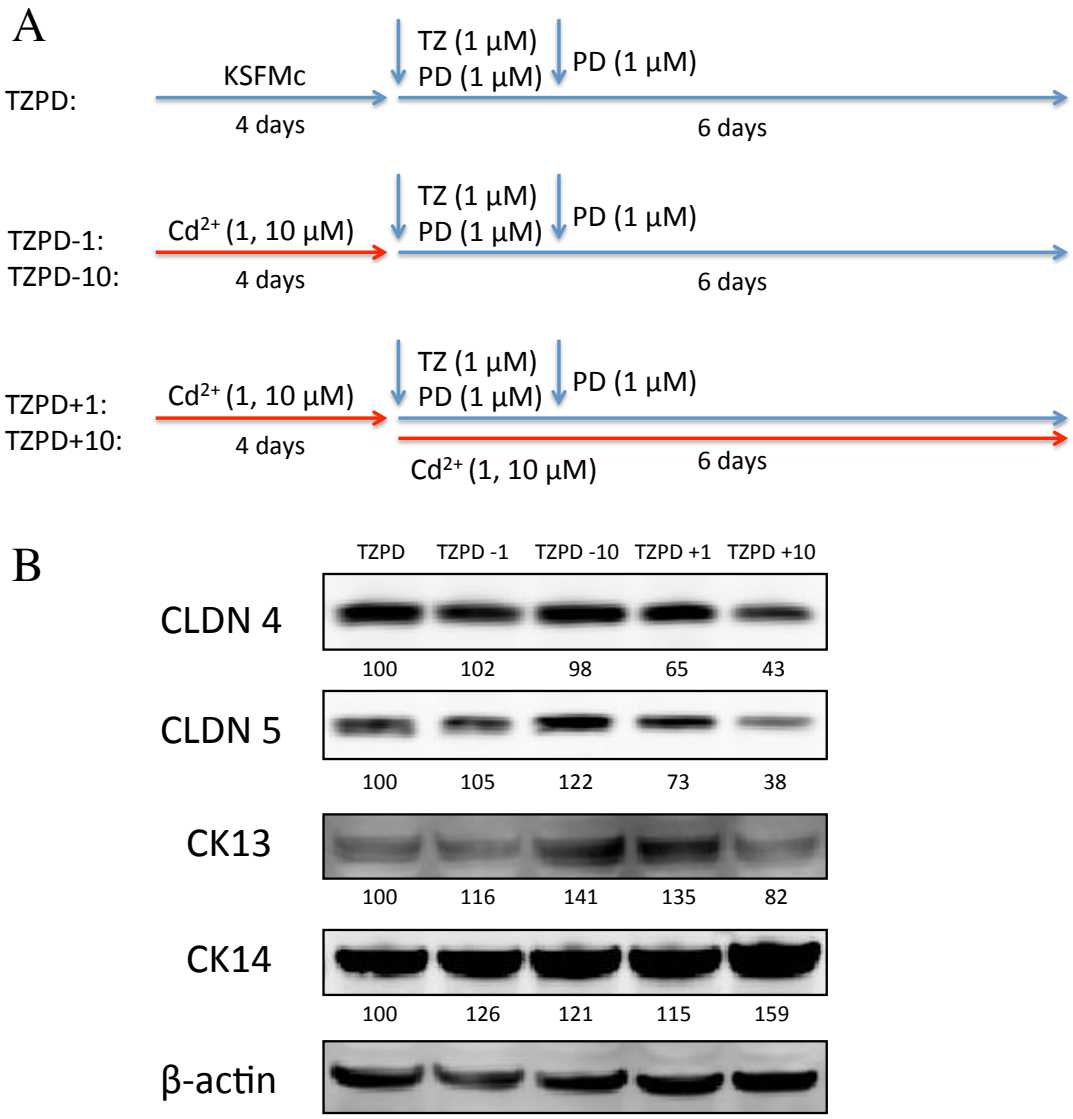

Figure 3.17. Western blot analysis of NHU cells pre-treated with KSFMc only , 1 µM $CdCl_2$ and 10 µM $CdCl_2$ before TZPD induced differentiation in the absence (-) or presence (+) of cadmium. A) Treatment timelines. B) Cells were lysed using SDS lysis buffer and then sonicated. Protein concentration was measured using a Bradford assay. 4-12% Bis-Tris gels were loaded with 20 µg of protein and run at 200 V in MES running buffer. Protein was blotted on to PVDF membranes using the Novex apparatus for 2 hours at 30 V. Membranes were blocked in Odyssey blocking buffer, incubated with primary antibodies overnight at 4°c, and secondary antibodies for one hour at ambient temperature then scanned on the Li-Cor imaging system. The fluorescence of each band was quantified and normalised to the loading control β-actin using Odyssey software.

Cadmium treatment during TZPD differentiation

Proliferative NHU cells were treated with or without TZPD in the absence or presence of cadmium for up to 7 days. At day 3 and day 7 time points the cells were harvested for mRNA with RTQPCR performed to measure the transcript expression of known differentiation markers.

It was found that exposure to cadmium resulted in a failure to upregulate KRT13 (Figure 3.18 C), a marker of transitional (or urothelial)-type differentiation, as well as the late archetypical differentiation-associated genes UPK1a (Figure 3.18 A), UPK2 (Figure 3.18 B) and KRT20 (Figure 3.18 D) at both day 3 and day 7.

There were statistically significant differences for all four differentiation-associated genes when comparing untreated with TZPD cell cultures and TZPD with TZPD Cd^{2+} treated cell cultures at day 3.

Further treatments with two independent NHU cell lines (Figure 3.19) confirmed the initial observation that cadmium exposure during TZPD differentiation led to a failure of NHU cell cultures to fully differentiate, as the four differentiation-associated genes UPK1a, UPK2, KRT13 and KRT20 all showed reduced expression when cadmium was present.

There were statistically significant differences for all four differentiation-associated genes when comparing untreated with TZPD cell cultures and TZPD with TZPD Cd^{2+} treated cell cultures.

A

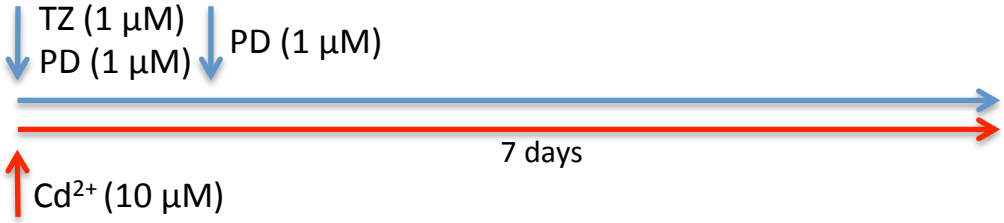
TZ (1 µM)
PD (1 µM)
PD (1 µM)
7 days
Cd2+ (10 µM)

B

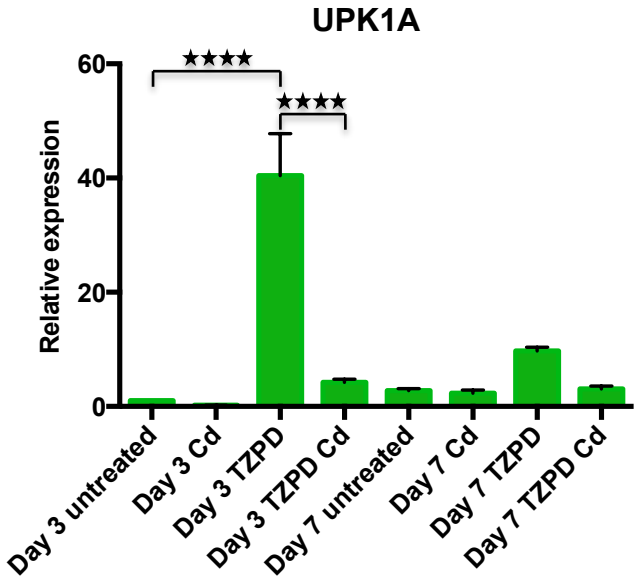
UPK1A
Relative expression
60
40
20
0
Day 3 untreated
Day 3 Cd
Day 3 TZPD
Day 3 TZPD Cd
Day 7 untreated
Day 7 Cd
Day 7 TZPD
Day 7 TZPD Cd

C

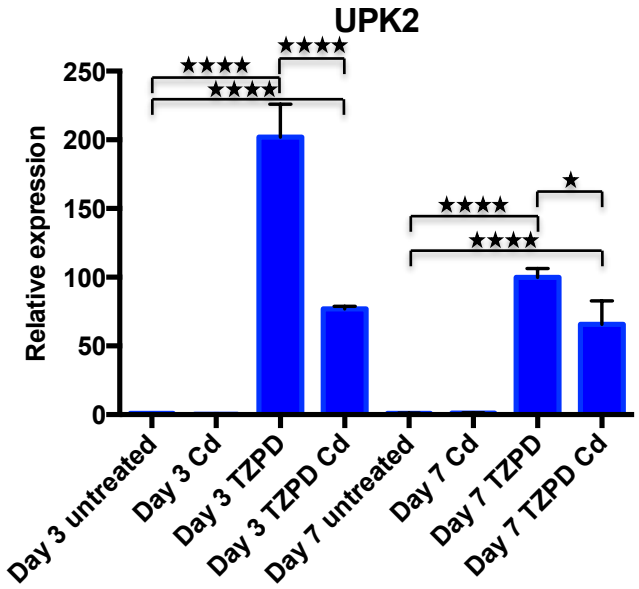
UPK2
Relative expression
250
200
150
100
50
0
Day 3 untreated
Day 3 Cd
Day 3 TZPD
Day 3 TZPD Cd
Day 7 untreated
Day 7 Cd
Day 7 TZPD
Day 7 TZPD Cd

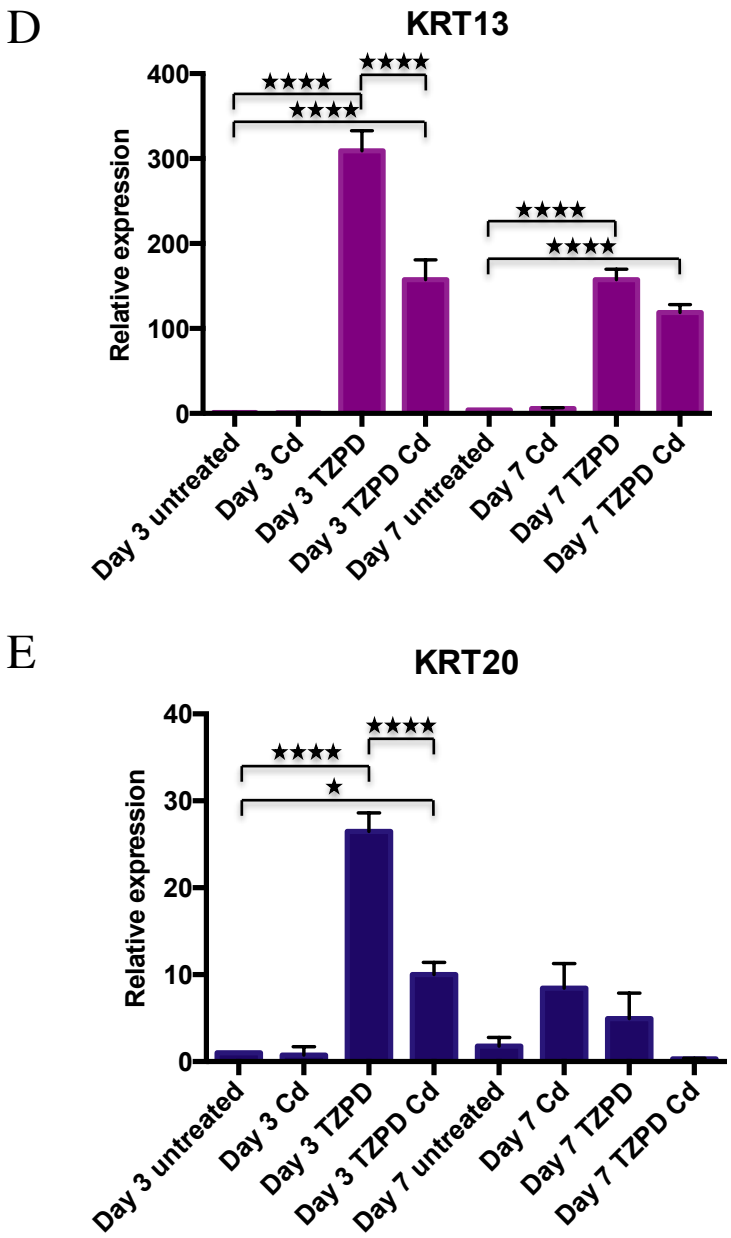

Figure 3.18. RT-QPCR data for four differentiation genes. Y1226 NHU cell cultures were treated ± TZPD ± 10 µM $CdCl_2$ for 7 days (A). mRNA was harvested from the cultures at day 3 and 7, with RTQPCR performed to quantify the relative expression of four differentiation-associated genes B) UPK1a, C) UPK2, D) KRT13 and E) KRT20. Each value is the average of 3 replicates with standard deviations shown by error bars. One-way ANOVAs with Tukey post testing was performed; where there are statistical differences between the TZPD treatments these are indicated on the graphs. * p<0.05 ** p<0.01, *** p<0.001, **** p<0.0001.

A

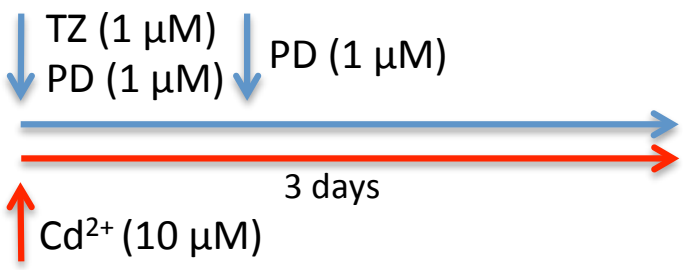
TZ (1 µM)
PD (1 µM)
PD (1 µM)
3 days
Cd2+ (10 µM)

B

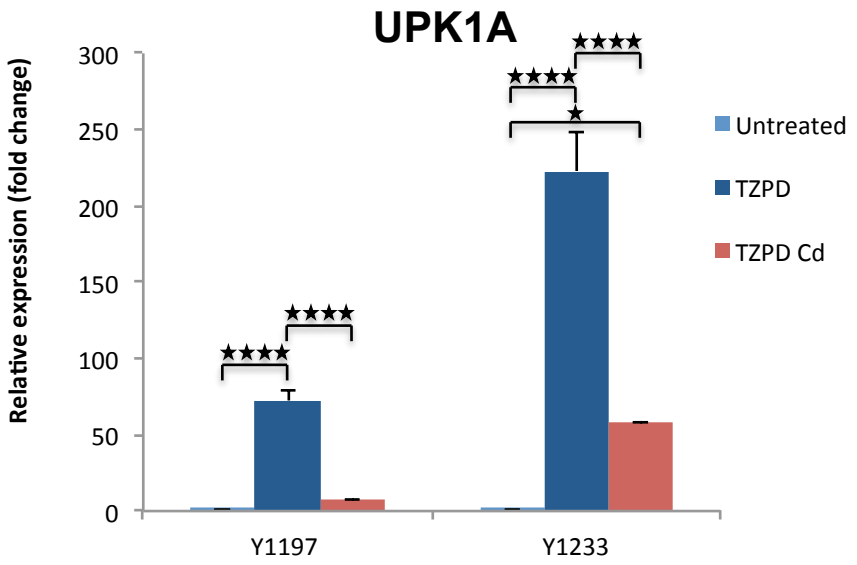
UPK1A
Relative expression (fold change)
300
250
200
150
100
50
0
Y1197
Y1233
Untreated
TZPD
TZPD Cd

C

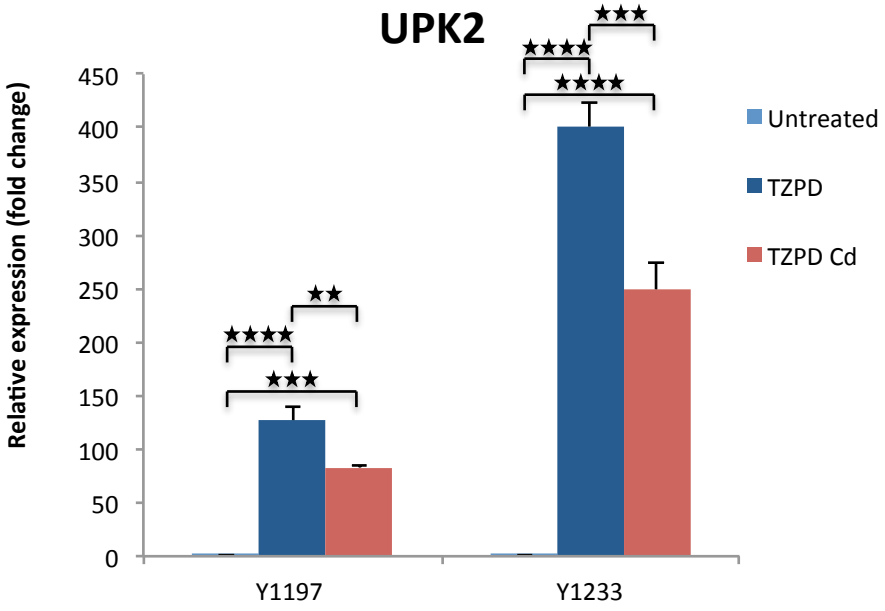
UPK2
Relative expression (fold change)
450
400
350
300
250
200
150
100
50
0
Y1197
Y1233
Untreated
TZPD
TZPD Cd

D

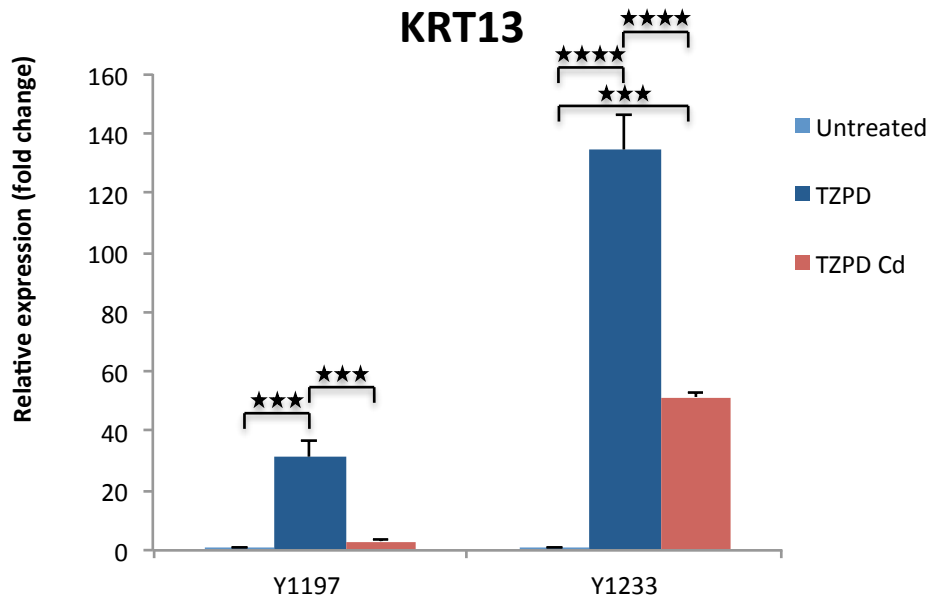

E

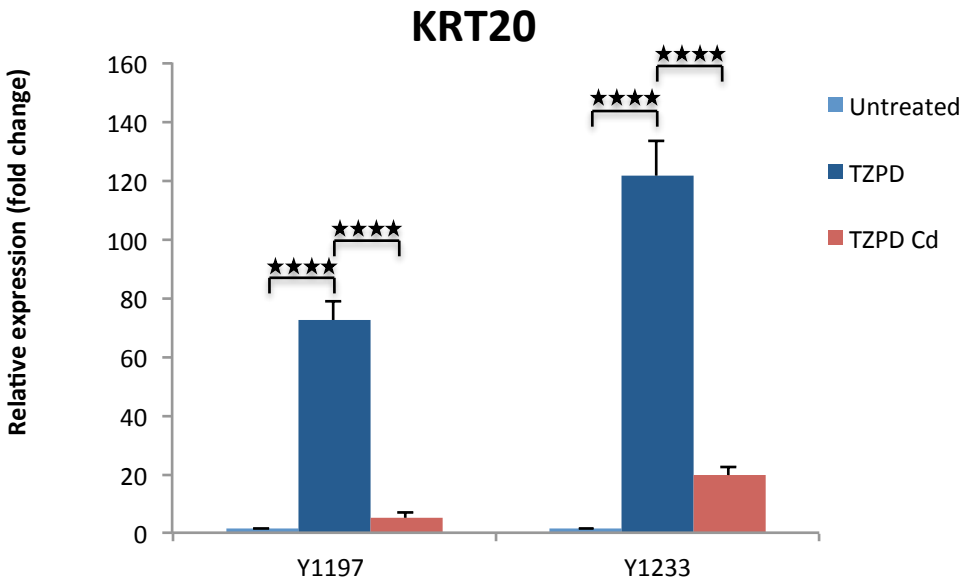

Figure 3.19. RT-QPCR data of four differentiation genes in two independent NHU cell lines. Y1197 and Y1233 NHU cell lines were cultured ± TZPD ± 10 µM $CdCl_2$ for 3 days before mRNA was harvested (A). RTQPCR was performed to quantify the relative expression of B) UPK1a, C) UPK2, D) KRT13 and E) KRT20. Each value is the average of 3 replicates with standard deviation shown as error bars. One-way ANOVAs with Tukey post testing was performed; where there are statistical differences between the treatments these are indicated on the graphs. * p<0.05 ** p<0.01, *** p<0.001, **** p<0.0001.

Immunofluorescence for CK20 was performed on NHU cell cultures which had been treated with or without TZ/PD and cadmium for 6 days (Figure 3.20A). TissueQuest software was then used to determine the percentage of CK20 labelled cells from the IF images (Figure 3.20B). These results support the RT-QPCR data shown above which show that CK20 expression was decreased in the presence of cadmium.

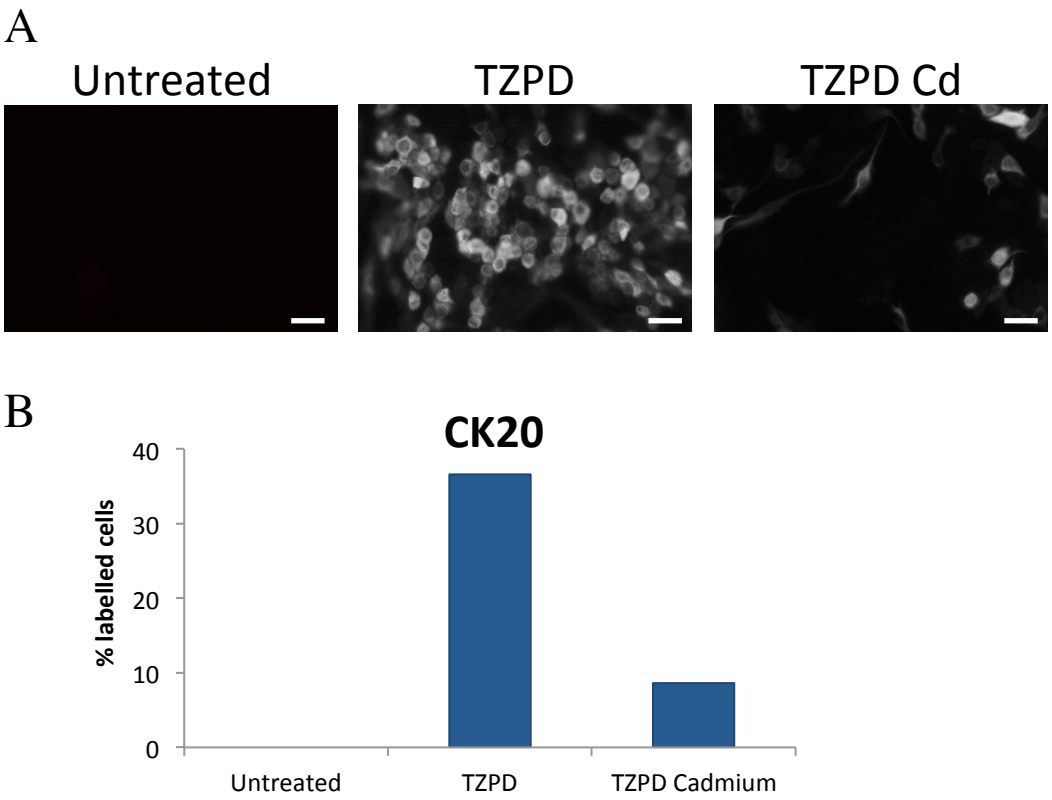

Figure 3.20. Cytokeratin 20 expression in cadmium exposed TZPD differentiating NHU cell cultures. A) Representative images of CK20 immunolabelled cells. NHU cells were seeded at a concentration of $1x10^5$ cells mL^{-1} on to 12-well slides. Cells were cultured for 6 days ± TZ/PD ± 10 µM $CdCl_2$ before being fixed in methanol:acetone. Cells were immunolabelled using mouse primary antibodies and goat anti-mouse secondary antibodies. Nuclei were stained with Hoechst 33258. Scale bar, 10 µM. B) Image analysis (TissueQuest by TissueGnostics) was used to quantify the percentage of CK20 labelled cells.

CK13/14 Switch and Cadmium

A switch in expression occurs between KRT14 and KRT13 in NHU cell cultures upon differentiation. KRT14 is a marker of squamous metaplasia and is expressed in proliferative, but not differentiated NHU cells, whereas KRT13 is only expressed in differentiated NHU cells. KRT14 transcript was not down regulated in the TZ/PD-differentiated cells in the presence of cadmium in two independent cell lines Y1226 (Figure 3.21 A) and Y1236 (Figure 3.21 B), suggesting the cells may have remained in a more squamous phenotype.

Immunofluorescence for CK14 was performed on NHU cell cultures that had been treated with or without TZ/PD and cadmium for 6 days (Figure 3.22 A). TissueQuest software was then used to determine the percentage of CK14 labelled cells from the IF images (Figure 3.22 B). These results support the RT-QPCR and western blot data (Figure 3.23), showing that in the presence of cadmium TZ/PD-induced differentiated cells continue to express CK14 while CK13 expression remained low.

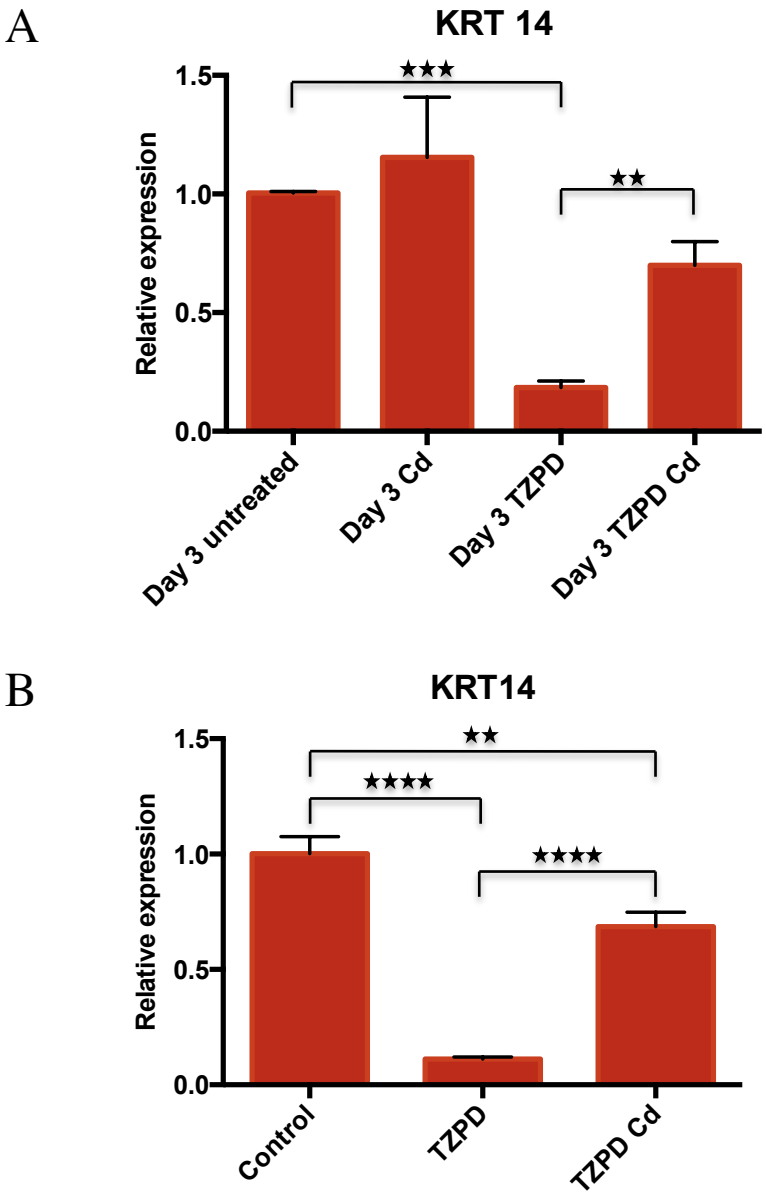

Figure 3.21. RTQPCR results of KRT14 mRNA expression in two independent NHU cell lines ± TZ/PD ± Cd. A) Y1226 NHU cell cultures were treated ± TZPD ± 10 µM $CdCl_2$ for 7 days. mRNA was harvested from the cultures at day 3 and 7, with RTQPCR performed to quantify the relative expression of KRT14. B) Y1197 NHU cell lines were cultured ± TZPD ± 10 µM $CdCl_2$ for 3 days before mRNA was harvested and RTQPCR performed to quantify the relative expression of KRT14. Each value is the average of 3 replicates with standard deviation shown. One-way ANOVAs with Tukey post testing was performed; where there are statistical differences between the treatments these are indicated on the graphs. * p<0.05 ** p<0.01, *** p<0.001, **** p<0.0001.

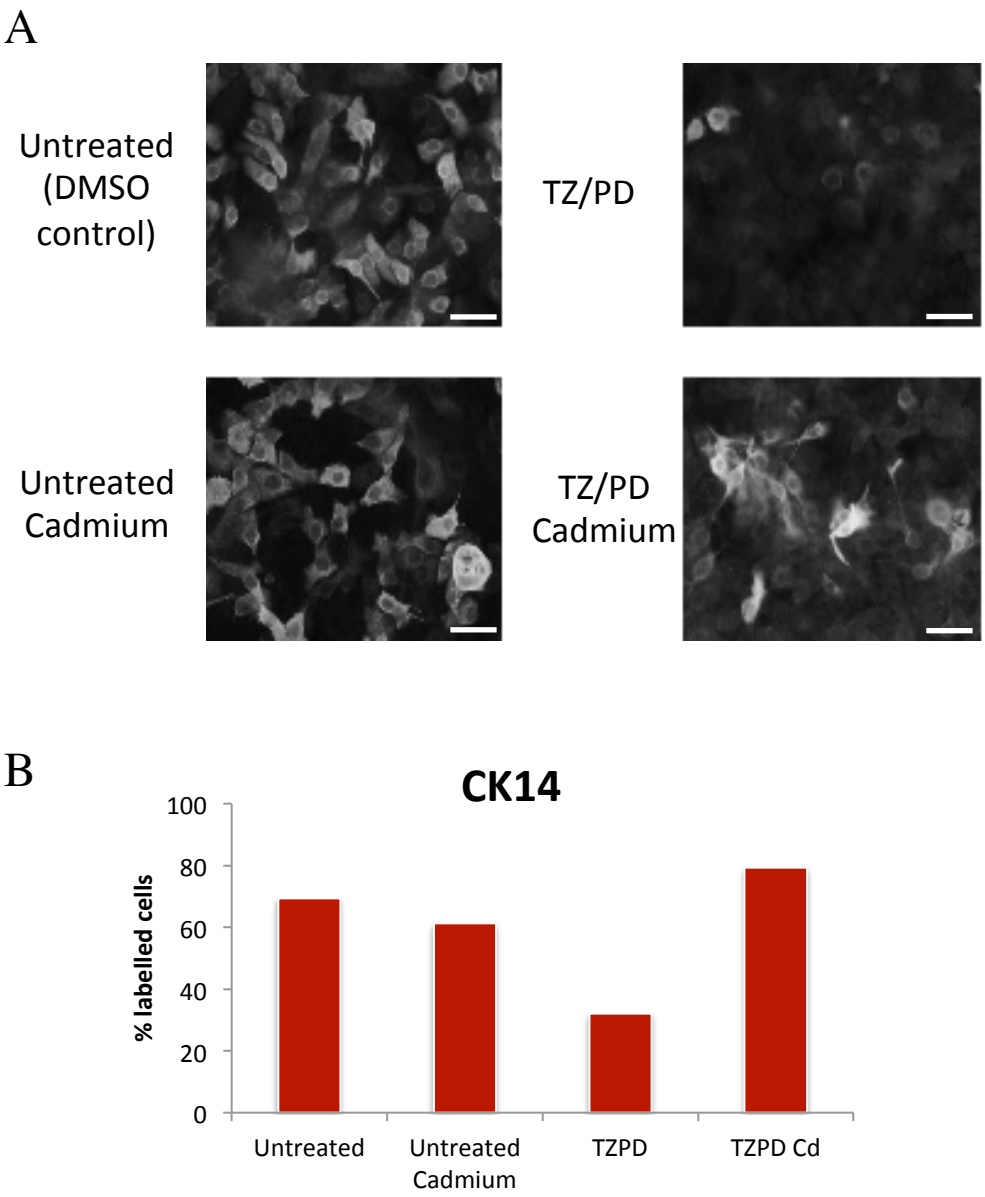

Figure 3.22. Effect of cadmium on CK14 protein expression. A) CK14 labelled immunofluorescence images of NHU cell cultures ± TZ/PD ± Cd. NHU cells were seeded at a concentration of $1x10^5$ cells mL^{-1} on to 12-well slides. Cells were cultured for 6 days before being fixed in methanol:acetone. Cells were immunolabelled using mouse primary antibodies and goat anti-mouse secondary antibodies. Nuclei were stained with Hoechst 33258. Scale bar, 10 µM. B) Quantification results from TissueQuest software, used to determine the percentage of labelled CK14 cells in the NHU cells cultures ± TZ/PD ± Cd.

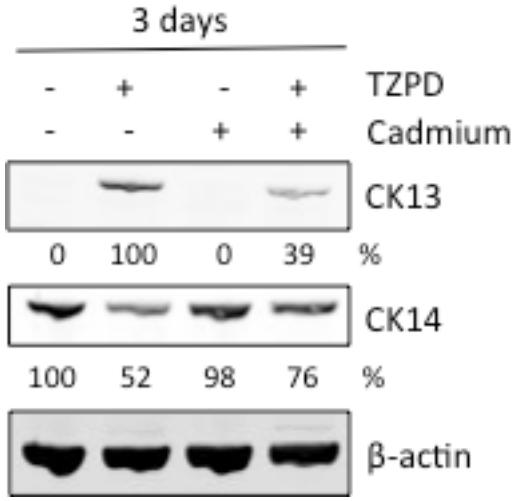

Figure 3.23. Western blot analysis for cytokeratin 13 and 14 in NHU cell cultures ±TZ/PD ± cadmium. Cells were lysed using SDS lysis buffer and then sonicated. Protein concentration was measured using a Bradford assay. 4-12% Bis-Tris gels were loaded with 20 µg of protein and run at 200 V using MES running buffer. Protein was blotted on to PVDF membranes using the Novex apparatus for 2 hours at 30 V. Membranes were blocked in Odyssey blocking buffer, incubated with primary antibodies overnight at 4°c, and secondary antibodies for one hour at ambient temperature then scanned on the Li-Cor imaging system. The fluorescence of each band was quantified and normalised to the loading control β-actin using the Odyssey software.

3.3.3 Transcription factors involved in urothelial differentiation

The expression of six transcription factors known to act downstream of PPARγ in urothelial differentiation (FOXA1, IRF1, GATA3, ELF3, KLF5 and GRHL3) was investigated using RT-PCR (Figure 3.24). An up regulation of all six transcription factors was seen between the proliferative DMSO treated control and TZPD induced differentiated cells. By contrast, no differences were seen between TZPD and TZPD Cd^{2+} treated NHU cell cultures.

Quantitative PCR looking at two known intermediary transcription factors, FOXA1 and IRF-1 showed that there was no statistical difference between transcript expression levels at day 1 and 3 in TZPD induced NHU cell cultures when cadmium was present or not (Figure 3.25).

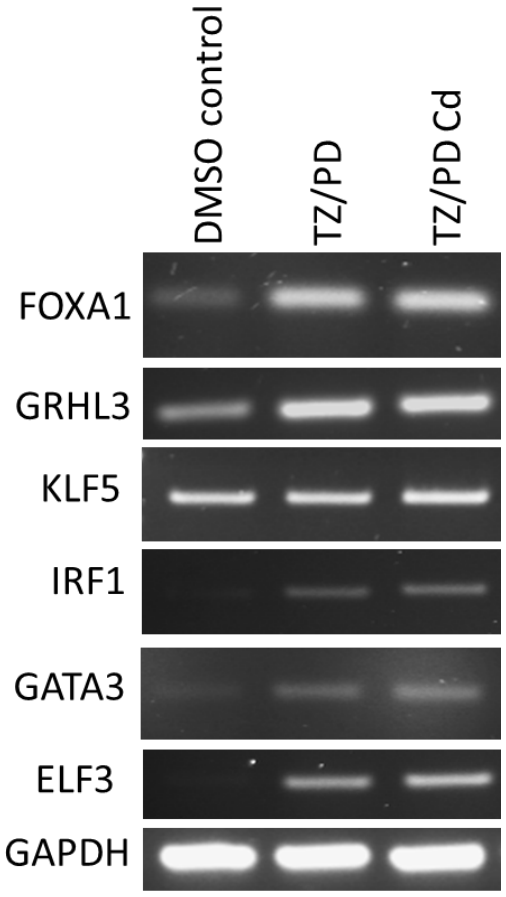

Figure 3.24. RTPCR of known transcription factors involved in urothelial differentiation. Y1236 NHU cell cultures were treated ± TZPD ± 10 µM $CdCl_2$ for 3 days before mRNA was harvested and RTPCR was performed to look at expression of known transcription factors involved in urothelial differentiation.

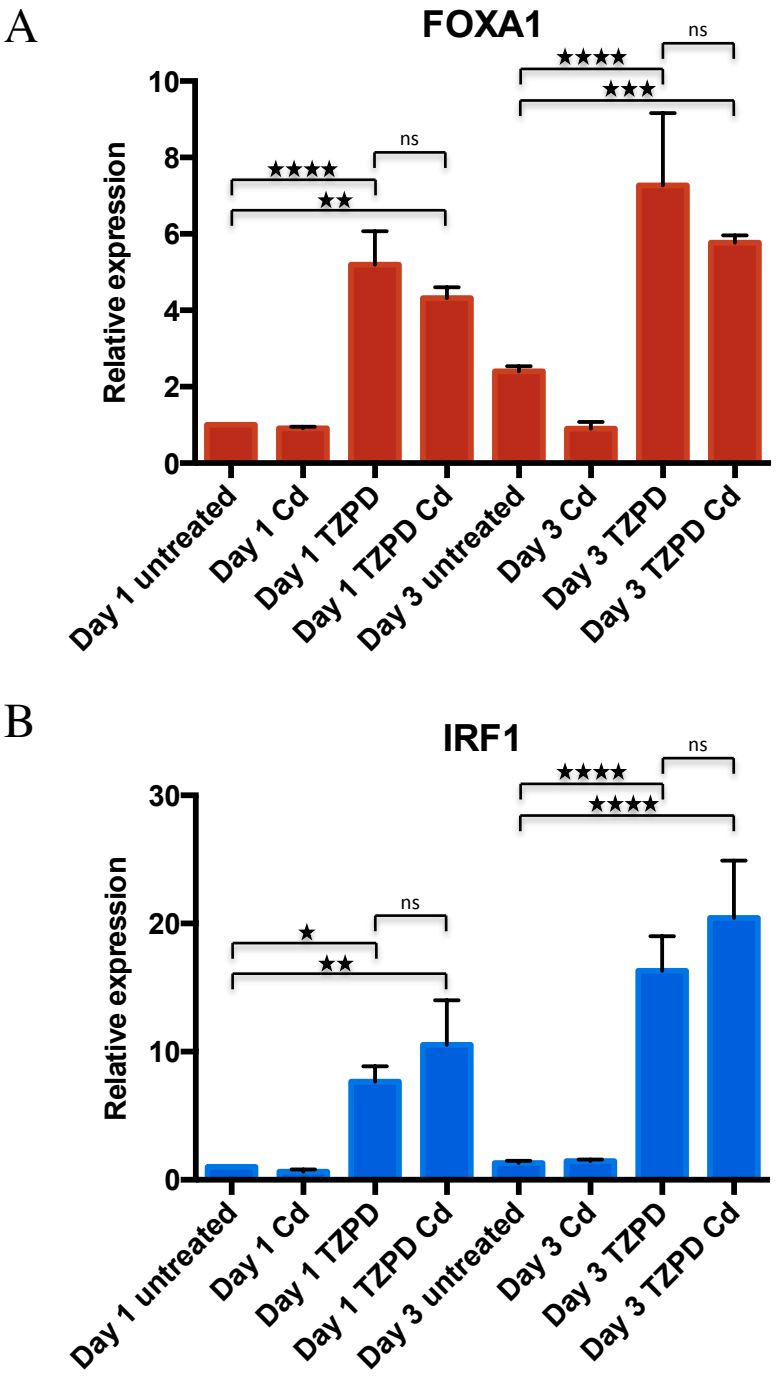

Figure 3.25. RT-QPCR data for two intermediary transcription genes involved in urothelial differentiation. Y1226 NHU cell cultures were treated ± TZPD ± 10 µM $CdCl_2$ for 3 days. mRNA was harvested from the cultures at day 1 and 3, with QPCR performed to quantify the relative expression of the two transcription factors A) FOXA1 and B) IRF-1. Each value is the average of 3 replicates with standard deviation shown. One-way ANOVAs with Tukey post testing was performed; where there are statistical differences between the TZPD treatments these are indicated on the graphs. * p<0.05 ** p<0.01, *** p<0.001, **** p<0.0001, ns not significant. Attention is drawn to the observation that there is no significant difference between TZPD and TZPD Cd at day 1 and day 3.

3.3.4 Tumour suppressor gene expression

The tumour suppressor, p16, was shown to be downregulated in cadmium exposed proliferative NHU cells, at transcript level (Figure 3.26) and at a protein level (Figure 3.27) and in TZ/PD-induced differentiated NHU cells (Figure 3.28).

NHU cell cultures were differentiated and seeded on to Snapwell™ membranes using the standard ABS/Ca^{2+} differentiation protocol. The NHU cell cultures were then treated with (1 or 10 µM) or without cadmium for ten days. Gene expression for tumour suppressor genes (p16, RASSF1A and APC) was then assessed by RTQPCR. Transcript expression for p16 and APC was significantly inhibited by cadmium treatment (Figure 3.29).

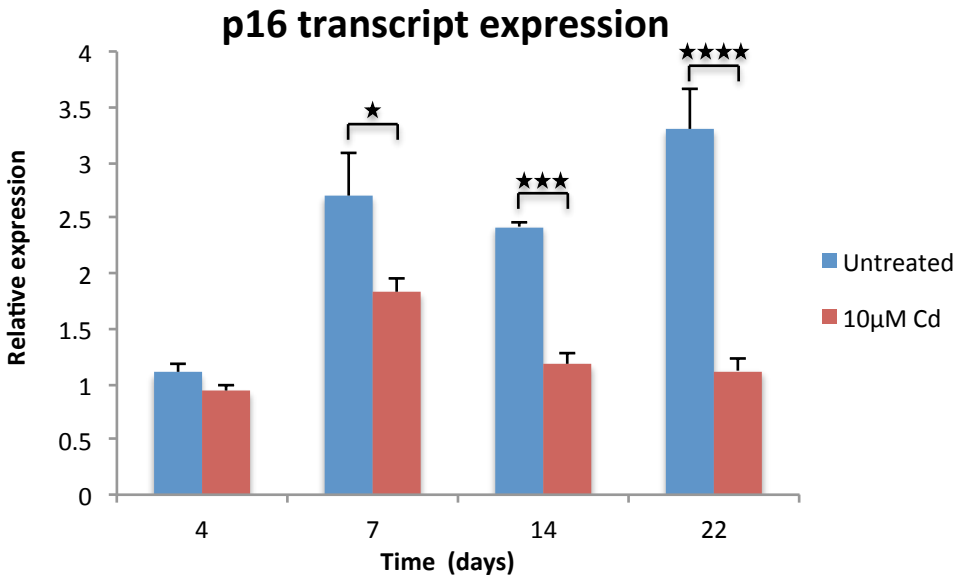

Figure 3.26. RT-QPCR for p16 transcript expression in proliferative NHU cell cultures. Proliferative NHU cell cultures (Y1233) were treated for ± 10 µM $CdCl_2$ 22 days. mRNA was harvested from the cultures at day 4, 7 , 14 and 22, with RTQPCR performed to quantify p16 transcript expression. Each value is the average of 3 technical replicates with standard deviation shown. One-way ANOVA with Tukey post testing was performed; where there are statistical differences between the treatments these are indicated on the graphs. * p<0.05 ** p<0.01, *** p<0.001, **** p<0.0001.

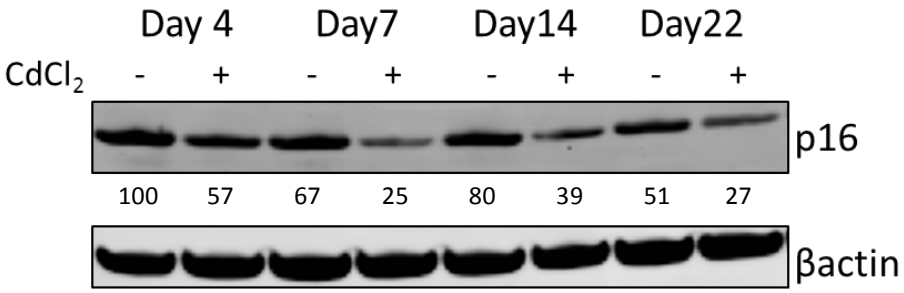

Figure 3.27. Western blot analysis for p16 expression in proliferative NHU cell cultures. Cells were lysed using SDS lysis buffer and then sonicated. Protein concentration was measured using a Bradford assay. 4-12% Bis-Tris gels were loaded with 20 µg of protein and run at 200 V using MES running buffer. Protein was blotted on to PVDF membranes using the Novex apparatus for 2 hours at 30 V. Membranes were blocked in Odyssey blocking buffer, incubated with primary antibodies overnight at 4°c, and secondary antibodies for one hour at ambient temperature then scanned on the Li-Cor imaging system. The fluorescence of each band was quantified and normalised to the loading control β-actin using the Odyssey software. Numbers quantifying the percentage intensity of the bands are displayed below the corresponding bands.

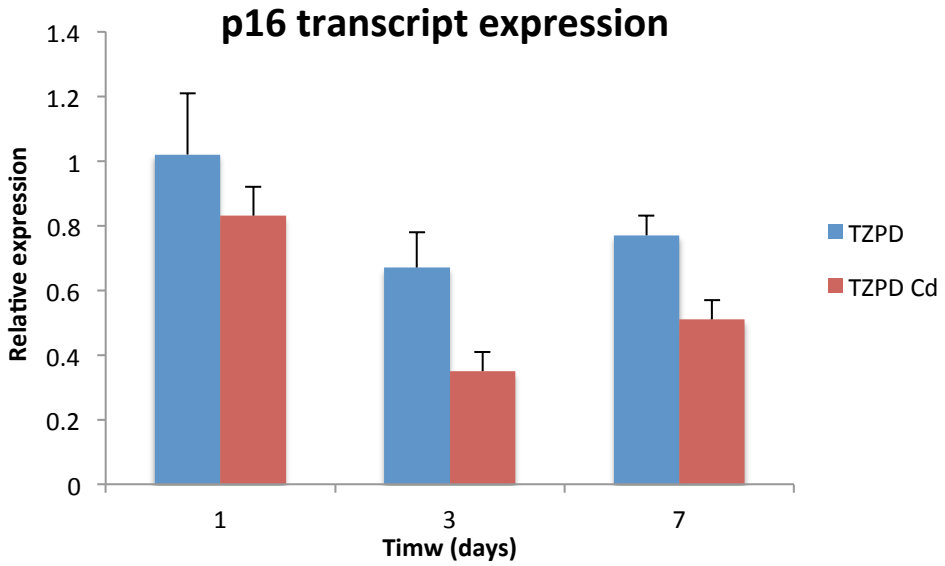

Figure 3.28. RT-QPCR for p16 transcript expression in TZPD-induced differentiated NHU cell cultures. Y1226 NHU cell cultures were treated ± TZPD ± 10 µM $CdCl_2$ for 7 days. mRNA was harvested from the cultures at day 1, 3 and 7, with RTQPCR performed to quantify transcript expression of p16. Each value is the average of 3 technical replicates with standard deviation shown.

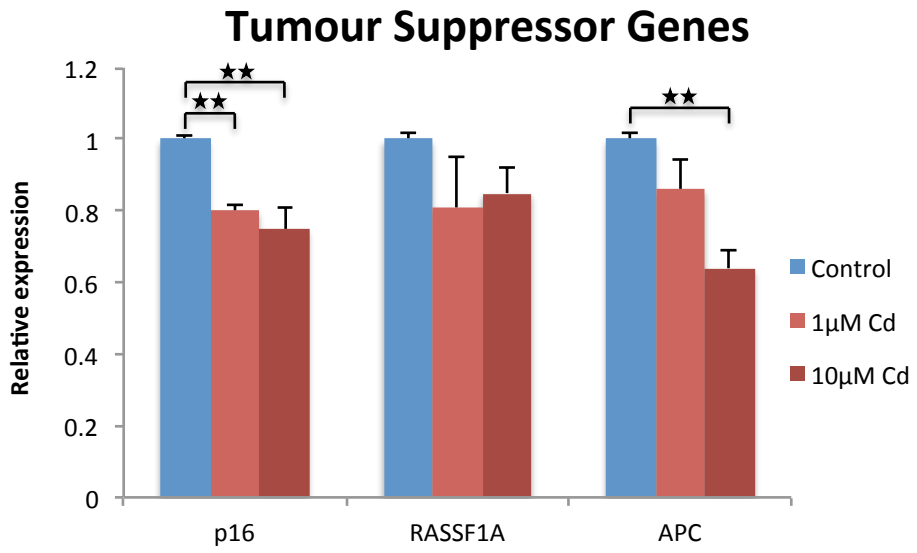

Figure 3.29. RT-QPCR for p16, RASSF1A and APC transcript expression in ABS/Ca2+ differentiated NHU cell cultures. Y1183 NHU cells were seeded on Snapwell™ membranes and differentiated in the absence or presence of cadmium for 10 days at which point mRNA was harvested and quantified using RT-QPCR. Each value is the average of 3 technical replicates with standard deviation shown. One-way ANOVAs with Tukey post testing were performed; where there are statistical differences between the treatments these are indicated on the graphs. * p<0.05 ** p<0.01, *** p<0.001, **** p<0.0001.

3.4 Summary

- **Proliferation**

Proliferative NHU cell cultures could be exposed to cadmium concentrations up to 10 μM $CdCl_2$ before cytotoxicity occurred; cultures exposed to 10 μM $CdCl_2$ showed a reduced proliferation rate, but this was reversible upon withdrawal of cadmium from the medium.

- **ABS/Ca^{2+} differentiation**

Pre-treatment of NHU cell cultures with cadmium before ABS/Ca^{2+} differentiation had no significant effect upon differentiation.

The presence of cadmium during differentiation had no effect on barrier formation as measured by TER, but it did affect the rate of barrier recovery following wounding. At the transcript expression level, three terminal markers of differentiation (UPK1a, UPK2 and KRT20) were shown to be downregulated as a consequence of cadmium exposure. The transitional differentiation marker CK13 was also downregulated by cadmium exposure during ABS/Ca^{2+} differentiation.

- **TZPD differentiation**

Exposure of NHU cell cultures to cadmium during TZ/PD-induced differentiation compromised their ability to undergo urothelial differentiation as shown by a decrease in transcript of four differentiation-associated genes (UPK1a, UPK2, KRT13 and KRT20). There was also a failure to downregulate KRT14, a maker of squamous metaplasia.

- **Transcription factors**

Cadmium exposure during TZ/PD-induced differentiation did not affect transcript expression of the PPARγ-induced intermediary transcription factors IRF-1 and FOXA1 or on four other transcription factors known to be involved in urothelial differentiation. These results suggest that cadmium affects urothelial differentiation downstream of the initial PPARγ -induced effects.

- **Tumour suppressor genes**

Expression of the tumour suppressor gene p16 was downregulated during cadmium treatment in proliferative and differentiating NHU cell cultures. Transcript

expression of two further tumour suppressor genes RASSF1A and APC was downregulated by cadmium exposure in ABS/Ca^{2+} differentiated cultures.

4 Epigenetic mechanisms in cadmium exposure

4.1 Aims

Trichostatin A (TSA), a HDAC inhibitor and 5-azacytidine, a DNA methyltransferase inhibitor are often used in studies to examine whether epigenetic mechanisms are involved (Vallot et al., 2010; Scholpa et al., 2014; Chen et al., 2015).

The aims of this chapter were to determine whether epigenetic mechanisms were involved in the ability of cadmium to silence differentiation-associated genes as reported in Chapter 3 and to identify gene expression changes that occur when NHU cell cultures were differentiated in the presence of cadmium and TSA.

The specific objectives of this chapter were to:

- Treat cadmium exposed differentiating NHU cell cultures with TSA or 5-azacytidine.
- Perform promoter analysis on differentiation-associated genes that responded differentially to TSA in order to identify transcription factor binding motifs that differ between them.
- Identify genes that were up/downregulated by cadmium and TSA in TZPD-differentiating NHU cell cultures using Agilent microarrays.
- Relate the changes determined from the microarrays to:
    1. Known markers of differentiation.
    2. Transcription factors involved in urothelial differentiation.
    3. Chromatin remodelling enzymes.

4.2 Experimental Approach

4.2.1 Cell culture

NHU cells were cultured until 80-90% confluent and then induced to differentiate using TZPD as described in section 2.5.3.1. Cadmium chloride (10 μM), TSA (400 nM) and 5-azacytidine (5aza) (1 μM) were applied to NHU cell cultures at the same time as TZPD. The concentrations used for the epigenetic modifiers were in line with those described in the literature and in particular those used by Vallot et al. (2010) when treating NHU cell cultures.

4.2.2 RTQPCR

RTQPCR was utilised in order to quantify changes in expression of known urothelial differentiation-associated genes following cadmium exposure and TSA or 5aza treatment. Genes examined included UPK1A, UPK2, KRT13, and KRT20. KRT14 expression was also examined as a marker of squamous metaplasia expressed in proliferative but not differentiated NHU cell cultures. Expression of all genes was calculated relative to the housekeeping gene, GAPDH.

4.2.3 Immunoblotting

Western blotting was performed to examine changes in CK13 protein expression following cadmium exposure and TSA treatment. Two independent NHU cell cultures, Y1197 and Y1223 were treated for 7 days ± TZPD ± 10 μM $CdCl_2$ ± 400 nM TSA. Upon completion of treatments, NHU cell cultures were lysed in situ with SDS lysis buffer to give whole cell lysates.

4.2.4 Immunofluorescence microscopy

Immunofluorescence microscopy was performed to examine protein expression and localisation of CK13 and CK14. NHU cells were seeded on to 12-well slides. Once cultures were 80-90% confluent, cells were treated ± TZPD ± 10 μM $CdCl_2$ ± 400 nM TSA for 3 days before being fixed in methanol:acetone. Following air-drying, cells were immunolabelled using CK13 or CK14 antibodies. Positive and negative controls for immunofluorescence microscopy were performed as described in section 2.7.

4.2.5 Promoter analysis

Promoter analysis for the four differentiation genes (UPK1A, UPK2, KRT13 and KRT20) was carried out using the PSCAN promoter analysis tool, which was run against the JASPAR database of transcription factor binding profiles (http://159.149.160.51/pscan/).

Following identification of transcription factor motifs that differed in the promoters, RTPCR was performed to see how the expression of these transcription factors changed following cadmium and TSA treatment. In order to examine protein expression and localization of the candidate transcription factors immunofluorescence microscopy was performed.

4.2.6 Gene expression analysis

Gene expression analysis was performed using Agilent SurePrint G3 Human Microarrays on two independent NHU cell lines (Y1441 and Y1451) which had been treated ± TZPD ± 10 μM $CdCl_2$ ± 400 nM TSA for 3 days. Microarrays were carried out by the Genomics Department of the Technology Facility at the University of York. Normalisation and fold change calculations were carried out by the Bioscience Technology Facility's Bioinformatics Laboratory. Normalised intensity values and fold change data was supplied in the form of Excel spreadsheets.

Gene ontology enrichment analysis was performed using the PANTHER Classification System (http://pantherdb.org/).

4.3 Results

4.3.1 Ability of cadmium to silence differentiation markers is associated with histone modifications

In order to determine if epigenetic mechanisms were involved in the process by which cadmium silenced differentiation genes as reported in Chapter 3, differentiating NHU cell cultures exposed to cadmium were treated with either TSA or 5aza for 3 days.

RTQPCR results showed that TSA was able to reverse the inhibitory effects of cadmium on the expression of UPK2 and KRT20 genes, but not for UPK1A and KRT13; KRT13 showed a further reduction upon TSA treatment (Figure 4.1). These results were statistically significant, whereas TSA alone had no affect on TZ/PD-induced differentiation on three of four differentiation-associated genes (UPK1A, UPK2 and KRT20).

RTQPCR results for 5-azacytidine treatments showed that 5aza was not able to reverse the inhibitory effects of cadmium (Figure 4.2). 5aza affected TZ/PD-induced differentiation in two of the four differentiation genes (UPK1A and KRT20).

Overall the results from the TSA and 5aza experiments indicated that histone modifications rather than DNA methylation may be responsible for the silencing of differentiation genes by cadmium.

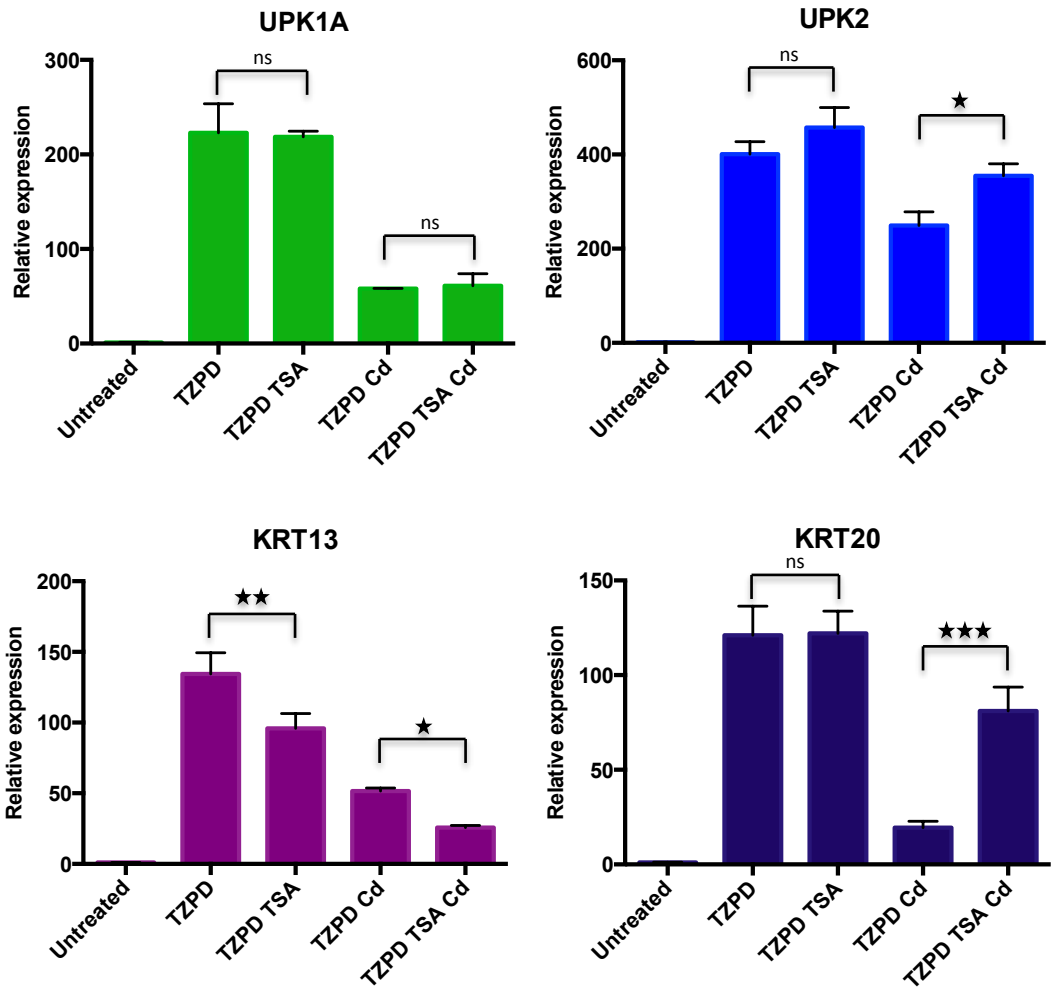

Figure 4.1. RTQPCR data for four differentiation genes from NHU cell cultures treated with TSA. Y1233 NHU cell cultures were treated ± TZPD ± 400 nM TSA ± 10 µM $CdCl_2$ for 3 days. mRNA was harvested from the cultures, cDNA was synthesised using random hexamers and then RTQPCR was performed to quantify the relative expression of four differentiation-associated genes UPK1A, UPK2, KRT13 and KRT20. Each value is the average of 3 technical replicates with standard deviations shown by error bars. One-way ANOVAs with Tukey post testing was performed (see Table 4.1) * p<0.05 ** p<0.01, *** p<0.001, **** p<0.0001, ns not significant. Note that TSA had no effect on the expression of the three terminal differentiation markers (UPK1A, UPK2 and KRT20), but TSA did reverse the inhibitory effects of cadmium for UPK2 and KRT20.

Table 4.1. Results of ANOVAs with Tukey post testing for the four differentiation genes in TSA treated NHU cell cultures. * p<0.05 ** p<0.01, *** p<0.001, **** p<0.0001, ns –not significant.

UPK1A	Control	TZPD	TZPD TSA	TZPD Cd	TZPD TSA Cd
Untreated	-	****	****	**	**
TZPD		-	ns	****	****
TZPD TSA			-	****	****
TZPD Cd				-	ns
TZPD TSA Cd					-

UPK2	Control	TZPD	TZPD TSA	TZPD Cd	TZPD TSA Cd
Untreated	-	****	****	****	****
TZPD		-	ns	***	ns
TZPD TSA			-	****	*
TZPD Cd				-	*
TZPD TSA Cd					-

KRT13	Control	TZPD	TZPD TSA	TZPD Cd	TZPD TSA Cd
Untreated	-	****	****	***	*
TZPD		-	**	****	****
TZPD TSA			-	***	****
TZPD Cd				-	*
TZPD TSA Cd					-

KRT20	Control	TZPD	TZPD TSA	TZPD Cd	TZPD TSA Cd
Untreated	-	****	****	ns	****
TZPD		-	ns	****	**
TZPD TSA			-	****	**
TZPD Cd				-	***
TZPD TSA Cd					-

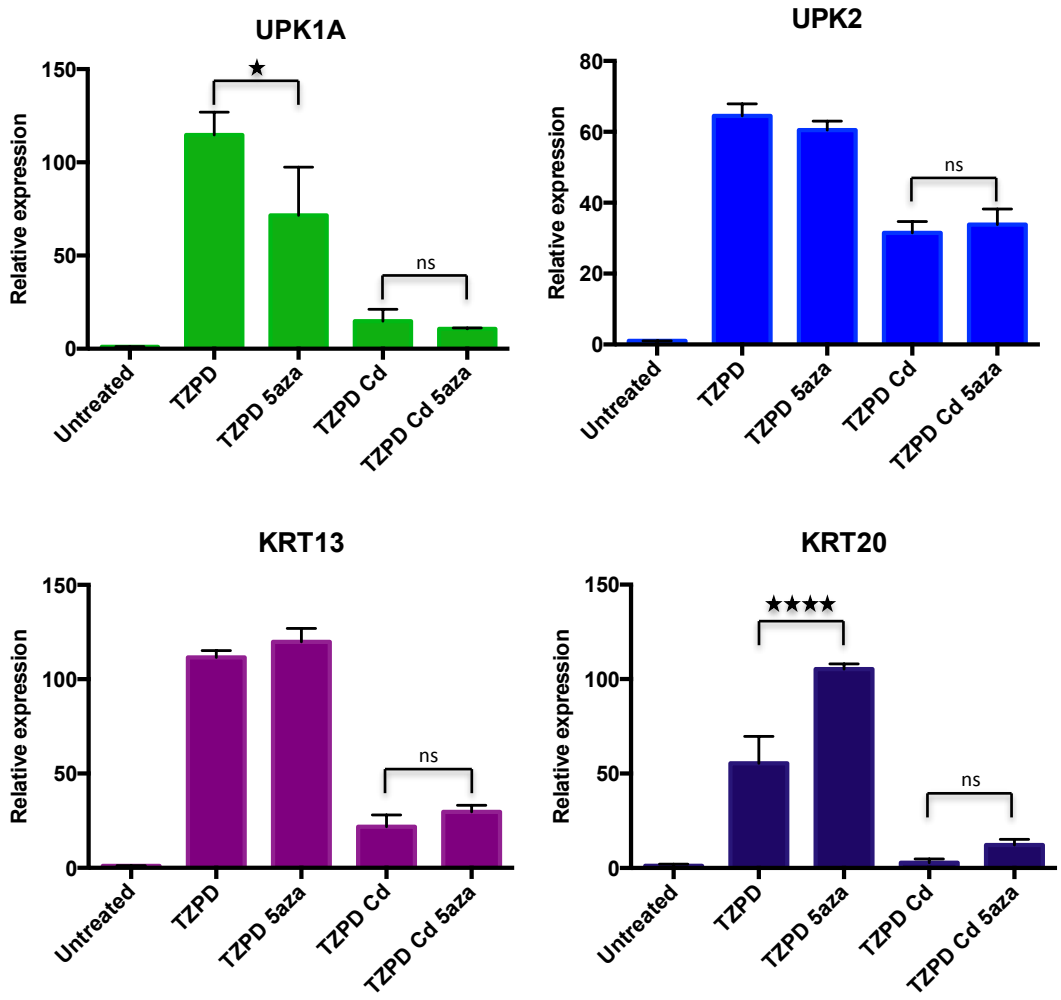

Figure 4.2. RTQPCR data for four differentiation genes from NHU cell cultures treated with 5-azacytidine. Y1236 NHU cell cultures were treated ± TZPD ± 1 µM 5aza ± 10 µM $CdCl_2$ for 3 days. mRNA was harvested from the cultures, cDNA was synthesised using random hexamers and then RTQPCR was performed to quantify the relative expression of four differentiation-associated genes UPK1A, UPK2, KRT13 and KRT20. Each value is the average of 3 technical replicates with standard deviations shown by error bars. One-way ANOVAs with Tukey post testing was performed (see Table 4.2) * $p<0.05$ ** $p<0.01$, *** $p<0.001$, **** $p<0.0001$, ns not significant. Note that 5-azacytidine did not reverse the inhibitory effects of cadmium but 5aza did affect the expression of two terminal differentiation markers in opposite directions (UPK1A and KRT20).

Table 4.2. Results of ANOVAs with Tukey post testing for the four differentiation genes in 5-azacytidine treated NHU cell cultures. * p<0.05 ** p<0.01, *** p<0.001, **** p<0.0001, ns –not significant.

UPK1A	Control	TZPD	TZPD 5aza	TZPD Cd	TZPD Cd 5aza
Untreated	-	****	***	ns	ns
TZPD		-	*	****	****
TZPD 5aza			-	**	**
TZPD Cd				-	ns
TZPD Cd 5aza					-

UPK2	Control	TZPD	TZPD 5aza	TZPD Cd	TZPD Cd 5aza
Untreated	-	****	****	****	****
TZPD		-	ns	****	****
TZPD 5aza			-	****	****
TZPD Cd				-	ns
TZPD Cd 5aza					-

KRT13	Control	TZPD	TZPD 5aza	TZPD Cd	TZPD Cd 5aza
Untreated	-	****	****	**	***
TZPD		-	ns	****	****
TZPD 5aza			-	****	****
TZPD Cd				-	ns
TZPD Cd 5aza					-

KRT20	Control	TZPD	TZPD 5aza	TZPD Cd	TZPD Cd 5aza
Untreated	-	****	****	ns	ns
TZPD		-	****	***	***
TZPD 5aza			-	****	****
TZPD Cd				-	ns
TZPD Cd 5aza					-

4.3.2 TSA treatments on two further independent NHU cell lines

Two further independent NHU cell lines (Y1197 and Y1357) were treated with TZPD, cadmium and TSA for 3 days. RTQPCR results for Y1197 (Figure 4.3) and Y1357 (Figure 4.4) confirmed the initial findings that TSA was able to reverse the cadmium reduced expression of UPK2 and KRT20 but was not able to reverse the cadmium-reduced expression UPK1A and KRT13.

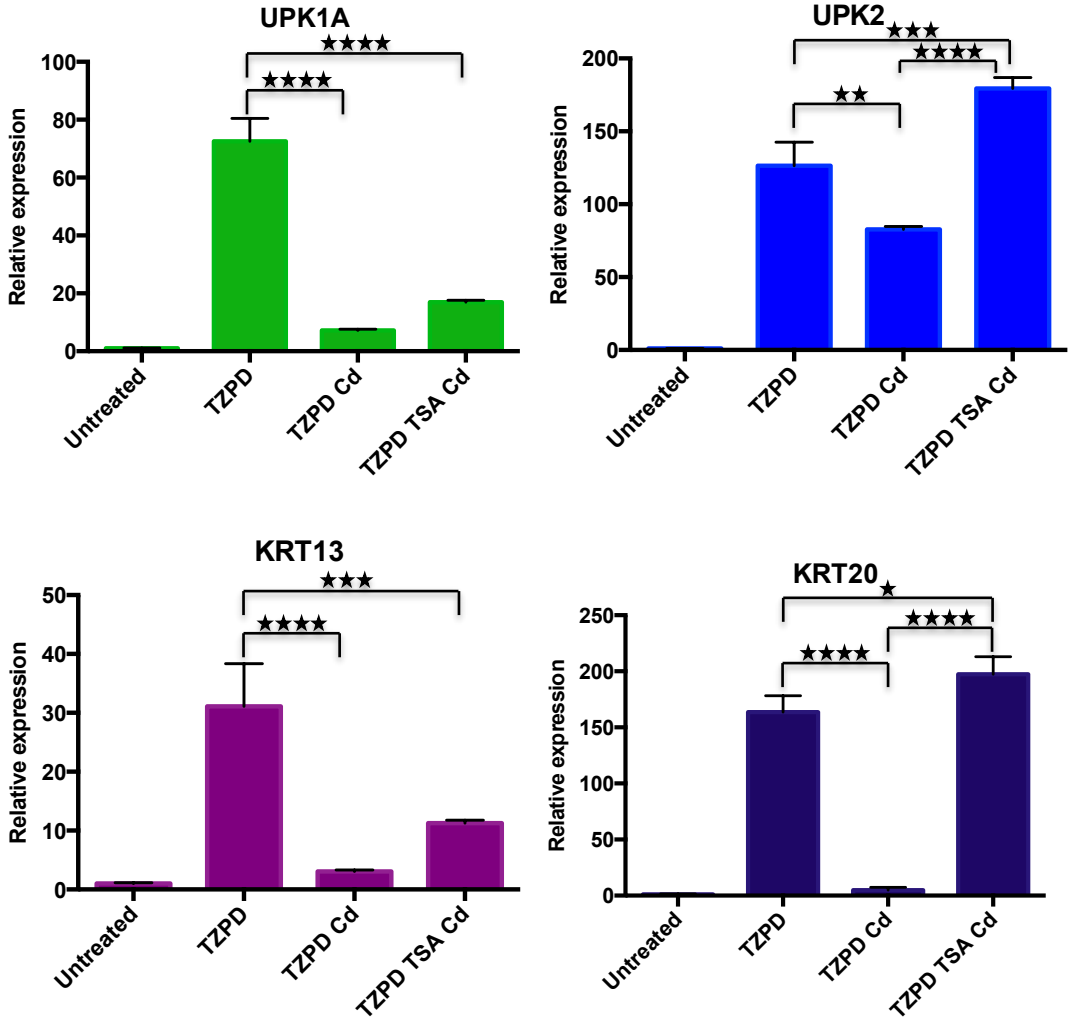

Figure 4.3. RTQPCR data for four differentiation genes from Y1197 NHU cultures. NHU cell cultures were treated ± TZPD ± 400 nM TSA ± 10 µM $CdCl_2$ for 3 days. mRNA was harvested from the cultures, cDNA was synthesised using random hexamers and then RTQPCR was performed to quantify the relative expression of four differentiation-associated genes UPK1A, UPK2, KRT13 and KRT20. Each value is the average of 3 technical replicates with standard deviations shown by error bars. One-way ANOVAs with Tukey post testing was performed; where there are statistical differences between the TZPD treatments these are indicated on the graphs. * p<0.05 ** p<0.01, *** p<0.001, **** p<0.0001.

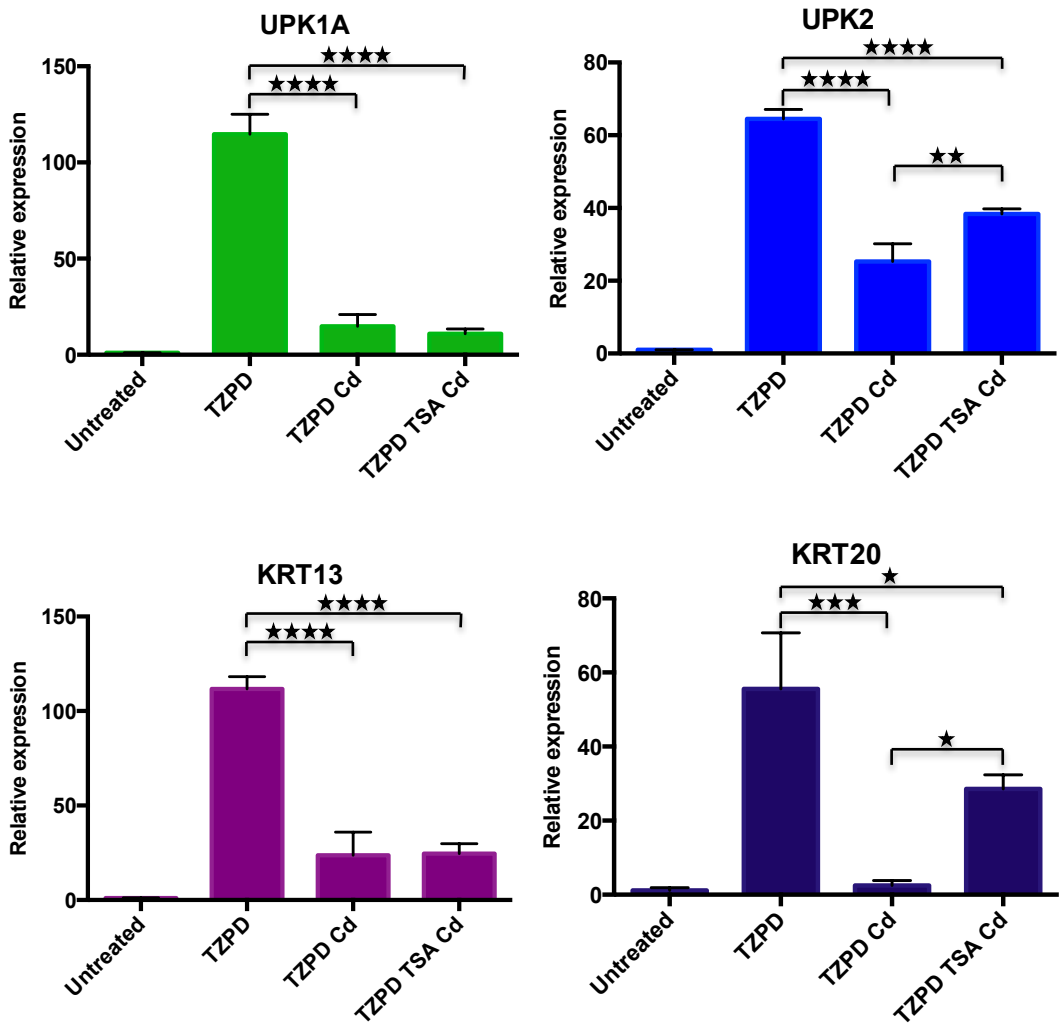

Figure 4.4. RTQPCR data for four differentiation genes from Y1357 NHU cultures. NHU cell cultures were treated ± TZPD ± 400 nM TSA ± 10 µM $CdCl_2$ for 3 days. mRNA was harvested from the cultures, cDNA was synthesised using random hexamers and then RTQPCR was performed to quantify the relative expression of four differentiation-associated genes UPK1A, UPK2, KRT13 and KRT20. Each value is the average of 3 technical replicates with standard deviations shown by error bars. One-way ANOVAs with Tukey post testing was performed; where there are statistical differences between the TZPD treatments these are indicated on the graphs. * p<0.05 ** p<0.01, *** p<0.001, **** p<0.0001.

4.3.3 CK13 protein expression

Immunoblotting for CK13, a transitional marker of urothelial differentiation, was performed using whole cell lysates from two independent NHU cell lines (Figure 4.5). CK13 was upregulated upon TZPD-induced differentiation in both cell lines. TSA alone led to slight increases in CK13. Upon exposure to cadmium CK13 expression was reduced in both cell lines with TSA leading to a slight rescue in the protein expression amounts in one cell line, while a reduction was observed in the other cell line. These results were consistent with transcript data for KRT13 reported above.

Immunofluorescence microscopy for CK13 (Figure 4.6) showed an upregulation of CK13 upon differentiation that was inhibited by cadmium exposure. TSA did not prevent the downregulation of CK13 caused by cadmium.

Overall these results showed that TSA did not affect the cadmium-reduced expression of CK13 protein in differentiated NHU cell cultures in two of out three independent cell lines.

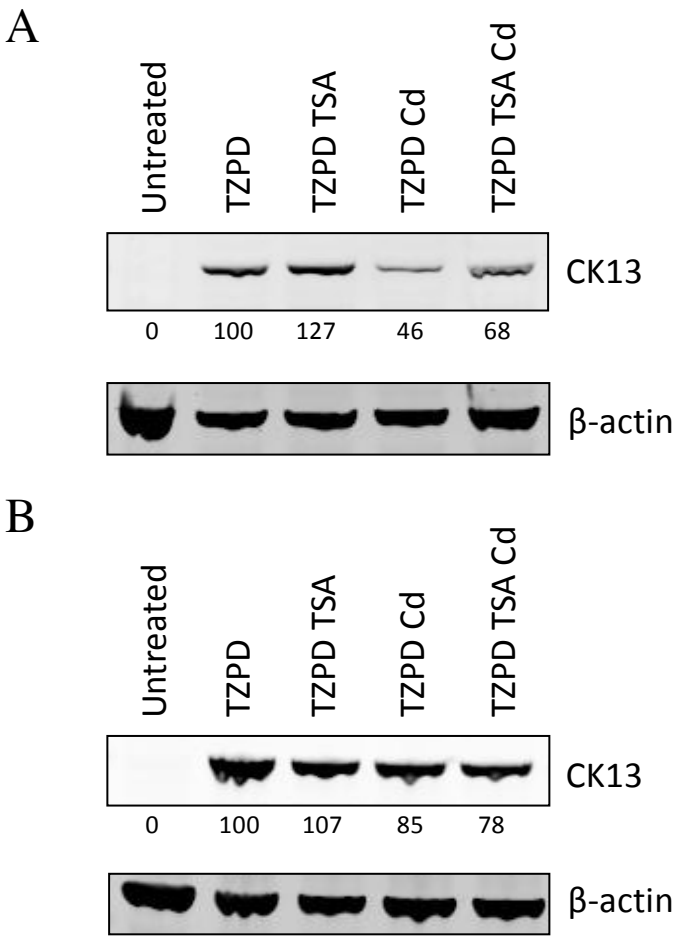

Figure 4.5. Western blot analysis of CK13 protein expression from two independent NHU cell lines. NHU cultures, Y1197 (A) and Y1223 (B), were treated for 7 days ± TZPD ± 10 µM $CdCl_2$ ± 400 nM TSA. Cultures were lysed in situ with SDS lysis buffer and then sonicated. Protein concentration was measured using a Bradford assay. 4-12% Bis-Tris gels were loaded with 20 µg of protein and run at 200 V in MES running buffer. Protein was blotted on to PVDF membranes using the Novex apparatus for 2 hours at 30 V. Membranes were blocked in Odyssey blocking buffer, incubated with primary antibodies overnight at 4°C, and secondary antibodies for one hour at ambient temperature then scanned on the Li-Cor imaging system. The fluorescence of each band was quantified and normalised to the loading control β-actin using the Odyssey software. Numbers quantifying the percentage intensity of the bands are displayed below the corresponding bands. Differentiation induced expression of CK13, which was further de-repressed by TSA. Cadmium inhibited differentiation-associated CK13 expression, which was partially alleviated by TSA in one cell line only.

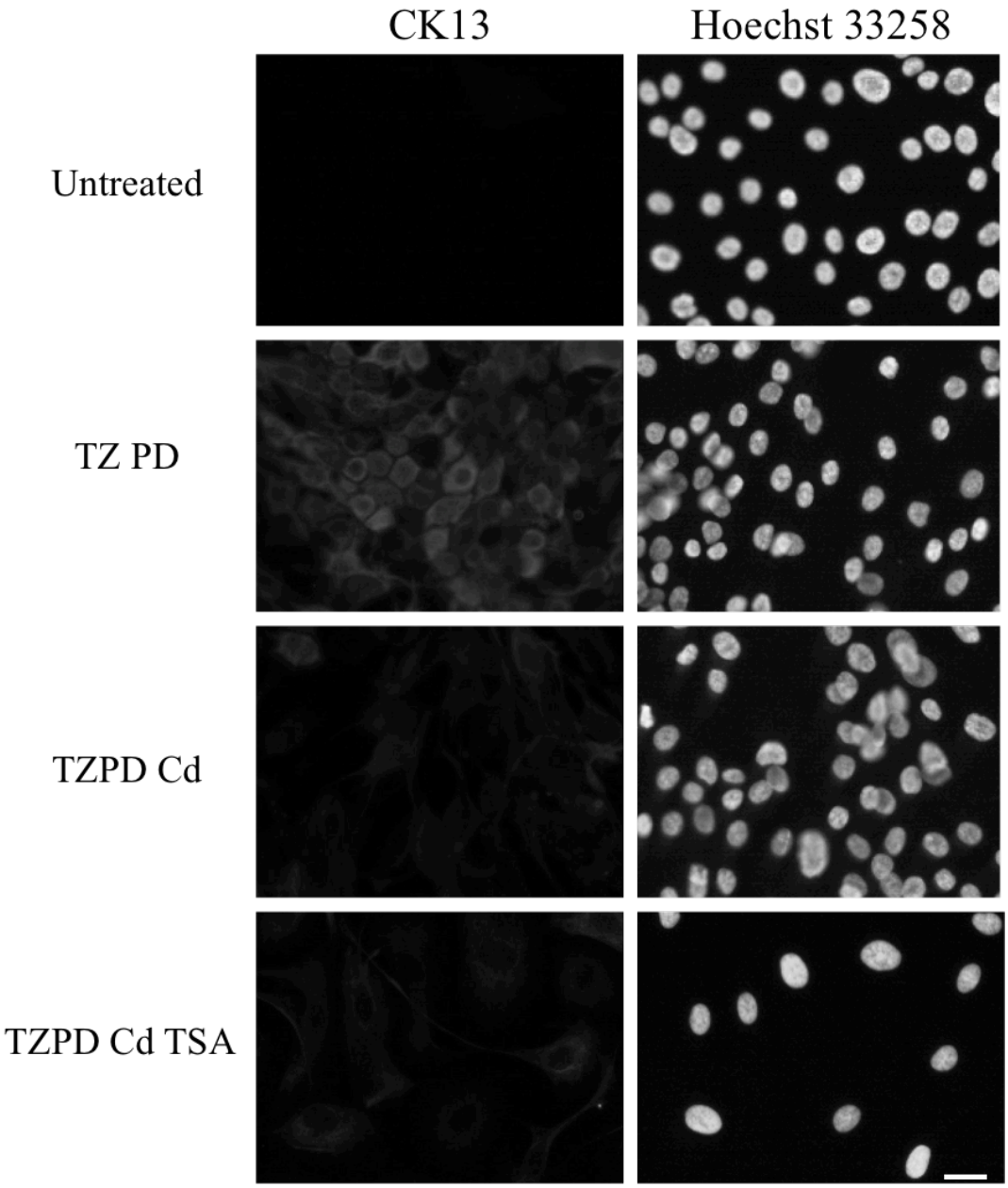

Figure 4.6. Immunofluorescence microscopy images for CK13. NHU cells (Y1357) were seeded at a concentration of $3x10^5$ cells mL^{-1} on to 12-well slides. Once cultures were 80-90% confluent cells were treated for 3 days ± TZPD ± 10 µM $CdCl_2$ ± 400 nM TSA before fixation in methanol:acetone. Following air-drying, cells were immunolabelled using anti-CK13 mouse primary antibodies and a goat anti-mouse secondary immunoconjugate. Nuclei were stained with Hoechst 33258. Scale bar, 10 µM.

4.3.4 CK14 transcript and protein expression

When differentiating NHU cell cultures were exposed to cadmium, there was a failure to downregulate KRT14, as reported in Chapter 3. TSA alone was shown to have no effect on the downregulation of KRT14 upon TZ/PD-induced differentiation (Figure 1.7A). TSA treatment enabled KRT14 to be downregulated when cadmium was present in Y1236 NHU cell cultures ($p<0.001$) (Figure 4.7B) but not in Y1197 NHU cell cultures (Figure 4.7A).

CK14 protein expression was examined by immunofluorescence microscopy (Figure 4.8). These results showed that upon differentiation CK14 was downregulated, however when cadmium was present downregulation of CK14 was inhibited. The addition of TSA to differentiating NHU cultures annulled the effect of cadmium and resulted in downregulation of CK14.

Together these results showed that the inhibition of cytokeratin 14 downregulation due to cadmium exposure could be prevented by TSA treatment in two out of three independent differentiating NHU cell cultures.

A

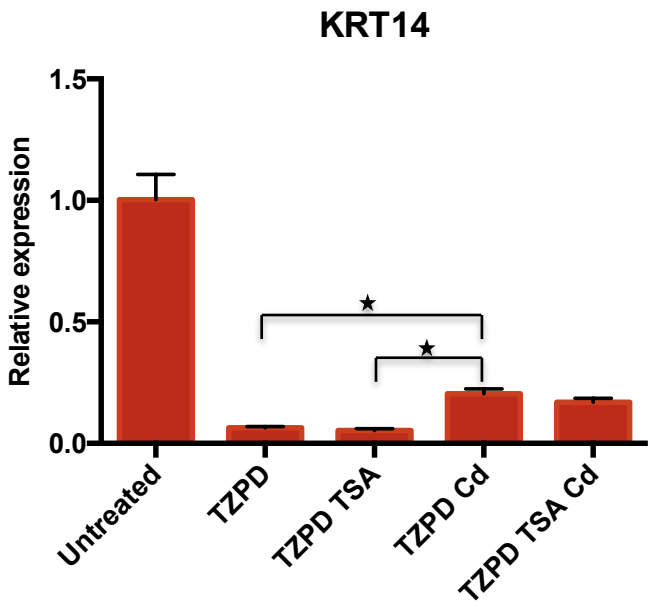

B

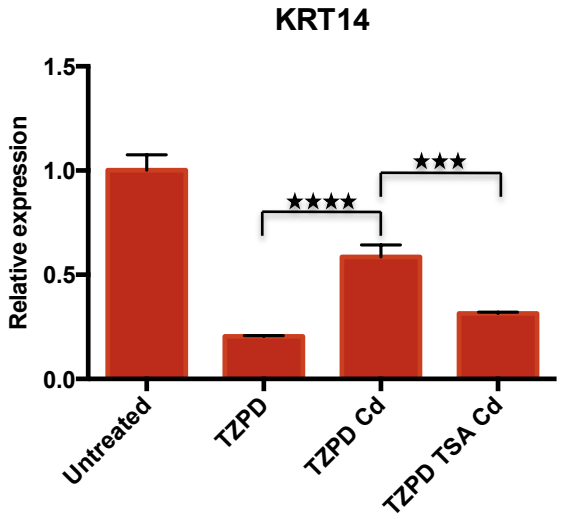

Figure 4.7. RTQPCR results for KRT14 transcript expression from two independent NHU cell lines treated with TSA. Y1197 (A) and Y1236 (B) NHU cell cultures were treated ± TZPD ± 400 nM TSA ± 10 µM $CdCl_2$ for 3 days. mRNA was harvested from the cultures, cDNA was synthesised using random hexamers and then RTQPCR was performed to quantify the relative expression of KRT14. Each value is the average of 3 technical replicates with standard deviations shown by error bars. One-way ANOVAs with Tukey post testing was performed; where there are statistical differences between the TZPD treatments these are indicated on the graphs. * p<0.05 ** p<0.01, *** p<0.001, **** p<0.0001.

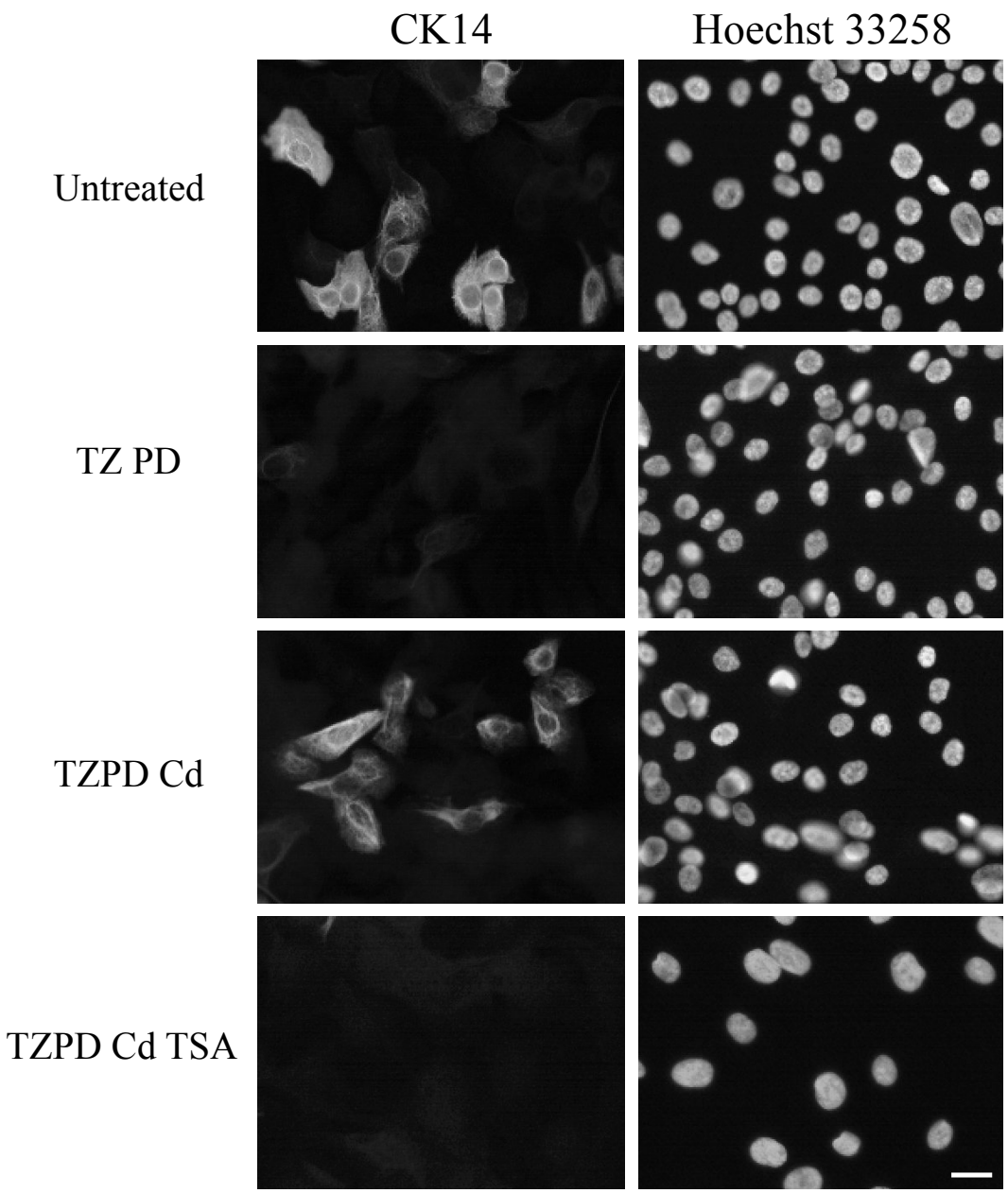

Figure 4.8. Immunofluorescence microscopy images for CK14. NHU cells (Y1357) were seeded at a concentration of $3x10^5$ cells mL^{-1} on to 12-well slides. Once cultures were 80-90% confluent cells were treated for 3 days ± TZPD ± 10 µM $CdCl_2$ ± 400 nM TSA before fixation in methanol:acetone. Following air-drying, cells were immunolabelled using anti-CK14 mouse primary antibodies and a goat anti-mouse secondary imunnoconjugate. Nuclei were stained with Hoechst 33258. Scale bar, 10 µM.

4.3.5 Promoter analysis for UPK1A, KRT13, UPK2 and KRT20

As UPK2 and KRT20 responded differently to TSA treatment compared to UPK1A and KRT13, a bioinformatics promoter analysis was performed for these genes. Promoter analysis was performed using the PSCAN promoter analysis tool applied to the JASPAR database of transcription factor binding motifs. When promoter regions for UPK1A and KRT13 were compared against UPK2 and KRT20, PSCAN results identified some potential candidates that differed between the two groups and many which did not (Figure 4.9).

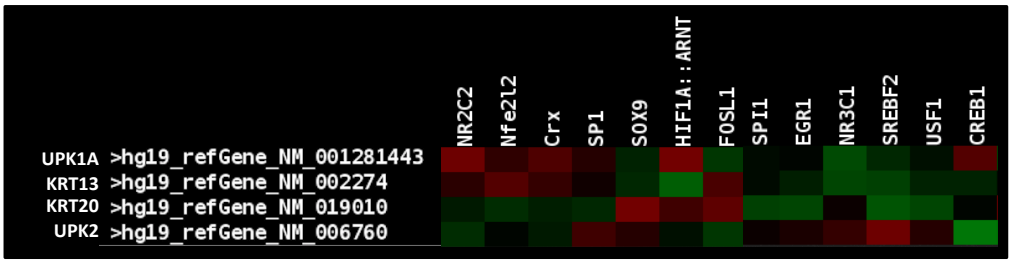

Figure 4.9. PSCAN promoter analysis performed using the JASPAR database of transcription factor binding site motifs. The 'heatmap' image shows the contribution of each input gene to the z-score of each transcription factor matrix; red spots correspond to scores higher than the genome-wide mean, green spots are scores lower than the genome-wide mean and black spots are around the average genome score. Therefore the motifs which are enriched in the promoter region of these genes will show as red. The following RefSeq mRNA IDs were input: NM_001281443, NM_002274, NM_019010 and NM_006760 representing UPK1A, KRT13, KRT20 and UPK2 respectively. Shown is a subset of the complete PSCAN analysis. SOX9 and NR3C1 motifs are shown enriched in UPK2 and KRT20.

Two motifs that were enriched in the promoter region for UPK2 and KRT20 but not UPK1A and KRT13 were SOX9 and NR3C1. RT-PCR was performed to see if cadmium exposure affected the transcript expression of these candidates. Results showed that SOX9 failed to downregulate upon differentiation when cadmium was present (Figure 4.10), whereas NR3C1 showed no change.

In order to examine SOX9 protein expression, immunofluorescence microscopy was performed. Results showed slight differences in SOX9 protein expression between cultures differentiated with or without cadmium. SOX9 labelling in TSA treated cells was more akin to the DMSO control cell cultures with labelling appearing greater in the nuclei compared to TZPD and TZPD Cd treated NHU cell cultures (Figure 4.11).

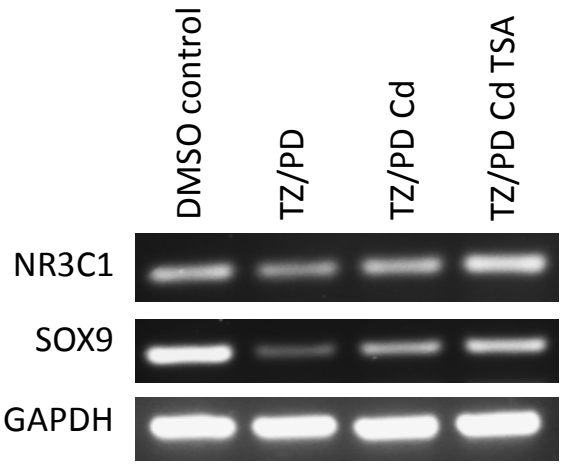

Figure 4.10. RTPCR results for NR3C1 and SOX9. Y1236 NHU cell cultures were treated ± TZPD ± 10 µM $CdCl_2$ ± 400 nM TSA for 3 days. mRNA was harvested from the cultures, cDNA was synthesised using random hexamers and RTPCR was performed to examine expression of NR3C1 and SOX9.

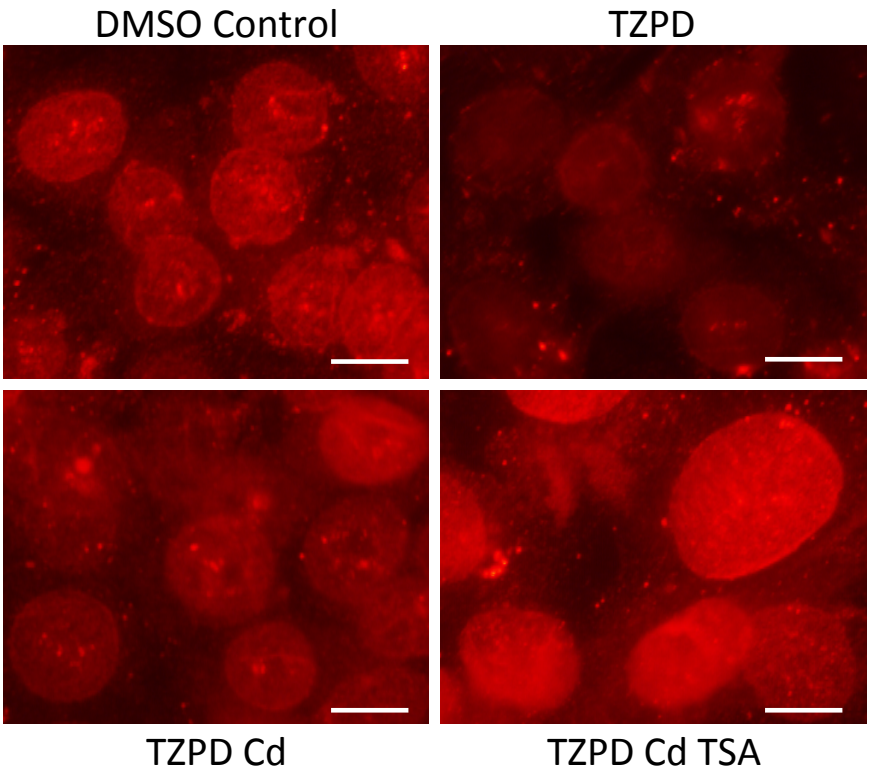

Figure 4.11. Immunofluorescence microscopy images for SOX9. NHU cells (Y1357) were seeded at a concentration of $3x10^5$ cells mL^{-1} on to 12-well slides. Once cultures were 80-90% confluent cells were treated for 3 days ± TZPD ± 10 µM $CdCl_2$ ± 400 nM TSA before fixation in methanol:acetone. Following air-drying, cells were immunolabelled using an anti-SOX9 goat primary antibody and a donkey anti-goat secondary immunoconjugate. Scale bar, 5 µM.

4.3.6 Gene expression analysis using Agilent microarrays

Agilent microarrays were used to identify genes that changed in expression when two independent NHU cell cultures were differentiated in the presence of cadmium and TSA.

Before microarrays were performed, confirmation that cadmium and TSA treatments had been successful was determined. A fraction of extracted RNA for each of the four treatments from the two NHU cell lines was synthesised into cDNA and RTQPCR was performed to examine the expression of the four urothelial differentiation-associated genes that were inhibited by cadmium exposure as reported in Chapter 3. Results showed that cadmium inhibited the expression of all four genes in both cell lines, with TSA reversing the inhibitory effects of cadmium for three terminal differentiation genes UPK1A, UPK2 and KRT20 (Figures 4.12 and 4.13). The reversal of the inhibitory effect of cadmium on UPK1A expression was in contrast to the results from three different NHU cell lines previously reported in this chapter.

Data obtained from microarray analysis revealed a number of genes that were differentially expressed due to cadmium exposure and TSA treatment (Figure 4.14). TZPD-induced differentiation of NHU cell cultures led to an upregulation of 1784 genes and a downregulation of 1503 genes when data was filtered for >2-fold up/down changes, $p<0.05$.

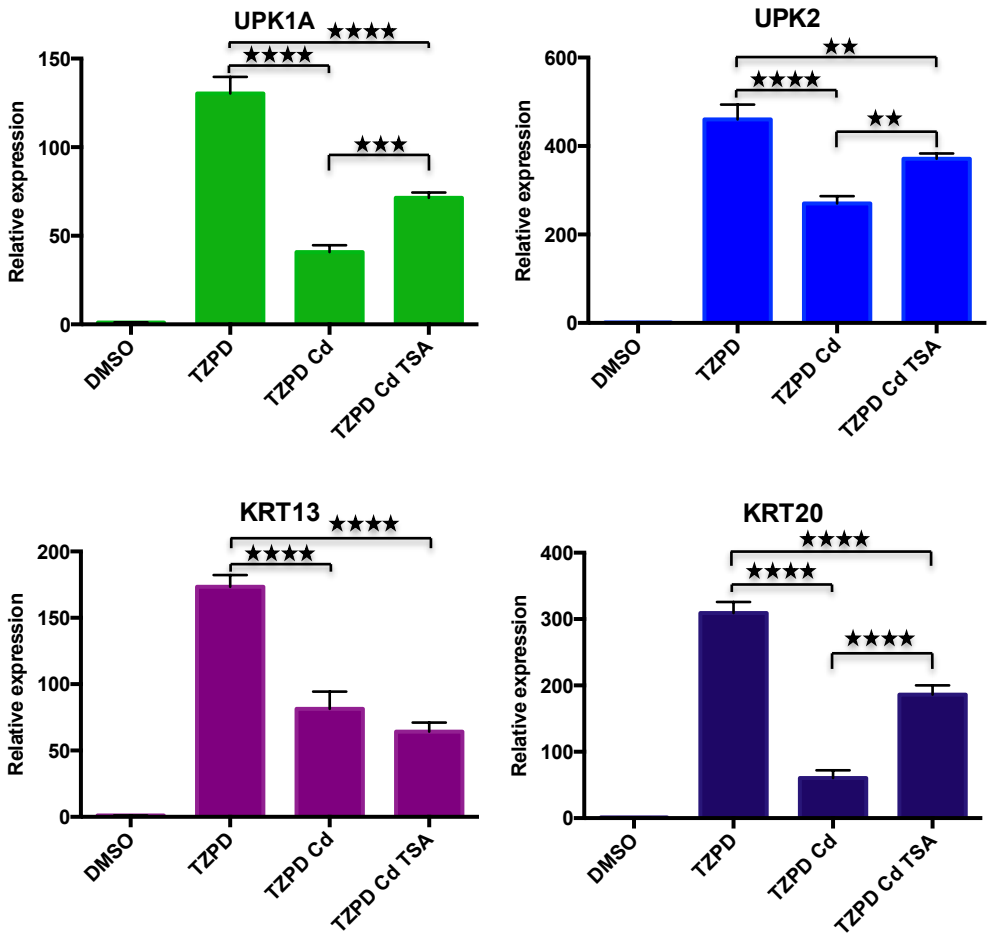

Figure 4.12. Confirmation of cadmium and TSA treatment in Y1441 NHU cell cultures. NHU cell cultures were treated ± TZPD ± 400 nM TSA ± 10 µM $CdCl_2$ for 72 hours. mRNA was harvested from the cultures, cDNA was synthesised using random hexamers and then RTQPCR was performed to quantify the relative expression of four differentiation-associated genes UPK1a, UPK2, KRT13 and KRT20. Each value is the average of 3 technical replicates with standard deviations shown by error bars. One-way ANOVAs with Tukey post testing was performed; where there are statistical differences between the TZPD treatments these are indicated on the graphs. * p<0.05 ** p<0.01, *** p<0.001, **** p<0.0001.

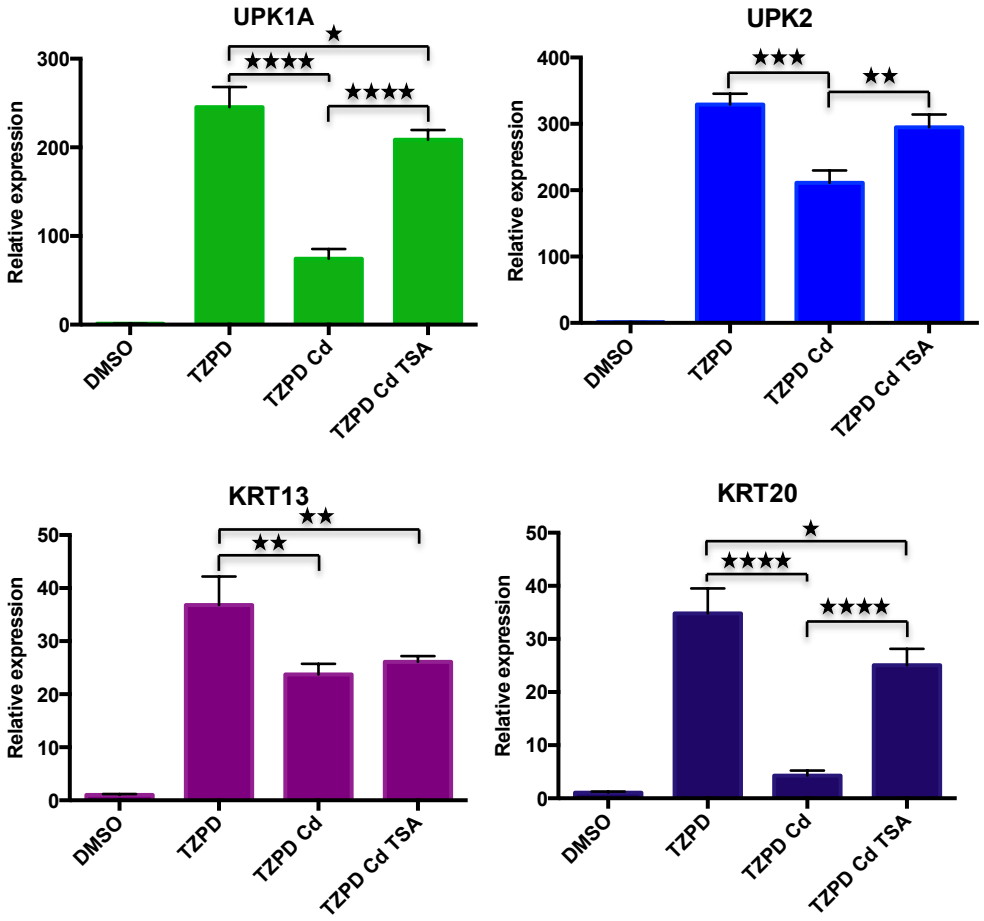

Figure 4.13. Confirmation of cadmium and TSA treatment in Y1451 NHU cell cultures. NHU cell cultures were treated ± TZPD ± 400 nM TSA ± 10 µM $CdCl_2$ for 72 hours. mRNA was harvested from the cultures, cDNA was synthesised using random hexamers and then RTQPCR was performed to quantify the relative expression of four differentiation-associated genes UPK1a, UPK2, KRT13 and KRT20. Each value is the average of 3 technical replicates with standard deviations shown by error bars. One-way ANOVAs with Tukey post testing was performed; where there are statistical differences between the TZPD treatments these are indicated on the graphs. * p<0.05 ** p<0.01, *** p<0.001, **** p<0.0001.

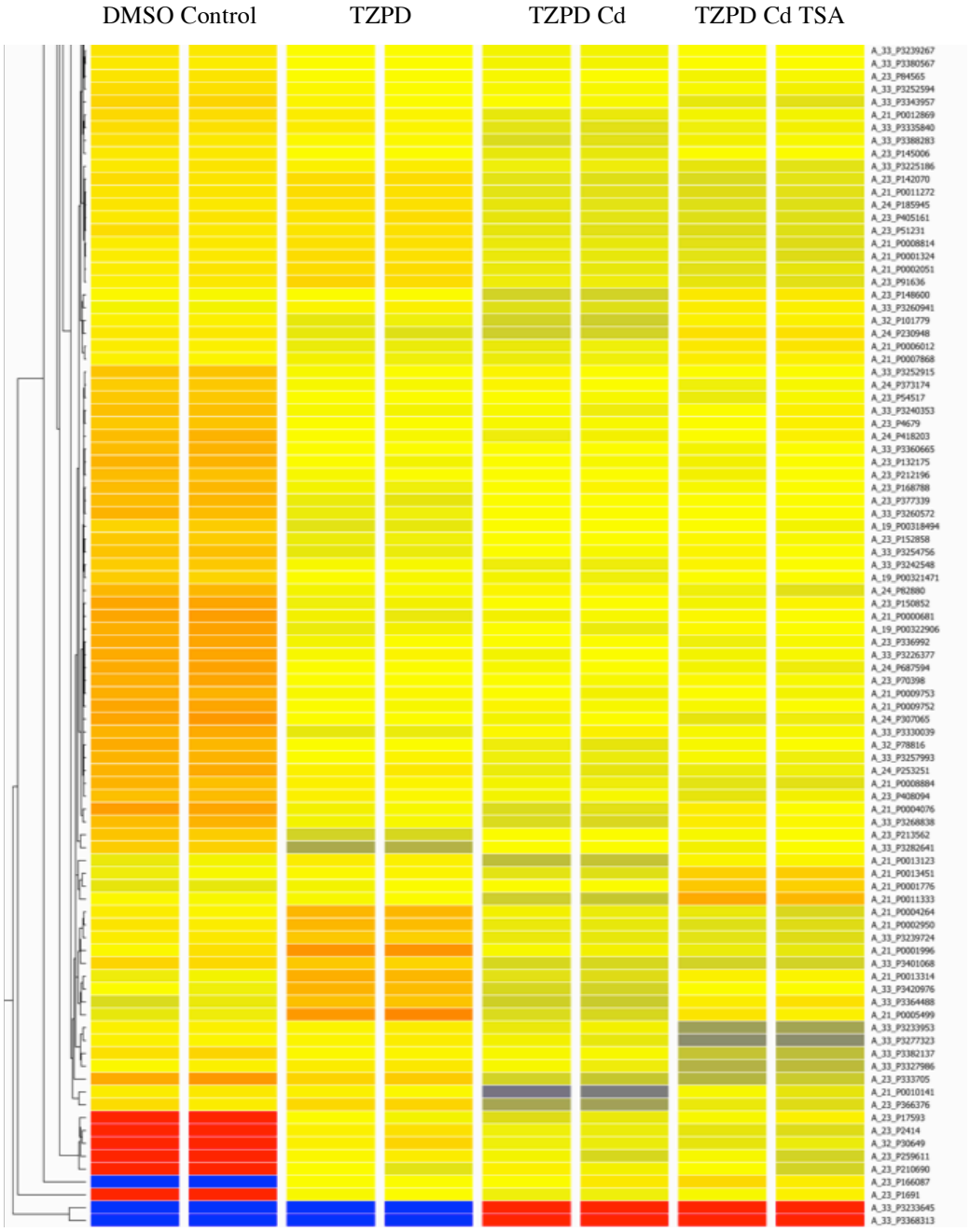

Figure 4.14. Section of a dendrogram heat map produced using GeneSpring GX software. Heat map shows genes with high expression levels (red), low expression levels (blue) or average expression values (yellow). Showed that changes in gene expression occurred when differentiating NHU cultures were treated with cadmium and TSA.

4.3.6.1 Confirmation of known differentiation-associated markers

The expression of known urothelial differentiation markers was analysed using fold change expression profiles. Fold changes were calculated using the combined microarray data of the two independent NHU cell lines (Y1441 and Y1451). Where more than one probe was present for a single gene the data was combined and standard deviations shown.

Uroplakin gene expression fold changes are shown in Figure 4.15. When TZPD-induced differentiated cell cultures were compared with DMSO control cultures all five uroplakin genes were shown to be upregulated. Cadmium exposure led to a decrease in expression of UPK1A, UPK2, UPK3A and UPK3B but not UPK1B. TSA reversed the inhibitory effect of cadmium by a 2 fold increase or more in three out of the four uroplakin transcripts (UPK1A, UPK3A and UPK3B) that were downregulated by cadmium.

Cytokeratin transcript fold changes are shown in Figure 4.16. KRT13, a transitional differentiation-associated gene, and KRT20 a terminal differentiation-associated gene were both upregulated in TZPD treated cell cultures. Cadmium exposure led to a 2.7 fold decrease in KRT20 expression with TSA shown to reverse this downregulation.

KRT14, KRT16, KRT17 and the KRT6 family all showed a marked reduction of transcript expression upon TZPD-induced differentiation. Cadmium treatment led to an increase of expression for all the transcripts when compared to TZPD only treated cultures. TSA alleviated the effects of cadmium exposure for two genes, KRT16 and KRT6C, by a 2 fold decrease or more.

Tight junction genes were also analysed and are shown in Figure 4.17. Tight junctions are built from 40 different proteins including claudins, occludin and zona occludens. Claudin 3 and 4 were shown to be upregulated upon differentiation. Cadmium exposure led to a very slight increase in expression of claudin 3 and 4, TSA was shown to reverse this increase. Occludin was shown to be upregulated upon differentiation of NHU cell cultures, with cadmium exposure leading to a slight decrease in occludin transcript expression, further treatment with TSA did not affect occludin expression. ZO-2 and ZO-3 were upregulated in differentiated NHU cell cultures, with cadmium and TSA only having a minimal effect on expression levels.

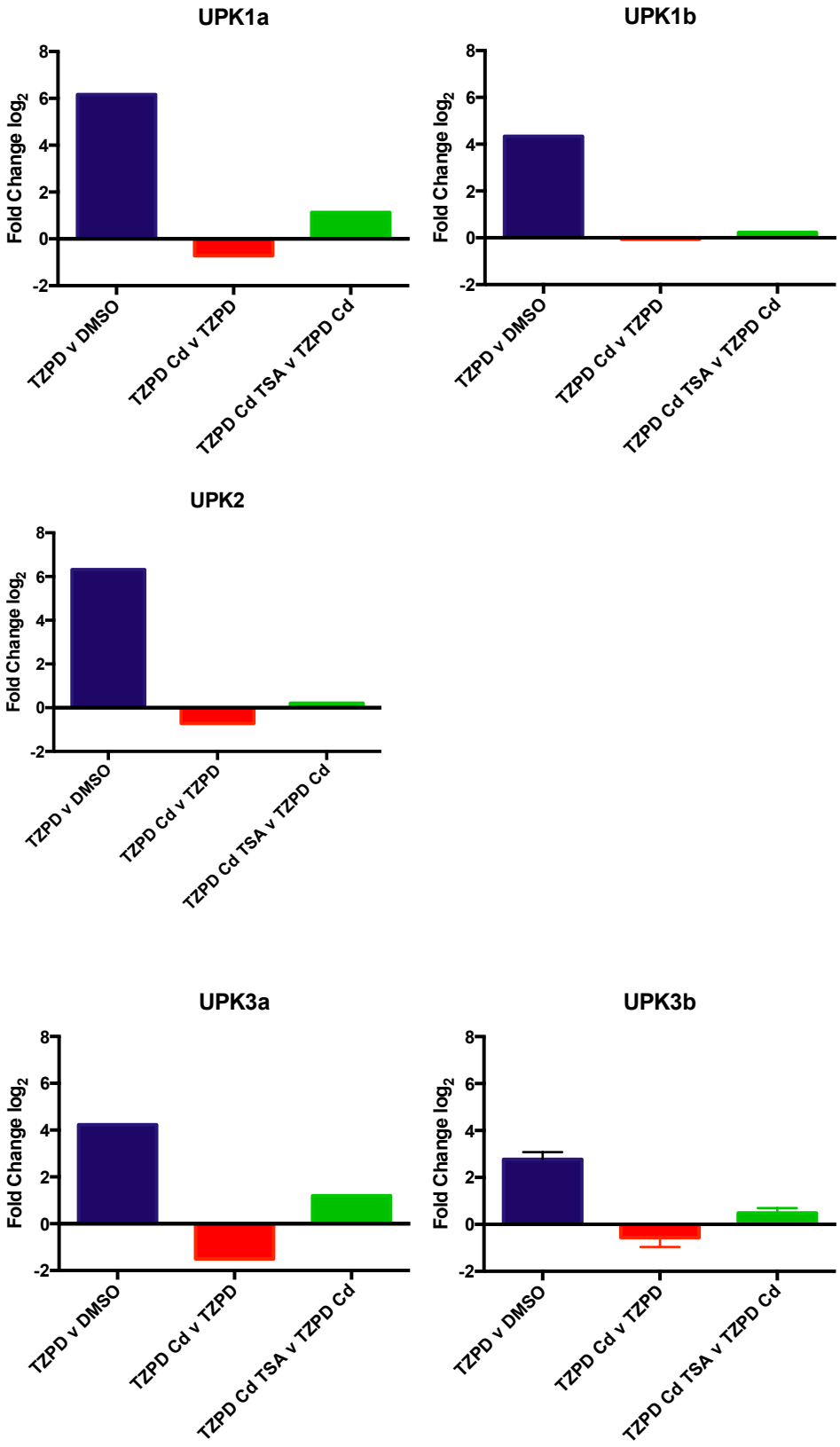

Figure 4.15. Agilent microarray analysis for uroplakin targets during urothelial differentiation, cadmium exposure and TSA treatment. Y1441 and Y1451 NHU cell cultures were treated ± TZPD ± 10 µM $CdCl_2$ ± 400 nM TSA. mRNA was collected at 72 hours and gene expression analysed using Agilent SurePrint G3 Human Microarrays.

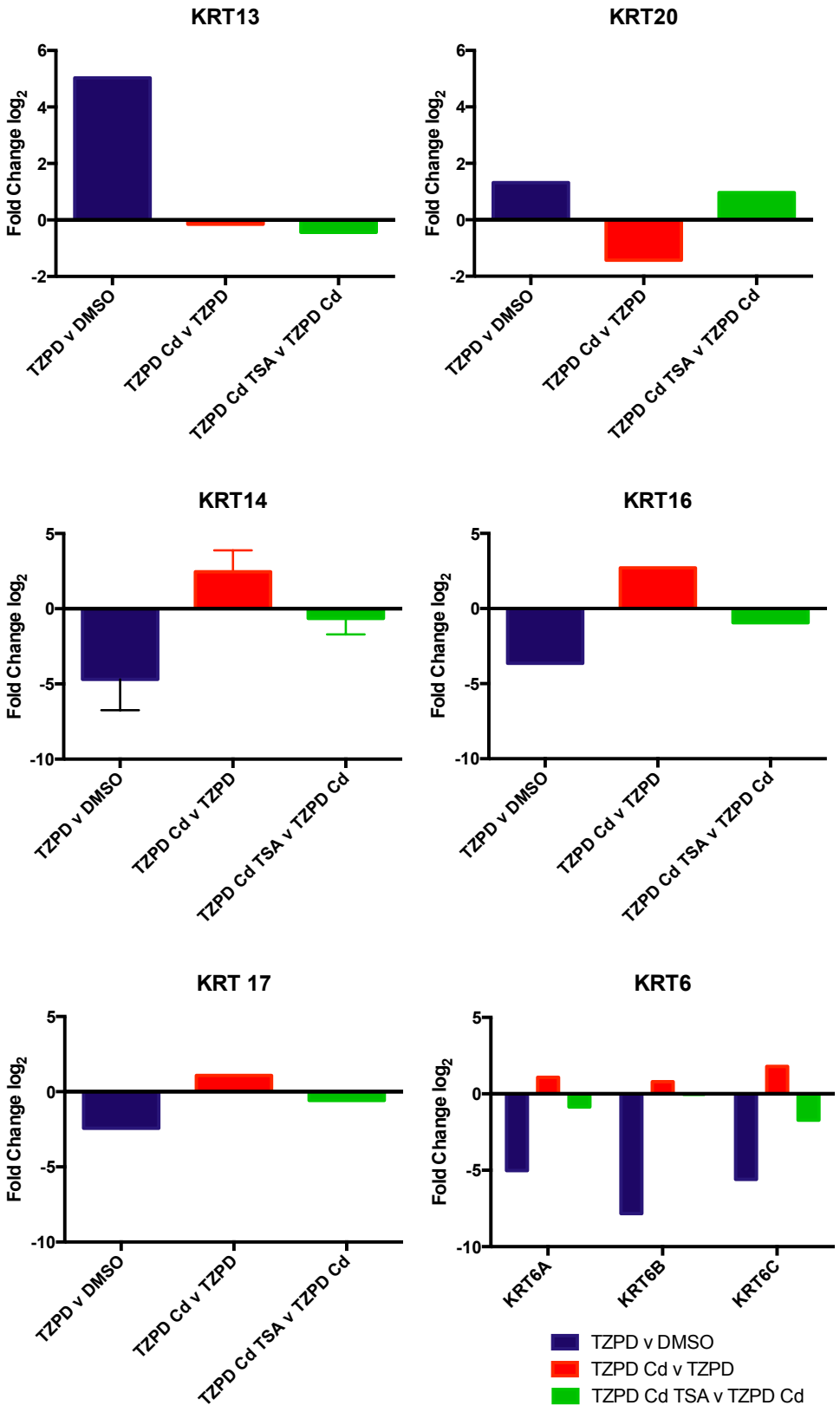

Figure 4.16. Agilent microarray analysis for cytokeratin targets during urothelial differentiation, cadmium exposure and TSA treatment. Y1441 and Y1451 NHU cell cultures were treated ± TZPD ± 10 µM $CdCl_2$ ± 400 nM TSA. mRNA was collected at 72 hours and gene expression analysed using Agilent SurePrint G3 Human Microarrays.

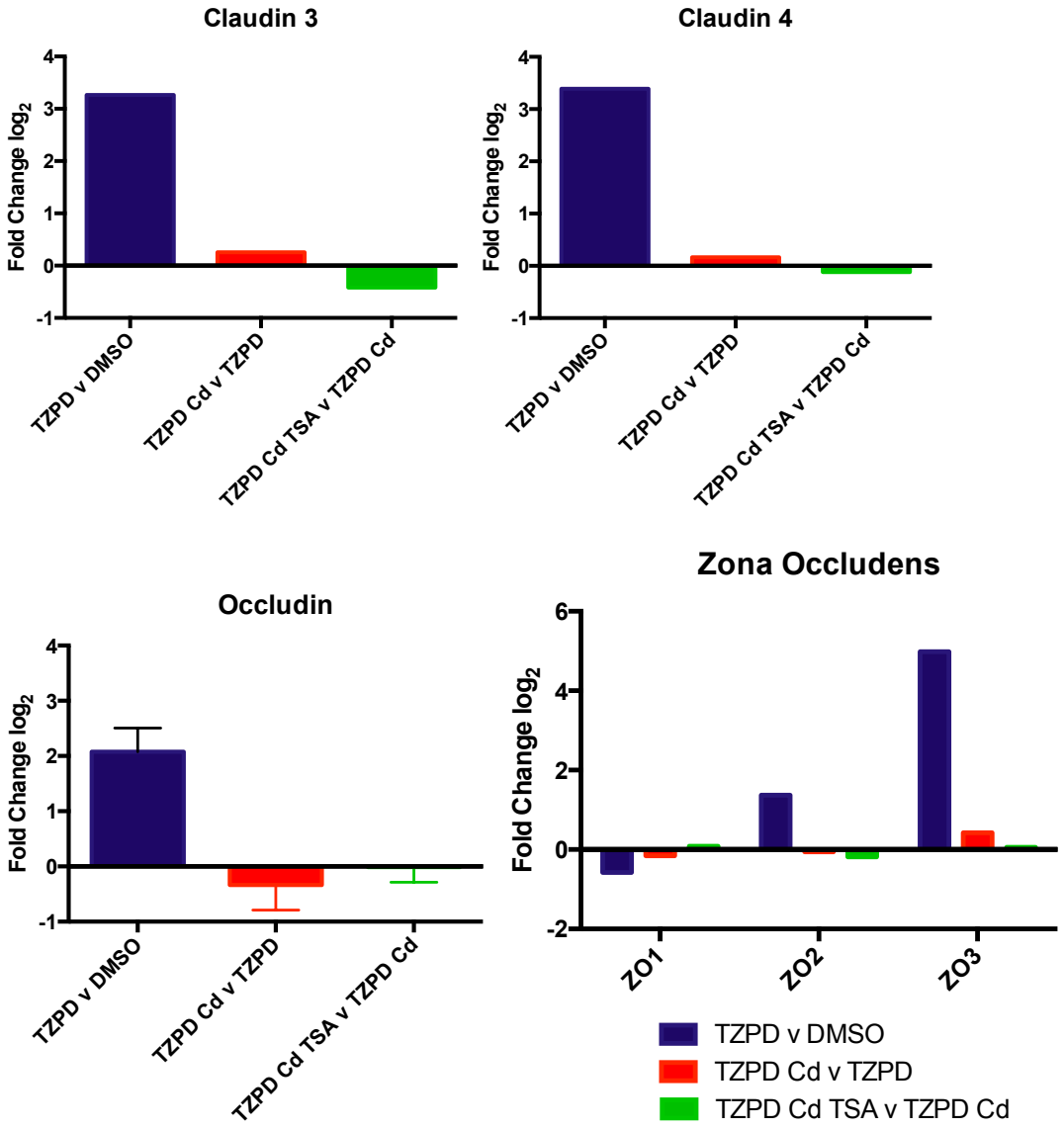

Figure 4.17. Agilent microarray analysis for tight junction targets during urothelial differentiation, cadmium exposure and TSA treatment. Y1441 and Y1451 NHU cell cultures were treated ± TZPD ± 10 µM $CdCl_2$ ± 400 nM TSA. mRNA was collected at 72 hours and gene expression analysed using Agilent SurePrint G3 Human Microarrays.

4.3.6.2 Expression of urothelial transcription factors

The expression of six transcription factors known to be involved in urothelial differentiation was analysed (Figure 4.18). All six transcription factors were shown to be upregulated in differentiation by at least 2-fold with ELF3 shown to be the most upregulated by 35-fold. Transcription factor expression was not affected by cadmium exposure or TSA, except for ELF3, which showed minor changes, however these changes in expression were both less than 1.5 fold changes.

These results were in agreement with the RTPCR and RTQPCR results reported in Chapter 3. Additionally they showed that TSA did not affect their expression.

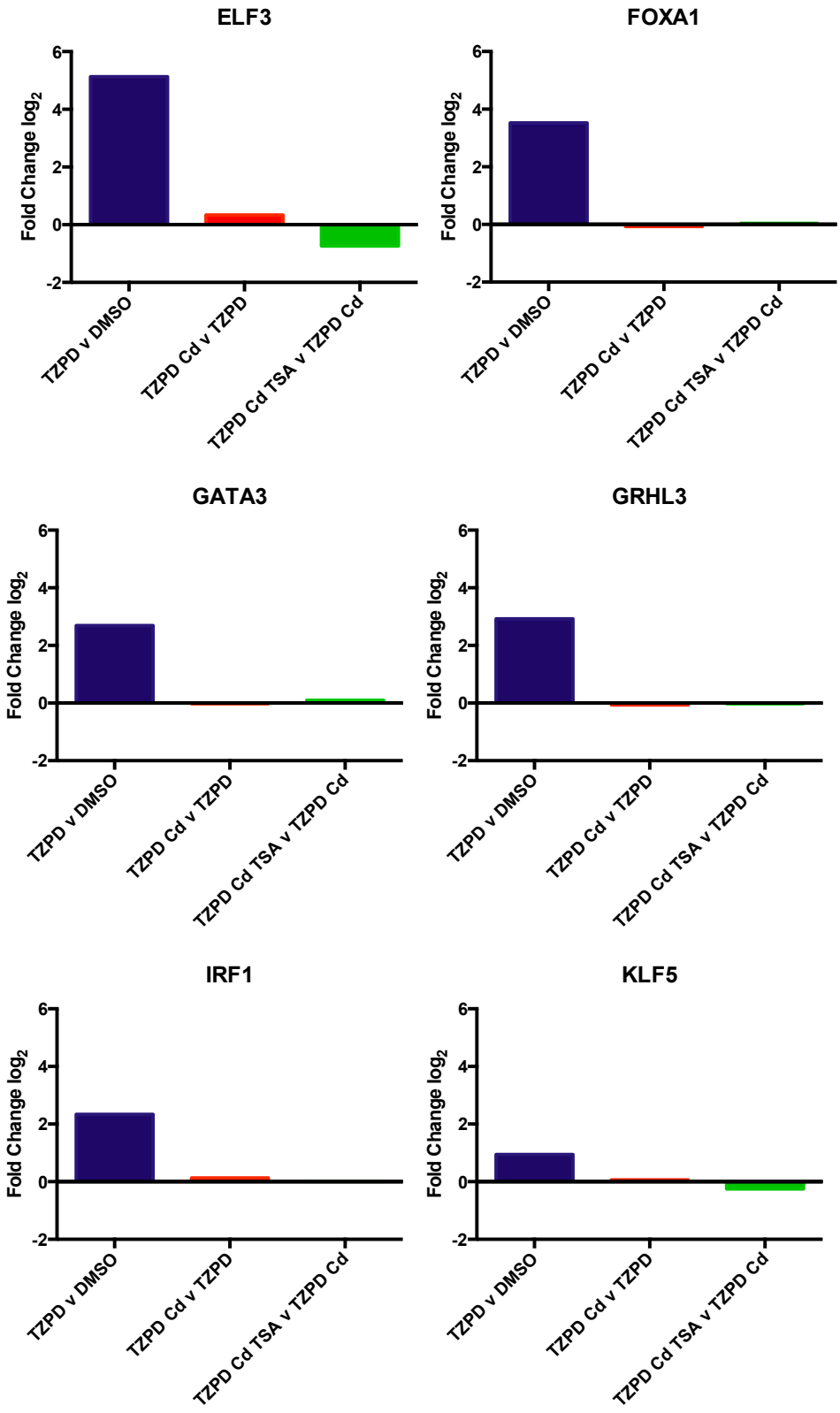

Figure 4.18. Agilent microarray analysis for transcription factors targets during urothelial differentiation, cadmium exposure and TSA treatment. Y1441 and Y1451 NHU cell cultures were treated ± TZPD ± 10 µM $CdCl_2$ ± 400 nM TSA. mRNA was collected at 72 hours and gene expression analysed using Agilent SurePrint G3 Human Microarrays.

4.3.6.3 Expression of chromatin modifying enzymes

As the results from the TSA experiments reported above indicated that histone modifications may be responsible for the silencing of differentiation genes by cadmium, the expression of chromatin modifying enzymes was analysed using the microarray data in order to investigate if histone modification changes were occurring during to a change in expression of these enzymes. In total six classses of chromatin modifying proteins were analysed.

Expression of polycomb group proteins which create and maintain repressive chromatin environments by forming two polycomb repressive complexes, PRC1 and PRC2 was analysed (Figure 4.19). Although differences were apparent upon differentiation, no differences greater than 1.5 fold change were noted during cadmium expoure.

Expression of herterochromatin protein (HP1) whch is a family of three proteins that are vital for the formation of transcriptionally inactive heterochromatin was analysed (Figure 4.20). No differences in their expression were found upon differentiation or cadmium and TSA treatment.

Three families of histone acetyltransferases (HATs) were analysed (Figure 4.21). The only change seen in expression amongst the HATs was for KAT2B upon differentiation. Cadmium exposure and TSA treatment did not affect HAT expression.

Expression of histone deacetylases (HDACs) was analysed (Figure 4.22). A few HDACs showed differential expression upon differentiation, but cadmium and TSA did not affect their expression.

Lysine methyltransferase (KMT) gene expression was analysed (Figure 4.23). Neither differentiation or cadmium and TSA treamtment affected the expression of KMTs.

Lysine demethylase (KDM) gene expression was analysed (Figure 4.24). Differentiation led to the uprgualtion of KDM1A, KDM3B and KDM7C by 2-fold change or greater and the downregualtion of KDM7A. Cadmium had no significant effect on expression of KDMs except for KDM1B which showed a 2-fold decrease in expression which was recovered by TSA.

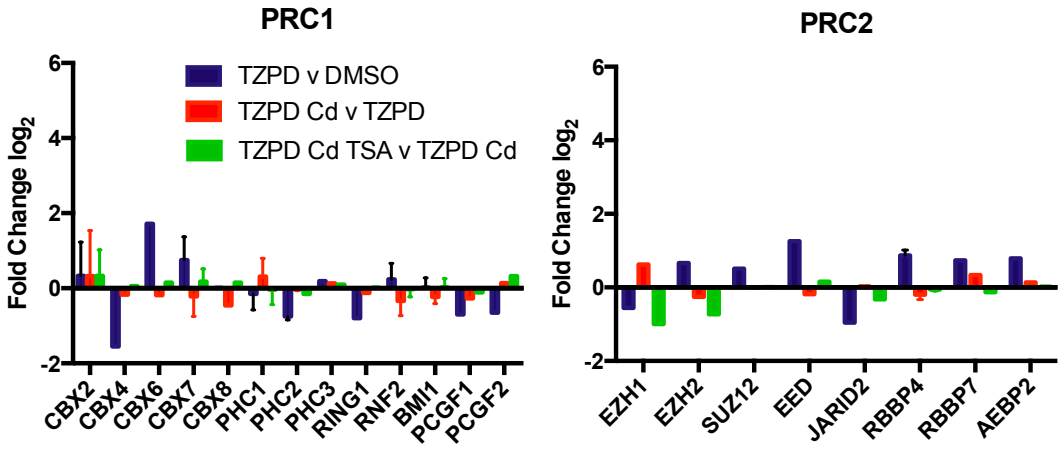

Figure 4.19. Agilent microarray analysis for the polycomb repressive complexes (PRC1 and PRC2) during urothelial differentiation, cadmium exposure and TSA treatment. Y1441 and Y1451 NHU cell cultures were treated ± TZPD ± 10 µM $CdCl_2$ ± 400 nM TSA. mRNA was collected at 72 hours and gene expression analysed using Agilent SurePrint G3 Human Microarrays.

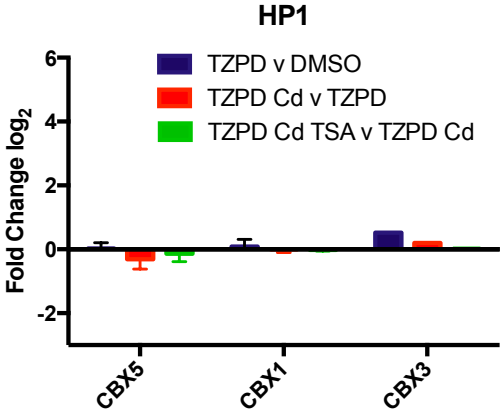

Figure 4.20. Agilent microarray analysis for herterochromatin protein (HP1) during urothelial differentiation, cadmium exposure and TSA treatment. Y1441 and Y1451 NHU cell cultures were treated ± TZPD ± 10 µM $CdCl_2$ ± 400 nM TSA. mRNA was collected at 72 hours and gene expression analysed using Agilent SurePrint G3 Human Microarrays.

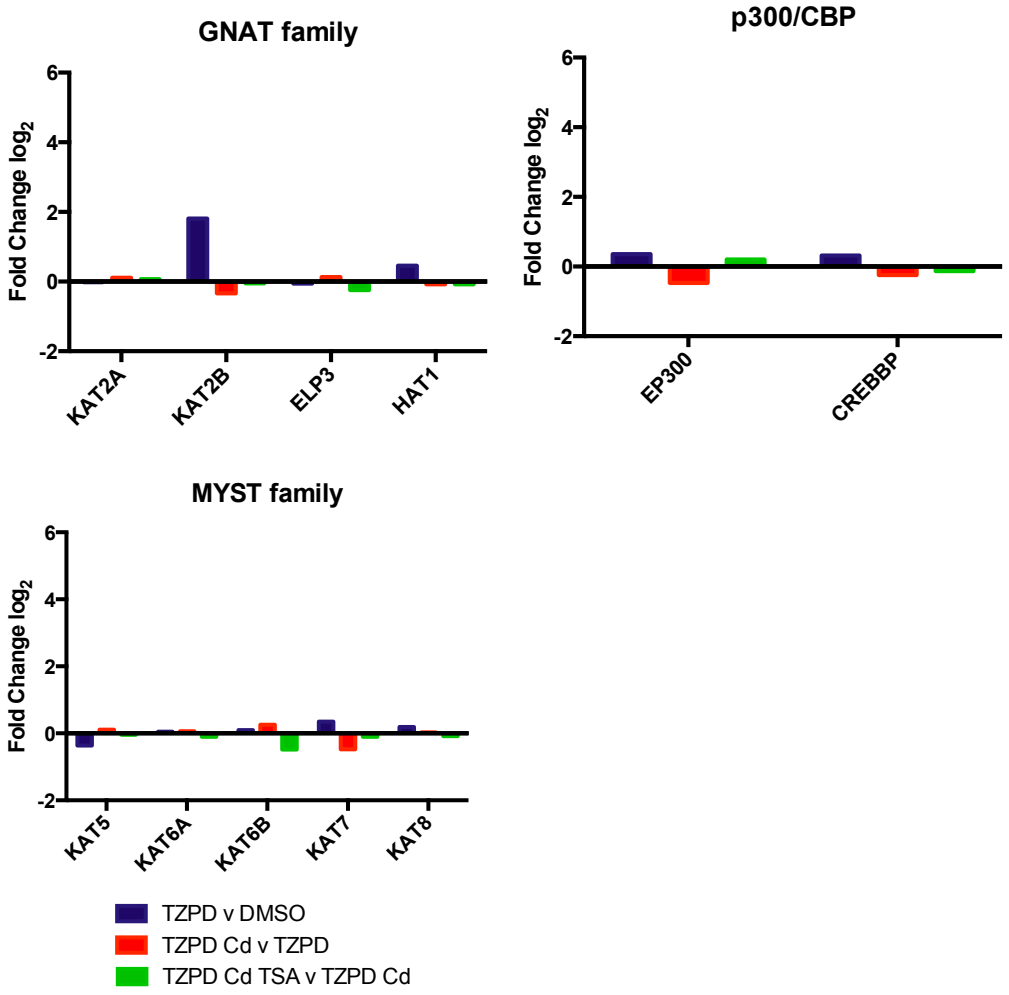

Figure 4.21. Agilent microarray analysis for histone acetyltransferases during urothelial differentiation, cadmium exposure and TSA treatment. Y1441 and Y1451 NHU cell cultures were treated ± TZPD ± 10 µM $CdCl_2$ ± 400 nM TSA. mRNA was collected at 72 hours and gene expression analysed using Agilent SurePrint G3 Human Microarrays

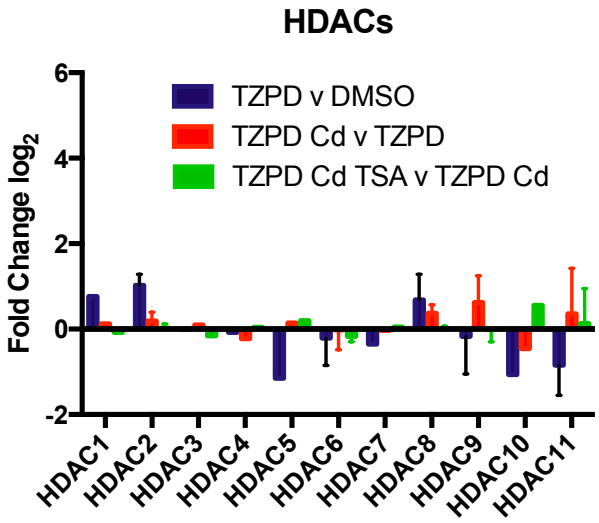

Figure 4.22. Agilent microarray analysis for histone deacetylases during urothelial differentiation, cadmium exposure and TSA treatment. Y1441 and Y1451 NHU cell cultures were treated ± TZPD ± 10 µM $CdCl_2$ ± 400 nM TSA. mRNA was collected at 72 hours and gene expression analysed using Agilent SurePrint G3 Human Microarrays.

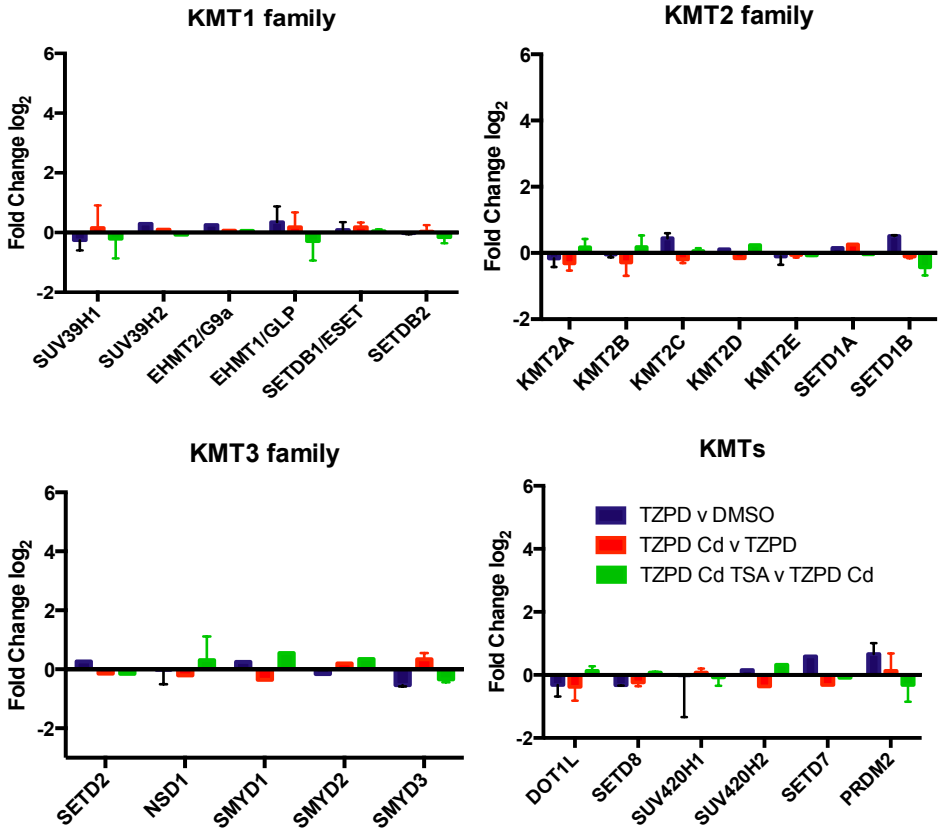

Figure 4.23. Agilent microarray analysis for lysine methltransferase (KMT) during urothelial differentiation, cadmium exposure and TSA treatment. Y1441 and Y1451 NHU cell cultures were treated ± TZPD ± 10 µM $CdCl_2$ ± 400 nM TSA. mRNA was collected at 72 hours and gene expression analysed using Agilent SurePrint G3 Human Microarrays.

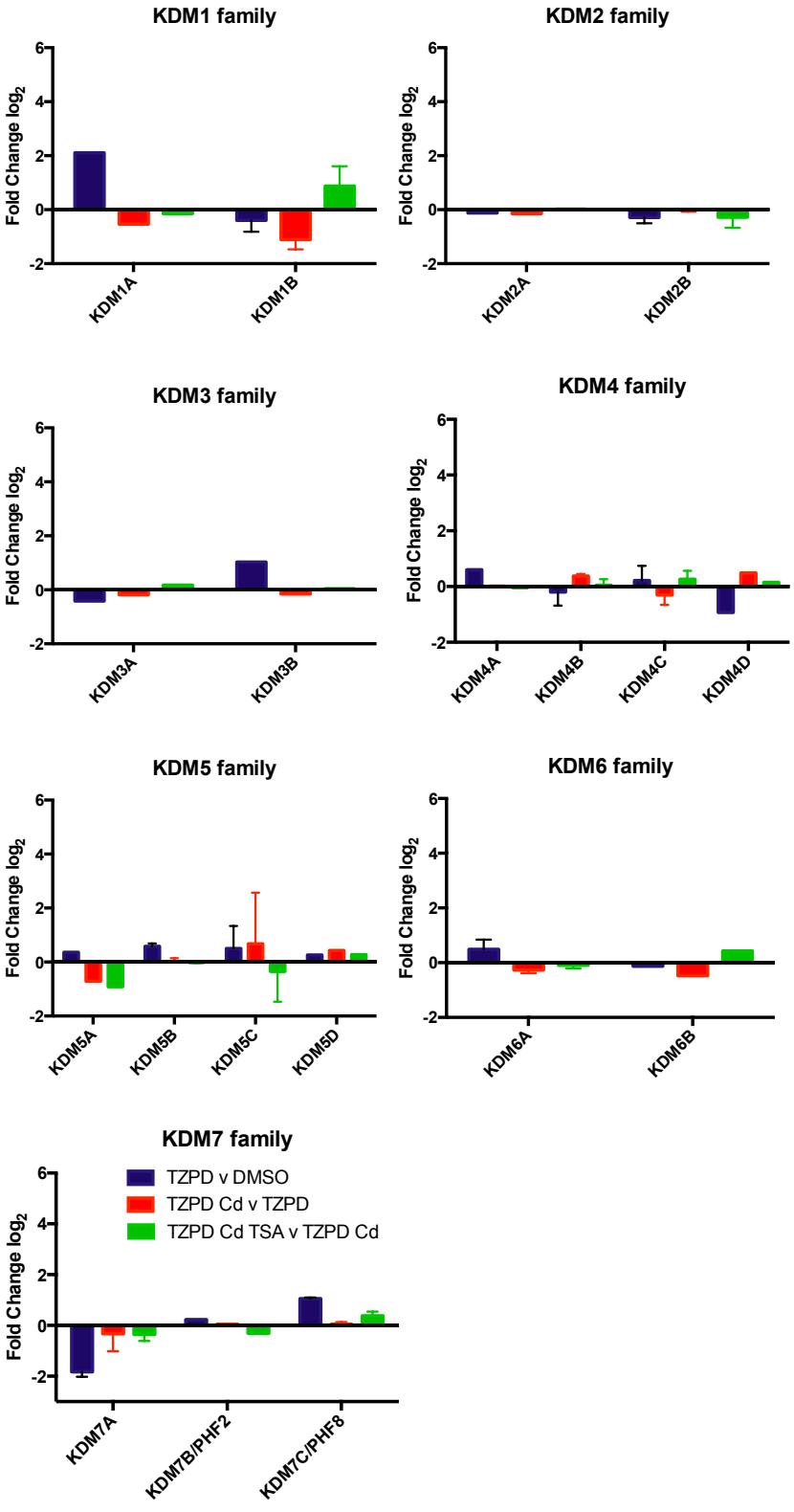

Figure 4.24. Agilent microarray analysis for lysine demethylases (KDM) during urothelial differentiation, cadmium exposure and TSA treatment. Y1441 and Y1451 NHU cell cultures were treated ± TZPD ± 10 µM $CdCl_2$ ± 400 nM TSA. mRNA was collected at 72 hours and gene expression analysed using Agilent SurePrint G3 Human Microarrays.

4.3.6.4 Identification of genes up/downregulated by cadmium and TSA

In order to identify genes that were affected by cadmium exposure, genes that had p values less than 0.05 were filtered for 2-fold up or down changes. Filtering of the upregulated genes selected 118 gene targets. The most upregulated genes are shown in Table 4.3. Filtering of the downregulated genes selected 588 gene targets, with the most downregulated genes shown in Table 4.4. Complete gene lists are shown in Appendix 4.

As expected, gene ontology enrichment analysis of the 118 genes upregulated in cadmium exposure (Figure 4.25) showed enrichment in GO biological process terms for a response to cadmium and zinc ions. This was due to the upregulation in metallothionein genes.

Other genes of note that were shown upregulated in response to cadmium included three zinc transporters (Figure 4.26).

When TSA was included in the treatment of NHU cell cultures, filtering produced 245 gene targets that were upregulated and 78 gene targets that were downregulated when compared to differentiating cultures exposed to cadmium (Appendix 4).

Table 4.3. Most upregulated genes by cadmium in TZPD-differentiating NHU cell cultures. Pairwise comparisons were performed between the two relevant treatment groups (TZPD and TZPD Cd) to identify genes that were differentially expressed, $p<0.05$.

Gene Symbol	Gene Name	Fold change log_2	GO biological process term
MT1G	Metallothionein 1G	14.5	Cellular response to cadmium/zinc ion
MT1H	Metallothionein 1H	11.8	Cellular response to cadmium/zinc ion
MT1M	Metallothionein 1M	8.4	Cellular response to zinc ion
MT1B	Metallothionein 1B	6.4	Cellular response to zinc ion
MT1L	Metallothionein 1L	6.4	Cellular response to zinc ion
MT1E	Metallothionein 1E	6.1	Cellular response to cadmium/zinc ion
MT1F	Metallothionein 1F	5.9	Cellular response to cadmium/zinc ion
MT1X	Metallothionein 1X	5.3	Cellular response to cadmium/zinc ion
MT1A	Metallothionein 1A	4.8	Cellular response to cadmium/zinc ion
MT2A	Metallothionein 2A	4.7	Cellular response to zinc ion
ALDH3A1	Aldehyde dehydrogenase 3 family, member A1	3.4	Response to hypoxia // positive regulation of cell proliferation // oxidation-reduction process
UCHL1	Ubiquitin carboxyl-terminal esterase L1 (ubiquitin thiolesterase)	3.1	Response to ischemia // protein deubiquitination // cell proliferation
HMOX1	Heme oxygenase (decycling) 1	2.8	Heme oxidation // angiogenesis // cellular response to cadmium ion
KRT16	Keratin 16	2.7	Cytoskeleton development // Keratinization // cell proliferation
TMEM71	Transmembrane protein 71	2.4	---

Table 4.4. Most downregulated genes by cadmium in TZPD-differentiating NHU cell cultures. Pairwise comparisons were performed between the two relevant treatment groups (TZPD and TZPD Cd) to identify genes that were differentially expressed, $p<0.05$.

Gene Symbol	Gene Name	Fold change log_2	GO biological process term
KRT8	Keratin 8	-4.1	Structural molecule activity
GPR179	G protein-coupled receptor 179	-3.2	Visual perception
BRIP1	BRCA1 interacting protein C-terminal helicase 1	-2.8	DNA duplex unwinding // DNA damage checkpoint // double-strand break repair
TDGF1	Teratocarcinoma-derived growth factor 1	-2.7	Cell differentiation // canonical Wnt signalling pathway
FCN2	Ficolin 2	-2.5	Complement activation // innate immune respnse
DTX1	Deltex 1, E3 ubiquitin ligase	-2.5	Notch signalling pathway //transcription
C4BPB	Complement component 4 binding protein, beta	-2.4	Complement activation, classical pathway
GRAMD1B	GRAM domain containing 1B	-2.4	---
CD200R1	CD200 receptor 1	-2.4	Regulation of immune response
FAM159B	Family with sequence similarity 159, member B	-2.3	---
TEX11	Testis expressed 11	-2.3	Negative regulation of apoptotic process
ZC3H12D	Zinc finger CCCH-type containing 12D	-2.3	Negative regulation of cell growth
FCAMR	Fc receptor, IgA, IgM, high affinity	-2.3	Immune system process
CD4	T-cell surface glycoprotein CD4	-2.3	Regulation of T cell activation // cell surface receptor signalling pathway
OR5J2	Olfactory receptor, family 5, subfamily J, member 2	-2.3	G-protein coupled receptor signalling pathway

	Homo sapiens (REF)	upload_1				
GO biological process experimental only	#	#	expected	Fold Enrichment	+/-	P value
cellular response to zinc ion	10	8	.05	> 5	+	1.26E-12
cellular response to cadmium ion	8	6	.04	> 5	+	1.03E-08
response to cadmium ion	10	6	.05	> 5	+	3.91E-08
response to zinc ion	14	8	.06	> 5	+	1.84E-11
response to transition metal nanoparticle	33	8	.15	> 5	+	1.63E-08
cellular response to metal ion	50	9	.23	> 5	+	9.87E-09
cellular response to inorganic substance	52	9	.24	> 5	+	1.39E-08
response to metal ion	92	9	.42	> 5	+	2.04E-06
response to inorganic substance	127	9	.58	> 5	+	3.26E-05
Unclassified	13320	46	60.80	.76	-	0.00E00

Figure 4.25. GO enrichment analysis for genes upregulated by cadmium exposure. T-tests were performed and genes were then filtered by 2-fold increase resulting in a list of 118 genes upregulated by cadmium exposure. This list was inputted in to the PANTHER Classification System; a PANTHER Overrepresentation Test was then performed using the annotation data set 'GO biological process experimental only'. The second column represents background frequency while the third column is sample frequency. Background frequency is the number of genes annotated to a GO term in the entire background set, while sample frequency is the number of genes annotated to that GO term in the input list. The symbols + and - indicate over or underrepresentation of a GO term.

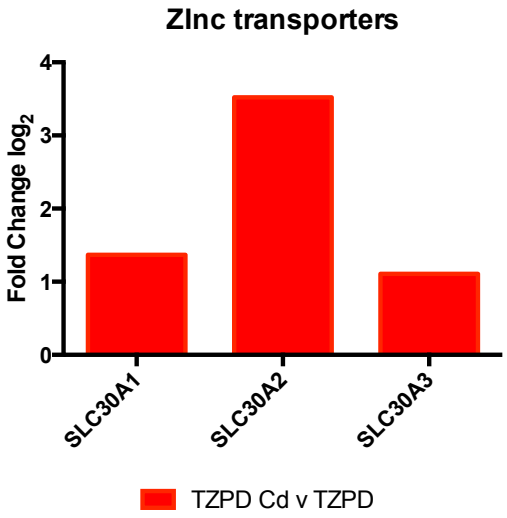

Figure 4.26. Upregulation of zinc transporters in TZPD-differentiating NHU cell cultures exposed to cadmium. Y1441 and Y1451 NHU cell cultures were treated with TZPD ± 10 µM $CdCl_2$. mRNA was collected at 72 hours and gene expression analysed using Agilent SurePrint G3 Human Microarrays.

4.4 Summary

- TSA treatment was able to reverse the inhibitory effects of cadmium for UPK2 and KRT20 (5/5), UPK1A (2/5) but not for KRT13 in five independent NHU cell lines. However, 5-azacytidine was not able to do the same. Overall the results from the TSA and 5aza experiments indicate that histone modifications rather than DNA methylation may be responsible for the silencing of differentiation-associated genes by cadmium.
- TSA did not affect the downregulation of CK13 protein by cadmium exposure in two out of three independent NHU cell lines.
- The inhibition of KRT14 downregulation at both transcript and protein level due to cadmium exposure reported in Chapter 3, could be prevented by TSA treatment.
- The SOX9 motif was shown to be enriched in the promoter regions for UPK2 and KRT20. SOX9 transcript was not downregulated upon differentiation when cadmium was present, although protein levels, assessed subjectively by immunofluorescence microscopy, remained unchanged.
- Results from Agilent microarrays showed:
    - Changes in uroplakin and cytokeratin gene expression following combined cadmium and TSA treatment
    - No significant changes in urothelial transcription factors or chromatin remodelling enzymes following cadmium and TSA treatment, with exception of KDM1B.
    - High induction of metallothionein genes upon cadmium exposure.

5 Cadmium Induced Post-translational Histone Modification Changes

5.1 Aims

Many metals, including arsenic, nickel and cobalt have been shown to induce post-translational histone modification changes in cell cultures. Histone modification changes implicated in arsenic exposure include alterations in global histone H3 methylation, with decreases in H3K27 trimethylation and increases in di- and trimethylated H3K4 (Zhou et al, 2008). Nickel exposure has been shown to lead to decreased histone acetylation of H2A, H2B, H3 and H4 (Broday et al., 2000; Golebiowski & Kasprzak, 2005; Ke et al., 2006), and increases in histone H3 lysine 9 dimethylation (Chen et al., 2006). Finally histone changes implicated with cobalt exposure include increases in H3K4me3, H3K9me2, H3K9me3, H3K27me3 and H3K36me3 and a decrease in acetylation of H4 (Li et al., 2009).

Reports of post-translational histone modification changes due to cadmium exposure are rather limited. However, one study reporting the epigenetic and genotoxic effects of cadmium telluride quantum dots in human breast carcinoma cells, found that free cadmium ions released in the cells led to chromatin condensation and global histone hypoacetylation (Choi et al., 2008).

The aims of this chapter were to:

- examine cadmium treated proliferative and differentiating NHU cell cultures for changes in global levels of post-translational histone modifications.
- determine if any of these changes correlate with the transcript expression decreases reported in Chapter 3 with the differentiation genes (KRT13, KRT20, UPK1A, UPK2) upon cadmium exposure.

5.2 Experimental Approach

5.2.1 Proliferative NHU cell cultures

Proliferative NHU cell cultures were treated with cadmium chloride concentrations ranging from 10 nM to 20 μM; medium was replaced every 48 hours. Control NHU cell cultures were maintained in KSFMc. Upon completion of cadmium treatment cultures was lysed using SDS lysis buffer to give whole cell lysates. Western blotting was performed to examine changes in known acetylation and methylation marks

present on the histone tails of H2A, H3 and H4. Equal quantities of protein were loaded per track and for quantification, final adjustments for loading were made using ß-actin as the housekeeping control protein. Densitometry was performed using LiCOR Odyssey software, and values were normalised to those obtained in the control (KSMFc) samples.

Antibodies used for histone acetylation marks included anti-H2AK5ac, anti-H3K9/14ac and anti-H4K5ac. Acetylation of histone tails by acetyltransferases induces chromatin decondensation, whereas the removal of acetyl groups by deacetylases promotes a tighter binding of the histones to the DNA.

Antibodies used for histone methylation marks included anti-H3K4me3, anti-H3K27me3 and anti-H4K20me3. Methylation of histones can be associated with either euchromatin or heterochromatin depending on the target histone residue. The tri-methylation of histone H3 lysine 27 (H3K27me3) is implicated in gene repression by promoting a compact chromatin structure (Ringrose et al., 2004). Tri-methylation of histone H4 lysine 30 (H4K20me3) is also associated with gene repression when present at promoters (Wang et al., 2008), whereas di/tri-methylated histone H3 lysine 4 (H3K4me2/me3) is associated with transcriptional activation, with the highest levels of this modification being observed near transcriptional start sites of highly expressed genes (Shi et al., 2004).

Immunofluorescence microscopy was performed to examine cellular localisations and confirm observations seen from the western blotting. NHU cells were seeded at a concentration of $1x10^5$ cells mL^{-1} on to 12-well slides. Cells were cultured for 5 days in the presence of 1 and 10 μM $CdCl_2$ before being fixed in methanol:acetone. Following air-drying, cells were immunolabelled using the H3K9/14ac and H4K5ac antibodies.

5.2.2 Differentiating NHU cell cultures

NHU cells were cultured until 80-90% confluent and then induced to differentiate using TZPD as described in Chapter 2. Cadmium chloride (concentration range 10 nM - 20 μM) and TSA (400 nM) were applied to NHU cell cultures at the same time as TZPD.

5.2.2.1 Quantification of histone changes using mass spectrometry

Quantification of global post-translational histone changes using mass spectrometry was performed in collaboration with Dr Mark Dickman and Tom Minshull from the Department of Chemical and Biological Engineering at the University of Sheffield. Cell culture treatments and preparation of histones was performed in York; RP-HPLC, MS/MS and MS analyses were performed in Sheffield.

NHU cell cultures were treated with TZPD ± 10 μM $CdCl_2$ for 72 hours. Histones were acid-extracted from cell cultures as described in Chapter 2, following the technique of Shechter et al (2007). Histones were quantified using a Bradford assay and purity tested via SDS/PAGE gel and staining with Coomassie Brilliant Blue solution. 10 μg of histone proteins were derivatized using propionic anhydride to neutralize charge and block lysine residues as described by Garcia et al (2007). Histones were digested by trypsin, which cleaved only at the arginine residues as all lysine residues were blocked by endogenous modifications or chemically by conversion to propionyl amides, to give reproducible histone H3 fragments (Figure 5.1).

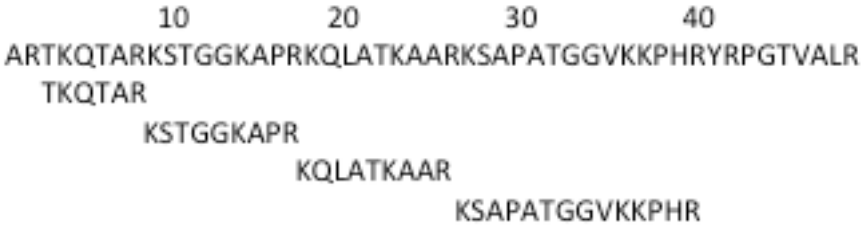

Figure 5.1. Peptides generated from the trypsin digestion of propionylated histone H3.

The histone peptides then underwent offline fractionation by reversed phase high performance liquid chromatography using a porous graphitic carbon (Hypercarb™) column before MS/MS analysis. Relative quantification of histone post-translational modifications was determined using the area under the extracted ion chromatogram peak corresponding to a specific modified peptide, normalized to the sum of the peak areas corresponding to all observed modified forms of such peptide.

5.2.2.2 Immunofluorescence microscopy

Immunofluorescence microscopy was performed to confirm the results seen from the MS analysis. NHU cells were seeded on to 12-well slides. Once cultures were 80-

90% confluent cells were treated ± TZPD ± $CdCl_2$ for 3 days before being fixed in methanol:acetone. Following air-drying, cells were immunolabelled using the H3K9me2 and H3K9me3 antibodies.

5.2.2.3 ChIP-(Q)PCR

In order to investigate if the silencing of differentiation genes brought about by cadmium exposure was associated with the H3K9me3 mark, ChIP-QPCR was performed.

ChIP-QPCR was performed using Dynabeads® as described by Collas (2011). Sonicated chromatin (100 bp-600bp) from formaldehyde-fixed cells, that had been treated ±TZPD ±$CdCl_2$ ±TSA for 3 days, was diluted in RIPA ChIP buffer and subjected to ChIP using antibodies targeted to either histone H3 trimethylated lysine 9 (H3K9me3), total histone H3 (positive control) or anti-rabbit IgG (negative control).

To confirm the success of the ChIP, PCR was performed with QPCR then utilised to quantify the changes observed for four known differentiation genes (KRT13, KRT20, UPK1A, UPK2).

5.2.2.4 Western blotting

Upon completion of cadmium treatment, cell cultures were either lysed in SDS lysis buffer to give whole cell lysates or underwent acid-extraction by 0.2 M H_2SO_4 to give histone proteins before western blotting was performed to examine changes in histone post-translational modifications in differentiating NHU cell cultures treated with cadmium.

Antibodies used for acetylation and methylation marks included anti-H3K9ac, anti-H3K18ac, anti-H3K23ac, anti-H3K9me2 and anti-H3K9me3. Total histone H3 was used as the loading control.

5.3 Results

5.3.1 Proliferative NHU cell cultures

To study whether cadmium exposure alters epigenetic marks on histones, proliferative NHU cell cultures (Y1054) were treated with 10 nM, 100 nM, 1 μM and 10 μM CdCl2 for 96 hours. Global levels of commonly studied histone modifications, including histone acetylation and methylation were assessed by western blot analysis. The results showed that global acetylation levels on histones H2A, H3 and H4 were reduced by cadmium treatment in a dose-dependent manner (Figure 5.2). However results for histone methylation marks differed across the cadmium chloride concentrations (Figure 5.3). Amounts of tri-methylation on H3 lysine 4 (H3K4me3) and tri-methylation on H3 lysine 27 (H3K27 me3) increased with lower doses (≤100 nM) of $CdCl_2$, but decreased with the highest dose (10 μM), while levels of tri-methylation on H4 lysine 20 (H4K20me3) decreased with doses above 100 nM $CdCl_2$.

Two further proliferative NHU cell lines, Y1141 and Y1220 were treated with 1 μM, 10 and 20 μM $CdCl_2$ for 72 and 96 hours respectively to assess global amounts of acetylation on histone H2A, H3 and H4. Both cell lines showed decreased global amounts of H2AK5ac, H3K9/14ac and H4K8ac with increasing concentrations of $CdCl_2$ (Figure 5.4, Figure 5.5).

Additionally, immunofluorescence microscopy was used to examine global amounts of histone acetylation. NHU cell cultures (Y1183) were treated with 1 and 10 μM $CdCl_2$ for 5 days before fixation with methanol:acetone, followed by immunolabelling using antibodies against H4K8ac and H3K9/14ac. All fluorescence images were taken at the same exposure and showed that H4K8ac and H3K9/14ac labelling was nuclear and appeared less bright in the cadmium exposed cell cultures (Figure 5.6).

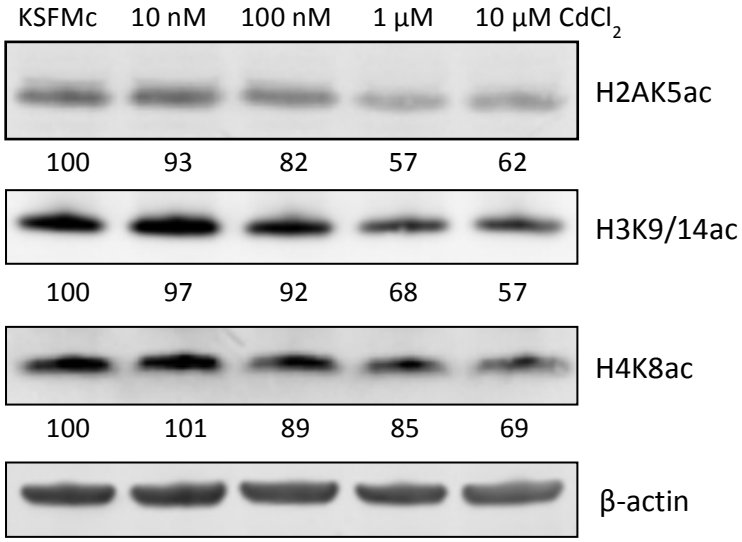

Figure 5.2. Western blot analysis for acetylation marks on histone H2A, H3 and H4 in proliferative NHU cell cultures (Y1054) treated with cadmium for 96 hours. Cells were lysed using SDS lysis buffer and then sonicated. Protein concentration was measured using a Bradford assay. 4-12% Bis-Tris gels were loaded with 20 µg of protein and run at 200 V in MES running buffer. Protein was blotted on to PVDF membranes using the Novex apparatus for 2 hours at 30 V. Membranes were blocked in Odyssey blocking buffer, incubated with primary antibodies overnight at 4°C, and secondary antibodies for one hour at ambient temperature then scanned on the Li-Cor imaging system. The fluorescence of each band was quantified and normalised to the loading control β-actin using the Odyssey software. Numbers quantifying the percentage intensity of the bands are displayed below the corresponding bands.

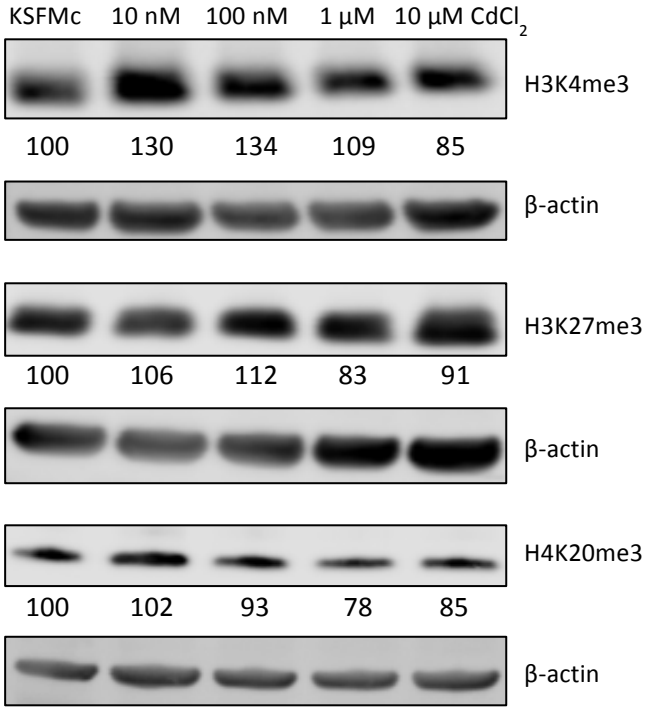

Figure 5.3. Western blot analysis for methylation marks on histone H3 and H4 in proliferative NHU cell cultures (Y1054) treated with cadmium for 96 hours. Cultures were lysed in situ with SDS lysis buffer and then sonicated. Protein concentration was measured using a Bradford assay. 4-12% Bis-Tris gels were loaded with 20 µg of protein and run at 200 V in MES running buffer. Protein was blotted on to PVDF membranes using the Novex apparatus for 2 hours at 30 V. Membranes were blocked in Odyssey blocking buffer, incubated with primary antibodies overnight at 4°C, and secondary antibodies for one hour at ambient temperature then scanned on the Li-Cor imaging system. The fluorescence of each band was quantified and normalised to the loading control β-actin using the Odyssey software. Numbers quantifying the percentage intensity of the bands are displayed below the corresponding bands.

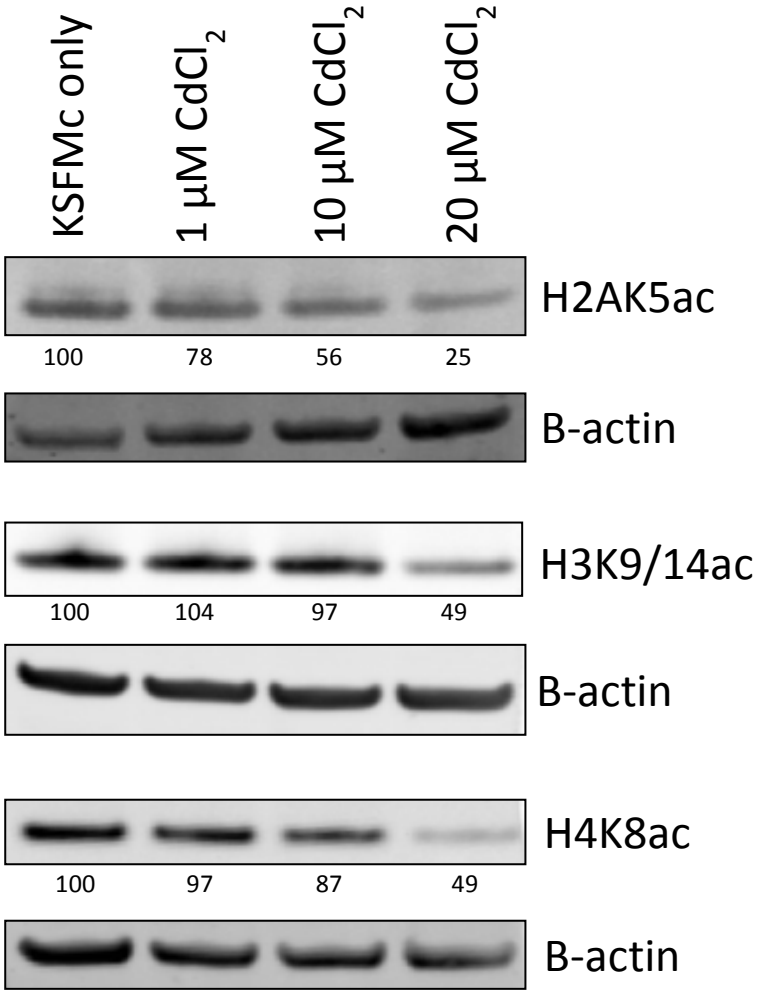

Figure 5.4. Western blot analysis for acetylation marks on histone H2A, H3 and H4 in NHU cell cultures (Y1141) treated with cadmium for 72 hours. Cultures were lysed in situ with SDS lysis buffer and then sonicated. Protein concentration was measured using a Bradford assay. 4-12% Bis-Tris gels were loaded with 20 µg of protein and run at 200 V in MES running buffer. Protein was blotted on to PVDF membranes using the Novex apparatus for 2 hours at 30 V. Membranes were blocked in Odyssey blocking buffer, incubated with primary antibodies overnight at 4°C, and secondary antibodies for one hour at ambient temperature then scanned on the Li-Cor imaging system. The fluorescence of each band was quantified and normalised to the loading control β-actin using the Odyssey software. Numbers quantifying the percentage intensity of the bands are displayed below the corresponding bands.

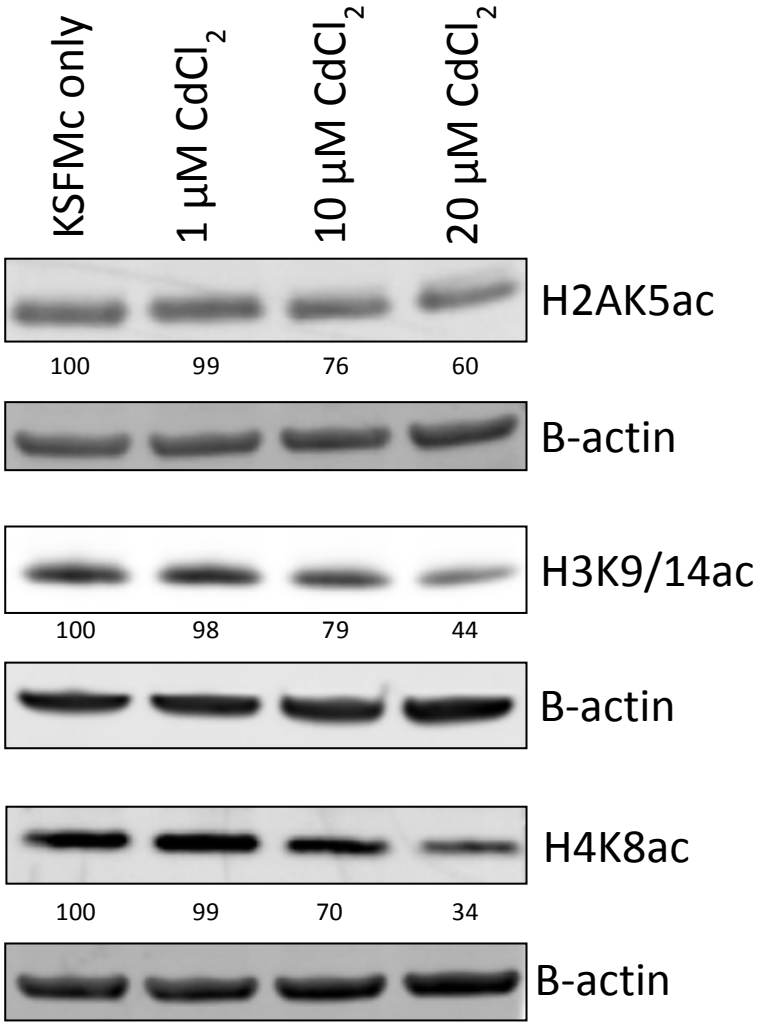

Figure 5.5. Western blot analysis for acetylation marks on histone H2A, H3 and H4 in NHU cell cultures (Y1202) treated with cadmium for 96 hours. Cultures were lysed in situ with SDS lysis buffer and then sonicated. Protein concentration was measured using a Bradford assay. 4-12% Bis-Tris gels were loaded with 20 µg of protein and run at 200 V in MES running buffer. Protein was blotted on to PVDF membranes using the Novex apparatus for 2 hours at 30 V. Membranes were blocked in Odyssey blocking buffer, incubated with primary antibodies overnight at 4°C, and secondary antibodies for one hour at ambient temperature then scanned on the Li-Cor imaging system. The fluorescence of each band was quantified and normalised to the loading control β-actin using the Odyssey software. Numbers quantifying the percentage intensity of the bands are displayed below the corresponding bands.

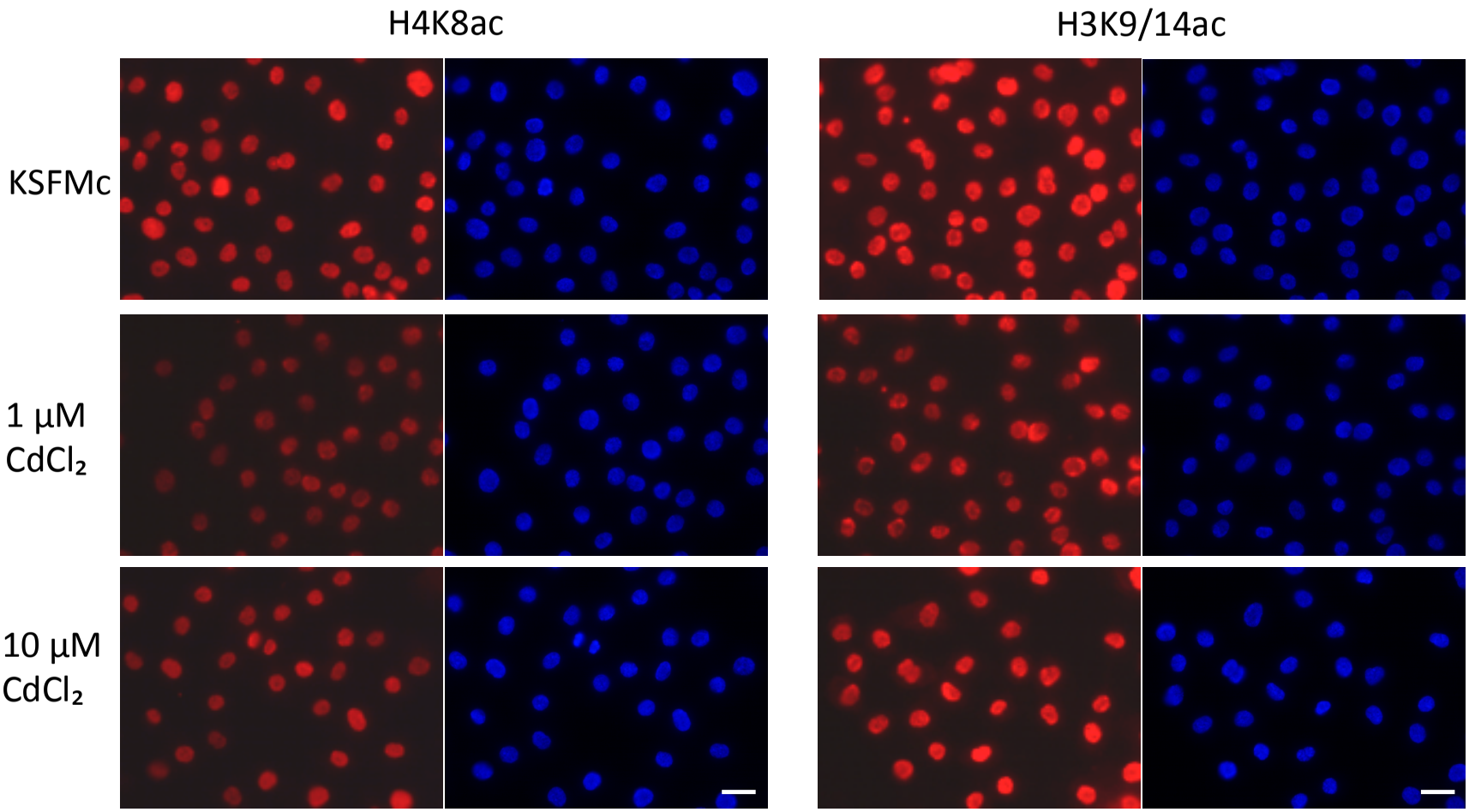

Figure 5.6. Immunofluorescence images of H3 and H4 acetylation marks in proliferative NHU cell cultures (Y1183) treated with cadmium chloride. NHU cells were seeded at a concentration of $1x10^5$ cells mL^{-1} on to 12-well slides. Cells were cultured for 5 days before being fixed in methanol:acetone. Cells were immunolabelled using rabbit primary antibodies to histone marks as indicated and goat anti-rabbit secondary antibodies (red). Nuclei were stained with Hoechst 33258 (blue). Scale bar, 10µM.

5.3.2 Differentiating NHU cell cultures

5.3.2.1 Mass spectrometry quantification of epigenetic marks on histone H3

Post-translational histone modifications of histone H3 were quantified using a mass spectrometry approach using histones isolated from differentiating NHU cell cultures (Y1202) that had been treated with or without 10 μM $CdCl_2$ for 72 hours.

Three peptides, K9-17, K18-26 and K27-40 of the H3 tail gave reliable identifications across all samples to allow quantification. In total 22 different combinations of histone modifications on 6 different lysine residues were manually verified and identified along the H3 tail. These modifications were quantified to give relative abundances per peptide (Figure 5.7). Due to overlapping retention times for acetylation on different positions of the same peptide (ie. K9ac v K14ac and K18ac v K23ac) an accurate percentage for each individual mark could not be ascertained, therefore in these cases relative abundance is given as the sum of both the individual marks.

The most profound change seen when cadmium was present was the change in methylation state of lysine 9 (K9). Mono and di-methylation (K9me1 and K9me2) were reduced with cadmium treatment whereas tri-methylation (K9me3), a repressive mark, was increased. Relative abundance reduced from 9.1% to 5.8% for K9me1 and 39.6% to 28.9% for K9me2 whereas K9me3 increased from 25.4% to 36% upon cadmium treatment.

Other changes of note include decreases in activating marks including K18/23ac and K9me1K14ac, although K9/14ac was increased, alongside increases in repressive marks including K27me2 and K27me3. Also the combinatorial mark K27me1K36me3 appears absent in cadmium treated cultures. Overall this indicated that cadmium treatment resulted in a more repressive chromatin state.

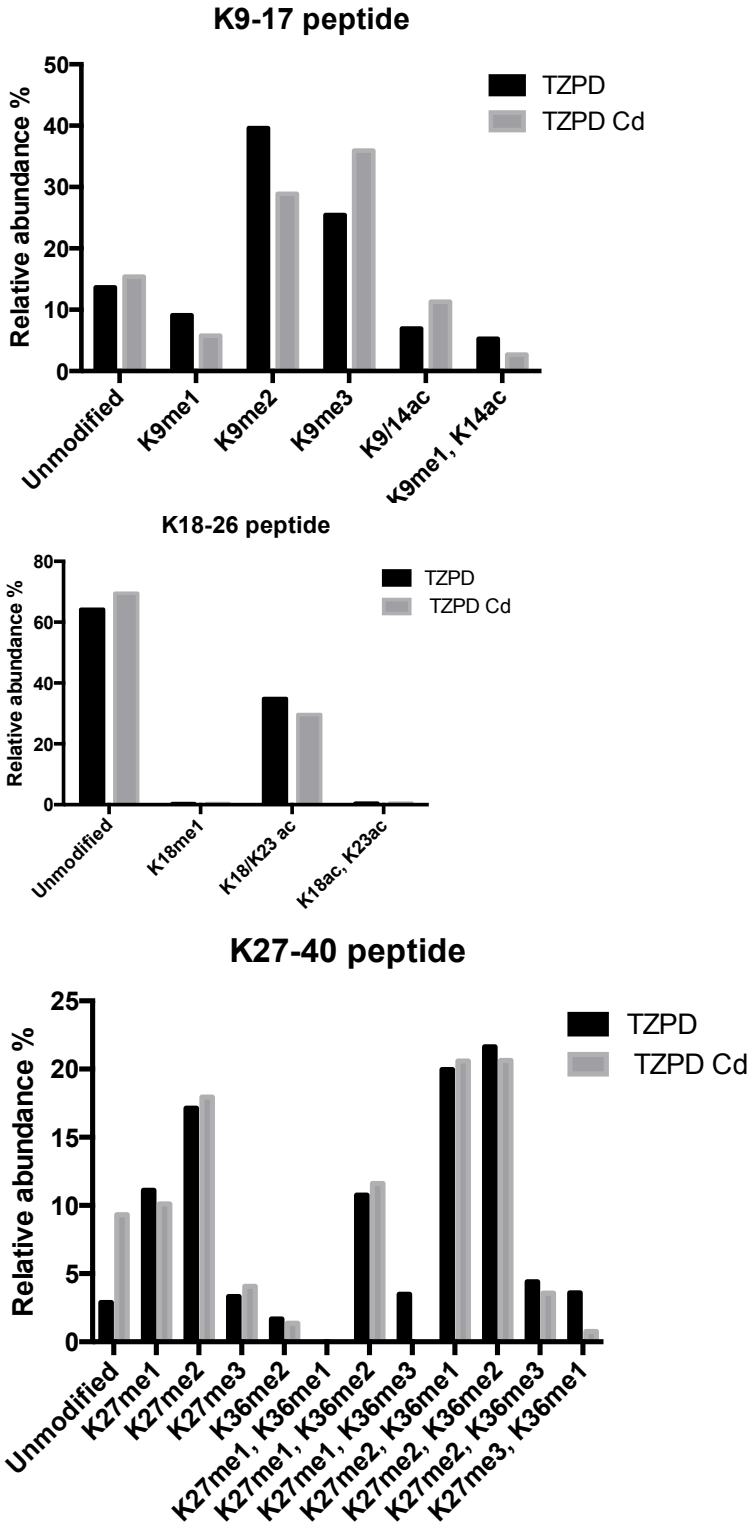

Figure 5.7. Mass spectrometry analysis of histone modification changes on histone H3 isolated from TZPD-induced differentiating NHU cell cultures (Y1202) treated with or without 10 µM $CdCl_2$ for 72 hours. Bar charts represent the relative abundance of the histone modifications for peptides covering residues 9-17 (KSTGGKAPR), 18-26 (KQLATKAAR) and 27-40 (KSAPATGGVKKPHR). MS data provided by Tom Minshull under the supervision of Dr Mark Dickman (University of Sheffield).

5.3.2.2 Immunofluorescence microscopy for H3K9me2 and H3K9me3

Immunofluorescence microscopy was used to further examine the H3K9me2 and H3K9me3 marks. NHU cell cultures (Y1357) were treated with TZPD or TZPD and 10 μM $CdCl_2$ alongside a DMSO control for 3 days. Immunofluorescence for H3K9me2 showed a change in shape and size of H3K9me2 foci between differentiated and non-differentiated (DMSO) cultures with H3K9me2 labelling appearing more punctate in TZPD and TZPD Cd treated cultures (Figure 5.8).

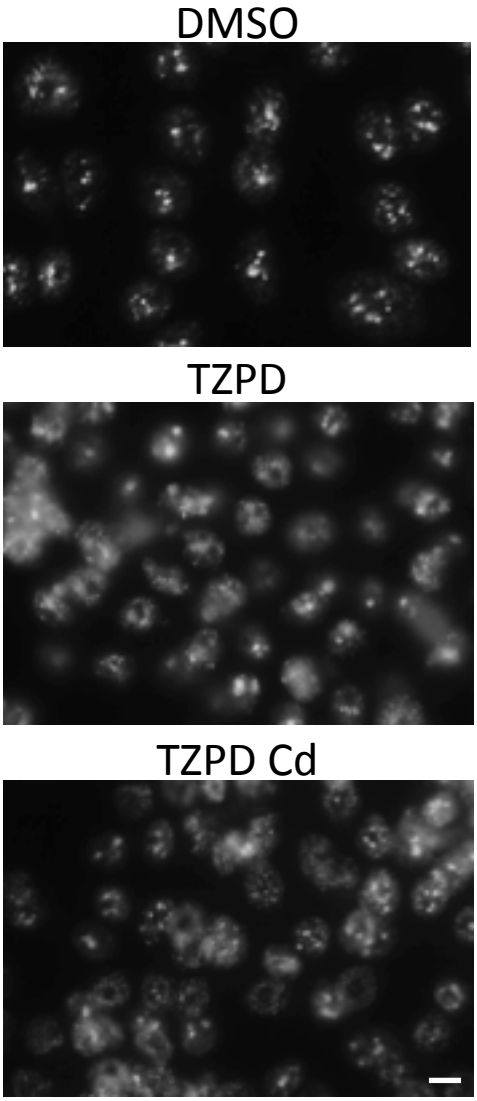

Figure 5.8. Immunofluorescence microscopy images for H3K9me2. NHU cells (Y1357) were seeded at a concentration of $3x10^5$ cells mL^{-1} on to 12-well slides. Once cultures were 80-90% confluent cells were treated for 3 days ± TZPD ± 10 μM $CdCl_2$ before being fixed in methanol:acetone. Cells were immunolabelled using anti-H3K9me2 rabbit primary antibodies and goat anti-rabbit secondary antibodies. Scale bar, 5 μM.

Immunofluorescence for H3K9me3 showed qualitative increases with differentiation and cadmium treatment compared to control cultures treated with DMSO only (Figure 5.9). Additionally, cadmium treatment showed increases in H3K9me3 at the nuclear periphery.

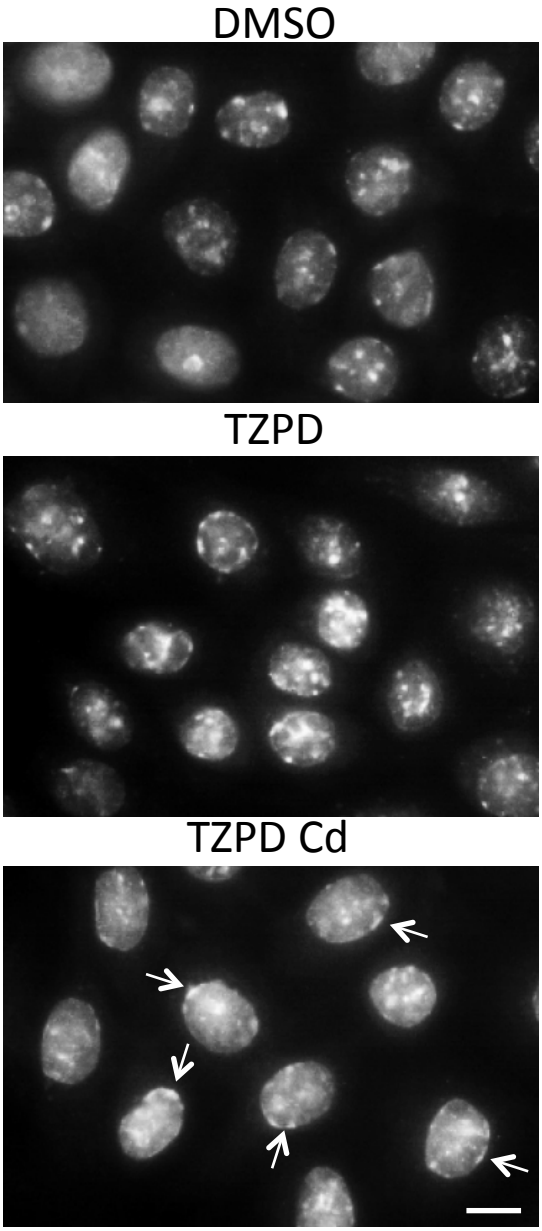

Figure 5.9. Immunofluorescence microscopy images for H3K9me3. NHU cells (Y1357) were seeded at a concentration of $3x10^5$ cells mL^{-1} on to 12-well slides. Once cultures were 80-90% confluent cells were treated for 3 days ± TZPD ± 10 µM $CdCl_2$ before being fixed in methanol:acetone. Cells were immunolabelled using anti-H3K9me3 rabbit primary antibodies and goat anti-rabbit secondary antibodies. Arrows indicate H3K9me3 labelling at the nuclear periphery. Scale bar, 5 µM.

5.3.2.3 Chromatin Immunoprecipitation

As the results from the MS analysis showed that the greatest change seen was with the H3K9me3 mark, ChIP-QPCR was performed using antibodies to this mark to see how H3K9me3 associated with four urothelial differentiation genes known to be downregulated due to cadmium exposure (KRT13, KRT20, UPK1A and UPK2).

Fragmented chromatin from NHU cell cultures (Y1141) that had been treated with either DSMO only, TZPD, TZPD $CdCl_2$ or TZPD $CdCl_2$ TSA for 72 hours was incubated with antibodies against H3K9me3, as well as H3 (positive control) and rabbit IgG (negative control). Anti-IgG Dynabeads were used to capture antibody-chromatin complexes; DNA was recovered by phenol-chloroform extraction.

In order to determine if ChIP had been successful, ChIP-isolated DNA was subjected to PCR using primers designed against the four differentiation genes. ChIP-PCR for H3K9me3 (Figure 5.10) showed that eluates from the positive control, H3, were positive in all samples and eluates from anti-rabbit IgG were negative in all samples. Differing amounts of PCR product for all four differentiation genes was present in each of the treated cell cultures; QPCR was used to quantify these changes.

ChIP-QPCR for H3K9me3 (Figure 5.11) showed that H3K9me3 occupancy at all four differentiation-associated genes was highest in the TZPD Cd samples.

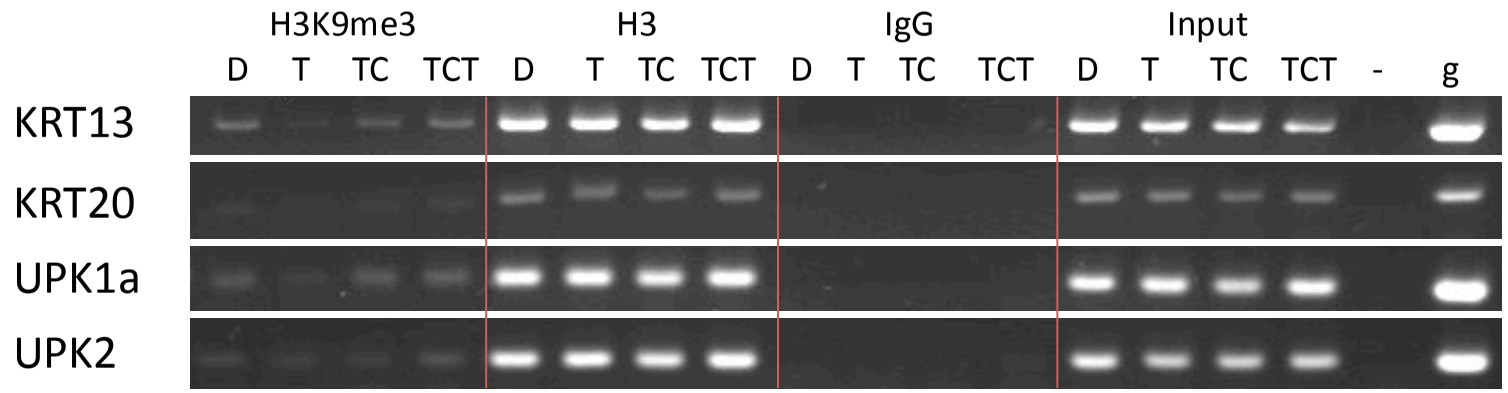

Figure 5.10. ChIP-PCR for H3K9me3. Y1441 NHU cell cultures were treated ±TZPD ±$CdCl_2$ ±TSA for 3 days before undergoing ChIP with anti-H3K9me2, anti-histone H3 and rabbit IgG. H3 was the positive control and rabbit IgG was the negative control. PCR was performed for 36 cycles. Genomic (g) DNA was used as a positive control and nuclease free H_2O was used as a no template control for the PCR reactions. D = DMSO, T = TZPD, TC = TZPD Cd and TCT = TZPD Cd TSA.

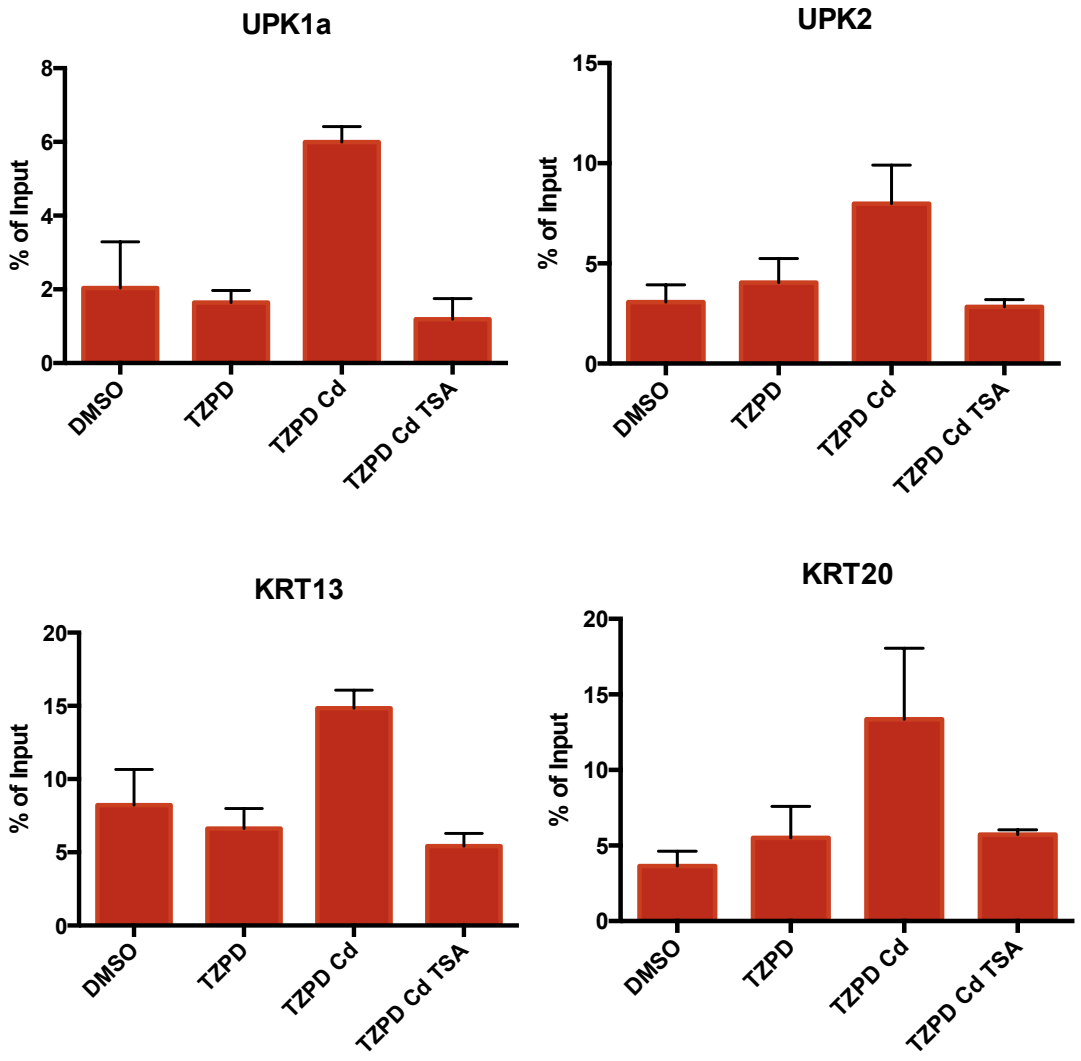

Figure 5.11. ChIP-QPCR analysis for H3K9me3. Data is represented as % of input where % of input = ($2^{-Ct\ IP}/2^{-Ct\ input}$) x 100. Error bars indicate standard deviation of three technical replicates.

5.3.2.4 Mass spectrometry quantification of epigenetic marks on histone H3 for a biological repeat

Post-translational histone modifications of histone H3 were quantified using a mass spectrometry approach using histones isolated from differentiating NHU cell cultures (Y1456) that had been treated with or without 10 μM $CdCl_2$ for 72 hours.

Overall the changes seen in histone modifications in the biological repeat Y1456 cultures (Figure 5.12) were not as profound as those seen in the Y1202 cultures, with only minor changes seen in the methylation states of K9. The greatest change seen due to cadmium treatment was the decrease in acetylation on K18 and K23 (K18/K23ac); relative abundance decreased from 34.9% in TZPD cultures to 22.8% in TZPD Cd cultures. Other notable changes include increases in the combinatorial marks K27me1K36me2, K27me2K36me2 and K27me2K36me3.

The two data sets for the biological replicates were combined to show the combined relative abundances and standard deviations against a DMSO treated non-differentiated culture (Figure 5.13). When comparing differentiating cultures (TZPD) with undifferentiated (DMSO) cultures, epigenetic marks that showed differences outside of the standard deviation of the measurements included decreases in all three of the unmodified peptides (K9-17, K18-26 and K27-40), decreases in K36me2, K27me1K36me1 and K27me1K36me2 and increases in K9me2, K18/23ac, K27me3, K27me2K36me3 and K27me3K36me1. When comparing TZPD Cd with TZPD treated cultures, changes in epigenetic marks that were outside of the standard deviation of the two biological replicates included increases in K27me3, K27me1K36me2 and unmodified K9-17 and K18-26 peptides along with a decrease in K18/23ac.

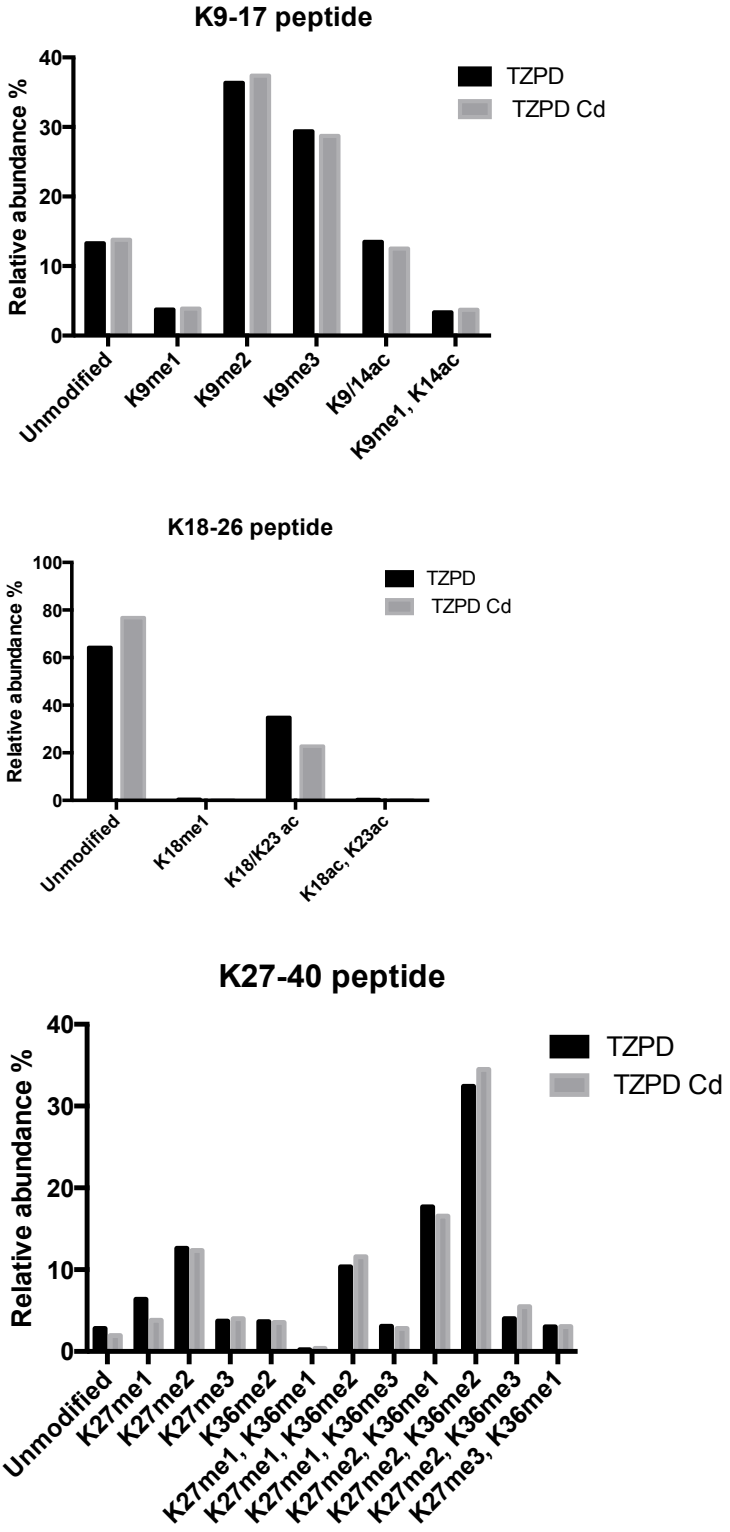

Figure 5.12. Mass spectrometry analysis of histone modification changes on histone H3 isolated from TZPD-induced differentiating NHU cell cultures (Y1456) treated with or without 10 µM $CdCl_2$ for 72 hours. Bar charts represent the relative abundance of the histone modifications for peptides covering residues 9-17 (KSTGGKAPR), 18-26 (KQLATKAAR) and 27-40 (KSAPATGGVKKPHR). MS data provided by Tom Minshull under the supervision of Dr Mark Dickman (University of Sheffield).

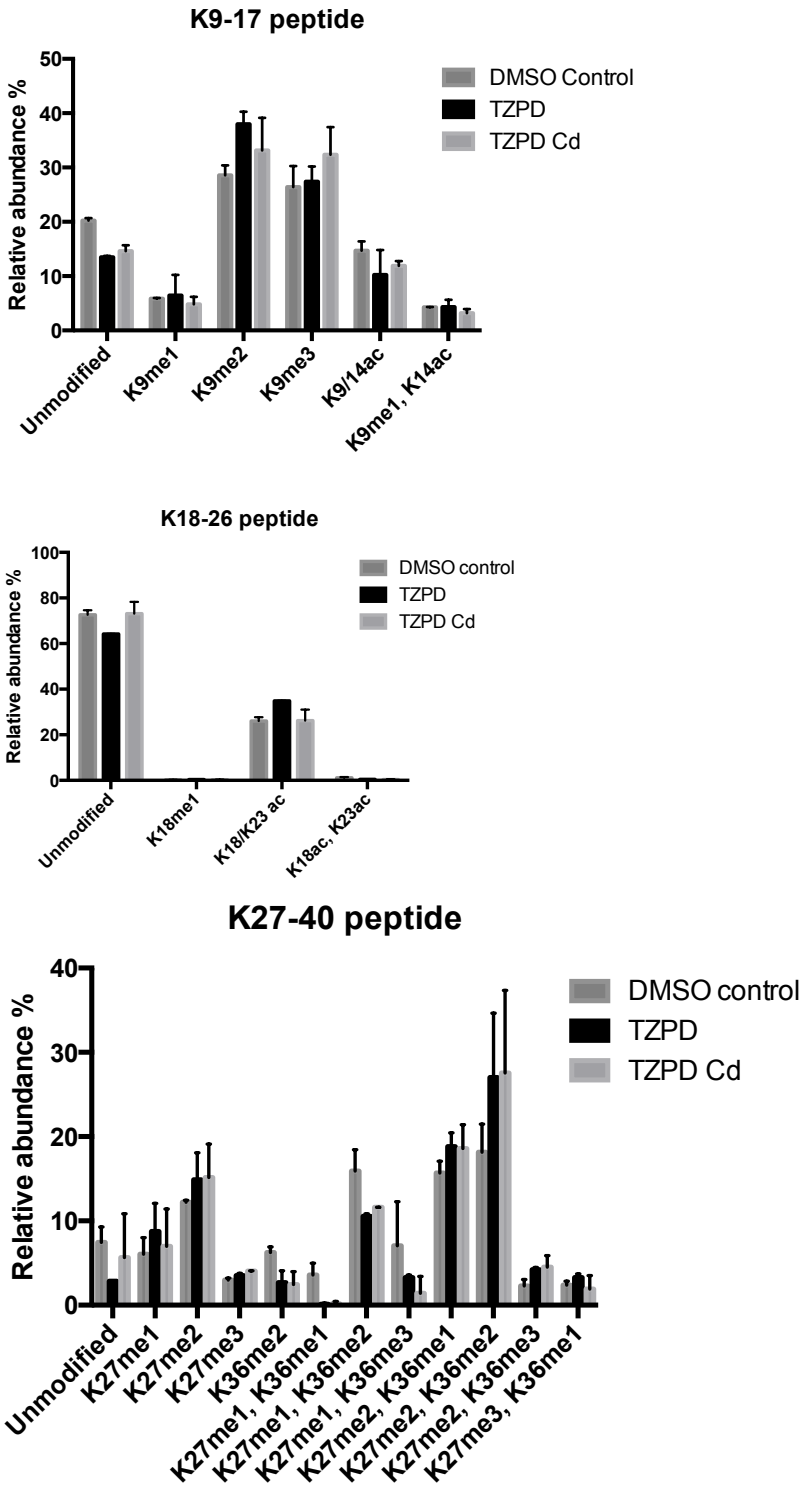

Figure 5.13. Mass spectrometry analysis of histone modification changes on histone H3 isolated from two NHU cell lines treated ± TZPD ± 10 µM $CdCl_2$ for 72 hours. Bar charts represent the relative abundance of the histone modifications for peptides covering residues 9-17 (KSTGGKAPR), 18-26 (KQLATKAAR) and 27-40 (KSAPATGGVKKPHR). Error bars indicate the SD of two independent biological replicates (Y1202 and Y1456) except for those for DMSO, which indicate the SD of two technical replicates (Y1456). MS data provided by Tom Minshull under the supervision of Dr Mark Dickman (University of Sheffield).

5.3.2.5 Immunoblotting for histone H3 epigenetic marks

To further explore changes in epigenetic marks on histone H3, immunoblotting against methylation on histone H3 lysine 9 and acetylation on histone H3 lysine 9, 18 and 23 was performed.

Western blots, carried out using whole cell lysates from two independent NHU cell lines treated with DMSO (control), TZPD or TZPD Cd, for H3K9me2, H3K18ac and H3K23ac showed that upon differentiation there was an increase in all three epigenetic marks (Figure 5.14). This was in agreement with the MS analysis. However cadmium treatment led to differing effects between the two cell lines. When TZPD and TZPD Cd treated cultures were compared, H3K9me2 was decreased in one cell line (Y1197) but slightly increased in the other (Y1223) and H3K23ac was increased in one (Y1197) and stayed the same in the other (Y1223). However, changes in H3K18ac were shown to be the same for both cell lines with expression of H3K18ac being decreased upon cadmium exposure.

Immunoblotting was performed on whole cell lysates from TZPD-differentiating cell cultures, treated with either 1 or 10 μM $CdCl_2$, in order to investigate changes in epigenetic marks caused by differing concentrations of cadmium. Cadmium treatments of 1 μM had a different effect compared to 10 μM treatments (Figure 5.15). 1 μM treatments led to increases in all four of the epigenetic marks (H3K9me2, H3K9me3, H3K18ac and H3K23ac). However, 10 μM treatments led to decreases in methylation marks (H3K9me2 and H3K9me3) but increases in the acetylation marks (H3K18ac and H3K23 ac).

Western blots were also performed on histones extracted from two independent NHU cell lines that had been treated with or without TZPD and $CdCl_2$. Results for acetylation marks on histone H3 (Figure 5.16), showed that upon differentiation (Cont v TZPD), acetylation at lysine 9, 18 and 23 increased in both cell lines. When differentiating cultures where treated with cadmium (TZPD Cd), acetylation was shown to increase for all three marks in one cell line (Y1335). However, the other cell line (Y1445) showed decreases in two of the acetylation marks (H3K18ac and H3K23ac) alongside an increase in H3K9ac which was in agreement with the MS results. Results for methylation at lysine 9 (Figure 5.17), showed a decrease for

H3K9me3 for both cell lines, whereas, H3K9me2 increased in one cell line and decrease in the other upon cadmium exposure.

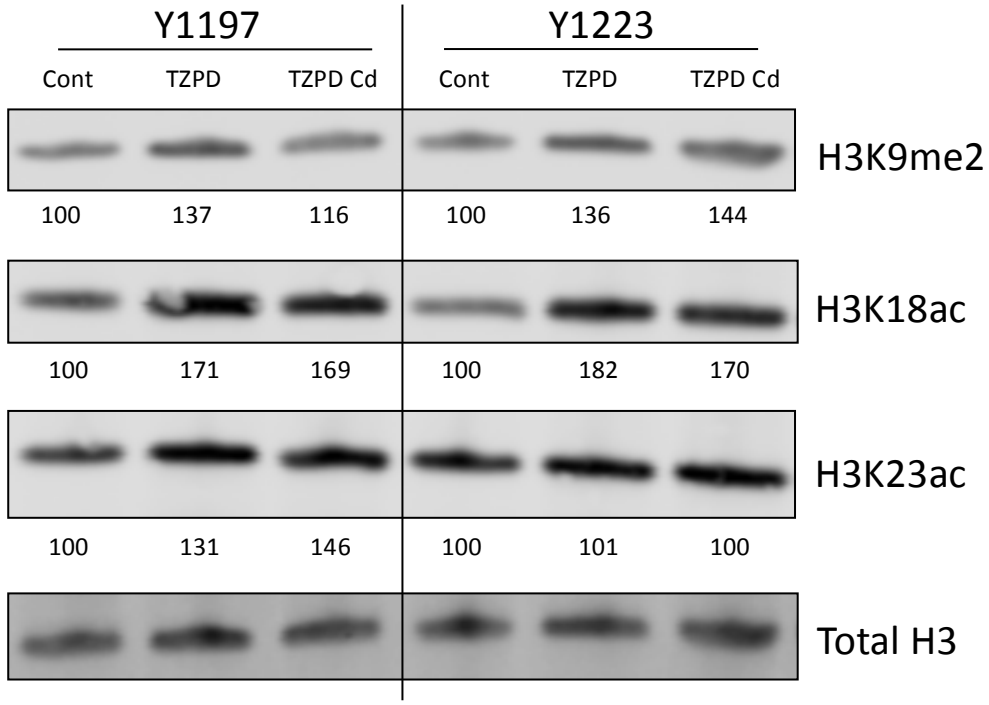

Figure 5.14. Western blot analysis of methylation and acetylation marks on histone H3 in whole cell lysates from two independent NHU cell lines. Cultures were treated ± TZPD ± 10 µM $CdCl_2$ for 6 days. Cultures were lysed in situ with SDS lysis buffer and then sonicated. Protein concentration was measured using a Bradford assay. 4-12% Bis-Tris gels were loaded with 20 µg of protein and run at 200 V in MES running buffer. Protein was blotted on to PVDF membranes using the Novex apparatus for 2 hours at 30 V. Membranes were blocked in Odyssey blocking buffer, incubated with primary antibodies overnight at 4°C, and secondary antibodies for one hour at ambient temperature then scanned on the Li-Cor imaging system. The fluorescence of each band was quantified and normalised to the loading control histone H3 using the Odyssey software. Numbers quantifying the percentage intensity of the bands are displayed below the corresponding bands.

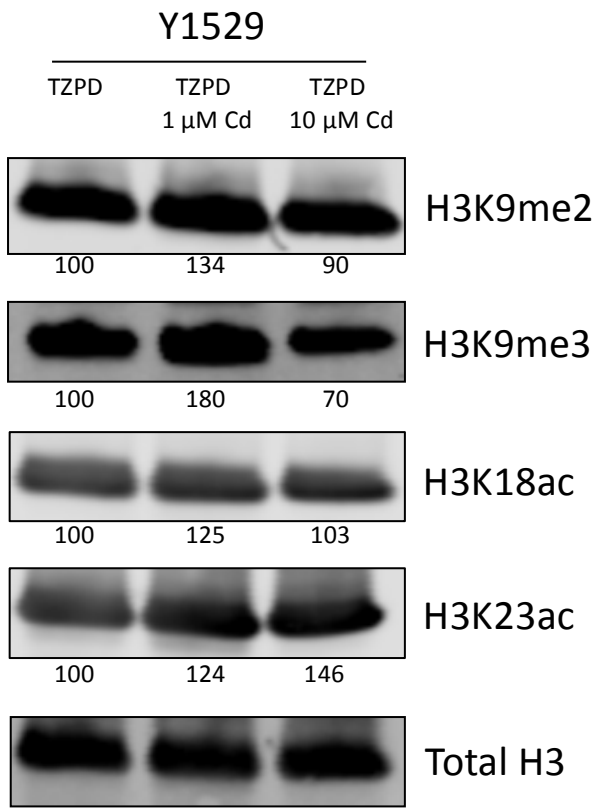

Figure 5.15. Western blot analysis of methylation and acetylation marks on histone H3 in whole cell lysates. Y1529 NHU cell cultures were treated with TZPD and either 1 or 10 µM $CdCl_2$ for 6 days. Cultures were lysed in situ with SDS lysis buffer and then sonicated. Protein concentration was measured using a Bradford assay. 4-12% Bis-Tris gels were loaded with 20 µg of protein and run at 200 V in MES running buffer. Protein was blotted on to PVDF membranes using the Novex apparatus for 2 hours at 30 V. Membranes were blocked in Odyssey blocking buffer, incubated with primary antibodies overnight at 4°C, and secondary antibodies for one hour at ambient temperature then scanned on the Li-Cor imaging system. The fluorescence of each band was quantified and normalised to the loading control histone H3 using the Odyssey software. Numbers quantifying the percentage intensity of the bands are displayed below the corresponding bands.

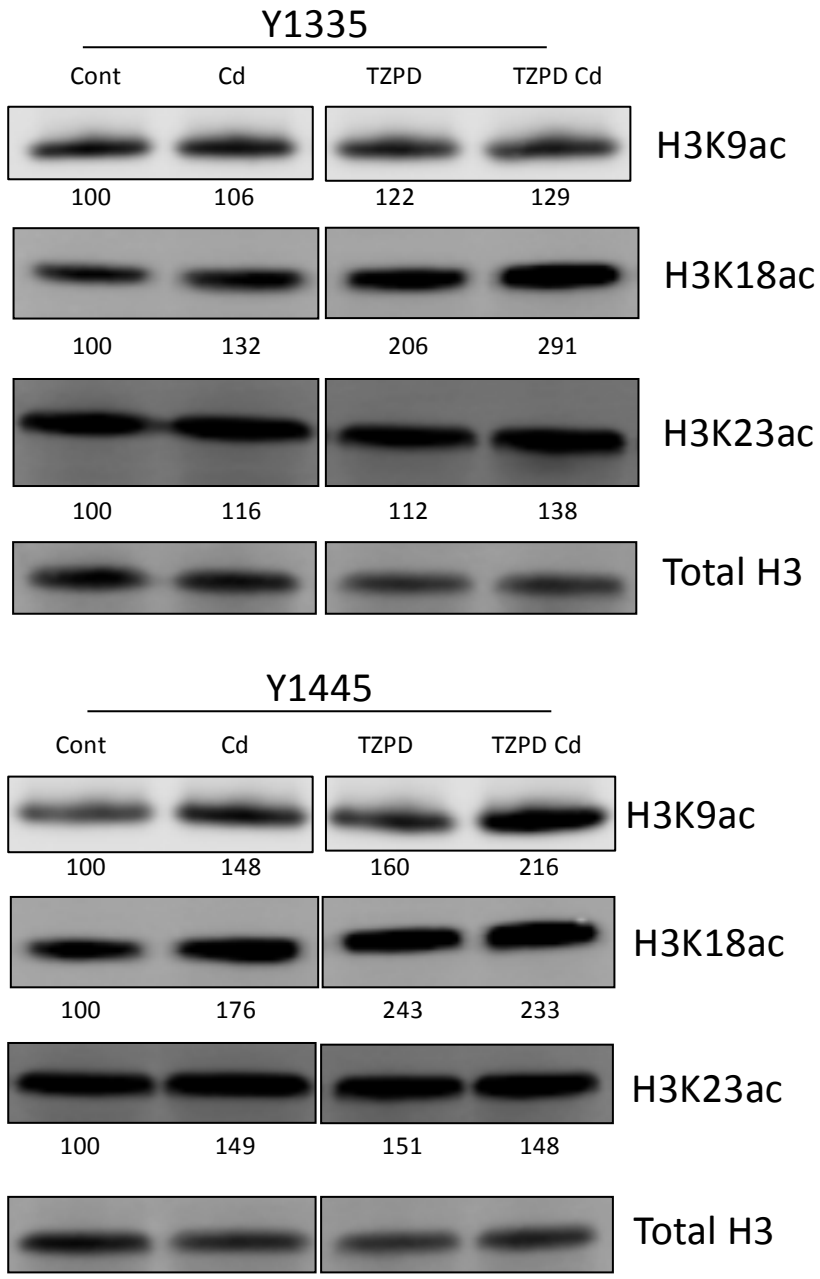

Figure 5.16. Western blot analysis for acetylation marks on histone H3 in acid extracted histones from two independent NHU cell lines. Cultures were treated ± TZPD ± 10 µM $CdCl_2$ for 72 hours. 4-12% Bis-Tris gels were loaded with 2.5 µg of isolated histones and run at 200 V in MES running buffer. Histone protein was blotted on to PVDF membranes using the Novex apparatus for 2 hours at 30 V. Membranes were blocked in Odyssey blocking buffer, incubated with primary antibodies overnight at 4°C, and secondary antibodies for one hour at ambient temperature then scanned on the Li-Cor imaging system. The fluorescence of each band was quantified and normalised to the loading control histone H3 using the Odyssey software. Numbers quantifying the percentage intensity of the bands are displayed below the corresponding bands.

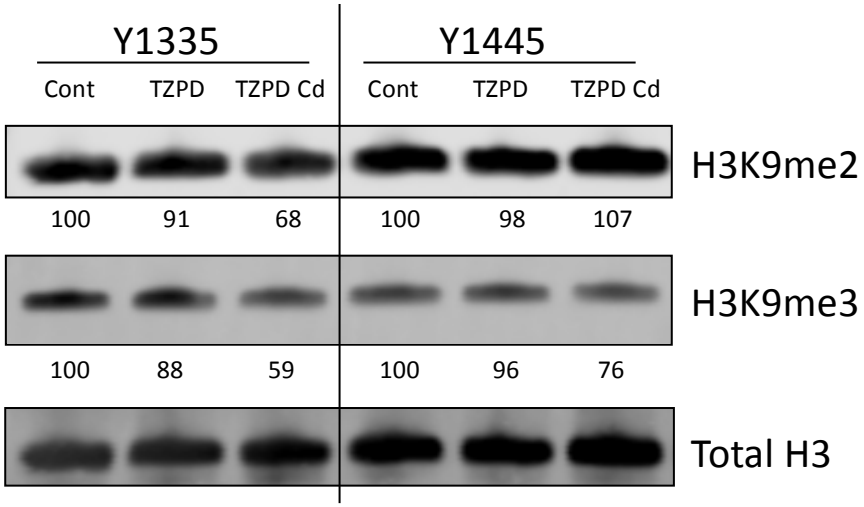

Figure 5.17. Western blot analysis for H3K9me2 and H3K9me3 marks in acid extracted histones from two independent NHU cell lines. Cultures were treated ± TZPD ± 10 µM $CdCl_2$ for 72 hours. 4-12% Bis-Tris gels were loaded with 2.5 µg of isolated histones and run at 200 V in MES running buffer. Histone protein was blotted on to PVDF membranes using the Novex apparatus for 2 hours at 30 V. Membranes were blocked in Odyssey blocking buffer, incubated with primary antibodies overnight at 4°C, and secondary antibodies for one hour at ambient temperature then scanned on the Li-Cor imaging system. The fluorescence of each band was quantified and normalised to the loading control histone H3 using the Odyssey software. Numbers quantifying the percentage intensity of the bands are displayed below the corresponding bands.

5.4 Summary

- **Proliferative NHU cultures**

Proliferative NHU cultures showed a decrease in global levels of histone acetylation on H2A lysine 5, H3 lysine 9 and 14 and H4 lysine 8 upon cadmium treatment. However histone methylation varied depending on cadmium concentration; H3K4me3 increased at low doses of cadmium, as did H3K27me3 but both marks showed a slight decrease when treated with 10 μM $CdCl_2$. Global H4K20me3 was shown to decrease with increasing concentrations of cadmium.

- **Differentiated NHU Cultures**

Mass spectrometry quantification of epigenetic marks on the tail of histone H3 in differentiating NHU cultures showed that upon cadmium exposure the relative abundance of H3K9me3 increased. ChIP-QPCR results showed that H3K9me3 occupancy for KRT13, KRT20, UPK1A and UPK2 was highest in TZPD-differentiating cultures exposed to cadmium.

MS data from two biological replicates showed that upon differentiation (TZPD v DMSO treated cultures) levels of H3K9me2, H3K18/23ac and H3K27me3 were all increased. The increase seen in H3K9me2 was supported by western blot analysis of whole cell lysates from two independent NHU cell lines. The increase in H3K18/23ac was supported by western blot analysis from four independent cell lines, two carried out using whole cell lysates and two performed on isolated histones.

Upon cadmium exposure, changes in epigenetic marks that were outside of the standard deviation of the two biological replicates included an increase in H3K27me3 and a decrease in H3K18/23ac. The decrease in amounts of H3K18/23ac was supported by western blots analysis carried out using whole cell lysates from two independent NHU cell lines and histones extracted from a further independent cell line.

When different concentrations of cadmium were used to treat the differentiating NHU cell cultures this led to differing effects on H3K9 methylation, as 1 μM $CdCl_2$ led to an increase in H3K9me2 and H3K9me3 whereas, 10 μM $CdCl_2$ led to a decrease in these marks.

6 Discussion

Mechanisms reported to be involved in cadmium carcinogenesis include induction of oxidative stress, aberrant gene regulation, repression of DNA repair, deregulation of cell proliferation and inhibition of apoptosis (reviewed by Joseph, 2009). However, the exact mechanism responsible for cadmium-induced carcinogenesis has not been identified. As cadmium is a weak mutagen, it has been proposed that epigenetic mechanisms could be involved in cadmium-induced carcinogenesis (Waalkes, 2003, Arita & Costa, 2009). Therefore cadmium carcinogenesis of human urothelial cells was investigated, with a focus on whether epigenetic modifications such as histone modifications were involved.

Experimental results support the initial hypothesis that exposure of urothelial cells to cadmium leads to downregulation of tumour suppressor genes and inhibition of differentiation via epigenetic dysregulation of gene expression.

The most important experimental findings were that:

- Cadmium exposure inhibits differentiation of NHU cell cultures *in vitro*.
- TSA reversed the inhibitory effect of cadmium on differentiation-associated genes.
- H3K9me3 may play a role in the silencing of differentiation-associated genes during cadmium exposure.
- Cadmium exposure downregulates expression of tumour suppressor genes p16, APC and RASSF1A.
- Cadmium alters histone modifications leading to a more repressive chromatin environment.

6.1 Exposure of urothelial cells to cadmium

Non-toxic cadmium chloride doses were determined by the use of an alamarBlue® assay and observations of NHU cell cultures. Cadmium chloride was cytotoxic to proliferative NHU cell cultures when concentrations exceeded 10 μM. However, ABS/Ca^{2+}-differentiated NHU cell cultures could still be maintained when exposed to 20 μM $CdCl_2$. After initial treatments of proliferative NHU cell cultures, cultures in all following experiments were exposed to non-toxic cadmium chloride concentrations. These doses were consistent with those used in other reported studies

including cadmium treatments on an immortalised human urothelial cell line that was exposed to 1, 5 and 9 μM $CdCl_2$ for 16 days (Sens et al., 2003). Other epithelial cell lines have also been exposed to similar cadmium chloride treatment doses including normal human bronchial epithelial (BEAS-2B) cells (Jing et al., 2012; Person et al., 2013). A study by Xiao et al. (2015) showed no significant change in the number of colonies formed by BEAS-2B cells treated with up to 10 μM cadmium compared to untreated cells. Additionally Chen at al. (2014) showed that there was no significant cytotoxicity in BEAS-2B cells after treatment with 10 μM $CdCl_2$ for 36 hours but 20 μM $CdCl_2$ significantly induced cytotoxicity after 36 hours of exposure.

It was observed that cadmium concentrations up to 20 μM did not adversely affect barrier function in ABS/Ca^{2+} differentiated cell cultures. This is consistent with a study examining tight junction permeability in differentiated human intestinal cells that found cadmium concentrations of 1 and 50 μM had no effect on TER values, whereas the very high concentrations (100 and 300 μM) caused time and concentration dependent decreases in TER (Rusanov et al., 2015). This may be due to these concentrations starting to become cytotoxic to the cells. The highest concentration of cadmium that ABS/Ca^{2+}-differentiated NHU cell cultures were exposed to was 20 μM and although this was shown to be cytotoxic for proliferative NHU cell cultures this was not the case for differentiated cultures.

Tight junctions regulate paracellular permeability (barrier function) and maintain cell polarity (Balda & Matter, 2008). Microarray results showed that cadmium exposure only had very minimal effects on gene expression of tight junction proteins. Claudin 3 knockdown in NHU cells has been shown to inhibit the formation of a tight barrier in three independent cell lines (Smith et al., 2015), therefore the slight increase in expression of claudin 3 and 4 upon cadmium exposure may explain the observation from Chapter 3 where 20 μM $CdCl_2$ treatment led to a tightening of the barrier compared to the control. By contrast, Schulzke et al. (2005) showed that occludin is not essential for barrier function in the urothelium. This may explain why even though occludin expression is reduced by cadmium exposure no reduction in barrier function was observed.

Rusanov et al. (2015) have recently studied the effects of cadmium on the functional state of human intestinal cells. Differentiated human intestinal epithelial Caco-2 cells

were treated with cadmium chloride concentrations ranging from 1 to 300 μM. They observed dose-dependent changes in mRNA expression levels of proteins involved in the formation of TJs (claudin 4 and ZO1) and adherens junctions (E-cadherin and p120-catenin). Claudin 4 expression was increased with increasing doses of cadmium while ZO1 expression was increased by 1 and 50 μM $CdCl_2$ but showed decreased expression when treated with 100 μM $CdCl_2$. In this thesis claudin 4 was shown to be slightly increased upon 10 μM cadmium exposure whereas ZO1 showed minimal changes in expression. E-cadherin and p120-catenin expression was shown to be the most sensitive to cadmium in Caco-2 cells, with the greatest induction in expression seen with 1 μM cadmium (Rusanov et al., 2015). Cadmium has been shown to specifically displace calcium from E-cadherin binding sites (Prozialeck & Lamar, 1999) and impair cell-cell adhesion in kidney epithelial cells (Prozialeck et al., 2003). This is because Cd^{2+} ions have ionic radii very similar to those of Ca^{2+} and therefore can substitute for Ca^{2+} in protein binding sites and interfere with the functions of numerous Ca^{2+}-transport and Ca^{2+}-dependent signalling proteins (Beyerssmann & Hartwig, 2008). However, in this thesis no indication of dysregulation of gene expression of E-cadherin was observed in cadmium exposed differentiating NHU cell cultures as gene expression analysis performed using Agilent microarrays showed no changes in the expression of E-cadherin or p120-catenin upon cadmium exposure.

It was also observed that barrier recovery was delayed in the presence of cadmium. Therefore in cases where urothelial injury has occurred, the lack of a fully functional permeability barrier and leaky tight junctions will allow intermediate and basal urothelial cells and underling tissue to be exposed to cadmium and other potential carcinogens that may be present in urine.

6.2 Induction of Metallothioneins

Metallothioneins (MTs) are low molecular weight proteins containing approximately 30% cysteine that bind transition metals with high affinity (Hamer, 1986; Andrews, 2000). They play an important role in cellular detoxification of inorganic species by sequestering metal ions that are present at elevated concentrations. Each MT protein molecule can bind up to seven cadmium atoms where Cd^{2+} is tetrahedrally coordinated to cysteine residues (Kagi & Valle, 1960; Otvos & Armitage, 1980;

Boulanger et al., 1982). Transcriptional activation of MT genes is mediated by MTF1, a metal-responsive transcription factor which binds to metal response elements (MREs) located upstream of the MT gene coding sequences (Stuart et al., 1984; Searle et al., 1985; Westin & Schaffner, 1988; Seguin & Prevost, 1988). The pattern of MT1/2 expression is distinct from that of MT3. MT1 and MT2 isoforms show a ubiquitous pattern of tissue expression and play a critical role in the homeostasis of essential metals ions such as Zn^{2+} and Cu^{2+} as well as in the detoxification of heavy metals such as cadmium. By contrast, MT3 expression is normally limited to neural tissues and is not metal responsive (Palmiter el al., 1992), but it does posses a neuronal cell growth inhibitory activity that the other MT genes do not (Uchida et al., 1991; Amoureux et al., 1995). Exposure to low concentrations of cadmium has been shown to result in a significant induction of MT genes in numerous cell lines and animal tissues including COS-7 (African green monkey kidney) cell lines (Lee et al., 2002) and adult male Wistar rats and adult male C57 and DBA mice tissues (Misra et al., 1997).

Metallothionein isoforms MT1 and MT2 were highly induced in NHU cell cultures upon cadmium exposure. This is consistent with a recent gene expression analysis of human hepatocarcinoma cells, performed using Affymetrix Human Gene 1.0 arrays, which showed that acute cadmium exposure (0.5 μM $CdCl_2$ for 24 hours) altered the expression of 333 genes, with the most upregulated being MT1G, MT1F, MT1M, MT1B, MT1X and MT1H (Cartularo et al., 2015).

Metallothioneins have been reported to be upregulated in bladder cancer. Sens et al. (2000) demonstrated that MT3 was upregulated in human bladder cancer and that levels of MT3 increased with increasing tumour grade as MT3 immunostaining was found to be high in both CIS and high-grade cancer with low to moderate staining observed in low-grade bladder cancer. MT3 was shown to be undetectable using immunohistochemical, western and RTPCR techniques in normal urothelium (Sens et al., 2000), this is consistent with experimental results for MT3 expression in NHU cell cultures. Somji et al. (2001) showed that MT1X was overexpressed in bladder cancer tissue compared to normal bladder tissue. Further investigation by Zhou et al. (2006), using an antibody that recognises both MT1 and MT2, found that there was no protein expression of MT1/2 in benign lesions and low-grade cancers, low expression in dysplastic lesions and high-grade cancers with no evidence of muscle

invasion, and significantly increased expression in high-grade cancers that had invaded the underlying matrix. Expression of MT1/2 was also determined in immortalised urothelial cells that had been malignantly transformed by Cd^{2+} and shown to be capable of tumour formation in nude mice. Expression of MT1/2 protein in the tumour heterotransplants was found to be similar to that found in high-grade bladder cancers.

6.3 Epigenetic dysregulation of differentiation

Normal human urothelium is commonly represented *in vitro* as immortalised cell lines. However, immortalised urothelial cells, such as those immortalised by the overexpression of human telomerase reverse transcriptase lose the potential to differentiate and form a functional barrier urothelium (Chapman et al., 2006; Georgopoulos et al., 2011). NHU cells can be induced to differentiate using two published methods (Cross et al., 2005; Varley et al., 2004); therefore NHU cells provide a relevant cell culture system to study the effect of cadmium on urothelial cytodifferentiation.

The potential of NHU cells to differentiate in the presence of cadmium was assessed, as exposure of the urothelium to cadmium was hypothesised to cause invasive urothelial cancer via epigenetic dysregulation of gene expression leading to field changes within the urothelium characteristic of dysplasia/carcinoma in situ (loss of differentiation). The observation that the urothelial differentiation markers KRT13 and KRT20 where downregulated upon cadmium exposure, whereas KRT6, KRT14, KRT16 and KRT17 where upregulated was consistent with previous studies examining cadmium transformed cell lines. Transformation of immortalised human urothelial cells (UROtsa) by cadmium or arsenic was shown to induce the expression of KRT6A mRNA and protein compared to non-transformed UROtsa cells (Somji et al., 2008). Immunostaining of keratin 6A in tumour heterotransplants showed focal staining of the tumour cells that was localised to the cytoplasm. Focal immunostaining was also found in some archival patient specimens of high-grade bladder cancer, confirming translation of the results to human bladder cancer. Microarray analysis on Cd^{2+} transformed cell lines and their respective transplants all had overexpression of KRT 6A, 16 and 17 mRNA and protein, which correlated with

the areas of urothelial tumours cells that had undergone squamous differentiation (Somji et al, 2011).

The cytokeratin expression profile of differentiating NHU cell cultures exposed to cadmium is similar to the recently described basal subtype of muscle invasive bladder cancer (MIBC; Sjodahl et al., 2012; 2013; Choi et al., 2014), where basal MIBCs characteristically express KRT5, KRT6, KRT14 and lack KRT20 expression. This indicates a link between cadmium exposure and invasive urothelial carcinoma.

Differentiation of NHU cells *in vitro* is known to occur via PPARγ activation (Varley et al., 2006) leading to the upregulation of transcription factors that play a role in inducing the expression of differentiation markers. FOXA1, IRF1, ELF3, GATA3, GRHL3 and KLF5 are known transcription factors involved in urothelial differentiation (Varley et al., 2009; Yu et al., 2009; Bell et al., 2011; Bock et al., 2014). It was observed that cadmium exposure did not affect the expression of these transcription factors. As the transcription factors include the pioneer factor FOXA1, whose differential binding to chromatin sites is dependent on the distribution of H3 lysine 4 dimethylation (Lupien et al., 2008), it was hypothesised that cadmium inhibits chromatin modifications associated with expression of terminal differentiation.

Differentiating NHU cell cultures were treated with two epigenetic modifiers to test this hypothesis. The epigenetic modifier, TSA was able to reverse the cadmium-induced down-regulation of three terminal differentiation markers whereas 5-azacytidine, a DNA-methylation inhibitor was not. This suggests that exposure to cadmium affects histone modifications required for the expression of these differentiation-associated genes. TSA has previously been used in the treatment of the human bladder cancer cell line CL1207 to show that epigenetic silencing of chromosomal regions was due to histone modifications, as TSA treatment was associated with the re-expression of most genes in the silenced regions (Vallot et al., 2010). It was found that the promoters of most genes in the silenced regions had high levels of the repressive marks H3K9me3 and H3K27me3. MS analysis of histone H3 modifications in NHU cell cultures exposed to cadmium showed increased levels of these two marks. H3K9me3 and H3K27me3 are characteristic of silent and heterochromatic regions of the genome (Greer & Shi, 2012). The observation that

H3K9me3 was increased at the nuclear periphery in cadmium exposed NHU cell cultures is consistent with a report that shows H3K9me3 associates with repressed genes at the nuclear periphery (Towbin et al., 2012). ChIP-QPCR results showed that H3K9me3 occupancy was highest in TZPD-differentiating cultures exposed to cadmium. However, these results were generated from only one NHU cell line, therefore repeats using additional independent NHU cell lines are needed in order to draw conclusions from this data. However, these results do suggest that in cultures treated with cadmium, H3K9me3 may play a role in suppressing the expression of KRT13, KRT20, UPK1A and UPK2. This is consistent with the role that H3K9me3 plays in the MRES phenotype identified by Vallot et al. (2011) that was found to be associated with muscle-invasive tumours and in particular the CIS pathway of tumour progression. Therefore the observation that cadmium exposure leads to dysregulation of differentiation and global increases in repressive marks implicates a link between cadmium exposure and the CIS pathway. Further studies will need to be carried out to address whether the inhibitory effects of cadmium on differentiation are sustained after cadmium is removed.

6.4 Inhibition of tumour suppressor genes

Cadmium is predominantly non-genotoxic (Valverde et al., 2001) and therefore may induce carcinogenesis via epigenetic mechanisms by altering the expression levels of various critical genes (reviewed by Wang et al., 2012). CIS and invasive bladder cancer is traditionally associated with the inactivation of tumour suppressor genes, including p53 (Fujimoto et al., 1992) CDKN2A (Cairns et al., 1993) RB1 (Cairns et al., 1991) and PTEN (Aveyard et al., 1999). Numerous other tumour suppressor genes have been implicated in bladder cancer including APC, RUNX3 and TSC1 (reviewed by Knowles & Hurst, 2015).

The tumour suppressor genes, APC, p16, RASSF1A and RUNX3 were all observed to be downregulated in cadmium-exposed NHU cell cultures.

The short arm of chromosome 9 (9p) contains a single region that encodes the known tumour suppressor genes p16 and p14 on alternate reading frames from the CDKN2A locus, and p15 from the CDKN2B locus (Cairns et al., 1994; Devlin et al., 1994; Orlow et al., 1995; Williamson et al., 1995; Berggren et al., 2003). More than 50% of all bladder tumours show chromosome 9 deletions (Cairns et al., 1993;

Linnenbach et al., 1993; Tsai et al., 1990). The majority of deletions are of CDKN2A. p16 is a negative regulator of the retinoblastoma **(**Rb) pathway and p14 is a negative regulator of the p53 pathway. CDKN2A deletions have been associated with high grade and stage bladder tumours (Chapman et al., 2005) and an increased risk of recurrence in Ta and T1 tumours (Bartoletti et al., 2007). However, a further study looking at homozygous deletions of exon 1B of CDKN2A found no association with tumour grade and stage (Berggren de Verdier et al., 2006).

RASSF1A is a tumour suppressor whose inactivation is implicated in the development of many human cancers (Dammann et al., 2001; Yan et al., 2003; Schagdarsurengin et al., 2003). Loss or significant reductions of RASSF1A was identified in 62% of bladder tumours (Lee et al., 2001). RASSF1A is believed to mediate microtubule stability, cell cycle progression and the induction of apoptosis (Amin & Banerjee, 2012). Loss of function of RASSF1A has been shown to lead to accelerated cell cycle progression and resistance to apoptotic signals.

RUNX3 is one of three Runt-domain transcription factors encoded by the RUNX gene family. In NHU cells exposed to cadmium RUNX3 microarray analysis showed -2.14 fold change compared to non-exposed cell cultures ($p<0.05$).

The APC gene encodes for the adenomatous polyposis coli protein, which is a component of the β-catenin destruction complex. The destruction complex is responsible for the ubiquitylation and subsequent proteasomal degradation of β-catenin. Inactivation of APC has been associated with human cancers including colon cancer (Markowitz & Bertagnolli, 2009).

Expression of APC and RASSF1A has been found to be decreased in muscle-invasive high-grade bladder cancer compared to non-muscle invasive low-grade bladder cancer and normal bladder mucosa (Bilgrami et al., 2014) and reduced expression of RASSF1A and p16 has previously been reported during cadmium-induced malignant transformation of human prostate cells (Benbrahim-Tallaa et al., 2007). Overall this suggests a link between cadmium exposure and invasive bladder cancer as cadmium exposure leads to the downregulation of tumour suppressor genes that are known to be associated with the CIS pathway and invasive high-grade bladder cancer. Future studies should identify if tumour suppressor genes remain downregulated in NHU cell cultures after cadmium exposure is removed.

The likely mechanism behind downregulation of tumour suppressor genes in cadmium-exposed cells may be DNA methylation as numerous reports have shown an association between reduced tumour suppressor expression and DNA hypermethylation. Hypermethylation of the RASSF1A promoter region is probably the most frequently described epigenetic inactivation event in human cancers (Pfeifer et al., 2002; Dammann et al., 2003). DNA hypermethylation of the RASSF1A promoter has been shown to correlate with overexpression of DNMT3b in cadmium-transformed prostrate epithelial cells (Benbrahim-Tallaa et al., 2007). RUNX3 inactivation by aberrant DNA methylation has been reported in bladder tumours (Kim at al., 2005), with a follow-up study by Kim et al. (2008) finding that RUNX3 methylation significantly correlated with the development of invasive tumours. APC promoter methylation has been significantly associated with urothelial cancer progression (Yates et al., 2007). Furthermore, DNA hypermethylation was detected in the promoter region of APC in lung tumours from workers who had been exposed to the metal chromium, (Ali et al., 2011). Additionally, arsenic exposure has been shown to cause promoter methylation of RASSF1A and p16 (Cui et al., 2006; Marsit et al., 2006; Chanda et al., 2006; Zhang et al. 2007). This indicates that non-genotoxic metals may share a similar mechanism that leads to aberrant DNA hypermethylation. Future work could utilise 5-azacytidine to identify if DNA methylation is responsible for APC, p16, RASSF1A and RUNX3 downregulation in cadmium exposed NHU cell cultures.

6.5 Alterations of histone modifications by cadmium

The greatest change observed in histone modifications in proliferative NHU cell cultures was in histone acetylation. Three independent NHU cell lines all showed a reduction in global acetylation at H2AK5, H3K9/14 and H4K8. Reduced acetylation will lead to more compact chromatin thereby resulting in gene repression and silencing (Grunstein, 1997; Turner, 2000). H4K20me3 global levels were shown to reduce slightly upon cadmium exposure. H4K20me3 is associated with repression of transcription when present at promoters (Wang et al., 2008). Additionally, loss of H4K20me3 has been identified as a hallmark of cancer (Fraga et al., 2005). Other epigenetic marks studied in proliferative NHU cell cultures were the repressive mark, H3K27me3 and the active mark H3K4me3. H3K27me3 is associated with promoter regions of repressed genes whereas H3K4me3 is found in promoter regions of

transcriptionally-active genes (Santos-Rosa et al., 2002; Mikkelsen et al., 2007). 10 nM and 100 nM $CdCl_2$ exposure led to an increase in these marks while 10 μM $CdCl_2$ exposure led to slight decreases. A non-linear dose response has also been reported in cadmium treatments of normal human bronchial epithelial (BEAS-2B) cells, where elevations of global H3K4me3 and H3K9me2 were less at 5 μM $CdCl_2$ than those at 2.5 μM $CdCl_2$ (Xiao et al., 2015). Additionally they also found that cadmium led to increases in global levels of a transcriptional activating mark and a repressing mark, this has also been reported in cells that have been exposed to other non-genotoxic metals including arsenic and nickel (Zhou et al., 2008; Zhou et al., 2009).

The use of a mass spectrometry (MS) approach to examine histone post-translational changes provides an unbiased method to quantify histone modifications and also offers the ability to examine the combinatorial nature of histone modifications (Britton et al., 2012). In this thesis two independent NHU cell lines underwent TZ/PD-induced differentiation either in the presence of absence of cadmium. Mass spectrometry results from the two cell lines showed that in both cell lines H3K18/23ac was decreased and H3K27me3 was increased upon cadmium treatment, indicating that cadmium exposure led to more repressive chromatin landscape. This may explain why microarray analysis, from Chapter 4, showed that 588 genes were downregulated but only 118 genes were upregulated during cadmium exposure.

A couple of epigenetic marks showed differential changes between the two NHU cell lines upon exposure to cadmium. One cell line showed a decrease in H3K9me2 alongside an increase in H3K9me3 whereas the other showed a slight increase in H3K9me2. This may be due to NHU cell lines being primary cells derived from different donors, therefore inter-individual variation in the epigenome may be present. Inter-individual variability of histone modifications and DNA methylation has been reported in rat and human cells (Rintisch et al., 2014; Wagner et al., 2014). Additionally, inter-individual variation in DNA repair gene expression was found between six independent NHU cell lines with the authors suggesting that donor genotype such as polymorphisms or epigenetic mechanisms may be responsible for the change in expression levels (Crallan et al., 2002). In order for conclusions to be drawn several NHU cell lines need to be analysed. This thesis has only used NHU cell cultures from two donors to quantify histone modifications by MS, therefore,

further independent NHU cell lines would need to be analysed to confirm histone modification changes.

The MS approach utilised in this study to quantify post-translational histone modifications has previously been used to identify and quantify histone modifications in honey bees (Dickman et al., 2013). This approach has a limitation in its ability to recover H3K4 peptides containing di-and tri-methyl marks; because of this H4K4 methylation in cadmium treated NHU cell cultures were not quantified by MS. Further limitations of this MS approach were that only acetylation and methylation on histone H3 were examined and also some of the combinatorial marks on lysine 9 had to be excluded from the MS analysis as they did not show reduction in signal in line with the dilution factor. Additional histone modifications that were not examined in this study include phosphorylation, ubiquitnation, sumoylation, citrullination and ADP-ribosylation.

The histone modification changes observed in western blots for NHU cell cultures where not as great as those that have recently been reported in HepG2 and BEAS-2B cells upon cadmium exposure (Cartularo et al., 2015; Xiao et al., 2015). However these two studies also showed contrasting results as global H3K9me2 was decreased in HepG2 cells upon cadmium exposure, whereas in BEAS-2B cell global H3K9me2 was increased. This may suggest that different cell types may show differential changes to histone modifications upon cadmium exposure.

The expression of numerous chromatin-remodelling genes involved in modifying histone modifications was analysed using Aglient microarrays. Genes analysed included those that encode for polycomb group proteins, HP1 proteins, histone acetyltransferases, histone deacetylases, lysine methyltransferases and lysine demethylases.

Polycomb group proteins are vital for maintenance of cell-type identity and differentiation by creating and maintaining repressive chromatin environments. Polycomb group proteins form two polycomb repressive complexes, PRC1 and PRC2. PRC2 is responsible for the di-and tri-methyaltion of lysine 27 of histone H3 (H3K27me2/3) by its catalytic subunits EZH1 and EZH2. H3K27me3 is then recognised by the CBX component of PRC1. The ubiquitin ligase RING1 then monoubiquitylates lysine 119 of histone H2A (H2AK119ub) leading to chromatin

compaction (Margueron & Reinberg, 2011). EZH2 has also been shown to serve as a recruitment platform for DNA methyltransfereases, thus forming a direct link between histone methylation and DNA methylation at represssed promoters (Vire et al., 2006).

HP1 is a family of three proteins, encoded by CBX5, CBX1 and CBX3, which are vital for the formation of transcriptionally inactive heterochromatin. HP1 proteins contain a methyl lysine binding chromodomain that binds methylated H3K9 (Jacobs et al., 2001) and a chromo-shadow domain that binds other HP1 proteins as well as numerous other interacting proteins (Lomberk et al., 2006). HP1 mediated heterochromatin formation occurs via the recruitment of CBX5/CBX1 by H3K9me2/3 which then recruits the H3K9 methyltransferase SUV39H1 (KMT1A). This leads to propagation of the H3K9me3 mark and HP1 down the chromosome as well as the binding of additional proteins such as DNA methyltransfereases leading to heterochromatin formation and gene silencing (Tamaru & Selker, 2001; Maison & Almouzni, 2004).

Histone acetyltransferases (HATs) acetylate lysine amino acids on histone proteins by transferring an acetyl group from acetyl-CoA. HATs can be grouped into several different families based on structural and functional similarity of their catalytic domains. The Gcn5-related *N*-acetyltransferase (GNAT) family are characterized by four conserved motifs found within the catalytic HAT domain and the presence of a bromodomain (Lee & Workman, 2007). The MYST family of HATs are characterized by the presence of the highly conserved MYST domain composed of an acetyl-CoA binding motif and a zinc finger (Avvakumov & Cote, 2007). The p300/CBP HATs have larger HAT domain than those present in the GNAT and MYST families, they also contain a bromodomain and three cysteine/histidine rich domains.

Histone deacetylases (HDACs) remove acetyl groups from lysine amino acids. HDACs are divided into four classes based on function and DNA sequence similarity. Class I, II and IV HDACs (HDAC1-11) all contain a zinc dependent active site.

Lysine methyltransferases (KMTs) catalyse mono-, di- or tri-methylation by transfering one, two or three methyl groups from S-adenosyl-L-methionine to the ε-

amino group of a lysine residue. All KMTs contain a conserved SET domain possessing the enzymatic activity except for KMT4/DOTIL (Qian & Zhou, 2006). Most KMTs also contain a defined protein domain or homologous sequence that is used to classify KMTs into distinct families (Aravind et al., 2011).

Two evolutionarily conserved families of histone demethylases, which utilise different reaction mechanisms to establish demethylation have been identified: LSD demethylases and Jumonji (JmjC) domain demethylases (Shi et al., 2004; Tsukada et al., 2006). Lysine demethylases (KDMs) are now classifed based on new nomenclature into several distinct groups based on their substrate specificities and protein domain organisation (Allis et al., 2007).

No significant changes in the expression of chromatin remodelling genes responsible for the reported histone modification changes were observed except for KDM1B. Cadmium has previously been shown to decrease H3 autophosphorylation *in vitro* by inhibition of the human vaccinia-related kinase VRK1/2 (Barcia-Sanjurjo et al., 2013); this study is one example of how cadmium exposure can impact histone modifications via inhibition of histone modifying enzymes without affecting expression of these enzymes. A more recent study has also reported histone modification changes that occurred due to cadmium inhibiting the activity rather than modulating the protein levels of two lysine demethylases, KDM5A and KDM3A (Xiao et al., 2015). Cd^{2+} ions have an analogous electron configuration with Zn^{2+} and despite having a larger radius (0.95 versus 0.74 Å), Cd^{2+} can often substitute for Zn^{2+} in zinc-dependent enzymes and disturb or abolish the biochemical functions of these proteins (Beyersmann, 1995; Nieboer et al., 1999; Hartwig, 2001). This may be a possible mechanism affecting chromatin remodelling proteins as many epigenetic enzymes bind zinc including class I, II and IV histone deacetylases and various histone acetyltransferases, lysine methyltransferases and lysine demethylases.

A two fold decrease in expression of KDM1B was observed upon cadmium exposure. However, upon TSA treatment this decrease in expression was reversed. KDM1B/LSD2 is a demethylase that can remove mono- and di-methyl but not tri-methyl groups from H3K4 (Karytinos et al., 2009). By contrast to its homologue KDM1A/LSD1, which functions at promoters, KDM1B removes intragenic H3K4 methylation (Fang et al., 2010). Changes in the epigenetic marks H3K4me1 and

H3K4me2 were not investigated in this thesis, therefore future work could include the examination of H3K4me1 and H4K4me2 changes in cadmium exposed cells as well as investigating histone modification positioning at either promoter or intragenic regions.

Future studies may consider:

- Investigating whether histone modification changes persist in NHU cell cultures through multiple generations after removal of cadmium from the medium. In the recently published study by Cartularo and colleagues (2015) cadmium chloride was removed from the cell culture media and HepG2 cells were then cultured for a further 72 hours in order to see if epigenetic changes caused by cadmium exposure persisted through at least three generations. It was found that histone H3 and H4 pan acetylation levels remained diminished, but not to the levels seen directly following treatment. Globally reduced levels of H4K16ac and H3K9me2 also remained diminished after 72 hours.
- Utilising *in vitro* assays in order to examine whether cadmium affects the activity of chromatin remodelling proteins. As it is has been proposed that cadmium may be affecting histone post-translational modifications during urothelial differentiation by modifying the activity of chromatin remodelling enzymes by substituting for zinc in zinc-dependent enzymes.

6.6 Cadmium molecular mechanism

As discussed above some of the effects of cadmium are thought to arise due to disruption of zinc-dependent processes, due to the structural and physical similarities between zinc and cadmium ions (Waalkes, 2003). Cadmium is believed to compete with zinc for a multitude of important binding sites within biomolecules, including sites important in gene regulation or enzymatic activity. This is supported by a study by Takiguchi and colleagues (2003) that showed that cadmium may inhibit DNMT activity by interacting with the DNA binding site, a zinc-binding domain. Cadmium ions exert high affinity towards SH groups, therefore potential targets are zinc finger proteins. Zinc finger proteins are a family of proteins where zinc is complexed through four cysteine and/or histidine residues to form a zinc finger domain. Zinc finger domains are mainly involved in DNA binding but can also be involved in

protein-protein interactions. Zinc replacement by cadmium in different eukaryotic zinc fingers has been studied with particular attention to the modulation of DNA binding activity, as cadmium substitution can lead to improper folding and structural rearrangement affecting the position of side chains involved in DNA recognition (Petering et al., 2000; Huang et al., 2004; Malgieri et al., 2011).

Kothinti el al. (2010) have reported that cadmium inhibited the DNA binding affinity of the transcription factor Sp1 by replacing zinc in its zinc finger DNA binding domain. Therefore it is possible that cadmium is substituting for zinc in some of the transcription factors involved in urothelial differentiation and affecting their ability to bind DNA, as their expression at mRNA level is still upregulated but their downstream targets are not. Urothelial transcription factors that contain zinc fingers include GATA3 and KLF5.

SOX9 is a transcription factor that is upregulated in basal and intermediate urothelial cells in response to injury and has been shown to be induced in CIS and invasive bladder tumours as well as many other types of cancer (Dong et al., 2004; Jo et al., 2014). SOX9 induction in urothelial carcinoma cell lines has been shown to occur through ligand-stimulated activation of EGFR and subsequent MAPK pathway activation (Ling et al., 2011). SOX9 was expressed in proliferative NHU cell cultures and downregulated upon differentiation by PPARγ activation. Panza et al. (2013) also found that PPARγ activation by a synthetic agonist for PPARγ (rosiglitazone) led to reduced expression of SOX9 mRNA in two colon cancer cell lines (CaCo2 and HT-29). When cadmium was present during urothelial cell differentiation SOX9 failed to downregulate. As SOX9 transcript failed to downregulate in the presence of cadmium it could be hypothesised that SOX9 may be inhibiting urothelial cytodifferentiation by promoting a proliferative phenotype. SOX9 protein expression was visualised by immunofluorescence microscopy. Decreased levels of SOX9 within nuclei were observed upon differentiation. This was consistent with CaCo2 cells that had been treated with rosiglitazone that also showed decreased levels of SOX9 staining within nuclei (Panza et al., 2013). Further investigation using immunoblotting techniques will need to be performed in order to fully characterise SOX9 protein expression changes upon cadmium exposure, with further study needed to investigate if SOX9 plays a role in the inhibition of urothelial differentiation and cadmium carcinogenesis.

CTCF is a highly conserved zinc finger protein involved in many cellular processes including transcriptional regulation, insulator activity and regulation of chromatin architecture (Phillips & Corces, 2009). Recently, Jose et al (2014) have shown that nickel, a non-genotoxic metal carcinogen, disrupted H3K9me2 domains, resulting in the spreading of H3K9me2 into active regions, which led to gene silencing in these regions. They found reduced CTCF binding at these sites, suggesting that a loss of CTCF-mediated insulation function maybe a potential reason for H3K9me2 domain disruption and spreading. Nickel, like cadmium, has also been linked with disrupting the structure and function of zinc finger domains of several transcription factors and enzymes leading to inhibition of DNA binding and alteration of DNA-binding specificity (Asmuss et al., 2000; Hartwig, 2001; Bal et al., 2003). Results from our laboratory show that greater amounts of CTCF are extracted in cadmium exposed cells following cytoskeletal salt extraction. This indicates that CTCF binding is weaker or reduced in cadmium exposed cells compared to control, suggesting that the mechanism of gene silencing described by Jose et al. may be present in NHU cell cultures exposed to cadmium.

The hypothesis that cadmium competes with zinc is supported by a recent study that found that cadmium exposure (10 μM $CdCl_2$) of HepG2 cells for 24 hours led to a large increase (93%) in intracellular zinc with cadmium displacing zinc from the zinc proteome (Urani et al., 2015). The study also reported the upregulation of the zinc transporter SLC30A1; this is in agreement with the upregulation of three zinc transporters (SLC30A1, SLC30A2 and SLC30A3) observed in differentiating NHU cell cultures exposed to cadmium. The SLC30 family of zinc transporters transport zinc and/or other metal ions from the cytoplasm into the lumen of intracellular organelles or to the outside of the cell (Palmiter & Huang, 2004). Therefore this upregulation of zinc transporters may be a way of regulating zinc homeostasis in NHU and HepG2 cell cultures by transporting excess Zn^{2+} ions out of the cytoplasm. Zinc transporters have also been implicated in the transport of Cd^{2+} into cells. The ZIP family of zinc transporters (SLC39) are responsible for the transport of zinc from the extracellular space or organellar lumen into the cytoplasm (Eide, 2004). ZIP8 (SLC39A8) and ZIP14 (SLC39A14) transporters have been shown to be responsible for Cd^{2+} transport in kidney, intestine and testis (Dalton et al., 2005; Girijashanker et al., 2008; Liu et al., 2008; He et al., 2009). Ajjimaporn et al. (2012) have shown that

ZIP8 is expressed in normal urothelium. Additional candidates for the transport of cadmium into cells include the Fe^{2+}/H^{+} cotransporter divalent metal transporter 1 (DMT/SLC11A2; Gunshin et al., 1997; Bannon et al., 2003), TRPM7 ion channel (Monteilh-Zoller et al., 2003) and CaV3.1 T-type Ca^{2+} channels (Lacinova et al., 2000, Diaz et al., 2005). Future studies examining NHU cell cultures for ZIP zinc transporters and other candidates proposed in cadmium transport would give insights into how cadmium is transported across the urothelial barrier and into urothelial cells.

6.7 Conclusions

Cadmium exposure changed the epigenome of NHU cells, leading to a more repressive chromatin landscape as evidenced by an increase in repressive marks such as H3K9me3 and H327me3 and a decrease in activation-associated acetylation marks including H3K18/23ac. Enzyme-catalysed post-translational modification of histones plays an important role in transcriptional processes. Disruption of the balance of histone modifications in cadmium-exposed cells could affect the normal expression of genes and contribute to cadmium carcinogenesis. Preliminary evidence supports a role for H3K9me3 inhibiting the expression of four representative differentiation-associated genes in NHU cell cultures exposed to cadmium. It was also found that cadmium exposure led to the downregulation of tumour suppressor genes p16, RASSF1A, APC and RUNX3. The inactivation of these tumour suppressor genes has previously been implicated in CIS and MIBC. Taken together, these observations provide evidence supporting the hypothesis that cadmium exposure gives rise to invasive urothelial cancers via epigenetic dysregulation of gene expression leading to field changes within the urothelium characteristic of dysplasia/carcinoma in situ. Additionally, cadmium exposure may play a role in bladder cancers caused by tobacco smoke, arylamines and polycyclic aromatic amines (Figure 6.1). Several studies have shown that cadmium inhibits DNA repair processes (Wieland et al., 2009; Viau et al., 2008, Schwerdtle et al., 2010; Zhou et al., 2012). A deficiency in DNA repair allows more DNA damages to remain in cells causing an increase in the frequency of mutations and eventually leading to cancer progression.

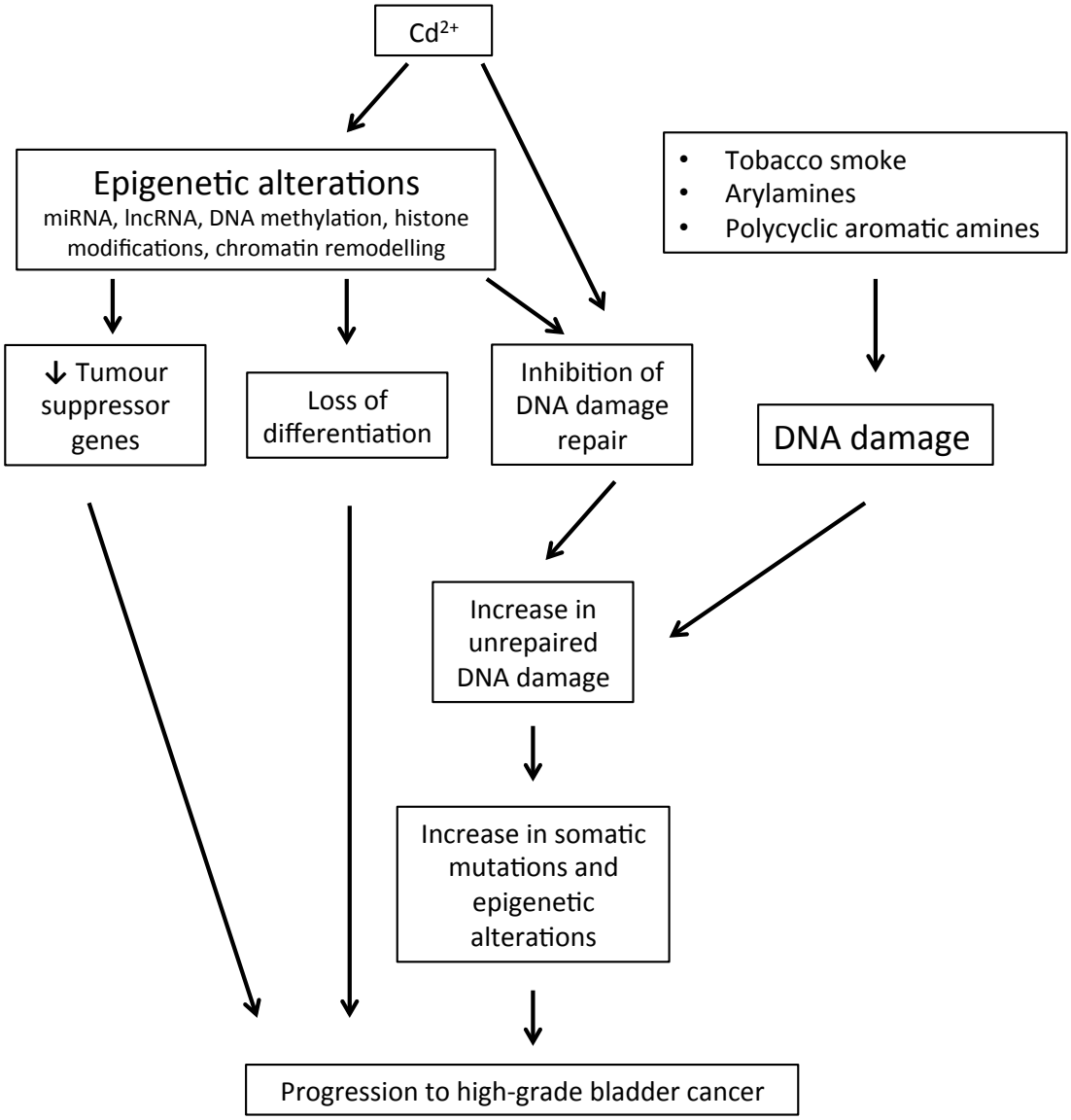

Figure 6.1. Hypothesis for the role of cadmium exposure in bladder cancer.

Cadmium is a complex carcinogen and the mechanisms involved in cadmium carcinogenesis are multifactorial. The overall effect of cadmium is likely due to a coherence of several mechanisms. Future studies should investigate the heritability of epigenetic marks and correlate them to heritable gene expression patterns. Additionally, studies into whether changes occur in the promoter or regulatory regions of dysregulated genes will provide further insight into the epigenetic mechanisms involved in cadmium-induced carcinogenesis.

7 Appendices

7.1 Appendix 1: List of Suppliers

Supplier	Contact details
Abcam	www.abcam.com
Abnova	www.abnova.com
Active Motif	www.activemotif.com
Agilent Technologies	www.agilent.com
Ambion	www.ambion.com
Applied Biosystems (ABI)	www.appliedbiosystems.com
Axygen	www.axygen.com
BD Biosciences	www.bdbiosciences.com
Bioline	www.bioline.com
Bio-Rad	www.bio-rad.com
Bruker Daltonics	www.bruker.com
CA Hendley	www.hendley-essex.com
Calbiochem	www.calbiochem.com
Cambridge Bioscience	www.bioscience.co.uk
CE Instruments	www.ceinstruments.co.uk
Cell Path	www.cellpath.co.uk
Cell Signalling	www.neb.uk.com
Clontech	www.clontec.com
Dako	www.dako.com

Diagenode	www.diagenode.com
Dionex	www.dionex.com
Dynex	www.dynextechnologies.com
ELGA	www.elgalabwater.com
Fisher Scientific	www.fisher.co.uk
Gibco	www.thermofisher.com/uk/en
Greiner	www.greinerbioone.com
Invitrogen	www.invitrogen.com
Leica	www.leicabiosystems.com
Li-Cor Biosciences	www.licor.com
Life Technologies	www.thermofisher.com/uk/en
Millipore	www.millipore.com
Molecular Probes	www.invitrogen.com
MSE	www.mseuk.co.uk
MWG Eurofins	www.eurofinsgenomics.eu
Nanoprop	www.nanodrop.com
New England Biolabs (NEB)	www.neb.uk.com
Nikon	www.nikon.com
Novex	www.thermofisher.com/uk/en
Nunc	www.nalgenunc.com
Olympus	www.olympus.co.uk
Philip Harris	www.philipharris.co.uk

Pierce	www.thermofisher.com/uk/en
Promega	www.promega.com
Qiagen	www.quigen.com
R&D Systems	www.rndsystems.com
RA Lamb	www.ralamb.co.uk
Rockland	www.rockland-inc.com
Santa Cruz	www.scbt.com
Serotech	www.abdserotec.com
Sigma	www.sigmaaldrich.com
SLS	www.scientificlabs.eu/
Star Lab	www.starlab-group.com/en/
Sarstedt	www.sarstedt.com
Seralab	www.seralab.co.uk
Syngene	www.syngene.com
Thermo Scientific	www.thermoscientific.com
TissueGnostics	www.tissuegnostics.com
Tocris	www.tocris.com
Vector Labs	www.vectorlabs.com
VWR	www.vwr.com
World Precision Instruments	www.wpiinc.com
Zeiss	www.zeiss.co.uk

7.2 Appendix 2: Buffers and Solutions

General Solutions

Phosphate Buffered Saline (PBS):

137mM NaCl, 2.7mM KCl, 3.2mM Na_2HPO_4 and 147mM KH_2PO_4, pH 7.2 in dH_2O PBS was prepared from tablets (Sigma) and autoclaved

Cell Culture Solutions

Cholera Toxin:

Diluted to 30µg/ml in KSFM. Diluted 1:1000 in KSFM for use.

Collagenase IV:

Diluted to 10,000 U in 100 mL Hank's Balanced Salt Solution (with Ca^{2+} and Mg^{2+} ions), 10 mM HEPES

Stripper Medium:

500 mL Hank's Balanced Salt Solution (without Ca^{2+} and Mg^{2+} ions), 10 mM HEPES, 500,000 kallikrein inactivating units (KIU) Trasylol and 0.1% (w/v) EDTA

Transport Medium:

500 mL Hank's Balanced Salt Solution (with Ca^{2+} and Mg^{2+} ions), 10 mM HEPES and 500,000 (KIU) Trasylol

10% (v/v) Formalin in PBSc:

100 mL 37% formalin, 900 mL PBSc (PBS containing 0.5 mM $MgCl_2$ and 0.9 mM $CaCl_2$)

Immunofluorescence Solutions

TBS for IF:

50mM Tris-HCl (pH 7.6), 150mM NaCl, 0.1% (w/v) NaN_3 and 0.1% (w/v) BSA

Antifade:

5% N-propyl Gallate (w/v) in 95% glycerol and 5% PBS

Histology Solutions

Citric acid Buffer:

0.8g Citric Acid in 350mls dH_2O, adjusted to pH 6.0 with NaOH

TBS Buffer for IHC:

0.05M Tris-HCl, 0.15M NaCl, pH 7.6 in dH_2O

Haematoxylin:

0.3g NaI, 1g Citric acid, 50g Chloral hydrate, 50g Aluminium potassium sulphate added sequentially to 850ml dH_2O, 20ml ethanol containing 15% (w/v) haematoxylin, and 120ml glycerol.

Scott's Tap Water:

2% (w/v) $MgSO_4$ and 0.35% (w/v) $NaHCO_3$ in dH_2O

Western Blotting Buffers

2x SDS Sample Buffer:

20% (v/v) glycerol, 2% (w/v) SDS, 125 mM Tris- HCl (pH 6.8), 200 mM NaF, 0.1 mM Na_3PO_4, 33 mM Na_3PO_4, with freshly added 13 mM DTT and 1:100 dilution of protease inhibitor cocktail (Sigma Aldrich)

Transfer Buffer:

20 % (v/v) methanol and 80 % (v/v) H_2O with final concentrations of 12 mM Tris and 96 mM glycine

Tris Buffered Saline (TBS):

10 mM Tris (adjusted to pH 7.4 with HCl) and 140 mM NaCl in H_2O

TBS – Tween 20:

0.1% Tween-20, 10 mM Tris (adjusted to pH 7.4 with HCl) and 140 mM NaCl in H_2O

Chromatin Immunoprecipitation Buffers

Swelling Buffer:

5mM PIPES (pH8) with 85 mM KCl in H_2O

TE buffer:

10 mM Tris-HCl (pH 8.0), 10 mM EDTA

***Radioimmunoprecipitation assay (RIPA) Buffer*:**

10 mM Tris-HCl (pH 7.5), 140 mM NaCl, 1 mM EDTA, 0.5 mM EGTA, 1% (v/v) Triton X-100 and 0.1% (w/v) SDS

RIPA-ChIP Buffer:

10 mM Tris-HCl (pH 7.5), 140 mM NaCl, 1 mM EDTA, 0.5 mM EGTA, 1% (v/v) Triton X-100, 0.1% (w/v) SDS with freshly added 1 mM PMSF and 1:100 dilution of protease inhibitor cocktail (Sigma Aldrich)

Elution Buffer:

20 mM Tris-HCl (pH 7.5), 5 mM EDTA and 50 mM NaCl

Complete Elution Buffer:

20 mM Tris-HCl (pH 7.5), 5 mM EDTA and 50 mM NaCl with freshly added 1% (w/v) SDS and 50 μg/mL proteinase K

Acid- Extraction Buffers

Hypotonic Lysis Buffer:

10 mM Tris-HCl (pH 8.0), 1 mM KCl, 1.5 mM MgCl2, with freshly added 1 mM DTT, 1 mM PMSF, 1:100 dilution of protease inhibitor cocktail (Sigma Aldrich) and 1:100 dilution of phosphatase inhibitor cocktails 2 and 3 (Sigma Aldrich)

Coomassie Brilliant Blue Solution:

0.1% (w/v) Brilliant Blue G-250 (BioRad), 50% methanol, 10% acetic acid in dH_2O

7.3 Appendix 3: Representative Western Blots

7.3.1 β-actin

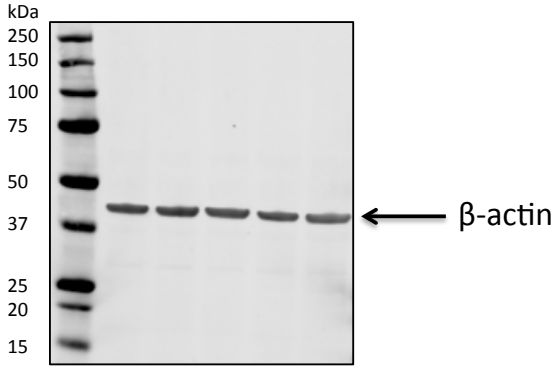

7.3.2 CK13

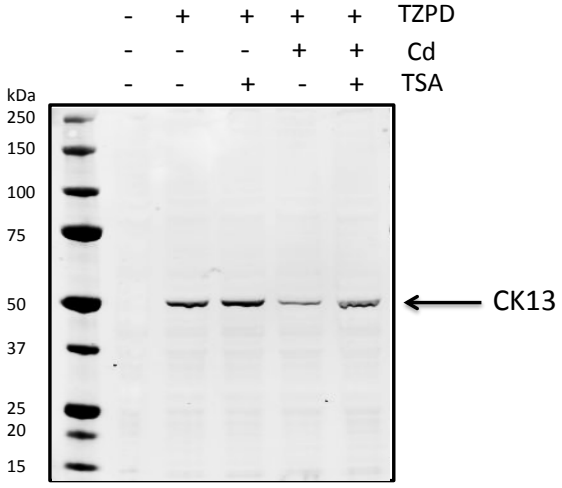

7.3.3 CK14

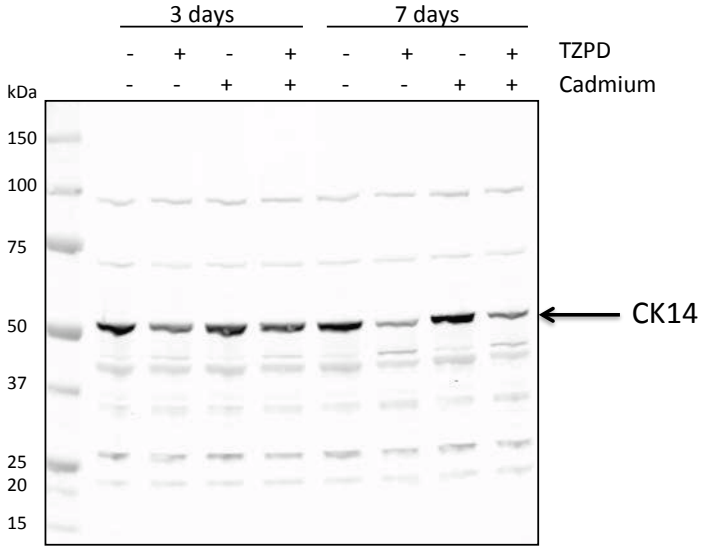

7.3.4 Claudin 4

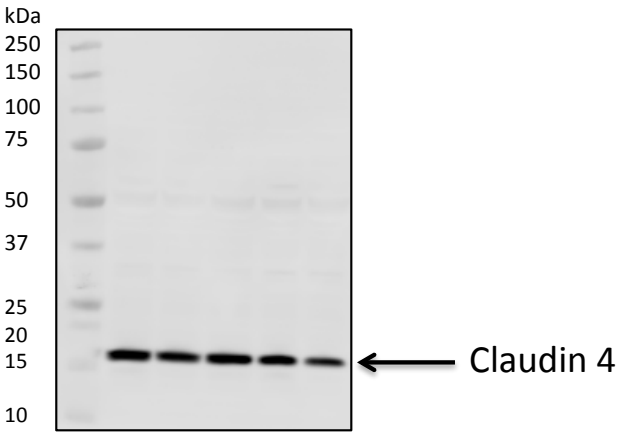

7.3.5 Claudin 5

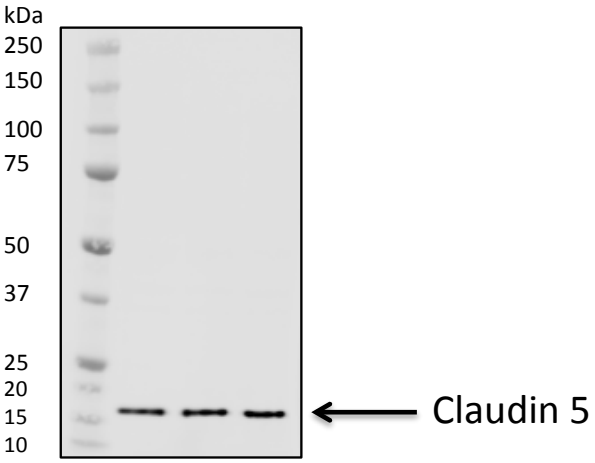

7.3.6 H2AK5ac

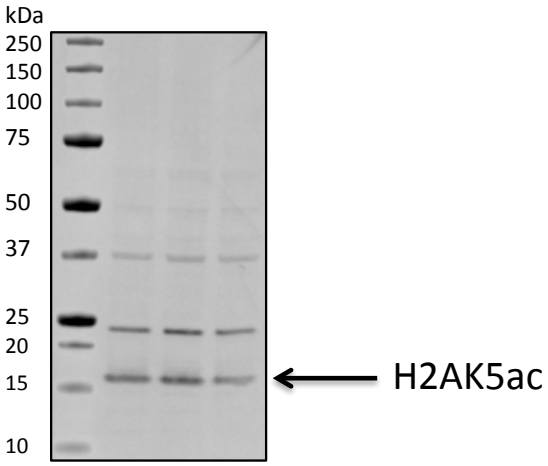

7.3.7 H3

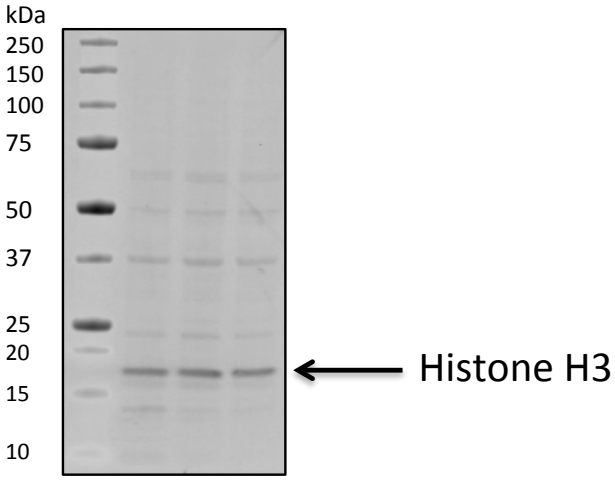

7.3.8 H3K4me3

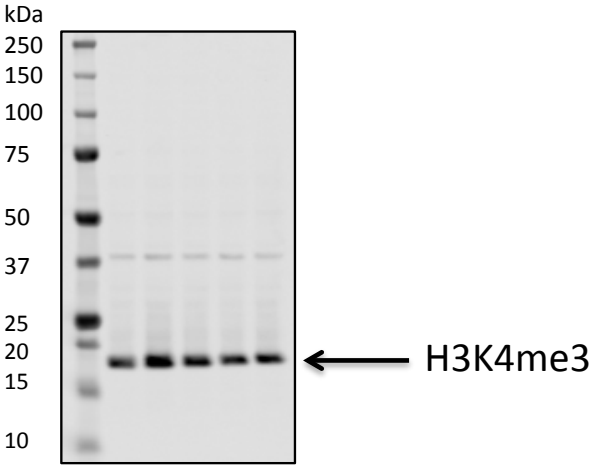

7.3.9 H3K9me2

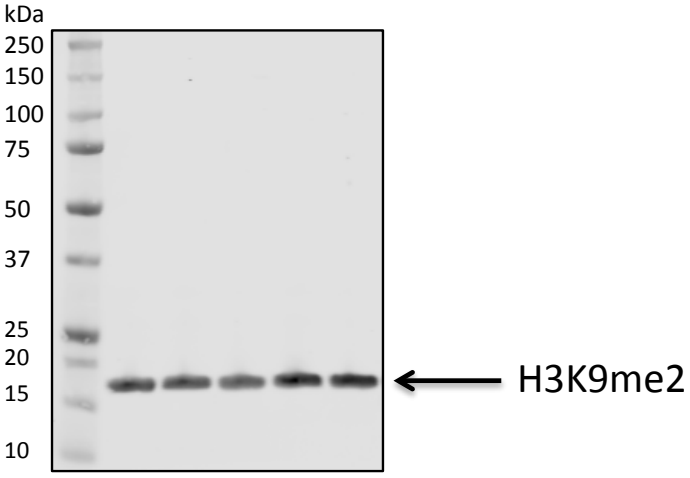

7.3.10 H3K9me3

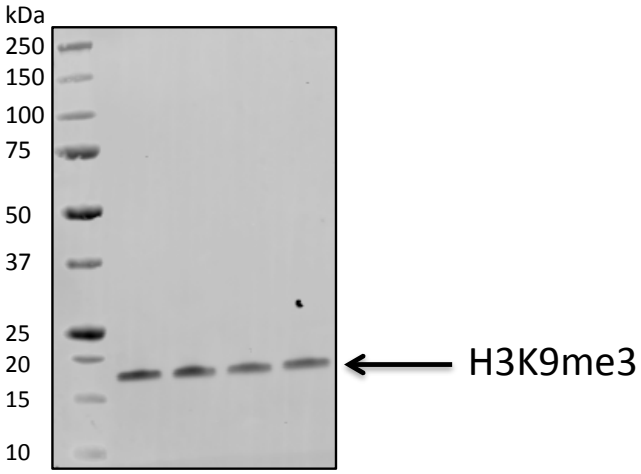

7.3.11 H3K9ac

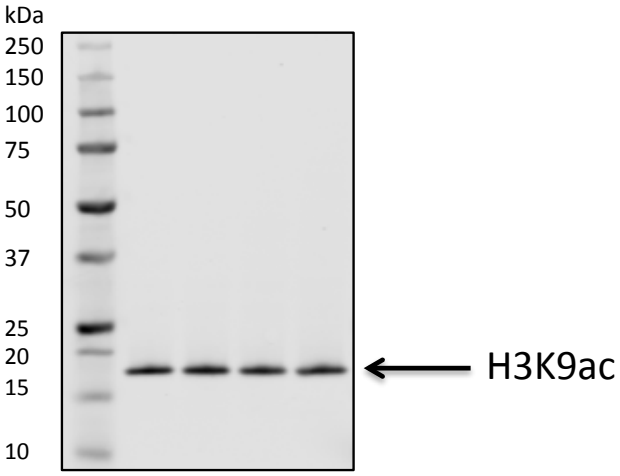

7.3.12 H3K9/14ac

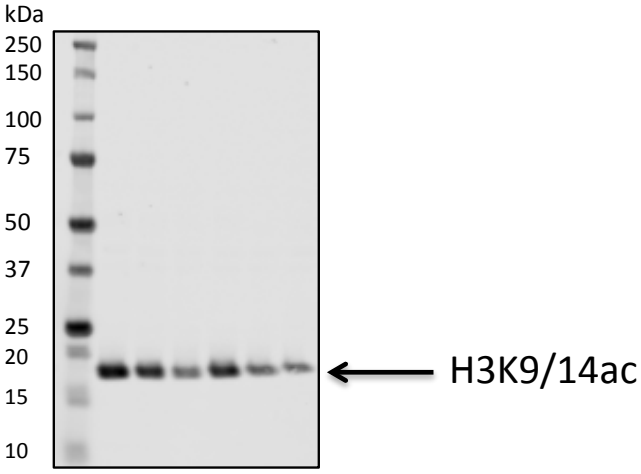

7.3.13 H3K18ac

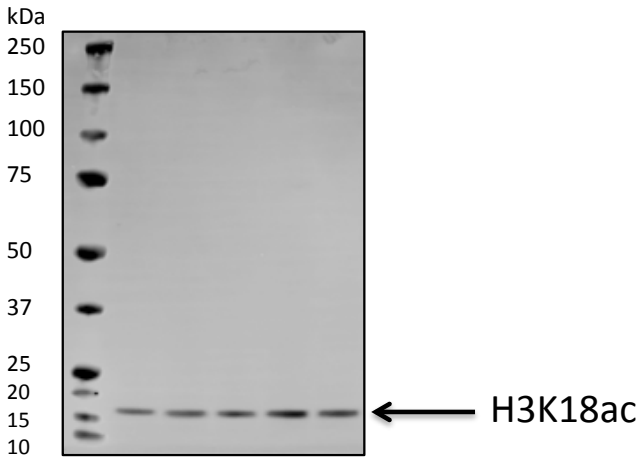

7.3.14 H3K23ac

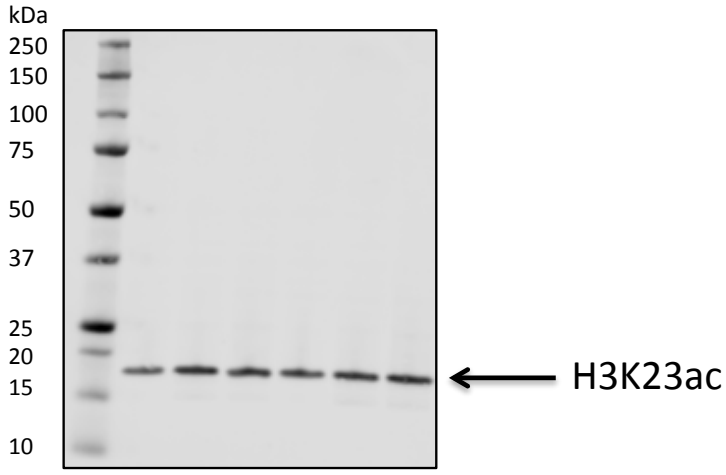

7.3.15 H3K27me3

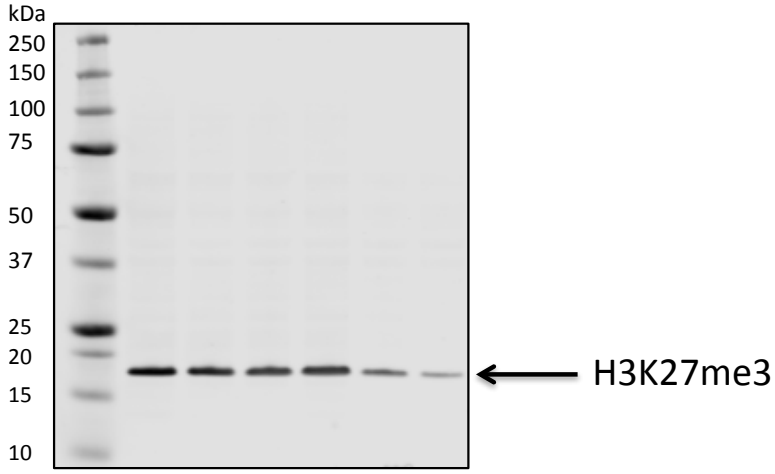

7.3.16 H4K8ac

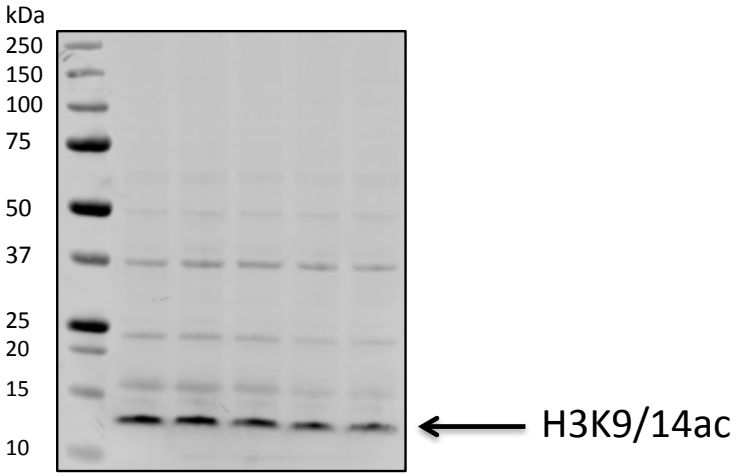

7.3.17 H4K20me3

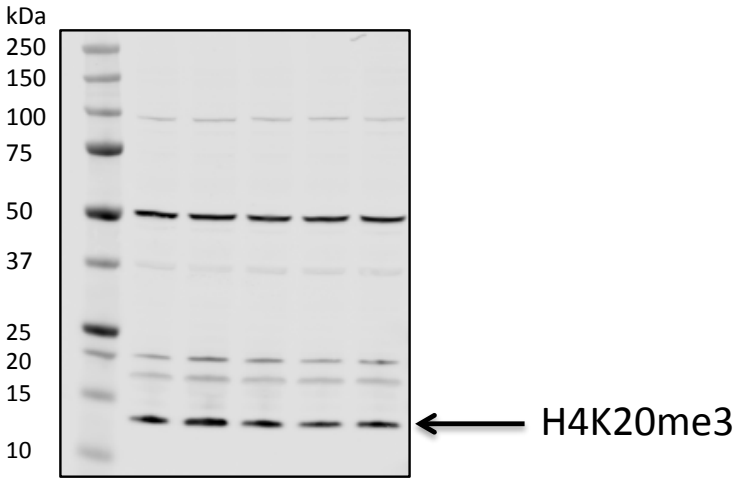

7.3.18 p16

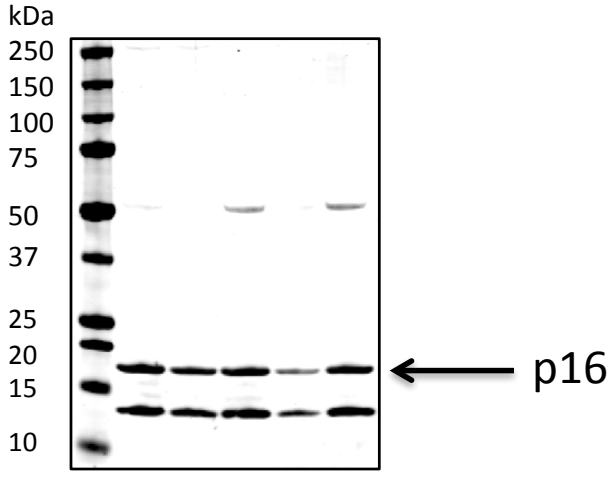

7.4 Appendix 4

7.4.1 Genes upregulated by >2-fold change during cadmium exposure (p > 0.05)

ADCK3
ALDH3A1
ANKRD35
AQP7P1
ARHGAP6
ARID5B
ASB2
ATP6V0A1
BIRC7
C17orf51
C21orf37
C3orf35
C9orf172
CCDC172
CCDC178
CCK
CCNB3
CD164L2
CDHR2
CLEC4GP1
CRABP2
CST7
CTSG
CYP2A7P1
CYP4Z1
DAB2
DDIT4L
EEF1A2
EMILIN2
ERC2
FLJ13744
FLJ32255
FOXL2
FPGT-TNNI3K
FXYD2
GATM
GIMAP6
GNAT2
GPR63
GPR78
HERC2
HMOX1
HRG
HSPB8
IGSF3
ITGB7
KRT14
KRT16
KRT16P2
KRT42P
KRTAP10-5
LHFPL1
LINC00633
LINC01121
LOC100505874
LOC100506379
LOC100506790
LOC100506795
LOC101927789
LOC101929553
LOC284561
LOC285629
LOC344887
LRP1B
MAPK8IP2
MEIOB
METTL10
MGC21881
MT1A
MT1B
MT1E
MT1F
MT1G
MT1H
MT1HL1
MT1IP
MT1L
MT1M
MT1X
MT2A
NCF2
NOX1
NTNG2
OTUB2
PALD1
PAMR1
PART1
PCDHGB2
PLA2G4C
PLAC1
PPAP2C
PRDM15
PTGDR
PTPRG
RABGEF1
RBM14
RBP7
RDH12
RNF32
S100A12
S100A8
SECISBP2
SLC30A1
SLC6A2
SLC9B1
SRD5A2
SSTR5
STXBP5-AS1
TBC1D21
TMEM71
TREM1
TRIL
TSPAN7
TTC24
TTYH2
UCHL1
UGT2B15
USP44

7.4.2 Genes downregulated by >2-fold change during cadmium exposure (p > 0.05)

A4GNT	C20orf166-AS1	CMTM5	ENDOU
ABAT	C20orf201	CNNM1	ENTHD1
ABCC12	C3orf49	CNTLN	ENTPD1
ABL2	C4BPB	COG6	EPHA10
ACAP1	C5AR2	COL6A3	EPHA8
ACBD7	C5orf48	COL6A4P1	ERCC5
ACP1	C5orf64	CPNE2	ERMN
ACSM4	C7orf13	CREB3L3	EXOG
ADAM2	C7orf33	CRHBP	F7
ADAM5	C7orf69	CRYBA1	FAM159B
ADH1A	C8orf44-SGK3	CSN2	FAM19A3
ADRA1D	C9orf169	CSN3	FAM205B
AICDA	CA6	CT64	FAM230C
ANKRD20A9P	CACNA2D2	CXorf21	FAM90A7P
ANKRD62	CALB1	CXorf27	FAM92B
APOL5	CALML3-AS1	CXorf38	FAM95B1
AQP4	CARD8	CYP26C1	FAM99A
AQP6	CASC15	CYP4Z2P	FBN1
ARAP1-AS2	CCDC147	DAB1	FCAMR
ARMCX4	CCDC64	DAW1	FCN1
ASB11	CD177	DBF4	FCN2
ASPM	CD1C	DCAF4L2	FCRL1
AZU1	CD200R1	DCD	FCRL5
BARHL2	CD247	DCLK2	FENDRR
BCOR	CD27-AS1	DEC1	FGF18
BLK	CD300LD	DEFA3	FGF5
BNC2	CD34	DEFB110	FGF8
BOLL	CD4	DEFB127	FGG
BPI	CDH26	DEFB130	FHL5
BRIP1	CDH6	DGKB	FLCN
BRWD1-AS1	CDKN2B-AS1	DHDDS	FLJ35282
BSX	CDRT15	DLX1	FLJ37786
C10orf53	CENPF	DMRTA2	FLJ43903
C10orf68	CENPW	DNTT	FLJ45482
C10orf71-AS1	CHGB	DOCK2	FLJ46284
C12orf39	CHRNA3	DOK7	FLT1
C12orf42	CHRNB2	DSCR8	FMNL3
C14orf64	CKLF	DTX1	FNDC1
C15orf54	CLDN22	DYNAP	FOXP2
C17orf74	CLEC2L	EBF1	FP2234
C1orf111	CLEC4M	EBF2	FRG2
C1orf227	CMA1	ECEL1P2	FXYD4
C1orf61	CMAHP	EML5	GALNT15
C1QL1	CMKLR1	EN1	GAS2L3

GATA1	ITGA4	LINC00669	LOC100507308
GATA3-AS1	IZUMO3	LINC00684	LOC100507353
GFRAL	JPH3	LINC00689	LOC100507431
GGNBP1	KCNA6	LINC00698	LOC100507477
GIGYF2	KCNJ9	LINC00858	LOC100507642
GIMAP4	KCNQ5	LINC00881	LOC100653005
GNAT3	KCTD21-AS1	LINC00893	LOC100996267
GNG3	KDM1B	LINC00894	LOC100996345
GOLGA6A	KIAA1211	LINC00911	LOC100996490
GPER1	KIRREL3-AS3	LINC00944	LOC100996701
GPR146	KLF6	LINC00950	LOC101805491
GPR179	KLK13	LINC01060	LOC101927165
GPR61	KLK14	LINC01088	LOC101927367
GPRIN1	KRT40	LINC01094	LOC101927381
GPX6	KRT8	LINC01095	LOC101927668
GRAMD1B	LAMB4	LINC01102	LOC101928058
GREB1	LDB2	LINGO1	LOC101928105
GRIN2A	LENG8	LIX1	LOC101928423
GTSE1	LGI4	LOC100127972	LOC101928895
GYG2P1	LHFPL3-AS1	LOC100128164	LOC101928956
HAVCR2	LIG4	LOC100128787	LOC101929125
HCG9	LINC00167	LOC100128840	LOC101929154
HCN2	LINC00200	LOC100129083	LOC101929416
HFE	LINC00208	LOC100129373	LOC101929578
HGC6.3	LINC00222	LOC100129393	LOC149351
HIST1H1D	LINC00277	LOC100129917	LOC151475
HIST1H4B	LINC00278	LOC100130071	LOC283177
HIST1H4D	LINC00299	LOC100130433	LOC283674
HIVEP3	LINC00307	LOC100130954	LOC284688
HLA-B	LINC00320	LOC100131510	LOC284751
HLX	LINC00327	LOC100131581	LOC284933
HMBOX1	LINC00328	LOC100131756	LOC284950
HMMR	LINC00348	LOC100131894	LOC285000
HOXC12	LINC00403	LOC100132005	LOC285043
HPD	LINC00446	LOC100132014	LOC285762
HSFY1P1	LINC00471	LOC100132069	LOC340515
HSPBAP1	LINC00473	LOC100133145	LOC388282
IDO2	LINC00478	LOC100133315	LOC400655
IFNA21	LINC00494	LOC100270679	LOC440416
IGFBP7-AS1	LINC00506	LOC100288102	LOC441204
IGSF1	LINC00544	LOC100288728	LOC441666
IGSF9B	LINC00582	LOC100289361	LOC441728
IKZF1	LINC00599	LOC100291323	LOC643037
IL12RB2	LINC00615	LOC100506272	LOC644852
IL20	LINC00622	LOC100506674	LOC645427
IL21R	LINC00643	LOC100506792	LOC646736
IL2RA	LINC00659	LOC100506827	LOC650226
IMPG1	LINC00661	LOC100506837	LOC727710

LOC728095
LOC728715
LOC729506
LOC729860
LOC729930
LOC731779
LONP2
LOXHD1
LOXL1
LPPR4
LRFN5
LRRIQ4
LRRTM2
LSM11
LST1
MAGEA4
MAGEA6
MAML3
MAP3K19
MAPK15
MATN2
MCHR2
MED27
MEGF11
METTL21EP
MEX3D
MGAT4C
MGC27382
MIEF2
MIPEPP3
MIR181A1HG
MIRLET7DHG
MMP21
MNDA
MPPED1
MROH2A
MROH7
MS4A2
MS4A8
MSMP
MTRNR2L1
MUC12
MUC5AC
MUC6
NAIP
NCAN
NDNF
NDST3
NDUFA6-AS1
NECAB1
NEK3
NKX2-2
NPPC
NPSR1-AS1
NPW
NPY2R
NRAP
NRK
NRXN1
NSD1
NUDT4
ODF3B
OR10A4
OR10J1
OR10K1
OR10R3P
OR10W1
OR13G1
OR14A16
OR1L3
OR2T4
OR4C12
OR4S2
OR51I1
OR51Q1
OR52B6
OR52J3
OR5D16
OR5J2
OR5M3
OR8A1
OTUD7A
PIGK
PIKFYVE
PNCK
PNPLA1
POLR2M
POM121L9P
POU4F3
PPP6R1
PRAMEF15
PRB4
PRDM14
PRKACG
PRRG3
PRX
PSIP1
PTF1A
PTGER3
PTGFR
PTPN5
QRFP
RACGAP1P
RASGEF1A
RAX
RBMY2EP
REM1
RERG
RGS6
RNA28S5
RNF17
RNU11
RPL13A
RSPH4A
RUNX3
RXFP2
S100G
SCARNA10
SCARNA22
SCARNA9L
SCGB1D4
SCN7A
SCTR
SEC16B
SHISA3
SIGLEC9
SLA2
SLC17A9
SLC22A24
SLC22A8
SLC24A4
SLC25A23
SLC2A13
SLC38A6
SLC39A12
SLC9A1
SMDT1
SMTN
SNAR-G1
SNORA2B
SNORD113-5
SNORD114-14
SNORD116-11
SNORD116-12
SNORD116-13
SNORD42A
SNORD59B
SNORD84
SNORD97
SORCS1
SOX14
SOX30
SPIC
SSMEM1
ST8SIA6
STC1
STX1B
STXBP5-AS1
SULT6B1
SYNGAP1
SYT1
TBC1D29
TCEB3C
TCL6
TCP10
TDGF1
TEX11
TEX13A
TEX26-AS1
TGIF2LY
TINAG
TMEM114
TMEM14E
TMEM151B
TMEM194A
TMEM262
TMEM56
TMEM88B
TMPO
TNFSF11
TNP1
TNS1
TPH2
TPTE2
TRERF1
TRIM15
TRIM61
TRPA1
TSG1
TSPAN16
TSPEAR
TTTY1

TTTY11
UNC80
UNC93A
VCAM1
VRTN
VWA3A
WDR33
WDR49
WIPF3
WNT2
WRAP53
WTAP
XKR5
ZBTB20
ZC3H12D
ZC3H13
ZEB2
ZNF29P
ZNF311
ZNF316
ZNF365
ZNF43
ZNF496
ZNF705B
ZNF732
ZNF804A
ZNF888
ZYG11A

7.4.3 Genes upregulated by >2-fold change by TSA (p > 0.05)

ABL2	DNER	IGSF6	LOC100996455
ACR	DNMT3B	IL21R	LOC101060442
ADORA2A-AS1	DOC2B	IL27	LOC101928761
AEBP1	DPF3	INE1	LOC101929765
AKAP4	DUX4L9	INTS1	LOC101930210
ALX4	ECEL1	JAKMIP2	LOC284757
ANKRD19P	EIF5A2	KCNA6	LOC339442
APBB1IP	EN1	KCNN1	LOC344887
AXIN2	ENTPD1	KCNV2	LOC388906
BMP4	ETV1	KCTD21-AS1	LOC644277
BMS1P20	EVX2	KIAA1161	LOC650226
BPI	F5	KRT8	LOC654841
BPIFB4	FAM189A2	KRTAP9-1	LOC728093
C12orf40	FAM216B	LGI3	LOC728445
C12orf42	FAM230C	LIF	LOC729739
C1orf189	FAM99A	LIMD2	LOC729866
C8orf44-SGK3	FBLN2	LINC00205	LRCOL1
CABP1	FCAMR	LINC00240	LRRTM4
CACNA1F	FERMT1	LINC00244	MAPT
CACNA2D2	FGF22	LINC00299	MNX1
CADPS	FLJ25363	LINC00307	MROH2A
CALML5	FRMPD4	LINC00313	MS4A3
CD3G	FRY	LINC00445	MSMP
CHGA	FUT10	LINC00462	MT1DP
CLEC2A	GLYATL2	LINC00478	MUC12
CLVS2	GNAS	LINC00630	MUC19
CNTLN	GNAZ	LINC00840	MUC3
COL6A4P2	GOLGA6A	LINC00879	MYH11
COMP	GOLGA7B	LINC00906	MYO3A
CPA5	GPR156	LINC00908	MZB1
CPA6	GPSM1	LINC01060	NHS
CPNE9	GSX2	LINC01088	NMNAT2
CRABP1	GYS2	LOC100128429	NPY2R
CRB1	HBA2	LOC100130761	NR5A1
CRLF1	HIST1H2APS1	LOC100131131	NR5A2
CT60	HLA-DPB2	LOC100133612	NRARP
CYP24A1	HRK	LOC100505902	NRK
CYP3A43	HSPA2	LOC100506351	OLAH
DCLK2	HSPB11	LOC100507236	OR14A16
DIO2	IFNA7	LOC100996380	OR1D5

OR2H1
OR51E2
OR52I2
OR52K2
OR6C76
OR7D4
OR8H1
OTOG
OTUD7A
P2RY10
PADI2
PCDHGA9
PCDHGC4
PDXK
PER3
PHOSPHO2-KLHL23
PKN2
PNKD
PON1
PRMT8
PROKR2
PRPH
PTCH1
PTN
PTPN5
PTPRVP
RAB43
RAP1GAP
RIMS1
RNF216
RPL36AP33
RRN3P2
SATL1
SBK1
SBK2
SBNO2
SCN5A
SCUBE1
SEC14L3
SEMA6B
SEPT12
SERPINA9
SFRP1
SH2B2
SLC24A4
SLC4A1
SLC5A1
SLC6A18
SLCO4C1
SNCB
SNORA39
SNORD113-5
SNORD114-9
SOGA1
SPATA25
SPDYE4
SPINK7
SSX7
STX1A
STXBP5-AS1
SUSD5
SYNGAP1
SYNJ2
SYT12
TACR2
TAS2R41
TCP10
TDGF1
TEX35
TEX37
TMEM59L
TNFRSF4
TNS1
TREM1
TRERF1
UCMA
UNC80
VAX1
VCY
VWA3B
WDR33
WFDC6
ZBTB20-AS1
ZFYVE28
ZNF29P

7.4.4 Genes downregulated by >2-fold change by TSA (p > 0.05)

ABLIM2
ACTG1
ADH4
ADORA3
AKT1S1
ANGPT1
ANKRD20A12P
ANKRD35
APCDD1L-AS1
ARMC12
BOD1L2
C9orf172
CAPN14
CARTPT
CD70
CHL1
COX8C
CRX
CYCSP52
CYP2A7P1
DCAF8
FAM133B
FGFBP1
FLNC
GBP1P1
GIMAP7
GUCY1B3
ICMT
IL18RAP
IL36RN
KRTAP29-1
LINC00112
LINC00371
LINC00424
LINC00617
LINC00683
LINC00841
LINC00963
LOC100129516
LOC100505716
LOC100506207
LOC100506276
LOC100506421
LOC101927630
LOC101928427
LOC101930083
LOC283484
LOC643406
NR2E1
OR2T8
OTC
OXCT2
PABPC3
PCDHGA5
PCDHGB2
PEG3-AS1
PIP5K1B
PPP1R14A
PPP1R27
PRKCQ-AS1
PRUNE2
PTPN11
SDCCAG8
SEMA3E
SH3RF3
SHANK2
SLC3A1
SLC9B1
SPATA41
TAGAP
TBC1D21
TDRG1
TEX9
TMEM33
TRIM36
TUBA3FP
ZC3H12D
ZNF577

8 Abbreviations

The following abbreviations are used throughout the text:

5aza	5-azacytidine (DNA methyltransferase inhibitor)
ABS	Adult bovine serum
ABS/Ca^{2+}	Treatment with 5% Adult bovine serum and 2 mM calcium
AUM	Asymmetric unit membrane
bp	Base pairs
BPE	Bovine pituitary extract
BSA	Bovine serum albumin
Ca^{2+}	Calcium
Cd^{2+}	Cadmium
$CdCl_2$	Cadmium chloride
ChIP	Chromatin Immunoprecipitation
CIS	Carcinoma in situ
CK	Cytokeratin protein
CMF	Cell multiplication factor (final cell number/initial cell number)
DAB	Diaminobenzidine
DEPC	Diethyl pyrocarbonate
DMSO	Dimethyl sulfoxide
DNMT	DNA methyltransferase
dNTP	Deoxynucleotide triphosphate
DPBS	Dulbecco's phosphate buffered saline
EDTA	Ethylenediaminetetraacetic acid
EGFR	Epidermal growth factor receptor
EZH2	Enhancer of zeste homolog 2
FBS	Fetal bovine serum
GAPDH	Glyceraldehyde 3-phosphate dehydrogenase
HAT	Histone acetyltransferase
HBSS	Hank's balanced salt solution
HDAC	Histone deacetylase
HPLC	High performance liquid chromatography
IEGs	Immediate early response genes

IF	Immunofluorescence
IHC	Immunohistochemistry
kDa	Kilo Dalton
KDM	Lysine demethylase
KMT	Lysine methyltransferase
KRT	Cytokeratin gene
KSFM(c)	Keratinocyte serum free medium (complete)
LDS	Lithium dodecyl sulfate
lncRNA	Long non-coding RNA
MAPK	Mitogen-activated protein kinase
MBD	Methyl-CpG-binding domain
MIBC	Muscle invasive bladder cancer
miRNA	Micro RNA
MRE	Metal response element
MRES	Multiple regional epigenetic silencing
MS	Mass spectrometry
MT	Metallothionein
MTF1	Metal regulatory transcription factor 1
NGFR	Nerve growth factor receptor
NHU	Normal human urothelial
NMIBC	Non-muscle invasive bladder cancer
PBS	Phosphate buffered saline
PD	PD153035 (EGFR inhibitor)
PPAR	Peroxisome proliferator activated receptor
PPRE	Peroxisome proliferator response element
PRC1	Polycomb repressive complex 1
PRC2	Polycomb repressive complex 2
PVDF	Polyvinyldifluoride
RT-QPCR	Reverse transcriptase - quantitative polymerase chain reaction
SAM	S-adenosyl methionine
SDS	Sodium dodecyl sulfate
Shh	Sonic hedgehog
TBS	Tris buffered saline

TER	Transepithelial electrical resistance
TJ	Tight junction
TSA	Trichostatin A (HDAC inhibitor)
TZ	Troglitazone (PPARγ agonist)
TZ/PD	Treatment with 1 μM troglitazone and 1 μM PD153035
UC	Urothelial carcimona
UPK	Uroplakin
Zn^{2+}	Zinc
ZO	Zona occludens

9 References

Achanzar WE, Achanzar KB, Lewis JG, Webber MM, Waalkes MP. (2000). Cadmium induces c-myc, p53 and c-jun expression in normal prostate epithelial cells as a prelude to apoptosis. *Toxicol Appl Pharmacol* 164:291-300.

Achtstatter T, Moll R, Moore B & Franke WW. (1985). Cytokeratin polypeptide patterns of different epithelia of the human male urogenital tract: immunofluorescence and gel electrophoretic studies. J Histochem Cytochem, 33: 415-426.

Adams SV, Newcomb PA, Shafer MM, Atkinson C, Bowles EJ, Newton KM, Lampe JW. (2011). Sources of cadmium exposure among healthy premenopausal women. *Sci Total Environ* 9(9):1632 –1637.

Agency for Toxic Substances and Disease Registry. (1999). Toxicological Profile for Cadmium. Department of Health and Human Services, Public Health Service, Atlanta, GA.

Ajjimaporn A, Botsford T, Garrett SH, Sens MA, Zhou XD, Dunlevy JR, Sens DA, Somji S. (2012). ZIP8 expression in human proximal tubule cells, human urothelial cells transformed by Cd+2 and As+3 and in specimens of normal human urothelium and urothelial cancer. *Cancer Cell Int* 12(1):16.

Ali AH, Kondo K, Namura T, Senba Y, Takizawa H, Nakagawa Y, Toba H, Kenzaki K, Sakiyama S, Tangoku A. (2011). Aberrant DNA methylation of some tumor suppressor genes in lung cancers from workers with chromate exposure. *Mol Carcinog* 50(2):89-99.

Allis CD, Berger SL, Cote J, Dent S, Jenuwien T, Kouzarides T, Pillus L, Reinberg D, Shi Y, Shiekhattar R, Shilatifard A, Workman J, Zhang Y. (2007). New nomenclature for chromatin-modifying enzymes. *Cell* 131(4):633-6.

Amaral AF, Cymbron T, Gärtner F, Lima M, Rodrigues AS. (2009). Trace metals and over-expression of metallothioneins in bladder tumoral lesions: a case-control study. *BMC Vet Res* 18:5–24.

Amin KS, Banerjee PP. (2012). The cellular functions of *RASSF1A* and its inactivation in prostate cancer . *J Carcinog* 11:3.

Amoureux MC, Wurch T, Pauwels PJ. (1995). Modulation of metallothionein-III mRNA content and growth rate of rat C6-glial cells by transfection with human 5-HT1D receptor genes. *Biochem Biophys Res Commun* 214(2):639-45.

Andersen O. (1984). Chelation of cadmium. *Environ Health Perspect* 54:249-66.

Andrews GK. (2000). Regulation of metallothionein gene expression by oxidative stress and metal ions. *Biochem Pharmacol* 59:95–104.

Aravind L, Abhiman S, Iyer LM. (2011). Natural history of the eukaryotic chromatin protein methylation system. *Prog Mol Biol Transl Sci* 101:105-76.

Arita A, Costa M. (2009). Epigenetics in metal carcinogenesis: nickel, arsenic, chromium and cadmium. *Metallomics* 1:222-228.

Asmuss M, Mullenders LH, Hartwig A. (2000). Interference by toxic metal compounds with isolated zinc finger DNA repair proteins. *Toxicol Lett* 112-113:227-31.

Asmuss M, Mullenders LH, Eker A, Hartwig A. (2000). Differential effects of toxic metal compounds on the activities of Fpg and XPA, two zinc finger proteins involved in DNA repair. *Carcinogenesis* 21:2097-2104.

Aveyard JS, Skilleter A, Habuchi T, Knowles MA. (1999). Somatic mutation of PTEN in bladder carcinoma. *Br J Cancer* 80(5-6):904-8.

Avvakumov N, Côté J. (2007). The MYST family of histone acetyltransferases and their intimate links to cancer. *Oncogene* 26(37):5395-407.

Bal W, Schwerdtle T, Hartwig A. (2003). Mechanism of nickel assault on the zinc finger of DNA repair protein XPA. *Chem Res Toxicol* 16(2):242-8.

Balda MS, Matter K. (2008). Tight junctions at a glance. *J Cell Sci* 121:3677–3682.Bannister AJ, Kouzarides T. (2011). Regulation of chromatin by histone modifications. *Cell Res* 21(3):381–395.

Bannon DI, Abounader R, Lees PS, Bressler JP. (2003). Effect of DMT1 knockdown on iron, cadmium, and lead uptake in Caco-2 cells. *Am J Physiol Cell Physiol* 284(1):C44-50.

Barcia-Sanjurjo I, Vázquez-Cedeira M, Barcia R, Lazo PA. (2013). Sensitivity of the kinase activity of human vaccinia-related kinase proteins to toxic metals. *J Biol Inorg Chem* 18(4):473-82.

Barsyte-Lovejoy D, Lau SK, Boutros PC, Khosravi F, Jurisica I, Andrulis IL, Tsao MS, Penn LZ. (2006). The c-Myc oncogene directly induces the H19 noncoding RNA by allele-specific binding to potentiate tumorigenesis. *Cancer Res* 66(10):5330-7.

Bartoletti R, Cai T, Nesi G, Roberta Girardi L, Baroni G, Dal Canto M. (2007). Loss of P16 expression and chromosome 9p21 LOH in predicting outcome of patients affected by superficial bladder cancer. *J Surg Res* 143(2):422-7.

Bell SM, Zhang L, Mendell A, Xu Y, Haitchi HM, Lessard JL, Whitsett JA. (2011). Kruppel-like factor 5 is required for formation and differentiation of the bladder urothelium. *Dev Biol* 358(1):79-90

Benbrahim-Tallaa L, Waterland RA, Dill AL, Webber MM, Waalkes MP. (2007). Tumor suppressor gene inactivation during cadmium-induced malignant

transformation of human prostate cells correlates with overexpression of de novo DNA methyltransferase. *Environ Health Perspect* 115(10):1454–1459.

Berggren P, Kumar R, Sakano S, Hemminki L, Wada T, Steineck G, Adolfsson J, Larsson P, Norming U, Wijkström H, Hemminki K. (2003). Detecting homozygous deletions in the CDKN2A(p16(INK4a))/ARF(p14(ARF)) gene in urinary bladder cancer using real-time quantitative PCR. *Clin Cancer Res* 9(1):235-42.

Berggren de Verdier PJ, Kumar R, Adolfsson J, Larsson P, Norming U, Onelöv E, Wijkström H, Steineck G, Hemminki K. (2006). Prognostic significance of homozygous deletions and multiple duplications at the CDKN2A (p16INK4a)/ARF (p14ARF) locus in urinary bladder cancer. *Scand J Urol Nephrol* 40(5):363-9.

Beyersmann D, Hartwig A. (1994). Genotoxic effects of metal compounds. *Arch Toxicol Suppl* 16:192-198.

Beyersmann D. (1995). Physiochemical aspects of the interference of detrimental metal ions with normal metal metabolism. In: Berthon G (ed) Handbook on metal-ligand interactions in biological fluids. Marcel Dekker, New York, pp813-826.

Beyersmann D, Hartwig A. (2008). Carcinogenic metal compounds: recent insight into molecular and cellular mechanisms. *Arch Toxicol* 82(8):493-512.

Bickenbach JR. (1981). Identification and behavior of label-retaining cells in oral mucosa and skin. *J Dent Res* 60 Spec No C:1611-20.

Bilgrami SM, Qureshi SA, Pervez S, Abbas F. (2014). Promoter hypermethylation of tumor suppressor genes correlates with tumor grade and invasiveness in patients with urothelial bladder cancer. *Springerplus* 3:178.

Billerey C, Chopin D, Aubriot-Lorton MH, Ricol D, Gil Diez de Medina S, Van Rhijn B, Bralet MP, Lefrere-Belda MA, Lahaye JB, Abbou CC, Bonaventure J, Zafrani ES, van der Kwast T, Thiery JP, Radvanyi F. (2001). Frequent FGFR3 mutations in papillary non-invasive bladder (pTa) tumors. *Am J Pathol* 158:1955-1959.

Blanquart C, Barbier O, Fruchart JC, Staels B, Glineur C. (2003). Peroxisome proliferator-activated receptors: regulation of transcriptional activities and roles in inflammation. *J Steroid Biochem Mol Bio* 85: 267-273.

Böck M, Hinley J, Schmitt C, Wahlicht T, Kramer S, Southgate J. (2014). Identification of ELF3 as an early transcriptional regulator of human urothelium. *Dev Biol* 386(2):321-30.

Boucherie S, Decaens C, Verbavatz JM, Grosse B, Erard M, Merola F, Cassio D, Combettes L. (2013). Cadmium disorganises the scaffolding of gap and tight junction proteins in the hepatic cell line WIF B9. *Biol Cell* 105(12):561-75.

Boulanger Y, Armitage IM, Miklossy KA, Winge DR. (1982). ^{113}Cd NMR study of a metallothionein fragment. Evidence for a two-domain structure. *J Biol Chem* 257:13717–19.

Bollati V, Marinelli B, Apostoli P, Bonzini M, Nordio F, Hoxha M, Pegoraro V, Motta V, Tarantini L, Cantone L, Schwartz J, Bertazzi PA, Baccarelli A. (2010). Exposure to metal-rich particulate matter modifies the expression of candidate microRNAs in peripheral blood leukocytes. *Environ Health Perspect* 118(6):763-8.

Britton LP, Gonzales-Cope M, Zee BM, Garcia BA. (2011). Breaking the histone code with quantitative mass spectrometry. *Expert Rev Proteomics* 8(5):631–643.

Broday L, Peng W, Kuo MH, Salinikow K, Zoroddu M, Costa M. (2000). Nickel compounds are novel inhibitors of histone H4 acetylation. *Cancer Res* 60:238-241.

Cairns P, Proctor AJ, Knowles MA. (1991). Loss of heterozygosity at the RB locus is frequent and correlates with muscle invasion in bladder carcinoma. *Oncogene* 6:2305–2309

Cairns P, Shaw ME, Knowles MA. (1993). Initiation of bladder cancer may involve deletion of a tumor-suppressor gene on chromosome 9. *Oncogene* 8:1083–1085.

Cairns P, Shaw ME, Knowles MA. (1993). Initiation of bladder cancer may involve deletion of a tumor-suppressor gene on chromosome 9. *Oncogene* 8:1083-1085.

Cairns P, Mao L, Merlo A, Lee DJ, Schwab D, Eby Y, Tokino K, van der Riet P, Blaugrund JE, Sidransky D. (1994). Rates of p16 (MTS1) mutations in primary tumors with 9p loss. *Science* 265(5170):415-7.

Cappellen D, De Oliveira C, Ricol D, de Medina S, Bourdin J, Sastre-Garau X, Chopin D, Thiery JP, Radvanyi F. (1999). Frequent activating mutations of FGFR3 in human bladder and cervix carcinomas. *Nat Genet* 23(1):18-20.

Cartularo L, Laulicht F, Sun H, Kluz T, Freedman JH, Costa M. (2015). Gene expression and pathway analysis of human hepatocellular carcinoma cells treated with cadmium. *Toxicol Appl Pharmacol* [Epub ahead of print].

Catto JW, Azzouzi AR, Rehman I, Feeley KM, Cross SS, Amira N, Fromont G, Sibony M, Cussenot O, Meuth M, Hamdy FC. Promoter hypermethylation is associated with tumor location, stage, and subsequent progression in transitional cell carcinoma. (2005). *J Clin Oncol* 23(13):2903-10.

Catto JW, Miah S, Owen HC, Bryant H, Myers K, Dudziec E, Larré S, Milo M, Rehman I, Rosario DJ, Di Martino E, Knowles MA, Meuth M, Harris AL,

Hamdy FC. (2009). Distinct microRNA alterations characterize high- and low-grade bladder cancer. *Cancer Res* 69(21):8472-8491.

Chanda S, Dasgupta UB, Guhamazumder D, Gupta M, Chaudhuri U, Lahiri S, Das S, Ghosh N, Chatterjee D. (2006). DNA hypermethylation of promoter of gene p53 and p16 in arsenic-exposed people with and without malignancy. *Toxicol Sci* 89(2):431-7.

Chapman EJ, Harnden P, Chambers P, Johnston C, Knowles MA. (2005). Comprehensive analysis of CDKN2A status in microdissected urothelial cell carcinoma reveals potential haploinsufficiency, a high frequency of homozygous co-deletion and associations with clinical phenotype. *Clin Cancer Res* 11(16):5740-7.

Chapman EJ, Hurst CD, Pitt E, Chambers P, Aveyard JS, Knowles MA. (2006). Expression of hTERT immortalises normal human urothelial cells without inactivation of the p16/Rb pathway. *Oncogene* 25(36):5037–45.

Chen DJ, Xu YM, Du JY, Huang DY, Lau AT. (2014). Cadmium induces cytotoxicity in human bronchial epithelial cells through upregulation of eIF5A1 and NF-kappaB. *Biochem Biophys Res Commun* 445:95-99.

Chen H, Ke Q, Kluz T, Yan Y, Costa M. (2006). Nickel ions increase histone H3 lysine 9 dimethylation and induce transgene silencing. *Mol Cell Biol* 26(10): 3728-3737.

Chen H, Zhang T, Sheng Y, Zhang C, Peng Y, Wang X, Zhang CJ. (2015). Methylation profiling of multiple tumor suppressor genes in hepatocellular carcinoma and the epigenetic mechanism of 3OST2 regulation. *J Cancer* 6(8):740-9.

Choi AO, Brown SE, Szyf M, Maysinger D. (2008). Quantum dot-induced epigenetic and genotoxic changes in human breast cancer cells. *J Mol Med (Berl)*, 86(3):291–302.

Choi W, Porten S, Kim S, Willis D, Plimack ER, Hoffman-Censits J, Roth B, Cheng T, Tran M, Lee IL, Melquist J, Bondaruk J, Majewski T, Zhang S, Pretzsch S, Baggerly K, Siefker-Radtke A, Czerniak B, Dinney CP, McConkey DJ. (2014). Identification of distinct basal and luminal subtypes of muscle-invasive bladder cancer with different sensitivities to frontline chemotherapy. *Cancer Cell* 25(2):152-65.

Christman JK, Mendelsohn N, Herzog D, Schneiderman N. (1983). Effect of 5-azacytidine on differentiation and DNA methylation in human promyelocytic leukemia cells (HL-60). *Caner Res* 43(2):763-9.

Christman JK. (2002). 5-Azacytidine and 5-aza-2'-deoxycytidine as inhibitors of DNA methylation: mechanistic studies and their implications for cancer therapy. *Oncogene* 21(35):5483-95.

Chu PG, Weiss LM. (2002). Keratin expression in human tissues and neoplasms. *Histopathology* 40(5):403-439.

Colopy SA, Bjorling DE, Mulligan WA, Bushman W. (2014). A population of progenitor cells in the basal and intermediate layers of the murine bladder urothelium contributes to urothelial development and regeneration. *Dev Dyn* 243(8):988-98.

Crallan RA1, Lord PG, Rees RW, Southgate J. (2002). Inter-individual variation in urothelial DNA repair gene expression in vitro. *Toxicol In Vitro* 16(4):383-7.

Creusot F, Acs G, Christman JK. (1982). Inhibition of DNA methyltransferase and induction of Friend erythroleukemia cell differentiation by 5-azacytidine and 5-aza-2'-deoxycytidine. *J Biol Chem* 257(4):2041-8.

Cross WR, Eardley I, Leese HJ & Southgate J. (2005). A biomimetic tissue from cultured normal human urothelial cells: analysis of physiological function. *Am J Physiol Renal Physiol* 289:F459-468.

Cui X, Wakai T, Shirai Y, Hatakeyama K, Hirano S. (2006). Chronic oral exposure to inorganic arsenate interferes with methylation status of p16INK4a and RASSF1A and induces lung cancer in A/J mice. *Toxicol Sci* 91(2):372-81.

Dally H, Hartwig A. (1997). Induction and repair inhibition of oxidative DNA damage by nickel(II) and cadmium(II) in mammalian cells. *Carcinogenesis* 18:1021-1026.

Dalton TP, He L, Wang B, Miller ML, Jin L, Stringer KF, Chang X, Baxter CS, Nebert DW. (2005). Identification of mouse SLC39A8 as the transporter responsible for cadmium-induced toxicity in the testis. *Proc Natl Acad Sci USA* 102:3401–3406.

Dammann R, Takahashi T, Pfeifer GP. (2001). The CpG island of the novel tumor suppressor gene RASSF1A is intensely methylated in primary small cell lung carcinomas. *Oncogene* 20:3563-7.

Dammann R, Schagdarsurengin U, Strunnikova M, Rastetter M, Seidel C, Liu L, Tommasi S, Pfeifer GP. (2003). Epigenetic inactivation of the Ras-association domain family 1 (RASSF1A) gene and its function in human carcinogenesis. *Histol Histopathol* 18(2):665-77.

Damrauer JS, Hoadley KA, Chism DD, Fan C, Tiganelli CJ, Wobker SE, Yeh JJ, Milowsky MI, Iyer G, Parker JS, Kim WY. (2014). Intrinsic subtypes of high-grade bladder cancer reflect the hallmarks of breast cancer biology. *Proc Natl Acad Sci USA* 111(8):3110-5.

Darewicz G, Malczyk E, Darewicz J. (1998). Investigations of urinary cadmium content in patients with urinary bladder carcinoma. *Int Urol Nephrol* 30:137–139.

Deng FM, Liang FX, Tu L, Resing KA, Hu P, Supino M, Hu CC, Zhou G, Ding M, Kreibich G, Sun TT. (2002). Uroplakin IIIb, a urothelial differentiation marker, dimerizes with uroplakin Ib as an early step of urothelial plaque assembly. *J Cell Biol* 159(4):685-694.

Devlin J, Keen AJ, Knowles MA. (1994). Homozygous deletion mapping at 9p21 in bladder carcinoma defines a critical region within 2cM of IFNA. *Oncogene* 9(9):2757-60.

Dhawan D, Hamdy FC, Rehman I, Patterson J, Cross SS, Feeley KM, Stephenson Y, Meuth M, Catto JW. (2006). Evidence for the early onset of aberrant promoter methylation in urothelial carcinoma. *J Pathol* 209(3):336-43.

Díaz D, Bartolo R, Delgadillo DM, Higueldo F, Gomora JC. (2005). Contrasting effects of Cd^{2+} and Co^{2+} on the blocking/unblocking of human Cav3 channels. *J Membr Biol* 207(2):91-105.

Dickman MJ, Kucharski R, Maleszka R, Hurd PJ. (2013). Extensive histone post-translational modification in honey bees. *Insect Biochem Mol Biol* 43(2):125-37.

Dong C, Wilhelm D, Koopman P. (2004). Sox genes and cancer. *Cytogenet Genome Res* 105:442-7.

Donninger H, Vos MD, Clark GJ. (2007). The RASSF1A tumor suppressor. *J Cell Sci* 120:3163-72.

Dubeau L, Jones PA. (1987). Growth of normal and neoplastic urothelium and response to epidermal growth factor in a defined serum-free medium. *Cancer Res* 47:2107-2112.

Dudziec E, Gogol-Döring A, Cookson V, Chen W, Catto J. (2012). Integrated epigenome profiling of repressive histone modifications, DNA methylation and gene expression in normal and malignant urothelial cells. *PLOS one* 7(3):e32750.

Dyrskjøt L, Kruhøffer M, Thykjaer, Marcussen N, Jensen JL, Møller K, Ørntoft TF. (2004). Gene expression in the urinary bladder: a common carcinoma *in situ* gene expression signature exists disregarding histopathological classification. *Cancer Res* 64:4040-4048.

Eide DJ. (2004). The SLC39 family of metal ion transporters. *Pflugers Arch* 447:796–800.

Fabbri M, Urani C, Sacco MG, Procaccianti C, Gribaldo L. (2012). Whole genome analysis and microRNAs regulation in HepG2 cells exposed to cadmium. *ALTEX* 29(2):173-82.

Fang R, Barbera AJ, Xu Y, Rutenberg M, Leonor T, Bi Q, Lan F, Mei P, Yuan GC, Lian C, Peng J, Cheng D, Sui G, Kaiser UB, Shi Y, Shi YG. (2010). Human

LSD2/KDM1b/AOF1 regulates gene transcription by modulating intragenic H3K4me2 methylation. *Mol Cell* 39(2):222-33.

Feki-Tounsi M, Olmedo P, Gil F, Khlifi R, Mhiri MN, Rebai A, Hamza-Chaffai A. (2013). Cadmium in blood of Tunisian men and risk of bladder cancer: interactions with arsenic exposure and smoking. *Environ Sci Pollut Res Int* 20(10):7204-13.

Feki-Tounsi M, Olmedo P, Gil F, Mhiri MN, Rebai A, Hamza-Chaffai A. (2014). Trace metal quantification in bladder biopsies from tumoral lesions of Tunisian cancer and controls subjects. *Environ Sci Pollut Res Int* 21(19):11433-8.

Fellows GJ, Marshall DH. (1972). The permeability of human bladder epithelium to water and sodium. *Invest Urol* 9:339-334.

Felsenfeld G, Groudine M. (2003). Controlling the double helix. *Nature* 421(6921):448-53.

Fleming JM. (2008) Regulation of Growth and Differentiation in Human Urothelium. PhD thesis, University of York.

Fraga MF, Ballestar E, Villar-Garea A, Boix-Chornet M, Espada J, Schotta G, Bonaldi T, Haydon C, Ropero S, Petrie K, Iyer NG, Pérez-Rosado A, Calvo E, Lopez JA, Cano A, Calasanz MJ, Colomer D, Piris MA, Ahn N, Imhof A, Caldas C, Jenuwein T, Esteller M. (2005). Loss of acetylation at Lys16 and trimethylation at Lys20 of histone H4 is a common hallmark of human cancer. *Nat Genet* 37(4):391-400.

Fromter E, Diamond J. (1972). Route of passive ion permeation in epithelia. *Nat New Biol* 235(53): 9-13.

Fujimoto K, Yamada Y, Okajima E, Kakizoe T, Sasaki H, Sugimura T, Terada M. (1992). Frequent association of p53 gene mutation in invasive bladder cancer. *Cancer Res* 52(6):1393-8.

Gandhi D, Molotkov A, Batourina E, Schneider K, Dan H, Reiley M, Laufer E, Metzger D, Liang F, Liao Y, Sun TT, Aronow B, Rosen R, Mauney J, Adam R, Rosselot C, Van Batavia J, McMahon A, McMahon J, Guo JJ, Mendelsohn C. (2013). Retinoid signaling in progenitors controls specification and regeneration of the urothelium. *Dev Cell* 26(5):469-82.

Georgopoulos NT, Kirkwood LA, Varley CL, MacLaine NJ, Aziz N, Southgate J. (2011). Immortalisation of normal human urothelial cells compromises differentiation capacity. *Eur Urol* 60(1):141–9.

Giepmans BNG. (2004). Gap junctions and connexin-interacting proteins. C*ardiovasc Res* 62:233–245.

Girijashanker K, He L, Soleimani M, Reed JM, Li H, Liu Z, Wang B, Dalton TP, Nebert DW. (2008). Slc39a14 gene encodes ZIP14, a metal/bicarbonate symporter: similarities to the ZIP8 transporter. *Mol Pharmacol* 73(5):1413-23.

Goering PL, Waalkes MP, Klaassen CD. (1994). Toxicology of cadmium. In *Handbook of Experimental Pharmacology: Toxicology of Metals, Biochemical Effects,* edited by Goyer RA, Cherian MG. New York: Springer-Verlag pp 189-214.

Golebiowski F, Kasprzak KS. (2005). Inhibition of core histones acetylation by carcinogenic nickel (II). *Mol Cell Biochem* 279:133-139.

Goll MG, Bestor TH. (2002). Histone modification and replacement in chromatin activation. *Genes Dev* 16:1739–1742.

Gottardo F, Liu CG, Ferracin M, Calin GA, Fassan M, Bassi P, Sevignani C, Byrne D, Negrini M, Pagano F, Gomella LG, Croce CM, Baffa R. (2007). Micro-RNA profiling in kidney and bladder cancers. *Urol Oncol* 25(5):387-92.

Grant PA. *(*2001). A tale of histone modifications. *Genome Biol*. *2(4)*REVIEWS0003.1-3.6

Greer EL, Shi Y. (2012). Histone methylation: a dynamic mark in health, disease and *inheritance. Nat Rev Genet 13(5):343-57.*

*Grewal SI, Moazed D. (*2003) Heterochromatin and epigenetic control of gene expression. *Science* 301:798–802.

Grunstein M. (1997). Histone acetylation in chromatin structure and transcription. *Nature* 389:349–352.

Guan Y, Zhang Y, Davis L, Breyer MD. (1997). Expression of peroxisome proliferator-activated receptors in urinary tract of rabbits and humans. *Am J Physiol* 273:F1013-1022.

Guancial EA, Bellmunt J, Yeh S, Rosenberg JE, Berman DM. (2014). The evolving understanding of microRNA in bladder cancer. *Urol Oncol* 32(1):41.

Gui Y, Guo G, Huang Y, Hu X, Tang A, Gao S, Wu R, Chen C, Li X, Zhou L, He M, Li Z, Sun X, Jia W, Chen J, Yang S, Zhou F, Zhao X, Wan S, Ye R, Liang C, Liu Z, Huang P, Liu C, Jiang H, Wang Y, Zheng H, Sun L, Liu X, Jiang Z, Feng D, Chen J, Wu S, Zou J, Zhang Z, Yang R, Zhao J, Xu C, Yin W, Guan Z, Ye J, Zhang H, Li J, Kristiansen K, Nickerson ML, Theodorescu D, Li Y, Zhang X, Li S, Wang J, Yang H, Wang J, Cai Z. (2011). Frequent mutations of chromatin remodelling genes in transitional cell carcinoma of the bladder. *Nat Genet* 43(9):875-8.

Guo G, Sun X, Chen C, Wu S, Huang P, Li Z, Dean M, Huang Y, Jia W, Zhou Q, Tang A, Yang Z, Li X, Song P, Zhao X, Ye R, Zhang S, Lin Z, Qi M, Wan S, Xie L, Fan F, Nickerson ML, Zou X, Hu X, Xing L, Lv Z, Mei H, Gao S,

Liang C, Gao Z, Lu J, Yu Y, Liu C, Li L, Fang X, Jiang Z, Yang J, Li C, Zhao X, Chen J, Zhang F, Lai Y, Lin Z, Zhou F, Chen H, Chan HC, Tsang S, Theodorescu D, Li Y, Zhang X, Wang J, Yang H, Gui Y, Wang J, Cai Z. (2013). Whole-genome and whole-exome sequencing of bladder cancer identifies frequent alterations in genes involved in sister chromatid cohesion and segregration. *Nat Genet* 45(12):1459-63.

Gunshin H, Mackenzie B, Berger UV, Gunshin Y, Romero MF, Boron WF, Nussberger S, Gollan JL, Hediger MA. (1997). Cloning and characterization of a mammalian proton-coupled metal-ion transporter. *Nature* 388(6641):482-8.

Günther V, Lindert U, Schaffner W. (2012). The taste of heavy metals: gene regulation by MTF-1. *Biochim Biophys Acta* 1823(9):1416-25.

Hamer DH. (1986). Metallothionein. *Annu Rev Biochem* 55:913–951.

Hammam O, Wishahiz M, Khalil H, El Ganzouri H, Badawy M, Elkhquly A, Elesaily K. (2014). Expression of cytokeratin 7, 20, 14 in urothelial carcinoma and squamous cell carcinoma of the Egyprian urinary bladder cancer. *J Egypt Soc Parasitol* 44(3):733-40.

Han Y, Chen J, Zhao X, Liang C, Wang Y, Sun L, Jiang Z, Zhang Z, Yang R, Chen J, Li Z, Tang A, Li X, Ye J, Guan Z, Gui Y, Cai Z. (2011). MicroRNA expression signatures of bladder cancer revealed by deep sequencing. *PLoS One* 6(3):e18286.

Han Y, Liu Y, Nie L, Gui Y, Cai Z. (2013). Inducing cell proliferation inhibition, apoptosis, and motility reduction by silencing long noncoding ribonucleic acid metastasis-associated lung adenocarcinoma transcript 1 in urothelial carcinoma of the bladder. *Urology* 81(1)209.e1-7.

Hart BA, Gong Q, Eneman JD. (1996). Pulmonary metallothionein expression in rats following single and repeated exposure to cadmium aerosols. *Toxicology* 112:205-218.

Hartmann A, Schlake G, Zaak D, Hungerhuber E, Hofstetter A, Hofstaedter F, Knuechel R. (2002). Occurrence of chromosome 9 and p53 alterations in multifocal dysplasia and carcinoma in situ of human urinary bladder. *Cancer Res* 62(3):809-18.

Hartwig A. (2001). Zinc finger proteins as potential targets for toxic metal ions: differential effects on structure and function. *Antioxid Redox Signal* 3:625-634.

Hatcher EL, Chen Y, Kang YJ. (1995). Cadmium resistance in A549 cells correlates with elevated glutathione content but not antioxidant enzymatic activities. *Free Radic Biol Med* 19:805-812.

He L, Wang B, Hay EB, Nebert DW. (2009). Discovery of ZIP transporters that participate in cadmium damage to testis and kidney. *Toxicol Appl Pharmacol* 238(3):250-7.

He W, Cai Q, Sun F, Zhong G, Wang P, Liu H, Luo J, Yu H, Huang J, Lin T. (2013). linc-UBC1 physically associates with polycomb repressive complex 2 (PRC2) and acts as a negative prognostic factor for lymph node metastasis and survival in bladder cancer. *Biochim Biophys Acta* 1832(10):1528-37.

Hicks RM. (1975). The mammalian urinary bladder: an accommodating organ. *Biol Rev Camb Philos Soc* 50:215-246.

Hopman AH, Kamps MA, Speel EJ, Schapers RF, Sauter G, Ramaekers FC. (2002). Identification of chromosome 9 alterations and p53 accumulation in isolated carcinoma in situ of the urinary bladder versus carcinoma in situ associated with carcinoma. *Am J Pathol* 161(4):1119-25.

Hu P, Deng FM, Liang FX, Hu CM, Auerbach AB, Shapiro E, Wu XR, Kachar B, Sun TT. (2000). Ablation of uroplakin III gene results in small urothelial plaques, urothelial leakage, and vesicoureteral reflux. *J Cell Biol* 151(5):961-972.

Hu P, Meyers S, Liang FX, Deng FM, Kachar B, Zeidel ML, Sun TT. (2002). Role of membrane proteins in permeability barrier function: uroplakin ablation elevates urothelial permeability. *Am J Physiol Renal Physiol* 283(6):F1200-1207.

Huang M, Krepkiy D, Hu W, Petering DH. (2004). Zn-, Cd-, and Pb-transcription factor IIIA: properties, DNA binding, and comparison with TFIIIA-finger 3 metal complexes. *J Inorg Biochem* 98(5):775-85.

Huang Q, Gumireddy K, Schrier M, le Sage C, Nagel R, Nair S, Egan DA, Li A, Huang G, Klein-Szanto AJ, Gimotty PA, Katsaros D, Coukos G, Zhang L, Puré E, Agami R. (2008). The microRNAs miR-373 and miR-520c promote tumour invasion and metastasis. *Nat Cell Biol* 10(2):202-10.

Hurst CD, Tomlinson DC, Williams SV, Platt FM, Knowles MA. (2008). Inactivation of the Rb pathway and overexpression of both isoforms of E2F3 are obligate events in bladder tumours with 6p22 amplification. *Oncogene* 27(19):2716-27.

Hutton KA, Trejdosiewicz LK, Thomas DF, Southgate J. (1993). Urothelial tissue culture for bladder reconstruction: an experimental study. *J Urol* 150:721-725.

Iizuka M, Smith MM. (2003). Functional consequences of histone modifications. *Curr Opin Genet Dev* 13:154*–160.*

International Agency for Research on Cancer. (1993). Beryllium, cadmium, mercury and exposures in the glass manufacturing industry. In: International Agency for Research on Cancer Monographs on the Evaluation of Carcinogenic Risks to Humans, vol. 58. IARC Scientific Publications, Lyon, pp. 119-237.

International Agency for Research on Cancer. (2012). Diesel and gasoline engine exhausts and some nitroarenes. In: International Agency for Research on

Cancer Monographs on the Evaluation of Carcinogenic Risks to Humans, vol. 105. IARC Scientific Publications, Lyon.

Itoh M, Furuse M, Morita K, Kubota K, Saitou M, Tsukita S. (1999). Direct binding of three tight junction-associated MAGUKs, ZO-1, ZO-2, and ZO-3, with the COOH termini of claudins. *J Cell Biol* 147(6):1351-1363.

Jacobs SA, Taverna SD, Zhang Y, Briggs SD, Li J, Eissenberg JC, Allis CD, Khorasanizadeh S. (2001). Specificity of the HP1 chromo domain for the methylated N-terminus of histone H3. *EMBO J* 20(18):5232-41.

Järup L, Akesson A (2009). Current status of cadmium as an environmental health problem. *Toxicol Appl Pharmacol* 238(3):201–8.

Jebar AH, Hurst CD, Tomlinson DC, Johnston C, Taylor CF, Knowles MA. (2005). FGFR3 and Ras gene mutations are mutally exclusive genetic events in urothelial cell carcinoma. *Oncogene* 24(33):5218-25.

Jensen TJ, Novak P, Eblin KE, Gandolfi AJ, Futscher BW. (2008). Epigenetic remodelling during arsenical-induced malignant transformation. *Carcinogenesis* 29:1500-1508.

Jenuwein T, Allis CD. (2001) Translating the histone code. *Science* 293:1074–1080.

Jin P, Ringertz NR. (1990). Cadmium induces transcription of proto-oncogenes c-jun and c-myc in rat L6 myoblasts. *J Biol Chem* 265:14061-14064.

Jin T, Lu J, Nordberg M. (1998). Toxicokinetics and biochemistry of cadmium with special emphasis on the role of metallothionein. *Neurotoxicology* 19(4-5):529–535.

Jing Y, Liu LZ, Jiang Y, Zhu Y, Guo NL, Barnett J, Rojanasakul Y, Agani F, Jiang BH. (2012). Cadmium increases HIF-1 and VEGF expression through ros, erk, and akt signaling pathways and induces malignant transformation of human bronchial epithelial cells. *Toxicol Sci* 125:10-19.

Jo A, Denduluri S, Zhang B, Wang Z, Yin L, Yan Z, Kang R, Shi LL, Mok J, Lee MJ, Haydon RC. (2014). The versatile functions of Sox9 in development, stem cells, and human diseases. *Genes Dis* 1(2):149-161.

Jo WJ, Ren X, Chu F, Aleshin M, Wintz H, Burlingame A, Smith MT, Vulpe CD, Zhang L. (2009). Acetylated H4K16 by MYST1 protects UROtsa cells from arsenic toxicity and is decreased following chronic arsenic exposure. *Toxicol Appl Pharmacol* 241:294-302.

Jones PA, Baylin SB. (2007). The epigenomics of cancer. *Cell* 23(4):683-92.

Joseph P. (2009). Mechanisms of cadmium carcinogenesis. *Toxicol Appl Pharmacol* 238:272-279.

Jost SP. (1989). Cell cycle of normal bladder urothelium in developing and adult mice. *Virchows Arch B Cell Pathol Incl Mol Pathol* 57: 27-36.

Kagi JHR, Vallee BL. (1960). Metallothionein, a cadmium- and zinc-containing protein from equine renal cortex. *J Biol Chem* 235:3460–65.

Karytinos A, Forneris F, Profumo A, Ciossani G, Battaglioli E, Binda C, Mattevi A. (2009). A novel mammalian flavin-dependent histone demethylase. *J Biol Chem* 284(26):17775-82.

Ke Q, Davidson T, Chen H, Kluz T, Costa M. (2006). Alterations of histone modifications and transgene silencing by nickel chloride. *Carcinogenesis* 27:1481-1488.

Kellen E, Zeegers MP, Hond ED, Buntinx F. (2007). Blood cadmium may be associated with bladder carcinogenesis: The Belgian case–control study on bladder cancer. *Cancer Detection and Prevention*, 31(1):77–82.

Kim EJ, Kim YJ, Jeong P, Ha YS, Bae SC, Kim WJ. (2008). Methylation of the RUNX3 promoter as a potential prognostic marker for bladder tumor. *J Urol* 180(3):1141-5.

Kim WJ, Kim EJ, Jeong P, Quan C, Kim J, Li QL, Yang JO, Ito Y, Bae SC. (2005). RUNX3 inactivation by point mutations and aberrant DNA methylation in bladder tumors. *Cancer Res* 65(20):9347-54.

Kirk D, Kagawa S, Vener G, Narayan KS, Ohnuki Y, Jones LW. (1985). Selective growth of normal adult human urothelial cells in serum-free medium. *In Vitro Cell Dev Biol* 21:165-171.

Knowles MA, Hurst CD. (2015). Molecular biology of bladder cancer: new insights into pathogenesis and clinical diversity. *Nat Rev Cancer* 15(1):25-41.

Kong XT, Deng FM, Hu P, Liang FX, Zhou G, Auerbach AB, Genieser N, Nelson PK, Robbins ES, Shapiro E, Kachar B, Sun TT. (2004). Roles of uroplakins in plaque formation, umbrella cell enlargement, and urinary tract diseases. *J Cell Biol* 167(6):1195-1204.

Kothinti RK, Blodgett AB, Petering DH, Tabatabai NM. (2010). Cadmium down-regulation of kidney Sp1 binding to mouse SGLT1 and SGLT2 gene promoters: possible reaction of cadmium with the zinc finger domain of Sp1. *Toxicol Appl Pharmacol* 244:254-62.

Kouzarides T. (2003). Chromatin modifications and their function. *Cell* 128:693-705.

Krause G, Winkler L, Mueller SL, Haseloff RF, Piontek J, Blasig IE. (2008). Structure and function of claudins. *Biochim Biophys Acta* 1778(3):631-645.

Kurzrock EA, Lieu DK, Degraffenried LA, Chan CW, Isseroff RR. (2008). Label-retaining cells of the bladder: candidate urothelial stem cells. *Am J Physiol Renal Physiol* 294(6):F1415-21.

Lacinová L, Klugbauer N, Hofmann F. (2000). Regulation of the calcium channel alpha(1G) subunit by divalent cations and organic blockers. *Neuropharmacology* 39(7):1254-66.

Lavelle J, Meyers S, Ramage R, Bastacky S, Doty D, Apodaca G, Zeidel ML. (2002). Bladder permeability barrier: recovery from selective injury of surface epithelial cells. *Am J Physiol Renal Physiol* 283:F242-F253.

Lee KK, Workman JL. (2007). Histone acetyltransferase complexes: one size doesn't fit all. *Nat Rev Mol Cell Biol* 8(4):284-95.

Lee MG, Kim HY, Byun DS, Lee SJ, Lee CH, Kim JI, Chang SG, Chi SG. (2001). Frequent epigenetic inactivation of RASSF1A in human bladder carcinoma. *Cancer Res* 61(18):6688-92.

Lee MJ, Nishio H, Ayaki H, Yamammoto M, Sumino K. (2002). Upregulation of stress response mRNAs in COS-7 cells exposed to cadmium. *Toxicology* 174:109-117.

Lewis SA, Diamond JM. (1975) Active sodium transport by mammalian urinary bladder. *Nature* 253(5494): 747-748.

Lewis SA, Diamond JM. (1976). Na+ transport by rabbit urinary bladder, a tight epithelium. *J Membr Biol* 28(1):1-40.

Lewis SA. (2000). Everything you wanted to know about the bladder epithelium but were afraid to ask. *Am J Physiol Renal Physiol* 2000, 278(6): F867-874.

Li Q, Ke Q, Costa M. (2009). Alterations of histone modifications by cobalt compounds. *Carcinogenesis* 30(7):1243-1251.

Lin S, Wein S, Gonzales-Cope M, Otte GL, Yuan ZF, Afjehi-Sadat L, Maile T, Berger SL, Rush J, Lill JR, Arnott D, Garcia BA. (2014). Stable Isotope labeled histone peptide library for histone post-translational modification and variant quantification by mass spectrometry. *Mol Cell Proteomics* 13:2450-66.

Linnenbach AJ, Pressler LB, Seng BA, Kimmel BS, Tomaszewski JE, Malkowicz SB. (1993). Characterization of chromosome 9 deletions in transitional cell carcinoma by microsatellite assay. *Hum Mol Genet* 2(9):1407-11.

Liu J, Qu W, Kadiiska MB. (2009). Role of oxidative stress in cadmium toxicity and carcinogenesis. *Toxicol Appl Pharmacol* 238:209-214.

Liu Z, Li H, Soleimani M, Girijashanker K, Reed JM, He L, Dalton TP, Nebert DW. (2008). Cd^{2+} versus Zn^{2+} uptake by the ZIP8 HCO3--dependent symporter: kinetics, electrogenicity and trafficking. *Biochem Biophys Res Commun* 365(4):814-20.

Lobban ED, Smith BA, Hall GD, Harnden P, Roberts P, Selby PJ, Trejdosiewicz LK, Southgate J. (1998). Uroplakin gene expression by normal and neoplastic urothelium. *Am J Pathol* 153(6):1957-67.

Lomberk G, Wallrath L, Urrutia R. (2006). The Heterochromatin Protein 1 family. *Genome Biol* 7(7):228.

Lowell BB. (1999). PPARgamma: an essential regulator of adipogenesis and modulator of fat cell function. *Cell* 99: 239-242.

Lu NZ, Cidlowski JA. (2004). The origin and functions of multiple human glucocorticoid receptor isoforms. *Ann N Y Acad Sci* 1024:102-23.

Luger K, Mäder AW, Richmond RK, Sargent DF, Richmond TJ. (1997). Crystal structure of the nucleosome core particle at 2.8 A resolution. *Nature* 389:251–260.

Luo M, Li Z, Wang W, Zeng Y, Liu Z, Qiu J. (2013). Long non-coding RNA H19 increases bladder cancer metastasis by associating with EZH2 and inhibiting E-cadherin expression. *Cancer Lett* 333(2)213-21.

Lupien M, Eeckhoute J, Meyer CA, Wang Q, Zhang Y, Li W, Carroll JS, Liu XS, Brown M. (2008). FoxA1 translates epigenetic signatures into enhancer-driven lineage-specific transcription. *Cell* 132(6):958-70.

Maison C, Almouzni G. (2004). HP1 and the dynamics of heterochromatin maintenance. *Nat Rev Mol Cell Biol* 5(4):296-304.

Malgieri G, Zaccaro L, Leone M, Bucci E, Esposito S, Baglivo I, Del Gatto A, Russo L, Scandurra R, Pedone PV, Fattorusso R, Isernia C. (2011). Zinc to cadmium replacement in the A. thaliana SUPERMAN Cys_2 His_2 zinc finger induces structural rearrangements of typical DNA base determinant positions. *Biopolymers* 95(11):801-10.

Margueron R, Reinberg D. (2011). The Polycomb complex PRC2 and its mark in life. *Nature* 469(7330):343-9.

Markowitz SD, Bertagnolli MM. (2009). Molecular origins of cancer: Molecular basis of colorectal cancer. *N Engl J Med* 361(25):2449-60.

Marsit CJ, Karagas MR, Danaee H, Liu M, Andrew A, Schned A, Nelson HH, Kelsey KT. (2006). Carcinogen exposure and gene promoter hypermethylation in bladder cancer. *Carcinogenesis* 27(1):112-6.

Martin C, Zhang Y. (2005). The diverse functions of histone lysine methylation. *Nature Rev Mol Cell Biol 6:*838–849.

Martinez-Zamudio R, Ha HC. (2011). Environmental epigentics in metal exposure. *Epigentics* 6:820-827.

Maruyama R, Toyooka S, Toyooka KO, Harada K, Virmani AK, Zöchbauer-Müller S, Farinas AJ, Vakar-Lopez F, Minna JD, Sagalowsky A, Czerniak B, Gazdar AF. (2001). Aberrant promoter methylation profile of bladder cancer and its relationship to clinicopathological features. *Cancer Res* 15;61(24):8659-63.

Matouk IJ, DeGroot N, Mezan S, Ayesh S, Abu-lail R, Hochberg A, Galun E. (2007). The H19 non-coding RNA is essential for human tumor growth. *PLos One* 2(9):e845.

Matsuoka M, Call KM. (1995). Cadmium-induced expression of immediate early genes in LLC-PK1 cells. *Kidney Int* 48:383-389.

Mi H, Muruganujan A, Casagrande JT, Thomas PD. (2013). Large-scale gene function analysis with the PANTHER classification system. *Nat Protoc* 8:1551-66**.**

Mikkelsen TS, Ku M, Jaffe DB, Issac B, Lieberman E, Giannoukos G, Alvarez P, Brockman W, Kim TK, Koche RP, Lee W, Mendenhall E, O'Donovan A, Presser A, Russ C, Xie X, Meissner A, Wernig M, Jaenisch R, Nusbaum C, Lander ES, Bernstein BE. (2007). Genome-wide maps of chromatin state in pluripotent and lineage-committed cells. *Nature* 448(7153):553-60.

Misra RR, Crance KA, Bare RM, Waalkes MP. (1997). Lack of correlation between the inducibility of metallothionein mRNA and metallothionein protein in cadmium-exposed rodents. *Toxicology* 117:99–109.

Moll R, Achtstatter T, Becht E, Balcarova-Stander J, Ittensohn M & Franke WW. (1988). Cytokeratins in normal and malignant transitional epithelium. Maintenance of expression of urothelial differentiation features in transitional cell carcinomas and bladder carcinoma cell culture lines. Am J Pathol, 132: 123-144.

Monteilh-Zoller MK, Hermosura MC, Nadler MJ, Scharenberg AM, Penner R, Fleig A. (2003). TRPM7 provides an ion channel mechanism for cellular entry of trace metal ions. *J Gen Physiol* 121(1):49-60.

Mysorekar IU, Isaacson-Schmid M, Walker JN, Mills JC, Hultgren SJ. (2009). Bone morphogenetic protein 4 signaling regulates epithelial renewal in the urinary tract in response to uropathogenic infection. Cell Host Microbe 5(5):463-75.

Nakagawa T, Kanai Y, Ushijima S, Kitamura T, Kakizoe T, Hirohashi S. (2005). DNA hypermethylation on multiple CpG islands associated with increased DNA methyltransferase DNMT1 protein expression during multistage urothelial carcinogenesis. *J Urol* 173(5):1767-71.

National Toxicology Program. (2000). Ninth report on carcinogens. Department of Health and Human Services, National Toxicology Program, Research Triangle Park, NC, USA.

Neely LA, Rieger-Christ KM, Neto BS, Eroshkin A, Garver J, Patel S, Phung NA, McLaughlin S, Libertino JA, Whitney D, Summerhayes IC. (2010). A microRNA expression ratio defining the invasive phenotype in bladder tumors. *Urol Oncol* 28(1):39-48.

Newell-Price J, Clark AJ, King P. (2000). DNA methylation and silencing of gene expression. *Trends Endocrinol Metab* 11(4):142-8.

Nieboer E, Fletcher GG, Thomassen Y. (1999). Relevance of reactivity determinants to exposure assessment and biological monitoring of the elements. *J Environ Monit* 1(1):1-14.

Nishiyama N, Arai E, Chihara Y, Fujimoto H, Hosoda F, Shibata T, Kondo T, Tsukamoto T, Yokoi S, Imoto I, Inazawa J, Hirohashi S, Kanai Y. (2010). Genome-wide DNA methylation profiles in urothelial carcinomas and urothelia at the precancerous stage. *Cancer Sci* 101(1):231-40.

Ochi T, Takahashi K, Ohsawa M. (1987). Indirect evidence for the induction of a pro-oxidant state by cadmium chloride in cultured mammalian cells and a possible mechanism for the induction. *Mutat Res* 180:257–266.

Orlow I, Lacombe L, Hannon GJ, Serrano M, Pellicer I, Dalbagni G, Reuter VE, Zhang ZF, Beach D, Cordon-Cardo C. (1995). Deletion of the p16 and p15 genes in human bladder tumors. *J Natl Cancer Inst* 87(20):1524-9.

Otvos JD, Armitage IM. (1980). Structure of the metal clusters in rabbit liver metallothionein. *Proc Natl Acad Sci USA* 77:7094–98.

Palmiter RD, Findley SD, Whitmore TE, Durnam DM. (1992). MT-III, a brain-specific member of the metallothionein gene family. *Proc Natl Acad Sci USA* 89(14):6333-7.

Palmiter RD, Huang L. (2004). Efflux and compartmentalization of zinc by members of the SLC30 family of solute carriers. *Pflugers Arch* 447:744–751.

Panza A, Pazienza V, Ripoli M, Benegiamo G, Gentile A, Valvano MR, Augello B, Merla G, Prattichizzo C, Tavano F, Ranieri E, di Sebastiano P, Vinciguerra M, Andriulli A, Mazzoccoli G, Piepoli A. (2013). Interplay between SOX9, β-catenin and PPARγ activation in colorectal cancer. *Biochim Biophys Acta* 1833(8):1853-65.

Papagiannakopoulos T, Shapiro A, Kosik KS. (2008). MicroRNA-21 targets a network of key tumor-suppressive pathways in glioblastoma cells. *Cancer Res* 68(19):8164-72.

Parsell DA, Lindquist S. (1994). Heat Shock Proteins and Stress Tolerance. In *The Biology of Heat Shock Proteins and Molecular Chaperones*, edited by Morimoto RI, Tissieres A, Georgopoulos C. New York: CSHL Press, 457-494.

Person RJ, Tokar EJ, Xu Y, Orihuela R, Ngalame NN, Waalkes MP. (2013). Chronic cadmium exposure in vitro induces cancer cell characteristics in human lung cells. *Toxicol Appl Pharmacol* 273:281-288.

Petering DH, Huang M, Moteki S, Shaw CF 3rd. (2000). Cadmium and lead interactions with transcription factor IIIA from Xenopus laevis: a model for

zinc finger protein reactions with toxic metal ions and metallothionein. *Mar Environ Res* 50(1-5):89-92.

Pfeifer GP, Yoon JH, Liu L, Tommasi S, Wilczynski SP, Dammann R. (2002). Methylation of the RASSF1A gene in human cancers. *Biol Chem* 383(6):907-14.

Phillips JE, Corces VG. (2009). CTCF: master weaver of the genome. *Cell* 137(7):1194-211.

Prozialeck WC, Lamar PC. (1999). Interaction of cadmium (Cd^{2+}) with a 13-residue polypeptide analog of a putative calcium-binding motif of E-cadherin. *Biochim Biophys Acta* 1451(1):93-100.

Prozialeck WC, Lamar PC, Lynch SM. (2003). Cadmium alters the localization of N-cadherin, E-cadherin, and beta-catenin in the proximal tubule epithelium. *Toxicol Appl Pharmacol* 189(3):180-95.

Puzio-Kuter AM, Castillo-Martin M, Kinkade CW, Wang X, Shen TH, Matos T, Shen MM, Cordon-Cardo C, Abate-Shen C. (2009). Inactivation of p53 and Pten promotes invasive bladder cancer. *Genes Dev* 23:675-680.

Qian C, Zhou MM. (2006). SET domain protein lysine methyltransferases: Structure, specificity and catalysis. *Cell Mol Life Sci* 63(23):2755-63.

Rahman Z, Reedy EA, Heatfield BM. (1987). Isolation and primary culture of urothelial cells from normal human bladder. *Urol Res* 15:315-320.

Reulen RC, Kellen E, Buntinx F, Brinkman M, Zeegers MP. (2008). A meta-analysis on the association between bladder cancer and occupation. *Scandinavian journal of urology and nephrology. Supplementum* (218)64–78.

Reznikoff CA, Johnson MD, Norback DH, Bryan GT. (1983). Growth and characterization of normal human urothelium in vitro. *In Vitro* 19:326-343.

Ringrose L, Ehret H, Paro R. (2004) Distinct contributions of histone H3 lysine 9 and 27 methylation to locus-specific stability of polycomb complexes. *Mol Cell* 16(4):641-53.

Rintisch C, Heinig M, Bauerfeind A, Schafer S, Mieth C, Patone G, Hummel O, Chen W, Cook S, Cuppen E, Colomé-Tatché M, Johannes F, Jansen RC, Neil H, Werner M, Pravenec M, Vingron M, Hubner N. (2014). Natural variation of histone modification and its impact on gene expression in the rat genome. *Genome Res* 24(6):942-53.

Rusanov AL, Smirnova AV, Poromov AA, Fomicheva KA, Luzgina NG, Majouga AG. (2015). Effects of cadmium chloride on the functional state of human intestinal cells. *Toxicol In Vitro* (5):1006-11.

Santos-Rosa H, Schneider R, Bannister AJ, Sherriff J, Bernstein BE, Emre NC, Schreiber SL, Mellor J, Kouzarides T. (2002). Active genes are tri-methylated at K4 of histone H3. *Nature* 419(6905):407-11.

Schaafsma HE, Ramaekers FC, van Muijen GN, Ooms EC, Ruiter DJ. (1989). Distribution of cytokeratin polypeptides in epithelia of the adult human urinary tract. *Histochemistry* 91(2):151-159.

Schagdarsurengin U, Wilkens L, Steinemann D, Flemming P, Kreipe HH, Pfeifer GP, Schlegelberger B, Dammann R. (2003). Frequent epigenetic inactivation of the RASSF1A gene in hepatocellular carcinoma. *Oncogene* 22:1866-71.

Schneeberger EE, Lynch RD. (2004). The tight junction: a multifunctional complex. *Am J Physiol Cell Physiol* 2004, 286(6):C1213-1228.

Scholpa NE, Zhang X, Kolli RT, Cummings BS. (2014). Epigenetic changes in p21 expression in renal cells after exposure to bromate. *Toxicol Sci* 141:432-40.

Schulzke JD, Gitter AH, Mankertz J, Spiegel S, Seidler U, Amasheh S, Saitou M, Tsukita S, Fromm M. (2005). Epithelial transport and barrier function in occludin-deficient mice. *Biochim Biophys Acta* 1669(1):34-42.

Schwerdtle T, Ebert F, Thuy C, Richter C, Mullenders LH, Hartwig A. (2010). Genotoxicity of soluble and particulate cadmium compounds: impact on oxidative DNA damage and nucleotide excision repair. *Chem Res Toxicol* 15;23(2):432-42.

Searle PF, Stuart GW, Palmiter RD. (1985). Building a metal-responsive promoter with synthetic regulatory elements. *Mol Cell Biol* 5:1480–1489.

Séguin C, Prévost J. (1988). Detection of a nuclear protein that interacts with a metal regulatory element of the mouse metallothionein 1 gene. *Nucleic Acids Res* 16:10547–10560.

Sens DA, Rossi M, Park S, Gurel V, Nath J, Garrett S, Sens MA, Somji S. (2003). Metallothionein isoform 1 and 2 gene expression in a human urothelial cell line (UROtsa) exposed to CdCl2 and NaAsO2. *J Toxicol Environ Health A* 66(21):2031-46.

Sens DA, Park S, Gurel V, Sens MA, Garrett SH, Somji S. (2004). Inorganic Cadmium- and Arsenite-Induced Malignant Transformation of Human Bladder Urothelial Cells. *Toxicological Sciences* 79(1):56–63.

Sens MA, Somji S, Lamm DL, Garrett SH, Slovinsky F, Todd JH,Sens DA. (2000). Metallothionein isoform 3 as a potential biomarker for human bladder cancer. *Environ Health Perspect* 108(5):413–418.

Shi Y, Lan F, Matson C, Mulligan P, Whetstine JR, Cole PA, Casero RA, Shi Y. (2004). Histone demethylation mediated by the nuclear amine oxidase homolog LSD1. *Cell* 119(7):941-53.

Shin K, Lee J, Guo N, Kim J, Lim A, Qu L, Mysorekar IU, Beachy PA. (2011). Hedgehog/Wnt feedback supports regenerative proliferation of epithelial stem cells in bladder. *Nature* 472(7341):110-4.

Siemiatycki J, Dewar R, Nadon L, Gerin M. (1994). Occupational Risk Factors for Bladder Cancer: Results from a Case-Control Study in Montreal, Quebec, Canada. *American Journal of Epidemiology* 140(12):1061–1080.

Sjödahl G, Lauss M, Lövgren K, Chebil G, Gudjonsson S, Veerla S, Patschan O, Aine M, Fernö M, Ringnér M, Månsson W, Liedberg F, Lindgren D, Höglund M. (2012). A molecular taxonomy for urothelial carcinoma. *Clin Cancer Res* 18(12):3377-86.

Sjödahl G, Lövgren K, Lauss M, Patschan O, Gudjonsson S, Chebil G, Aine M, Eriksson P, Månsson W, Lindgren D, Fernö M, Liedberg F, Höglund M. (2013). Toward a molecular pathologic classification of urothelial carcinoma. *Am J Pathol* 183(3):681-91.

Smith NJ, Hinley J, Varley CL, Eardley I, Trejdosiewicz LK, Southgate J. (2015). The human urothelial tight junction: claudin 3 and the ZO-1α^{+} switch. *Bladder* 2(1):e9.

Somji S, Sens MA, Lamm DL, Garrett SH, Sens DA. (2001). Metallothionein isoform 1 and 2 gene expression in the human bladder: evidence for upregulation of MT-1X mRNA in bladder cancer. *Cancer Detect Prev* 25(1):62–75.

Somji S, Bathula CS, Zhou XD, Sens MA, Sens DA, Garrett SH. (2008). Transformation of human urothelial cells (UROtsa) by as and cadmium induces the expression of keratin 6a. *Environ Health Perspect* 116(.4):434–440.

Somji S, Cao L, Mehus A, Zhou XD, Sens MA, Dunlevy JR, Garrett SH, Zheng Y, Larson JL, Sens DA. (2011). Comparison of expression patterns of keratin 6, 7, 16, 17, and 19 within multiple independent isolates of As(+3)- and Cd (+2)-induced bladder cancer: keratin 6, 7, 16, 17, and 19 in bladder cancer. *Cell Biol Toxicol* 27:381–396.

Somji S, Garrett SH, Toni C, Zhou XD, Zheng Y, Ajjimaporn A, Sens MA, Sens DA. (2011). Differences in the epigenetic regulation of MT-3 gene expression between parental and Cd^{+2} or As^{+3} transformed human urothelial cells. *Cancer Cell International* 11:2.

Southgate J, Hutton KA, Thomas DF, Trejdosiewicz LK. (1994). Normal human urothelial cells in vitro: proliferation and induction of stratification. *Lab Invest* 71:583-594.

Southgate J, Masters JR, Trejdosiewicz LK. (2002). Culture of human urothelium. In *Culture of Epithelial Cells*, edited by Freshney RI, Freshney MG. New York: Wiley, 381-400.

Stohs SJ, Bagchi D, Hassoun E, Bagchi M. (2001). Oxidative mechanisms in the toxicity of chromium and cadmium ions. *J Environ Pathol Toxicol Oncol* 20:77–88.

Stransky N, Vallot C, Reyal F, Bernard-Pierrot I, de Medina SG, Segraves R, de Rycke Y, Elvin P, Cassidy A, Spraggon C, Graham A, Southgate J, Asselain B, Allory Y, Abbou CC, Albertson DG, Thiery JP, Chopin DK, Pinkel D, Radvanyi F. (2006). Regional copy number-independent deregulation of transcription in cancer. *Nat Genet* 38:1386-1396.

Stuart GW, Searle PF, Chen HY, Brinster RL, Palmiter RD. (1984). A 12-base-pair DNA motif that is repeated several times in metallothionein gene promoters confers metal regulation to a heterologous gene. *Proc Natl Acad Sci* 81:7318–7322.

Stuart GW, Searle PF, Palmiter RD. (1985). Identification of multiple metal regulatory elements in mouse metallothionein-I promoter by assaying synthetic sequences. *Nature* 317(6040):828-31.

Sun DK, Wang JM, Zhang P, Wang YQ. (2015). MicroRNA-138 Regulates Metastatic Potential of Bladder Cancer Through ZEB2. *Cell Physiol Biochem* 37(6):2366-74.

Sun TT, Liang FX, Wu XR. (1999). Uroplakins as markers of urothelial differentiation. *Adv Exp Med Biol* 462:7-18.

Sun W, Wilhelmina Aalders T, Oosterwijk E. (2014). Identification of potential bladder progenitor cells in the trigone. *Dev Biol* 393(1):84-92.

Takenaka S, Oldiges H, Konig H, Hochrainer D, Oberdorster G. (1983). Carcinogenicity of cadmium chloride aerosols in W rats. *Journal of the National Cancer Institute*, 70(2):367–373.

Takiguchi M, Achanzar WE, Qu W, Li G, Waalkes MP. (2003). Effects of cadmium on DNA-(cytosine-5) methyltransferase activity and DNA methylation status during cadmium-induced cellular transformation. *Exp Cell Res* 286:355-365.

Tamaru H, Selker EU. (2001). A histone H3 methyltransferase controls DNA methylation in Neurospora crassa. *Nature* 414(6861):277-83.

Tani H, Onuma Y, Ito Y, Torimura M. (2014). Long non-coding RNAs as surrogate indicators for chemical stress responses in human-induced pluripotent stem cells. *PLoS One* 9(8) e106282.

Taylor SM, Jones PA. (1982). Mechanism of action of eukaryotic DNA methyltransferase. Use of 5-azacytosine-containing DNA. *J Mol Biol* 162(3):679-92.

Thangappan R, Kurzrock EA. (2009). Three clonal types of urothelium with different capacities for replication. *Cell Prolif* 42(6):770-9.

Tokar EJ, Benbrahim-Tallaa L, Waalkes MP. (2011). Metal ions in human cancer development. *Met Ions Life Sci* 8:375-401.

Towbin BD, González-Aguilera C, Sack R, Gaidatzis D, Kalck V, Meister P, Askjaer P, Gasser SM. (2012). Step-wise methylation of histone H3K9 positions heterochromatin at the nuclear periphery. *Cell* 150(5):934-47.

Tsai YC, Nichols PW, Hiti AL, Williams Z, Skinner DG, Jones PA. (1990). Allelic losses of chromosomes 9, 11, and 17 in human bladder cancer. *Cancer Res* 50(1):44-7.

Tsujimura A, Koikawa Y, Salm S, Takao T, Coetzee S, Moscatelli D, Shapiro E, Lepor H, Sun TT, Wilson EL. (2002). Proximal location of mouse prostate epithelial stem cells: a model of prostatic homeostasis. *J Cell Biol* 157(7):1257-65.

Tsukada Y, Fang J, Erdjument-Bromage H, Warren ME, Borchers CH, Tempst P, Zhang Y. (2006). Histone demethylation by a family of JmjC domain-containing proteins. *Nature* 439(7078):811-6.

Turner BM. (2000*)*. Histone acetylation and an epigenetic code. *Bioessays* 22*:*836–845.

Turner BM. (2002). Cellular memory and the histone code. *Cell* 111:285–291.

Uchida Y, Takio K, Titani K, Ihara Y, Tomonaga M. (1991). The growth inhibitory factor that is deficient in the Alzheimer's disease brain is a 68 amino acid metallothionein-like protein. *Neuron* (2):337-47.

Umeda K, Ikenouchi J, Katahira-Tayama S, Furuse K, Sasaki H, Nakayama M, Matsui T, Tsukita S, Furuse M, Tsukita S. (2006). ZO-1 and ZO-2 idenependently determine where claudins are polymerized in tight-junction strand formation. *Cell* 126(4): 741-754.

Urani C, Melchioretto P, Gribaldo L. (2010). Regulation of metallothioneins and ZnT-1 transporter expression in human hepatoma cells HepG2 exposed to zinc and cadmium. *Toxicol In Vitro* 24(2):370-4.

Urani C, Melchioretto P, Bruschi M, Fabbri M, Sacco MG, Gribaldo L. (2015). Impact of Cadmium on Intracellular Zinc Levels in HepG2 Cells: Quantitative Evaluations and Molecular Effects. *Biomed Res Int* [Epub ahead of print] 949514.

Valko M, Rhodes CJ, Moncol J, Izakovic M, Mazur M. (2006). Free radicals, metals and antioxidants in oxidative stress-induced cancer. *Chem Biol Interact* 160:1–40.

Vallot C, Stransky N, Bernard-Pierrot I, Hérault A, Zucman-Rossi J, Chapeaublanc E, Vordos D, Laplanche A, Benhamou S, Lebret T, Southgate J, Allory Y, Radvanyi F. (2011). A novel epigenetic phenotype associated with the most

aggressive pathway of bladder tumor progression. *J Natl Cancer Inst* 103:47-60.

Valverde M, Trejo C, Rojas E. (2001). Is the capacity of lead acetate and cadmium chloride to induce genotoxic damage due to direct DNA-metal interaction? *Mutagenesis* 16(3):265-70.

Varley CL, Stahlschmidt J, Smith B, Stower M, Southgate J. (2004). Activation of peroxisome proliferator-activated receptor-gamma reverses squamous metaplasia and induces transitional differentiation in normal human urothelial cells. *Am J Pathol* 164(5):1789-98.

Varley CL, Stahlschmidt J, Lee WC, Holder J, Diggle C, Selby PJ, Trejdosiewicz LK, Southgate J. (2004). Role of PPARγ and EGFR signalling in the urothelial terminal differentiation programme. *J Cell Sci* 117:2029-2036.

Varley CL, Hill G, Pellegrin S, Shaw NJ, Selby PJ, Trejdosiewicz LK, Southgate J. (2005). Autocrine regulation of human urothelial cell proliferation and migration during regenerative responses in vitro. *Exp Cell Res* 306:216-229.

Varley CL, Garthwaite MA, Cross W, Hinley J, Trejdosiewicz LK, Southgate J. (2006). PPARgamma-regulated tight junction development during human urothelial cytodifferentiation. *J Cell Physiol* 208(2):407-17.

Varley CL, Southgate J. (2008). Effects of PPAR agonists on proliferation and differentiation in human urothelium. *Exp Toxicol Pathol* 60(6):435-41.

Varley CL, Bacon EJ, Holder JC, Southgate J. (2009). FOXA1 and IRF-1 intermediary transcriptional regulators of PPARgamma-induced urothelial cytodifferentiation. *Cell Death Differ* 16(1):103-14.

Veerla S, Lindgren D, Kvist A, Frigyesi A, Staaf J, Persson H, Liedberg F, Chebil G, Gudjonsson S, Borg A, Månsson W, Rovira C, Höglund M. (2009). MiRNA expression in urothelial carcinomas: important roles of miR-10a, miR-222, miR-125b, miR-7 and miR-452 for tumor stage and metastasis, and frequent homozygous losses of miR-31. *Int J Cancer* 124(9):2236-42.

Verougstraete V, Lison D, Hotza P. (2002). A systematic review of cytogenetic studies conducted in human populations exposed to cadmium compounds. *Mutat Res* 511:15-43.

Viau M, Gastaldo J, Bencokova Z, Joubert A, Foray N. (2008). Cadmium inhibits non-homologous end-joining and over-activates the MRE11-dependent repair pathway. *Mutat Res* 654(1):13-21.

Viré E, Brenner C, Deplus R, Blanchon L, Fraga M, Didelot C, Morey L, Van Eynde A, Bernard D, Vanderwinden JM, Bollen M, Esteller M, Di Croce L, de Launoit Y, Fuks F. (2006). The Polycomb group protein EZH2 directly controls DNA methylation. *Nature* 439(7078):871-4.

Waalkes MP, Anver M, Diwan BA. (1999a). Carcinogenic effects of cadmium in the noble NBL/Cr) rat: induction of pituitary, testicular,and injection site tumors and intraepithelial proliferative lesions of the dorsolateral prostate. *Toxicol Sci* 52:154–161.

Waalkes MP, Anver MR, Diwan BA. (1999b). Chronic toxic and carcinogenic effects of oral cadmium in the Noble (NBL/Cr) rat: induction of neoplastic and proliferative lesions of the adrenal, kidney, prostate, and testes. *J Toxicol Environ Health A* 58:199–214.

Waalkes MP, Rehm S, Cherian MG. (2000). Repeated cadmium exposures enhance the malignant progression of ensuing tumors in rats. *Toxicol Sci* 54:110–120.

Waalkes MP. (2000). Cadmium carcinogenesis in review. *J Inorg Biochem* 79:241–244.

Waalkes MP. (2003). Cadmium carcinogenesis. *Mutat Res* 533:107-120.

Wagner JR, Busche S, Ge B, Kwan T, Pastinen T, Blanchette M. (2014). The relationship between DNA methylation, genetic and expression inter-individual variation in untransformed human fibroblasts. *Genome Biol* 15(2):R37.

Waisberg M, Joseph P, Hale B, Beyersmann D. (2003). Molecular and cellular mechanisms of cadmium carcinogenesis. *Toxicology* 192:95–117.

Wang B, Li Y, Shao C, Tan Y, Cai L. (2012). Cadmium and its epigenetic effects. *Curr Med Chem* 19(16):2611-20.

Wang Z, Zang C, Rosenfeld JA, Schones DE, Barski A, Cuddapah S, Cui K, Roh TY, Peng W, Zhang MQ, Zhao K. (2008). Combinatorial patterns of histone acetylations and methylations in the human genome. *Nat Genet* 40(7):897-903.

Westin G, Schaffner W. (1988). A zinc-responsive factor interacts with a metal-regulated enhancer element (MRE) of the mouse metallothionein-I gene. *EMBO J* 7:3763–3770.

Wezel F, Pearson J, Southgate J. (2014). Plasticity of in vitro-generated urothelial cells for functional tissue formation. Tissue Eng Part A 20(9-10):1358-68.

Wieland M, Levin MK, Hingorani KS, Biro FN, Hingorani MM. (2009). Mechanism of cadmium-mediated inhibition of Msh2-Msh6 function in DNA mismatch repair. *Biochemistry* 48(40):9492-502.

Williamson MP, Elder PA, Shaw ME, Devlin J, Knowles MA. (1995). p16 (CDKN2) is a major deletion target at 9p21 in bladder cancer. *Hum Mol Genet* 4(9):1569-77.

Wolf C, Strenziokb R, Kyriakopoulosa A. (2009). Elevated MT-bound Cadmium concentrations in urine from bladder carcinoma patients, investigated by size exclusion chromatography-inductively coupled plasma mass spectrometry. *Anal Chim Acta* 631(2): 218-222.

Wu XR, Manabe M, Yu J, Sun TT. (1990). Large scale purification and immunolocalization of bovine uroplakins I, II, and III. Molecular markers of urothelial differentiation. *J Biol Chem* 265(31):19170-19179.

Wu XR, Lin JH, Walz T, Haner M, Yu J, Aebi U, Sun TT. (1994). Mammalian uroplakins. A group of highly conserved urothelial differentiation-related membrane proteins. *J Biol Chem* 269(18):13716-13724.

Wu Z, Liu K, Wang Y, Xu Z, Meng J, Gu S. (2015). Upregulation of microRNA-96 and its oncogenic functions by targeting CDKN1A in bladder cancer. *Cancer Cell Int* 15:107.

Xiao C, Liu Y, Xie C, Tu W, Xia Y, Costa M, Zhou X. (2015). Cadmium induces histone H3 lysine methylation by inhibiting histone demethylase activity. *Toxicol Sci* 145(1):80-9.

Yan PS, Shi H, Rahmatpanah F, Hsiau TH, Hsiau AH, Leu YW, Liu JC, Huang TH. (2003). Differential distribution of DNA methylation within the RASSF1A CpG island in breast cancer. *Cancer Res* 63:6178-86.

Yang F, Bi J, Xue X, Zheng L, Zhi K, Hua J, Fang G. (2012). Up-regulated long non-coding RNA H19 contributes to proliferation of gastric cancer cells. *FEBS J* 279(17):3159-65.

Yates DR, Rehman I, Abbod MF, Meuth M, Cross SS, Linkens DA, Hamdy FC, Catto JW. (2007). Promoter hypermethylation identifies progression risk in bladder cancer. *Clin Cancer Res* 13(7):2046-53.

Yoshida M., Horinouchi S., Beppu T. (1995). Trichostatin A and trapoxin: novel chemical probes for the role of histone acetylation in chromatin structure and function. *BioEssays,* 17*:* 423-430.

Yu J, Lin JH, Wu XR, Sun TT. (1994). Uroplakins Ia and Ib, two major differentiation products of bladder epithelium, belong to a family of four transmembrane domain (4TM) proteins. *J Cell Biol* 125:171-182.

Yu Z, Mannik J, Soto A, Lin KK, Andersen B. (2009). The epidermal differentiation-associated Grainyhead gene Get1/Grhl3 also regulates urothelial differentiation. *EMBO J* 28(13):1890-903.

Zambelli F, Pesole G, Pavesi G. (2009). Pscan: finding over-represented transcription factor binding site motifs in sequences from co-regulated or co-expressed genes. *Nucleic Acids Res* 37:247-52.

Zhang AH, Bin HH, Pan XL, Xi XG. (2007). Analysis of p16 gene mutation, deletion and methylation in patients with arseniasis produced by indoor unventilated-stove coal usage in Guizhou, China. *J Toxicol Environ Health A* 70(11):970-5.

Zhang B, Georgiev O, Hagmann M, Günes C, Cramer M, Faller P, Vasák M, Schaffner W. (2003). Activity of metal-responsive transcription factor 1 by toxic heavy metals and H2O2 in vitro is modulated by metallothionein. *Mol Cell Biol* 23:8471-85.

Zhou X, Sun H, Ellen TP, Chen H, Costa M. (2008). Arsenite alters global histone H3 methylation. *Carcinogenesis* 29:1831-1836.

Zhou X, Li Q, Arita A, Sun H, Costa M. (2009). Effects of nickel, chromate, and arsenite on histone 3 lysine methylation. *Toxicol Appl Pharmacol* 236:78-8.

Zhou XD, Sens DA, Sens MA, Namburi VB, Singh RK, Garrett SH, Somji S. (2006). Metallothionein-1 and -2 expression in cadmium- or arsenic-derived human malignant urothelial cells and tumor heterotransplants and as a prognostic indicator in human bladder cancer. *Toxicol Sci* 91(2):467–475.

Zhou XD, Sens MA, Garrett SH, Somji S, Park S, Gurel V, Sens DA. (2006). Enhanced expression of metallothionein isoform 3 protein in tumor heterotransplants derived from As+3- and Cd+2-transformed human urothelial cells. *Toxicol Sci* 93(2):322-30.

Zhou Z, Liu H, Wang C, Lu Q, Huang Q, Zheng C, Lei Y. (2015). Long non-coding RNAs as novel expression signatures modulate DNA damage and repair in cadmium toxicology. *Sci Rep* 5:15293.

Zhou ZH, Lei YX, Wang CX. (2012). Analysis of aberrant methylation in DNA repair genes during malignant transformation of human bronchial epithelial cells induced by cadmium. *Toxicol Sci* 125(2):412-7.